



University
of Glasgow

Toole, Joseph (1984) *Marine chemistry of uranium: studies by particle track analysis and alpha spectrometry*. PhD thesis.

<http://theses.gla.ac.uk/5919/>

Copyright and moral rights for this thesis are retained by the author

A copy can be downloaded for personal non-commercial research or study, without prior permission or charge

This thesis cannot be reproduced or quoted extensively from without first obtaining permission in writing from the Author

The content must not be changed in any way or sold commercially in any format or medium without the formal permission of the Author

When referring to this work, full bibliographic details including the author, title, awarding institution and date of the thesis must be given

MARINE CHEMISTRY OF URANIUM : STUDIES BY PARTICLE
TRACK ANALYSIS AND ALPHA SPECTROMETRY

A thesis submitted to
the University of Glasgow
in fulfilment of the requirements
for the degree of

Doctor of Philosophy

by

JOSEPH TOOLE

November 1984

DEPARTMENT OF CHEMISTRY
UNIVERSITY OF GLASGOW
GLASGOW G12 8QQ

ACKNOWLEDGEMENTS

I am indebted to the many people who have assisted me, either academically or otherwise, through the course of this project. In particular, the expert advice and guidance of both my supervisors, Dr. Murdoch S. Baxter at Glasgow and Dr. John Thomson at the Institute of Oceanographic Sciences, is gratefully acknowledged.

Other scientific personnel at I.O.S. are also acknowledged, particularly Drs. T. Roger Wilson, David J. Hydes and Sarah Colley, for their provision of deep sea core and pore water samples, auxiliary data and for valuable discussion of results. My thanks also go to M.B.A. Plymouth (Dr. Mike Whitfield), the Department of Earth Sciences, Leeds University (Russell Alexander, Robert Upstill-Goddard and Dr. Harry Elderfield), the Clyde and Forth River Purification Boards (Drs. Andrew J. Newton and Tom M. Leatherland) and the crews of these institutes' respective research vessels for their organisation of field trips and help during sample collection. Provision of neutron irradiation facilities by Dr. Angus B. Mackenzie and the control room staff at the Scottish Universities Research and Reactor Centre is also acknowledged. In addition, my thanks go to Professor Adam S. G. Curtis for technical advice and access to a Quantimet Image Analyser system, to the staff of the mechanical, electronic and glassblowing workshops for furnishment and maintenance of essential equipment, and to Mr. Robert Munro for photographic assistance and prints.

I am also indebted to Dr. J. Kirk Cochran for provision of pore water samples and for his participation in an inter-calibration exercise.

At work and on a social level, Dr. Gordon T. Cook, Dr. Ron W. Crawford, Miss Beatrice Economides, Mr. Francis R. Livens, Mr. Richard Malcolmson, Mr. Martin McCartney, Mrs. Alison McDonald, Mr. Paul McDonald, Dr. William A. McKay, Mr. Keith McKay/

McKay, Mr. Azizan Saad and Dr. Mike J. Stenhouse formed an inspiring group of friends at the University of Glasgow and provided a stimulating scientific environment in which I was privileged to work.

This research could not have been performed without the support and encouragement of my parents to whom I extend my warmest thanks. I am especially grateful to Pauline for her enthusiastic support and help with diagrams. I am also deeply indebted to Mrs. Ella Clark for her many hours of patient and precise work during the typing and photocopying of this thesis.

Finally, I gratefully acknowledge the financial support of the Natural Environment Research Council.

C O N T E N T S

PAGE

List of Figures

List of Tables

Abstract

CHAPTER ONE - INTRODUCTION

1.1	Marine Geochemistry of Uranium	1
1.2	Deep-sea and Nearshore Pore Waters	12
1.3	Aims of the Project	30

CHAPTER TWO - EXPERIMENTAL METHODS

2.1	Introduction	32
2.2	Deep-sea Sediments and Pore Waters	36
2.3	Estuarine Pore Waters	45
2.4	Rivers and Estuaries	47
2.5	Particulates from the Vicinity of Nuclear Installations and Miscellaneous Samples	51
2.6	Fission Track Method	54
2.6.1	Solid Samples	55
2.6.2	Aqueous Samples	58
2.6.3	Track Counting	67
2.6.4	Sample Irradiations	69
2.7	Alpha Track Method	80
2.8	Alpha Spectrometry	88
2.8.1	Aqueous Samples	88
2.8.2	Solid Samples	94
2.8.3	Alpha Spectrometry - Theory and Instrumentation	97
2.8.4	Spike Solutions	101

	<u>PAGE</u>
<u>CHAPTER THREE - RESULTS AND DISCUSSION</u>	
3.1 Particle Track Dating of Deep-sea Core 9936K	104
3.2 Uranium in Pore Waters of Deep-sea Sediments	118
3.3 Uranium in Pore Waters of Estuarine Sediments	155
3.4 Uranium in Rivers and Estuaries	164
3.5 Further Applications of Particle Track Analysis	199
 <u>APPENDIX A</u>	
Sample Calculations, Errors and Statistics	217
 <u>APPENDIX B</u>	
Fortran IV Computer Programme for Neutron Flux Calculation	220
 <u>APPENDIX C</u>	
Fortran IV Computer Programme for Evaluation of the Uranium Activity of Natural Waters	221
 <u>REFERENCES</u>	 223

LIST OF FIGURES

<u>Figure</u>		<u>Page</u>
1.1	Radioactive decay series of ^{238}U and ^{235}U through their first few daughters	3
1.2	Idealised schematic representation of the changes in concentration of some major redox indicators in pore waters	15
1.3	Eh-pH diagram of uranium species in the presence of CO_2	24
2.1	Locations of deep-sea cores sampled by R.R.S. Discovery	37
2.2	Diagram of the Hydrowerkstätten Kastenlot corer	39
2.3	Schematic diagram of the box corer in operation	40
2.4	Schematic diagram of the I.O.S. Mark II pore water sampler in operation at the sea bed	42
2.5	Schematic diagram of the I.O.S. Mark II pore water sampler	43
2.6	Sampling sites in the Tamar estuary	46
2.7	Sampling sites in the Clyde estuary	48
2.8	Sampling sites in the Forth estuary	50
2.9	Fission star or 'hotspot' from a uranium-bearing mineral in a solid sample	
2.10	Homogeneous track distribution from a sea water sample using 15ul ethylene glycol as spreading agent	60
2.11	Non-homogeneous track distribution from a sea water sample. No spreading agent used	61
2.12	Linearity obtained between uranium concentration of standards and samples and their corresponding track density observed by the Quantimet	63
2.13	Appearance of fission tracks (a) etched at 45°C for 60 minutes (b) etched at 80°C for 20 minutes	70
2.14	Abrasion of Lexan by a sandwiched seasalt deposit	72
2.15	The UTR-300 Research Reactor	74
2.16	Variation of thermal neutron flux with distance : from core in the UTR-300 research reactor	75
2.17	Track densities at the various reactor positions normalised to the integrated flux at the C.V.S. position	77
2.18/		

<u>Figure</u>		<u>Page</u>
2.18	Background-corrected track interference from fast fission of ^{232}Th	79
2.19	(a) Homogeneous and (b) heterogeneous alpha track distribution in cellulose nitrate detector	84
2.20	Typical alpha track distribution from a 13 mm sediment pellet, application time 8 months	85
2.21	Electrodeposition cell, dismantled	93
2.22	Typical alpha spectrum	102
3.1	Depth profile of total alpha track rate in core 9936K	108
3.2	Depth profiles of uranium levels in core 9936K from both fission track and alpha spectrometry techniques	110
3.3	Depth profiles of (a) excess alpha track rate and (b) unsupported ^{230}Th activity in core 9936K	111
3.4	Plot of uranium against calcium carbonate content for core 9936K	114
3.5	Uranium concentrations in the pore waters of cores from the Cape Verde abyssal plain	120
3.6	Alkalinity in the pore waters of cores from the Cape Verde abyssal plain	121
3.7	Uranium concentrations in the pore waters of cores from the Nares abyssal plain	126
3.8	Uranium and phosphate concentrations in the pore waters from core 10189 4B in the Bauer basin	131
3.9	Uranium concentrations in the pore waters of cores from the Madeira abyssal plain	135
3.10	Alkalinity in the pore waters of cores from the Madeira abyssal plain	136
3.11	Uranium, alkalinity and phosphate in the pore waters of eastern Atlantic core 10549 6K	143
3.12	Pore water uranium and solid phase uranium and organic carbon in east Mediterranean core 10103 1B	149
3.13	Pore water uranium in east Mediterranean core 10103 6B	150
3.14	Pore water uranium in east Mediterranean core 10103 3K	151
3.15/		

<u>Figure</u>		<u>Page</u>
3.15	Pore water uranium, iron and manganese in core 054 from the Tamar estuary	158
3.16	Pore water uranium, iron and manganese in core 053 from the Tamar estuary	159
3.17	Pore water uranium, iron and manganese in core 075 from the Tamar estuary	160
3.18	Variation in uranium concentration with salinity in the waters of the Clyde estuary	169
3.19	Variation in the $^{234}\text{U}/^{238}\text{U}$ activity ratio with salinity in the waters of the Clyde estuary	170
3.20	Plot of A.R. against $1/\text{U}$ as an indication of the conservativeness of mixing of the fresh and saline water end-members in the Clyde estuary	171
3.21	Variation in uranium concentration with salinity in the waters of the Tamar estuary	180
3.22	Variation in the $^{234}\text{U}/^{238}\text{U}$ activity ratio with salinity in the waters of the Tamar estuary	181
3.23	Concentration of suspended solids (turbidities) at time of sampling in three U.K. estuaries	186
3.24	Variation in phosphate concentration with salinity in the waters of the Forth estuary	187
3.25	Variation in uranium concentration with salinity in the waters of the Forth estuary	190
3.26	Variation in the $^{234}\text{U}/^{238}\text{U}$ activity ratio with salinity in the waters of the Forth estuary	191
3.27	Variation in the ^{234}U concentration with salinity in the waters of the Forth estuary	192
3.28	Uranium-salinity relationship for all three U.K. estuaries	197
3.29	Alpha track clusters in cellulose nitrate from filtered particulates of the Esk estuary	201
3.30	Enlarged alpha hot-spot from filtered particulates of the Esk estuary	202
3.31	(a) Fission track and (b) alpha-track hot-spots from material scraped from rocks near Dounreay, Caithness	205
3.32	Alpha-autoradiograph of the upper edge of a hydrothermal manganese deposit	208
3.33/		

<u>Figure</u>		<u>Page</u>
3.33	Complete alpha-autoradiograph of a hydrothermal manganese deposit	210
3.34	Alpha-autoradiograph of a planchet containing about 4 dpm ^{232}U	212
3.35	Alpha-autoradiograph of a planchet containing Pu isotopes	213
3.36	Alpha-autoradiograph of a planchet containing 47.7 dpm of alpha-emitting Pu isotopes	214
3.37	Fission track distribution produced by irradiation of a planchet containing Pu isotopes	215

LIST OF TABLES

<u>Table</u>		<u>Page</u>
2.1	Sampling data from all cruises	38
2.2	Environmental particulate samples from near Dounreay, Caithness	52
2.3	I.O.S. sea water replicates fission track counts	65
2.4	Alpha spectrometry/fission track analysis pore water intercalibration	66
2.5	Fission track counts from N.B.S. Standard Glass	71
2.6	Typical Quantimet alpha track count of a sediment pellet	86
2.7	Detector backgrounds	100
3.1	Particle track data for core 9936K	106
3.2	Alpha spectrometric data for core 9936K	107
3.3	Pore water uranium and alkalinity data for station 10552	119
3.4	Uranium concentrations in pore waters from station 10164 and 10165	125
3.5	Uranium concentrations in pore waters from station 10189	130
3.6	Uranium and alkalinity data for station 10554	134
3.7	Uranium, alkalinity and phosphate data for station 10549	142
3.8	Uranium data for station 10103	148
3.9	Pore water uranium data for cores from the Tamar estuary	157
3.10	Uranium concentrations and activity ratios in the Clyde estuary	168
3.11	Uranium concentrations and activity ratios in Clyde muds	176
3.12	Uranium concentrations and activity ratios in the Tamar estuary	179
3.13	Uranium concentrations in the muds from the Tamar estuary, as determined by fission track analysis	184
3.14	Uranium concentrations and activity ratios in the Forth estuary	189
3.15	Radionuclide activities in particulate material from the Esk estuary, Cumbria	200
3.16	Plutonium and uranium concentrations of samples collected in the vicinity of Dounreay Nuclear Power Development Establishment, Caithness.	204

ABSTRACT

Refinement of the fission track analysis technique has enabled accurate and reproducible determination of uranium in sediment pore waters at the sub-nanogram level, that is, with a sensitivity superior to that of the conventional radiochemical/ α -spectrometric procedure. Since the former technique requires a simple polymeric track recording medium rather than stable electronic nuclear counting equipment, with its associated high vacuum systems, it is inherently less expensive and more portable. Other advantages are the low track backgrounds recorded by the track detector itself, the minimal degree of chemical processing required, the small sample sizes assayable (0.1 g or 0.1 ml) and the ability to increase or decrease the sensitivity as required by using neutron irradiations of variable flux and duration.

Results from oxic, deep-sea carbonate sediments show that the levels of dissolved uranium in squeezed pore waters are significantly less than those measured in the same pore waters collected by an in-situ device. This important discrepancy is explained by the presence of a pressure effect which acts on cores retrieved from the sea-bed such that CO_2 is lost as the core is brought to ambient pressures. This artificial perturbation of the carbonate equilibrium system therefore leads to precipitation of calcium carbonate which, in turn scavenges some uranium from solution.

In deep-sea cores which exhibit anoxia, it is confirmed that the pore water uranium content is enhanced relative to sea water values. In-situ samples from one such core, containing a 20 cm thick turbidite layer, have provided the first direct evidence for a uranium flux within the pore waters, upwards into sea water. The flux is estimated at $0.94 \times 10^{-8} \text{ g U cm}^{-2} \text{ yr}^{-1}$. The geochemical behaviour of uranium in pore waters, however, seems to be less than straightforward, being dependent on a number of parameters such as alkalinity, organic carbon content and redox status of the sediment, with the major speciations being uncertain.

In/

In shallow nearshore sedimentary pore waters, uranium is fixed in the solid phase close to the sediment : water interface where anoxic to suboxic conditions are attained. Increases in the pore water uranium content at greater depths (below ~12 cm) in these sediments were regularly observed, indicating release from the sediment by a solubilisation mechanism.

The behaviour of uranium during estuarine mixing was studied in three British estuaries by the radiochemical/ α -spectrometric analysis of water samples. The Clyde and Tamar estuaries exhibited conservative behaviour, i.e. uranium concentration varied only with salinity. The Forth estuary, in contrast, showed evidence of uranium removal at salinities $<10^{\circ}/\infty$, where high particulate loads of up to 180 mg l^{-1} occurred. Large fluxes of phosphate removal were also found. The uranium concentrations and $^{234}\text{U}/^{238}\text{U}$ activity ratios for the Clyde, Tamar and Forth rivers were, respectively, 0.15 ug l^{-1} and 1.65, 0.04 ug l^{-1} and 1.44, 0.09 ug l^{-1} and 1.50. The removal rate of uranium in the upper part of the Forth estuary was estimated at about 44 kg. yr^{-1} and consequently does not represent a significant removal mechanism when compared to the total oceanic uranium input value of $1 \text{ to } 2 \times 10^{10} \text{ gy r}^{-1}$.

Alpha-particle track analysis, which shares many of the advantages of the fission track technique, is in addition non-destructive. However, it can sometimes require prolonged exposure periods for low-activity samples, it has a lower sensitivity than α -spectrometry and is not nuclide-specific. Nonetheless, it has been shown here to be useful in the dating of deep-sea sediment cores when combined with the fission track technique. Good agreement was found between the solid-phase uranium data generated by the fission track method and those from α -spectrometry, while the α -track results, in combination with these uranium data, gave a similar sedimentation rate ($0.26 \pm 0.06 \text{ cm kyr}^{-1}$) to that determined by direct ^{230}Th measurement ($0.26 \pm 0.02 \text{ cm kyr}^{-1}$).

The role of the α -track method in an autoradiographic mode was illustrated by exposure of the α -sensitive plastic to electroplated sources of various radionuclides and to some specially-prepared environmental thick sources. Sites of variable α -radiative intensity can be clearly identified, permitting semi-quantitative conclusions to be drawn. For example, the presence of 'hot particles' thought to contain/

contain Pu isotopes, was confirmed in estuarine particulates, while an autoradiograph from a hydrothermal ferromanganese nodule showed that diffusion of ^{222}Rn was occurring along microcracks and that α -emitting nuclides were concentrated at the surface which was exposed to sea water.

The relative ease of use of dielectric track detectors makes them invaluable as analytical tools for the environmental radiochemist, either in their own right, as in fission track analysis, or in a complementary role with the more accepted and widely-used wet radiochemical methods.

CHAPTER ONE

INTRODUCTION

1.1 Marine Geochemistry of Uranium

The concentration of uranium in the open ocean has been found to be roughly constant, varying only with salinity (Sackett and Cook, 1969; Turekian and Chan, 1971; Burton, 1975; Ku et al., 1977), but, in nearshore and coastal waters, it is variable, being primarily related to the uranium contents of rivers entering these zones (Blanchard and Oakes, 1965; Sackett and Cook, 1969; Bhat and Krishnaswami, 1969; Bhat et al., 1969; Borole et al., 1977; Martin et al., 1978 a,b; Nikolayev et al., 1979; Maeda and Windom, 1982; Borole et al., 1982).

The behaviour of uranium in the estuarine zone, however, where mixing of these marine and riverine end-members occurs, is not well known. This mixing region is one in which the uranium input in fresh water could be either enhanced, by leaching from particulates, or lowered, by adsorption or flocculation and scavenging. In either case, the finite input from rivers and the constancy of the sea water content call for the removal of uranium from solution in areas on or beyond the continental shelves. Many such sinks have been identified and attempts made to quantify them. They include nearshore carbonate deposits (Sackett and Cook, 1969); organic-rich anoxic sediments, (Veeh, 1967; Mo et al., 1973; Kolodny and Kaplan, 1973) metalliferous ridge-crest deposits (Fisher and Bostrom, 1969; Bertine et al., 1970; Bender et al., 1971; Veeh and Bostrom, 1971; Bloch, 1980) and oceanic basalts (Aumento, 1971; Macdougall, 1977; Bloch, 1980). Minor removal occurs in the pelagic clays and silicious oozes (Cochran, 1982).

The continuous chemical diagenesis within deep-sea sediments can give rise to reducing conditions at depth and there concentrations of uranium in both the solid phase (Bonatti et al., 1971; Boulad and Michard, 1976; Aller and Cochran, 1976) and in pore waters (Baturin and Kochenov, 1973; Boulad/ -

Boulad and Michard, 1976) which are enhanced over the oxic core sections above, have been observed. Diffusion upwards into the overlying sea water may result in a globally significant uranium flux if such sediments cover a sufficiently large area of the sea floor. Most workers, assuming a steady state for uranium, have performed calculations to establish whether or not the various known inputs and outputs indicate a balanced uranium budget and to derive limits for the flux values (Veeh, 1967; Bhat and Krishnaswami, 1969; Ku et al., 1977; Turekian and Cochran, 1978; Mangini et al., 1979; Borole et al., 1982).

Naturally-occurring uranium consists of three isotopes, namely ^{238}U , ^{235}U and ^{234}U , the former two being the primordial parent nuclides of two separate decay series which ultimately yield the stable isotopes ^{206}Pb and ^{207}Pb respectively (Figure 1.1). Little natural fractionation of ^{238}U and ^{235}U has been observed and thus today almost all terrestrial materials contain ^{235}U in constant ratio to ^{238}U i.e. in a $^{238}\text{U}/^{235}\text{U}$ atom ratio of 137.88. [The one notable exception to this generality is at the natural fission reactor environment in Oklo (Gabon), a uraninite deposit where considerably lower ^{235}U contents have been found due to consumption in a natural reactor occurrence some 1.8×10^9 years ago (West, 1976)]. The third isotope of uranium, ^{234}U , is an intermediate daughter in the decay series of ^{238}U and is formed from this precursor by the emission of one α and two β particles (Figure 1.1). At secular equilibrium, therefore, the abundance ratio of $^{234}\text{U}/^{238}\text{U}$ in atomic terms is equal to the corresponding half-life ratio, i.e. ^{234}U comprises only $5.6 \times 10^{-3}\%$ of total natural uranium (Rogers and Adams, 1969). Since chemical fractionation processes for these heavy nuclides might be expected to be negligible in the natural environment, the α - activity ratio of ^{234}U to ^{238}U should equal the secular equilibrium value of 1.00 and that for $^{235}\text{U}/^{238}\text{U}$ or $^{235}\text{U}/^{234}\text{U}$ should be 0.046, as calculated from the equation

$$A = \frac{x}{M} N \frac{0.693}{t_{1/2}} \dots\dots\dots(1.1)$$

Here/

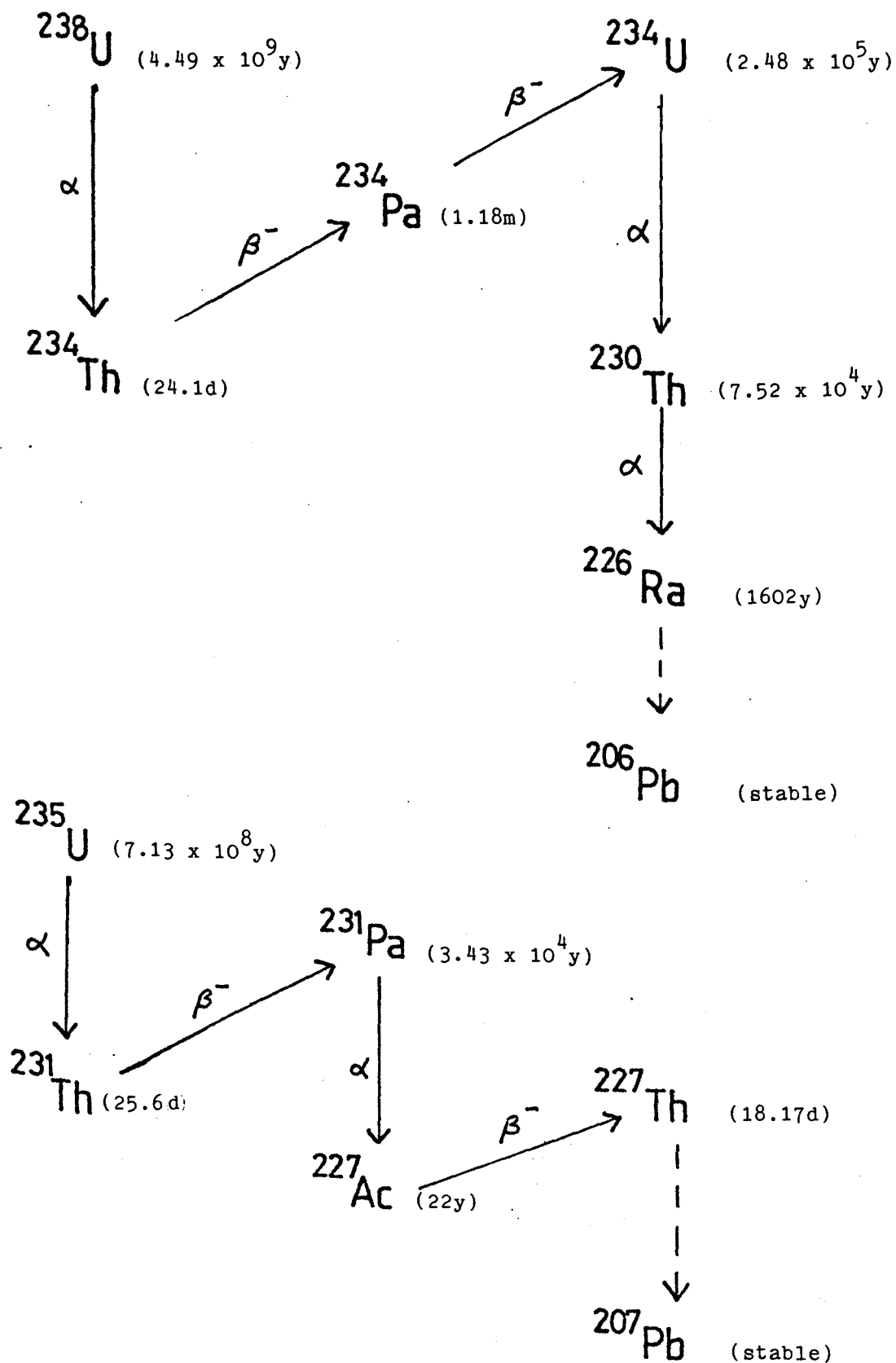


Figure 1.1. Radioactive decay series of ^{238}U and ^{235}U through their first few daughters ($t_{1/2}$ values in parenthesis)

Here, A is the activity in disintegrations per unit time per unit mass of the particular uranium isotope, x is the mass of uranium isotope present and M is its atomic mass, N is Avogadro's constant and $t_{1/2}$ is the half-life of the particular isotope. However, as early as 1955, Cherdynstsev observed large fractionations of the isotopes ^{234}U and ^{238}U in rocks and in their leach solutions (Cherdynstsev et al., 1955), while Thurber (1962) later found $^{234}\text{U}/^{238}\text{U}$ activity ratios greater than 1.00 for ocean water, as inferred from carbonate deposits. It soon became apparent that such uranium disequilibrium was widespread, occurring in most natural waters and sediment samples, with the equilibrium situation being exceptional.

The principal sources of uranium are in continental igneous rocks, particularly the silicic type in which uranium is concentrated relative to ultramafic rock. These contain one or more ferromagnesian minerals with little or no silica indicating that uranium is strongly fractionated from other elements into early-melting, silica-rich phases. Uranium is distributed in the igneous rocks mainly as minor or major components of accessory minerals like zircon and monazite, and by adsorption onto crystal and grain boundaries. Fission-track studies (Hamilton, 1966; Fleischer et al., 1975) have confirmed such distribution patterns. The solubility of uraninite, UO_2 , in distilled water is very low being $<0.01\mu\text{g l}^{-1}$ between pH 2 and 7 (Langmuir, 1978), but increases by several orders of magnitude in oxidising environments due to the formation of the uranyl ion UO_2^{2+} , its solubility being enhanced in the presence of complexing ions (Allard et al., 1984). The important uranyl species between pH 6 and 8 are UO_2OH^+ and $(\text{UO}_2)_3(\text{OH})_5$ when other complexing ions are absent but, even at low concentrations of CO_2 , the mono-, di- and tricarbonates complexes $\text{UO}_2(\text{CO}_3)_n^{2(n-1)-}$ ($n=1,2,3$), are the dominant species (Langmuir, 1978; Allard et al., 1984). Another soluble complex, $\text{UO}_2(\text{HPO}_4)_2^{2-}$, can also be formed between pH 4 and 7.5 at phosphate concentrations as low as 0.1ppm. Humic and/

and fulvic substances can also be responsible for the mobility and deposition of uranium (Halbach et al., 1980) due to the small changes in pH which govern the solubility of the uranium humates and fulvates. If dissolved phosphate concentrations are low, complexation by such organic compounds may reduce the uranyl ion to the uranous state due to the decreasing redox potential associated with the oxidation of organic matter in early diagenesis (Froelich et al., 1979). This ability of uranium to undergo inorganic/organic dissolution and reprecipitation is probably the most important natural process to cause disequilibrium between ^{234}U and ^{238}U (Gascoyne, 1982). In conjunction with this, however, various physico-chemical processes have been proposed to explain the small excesses of ^{234}U and some of these postulated mechanisms have been substantiated by laboratory experiments. Osmond and Cowart (1976) classified the various radiogenic fractionation processes which favour the preferential removal from minerals of the uranium daughter. These were (i) direct transfer of ^{234}U into solution by α -recoil across the solid/liquid phase boundary, (ii) increased vulnerability to leaching of α -recoiled ^{234}U arising from bond breakage and lattice disruption, the daughter atom ending up in an unstable location, and (iii) oxidation of ^{234}U by removal of orbital electrons during α decay of ^{238}U or during β decay of the intermediate nuclides ^{234}Th and ^{234}Pa , ultimately forming $^{234}\text{U}^{6+}$, or oxidation due to the change in energy levels between the original ^{238}U atom site and the dislocated site occupied by its α decay product. The uranyl ion so produced is more soluble than its uranous predecessor. Process (i) was demonstrated by Kigoshi (1971), who showed that there was a time-related increase of ^{234}Th in the aqueous phase of a suspension of zircon powder (360ppm uranium), and by Fleischer and Raabe (1978), who showed by inducing fission that daughter ^{235}U atoms from a $^{239}\text{PuO}_2$ source were directly embedded in a quartz detector placed 0.5mm distance away. Fleischer (1980) has also indicated that, in addition to direct recoil ejection into the surrounding liquid (process (iii)), a second mechanism of ^{234}U displacement results when recoiled nuclei become embedded in adjacent grains producing α -recoil tracks which are subsequently etched/

etched by natural solutions and release some of the recoil nuclei.

The outcome of all or some of the above fractionation processes is to produce natural waters whose $^{234}\text{U}/^{238}\text{U}$ α -activity ratio (A.R.) is >1.00 . This is more readily seen in groundwaters and aquifers (Osmond and Cowart, 1976; Asikainen, 1981; Osmond and Cowart, 1982) where minerals and waters are intimately mixed. Here, surface areas, porosity and water residence times have large values and the physico-chemical fractionation processes have enhanced opportunities to operate and manifest themselves. Groundwater samples with A.R. values of greater than 30 have been analysed (Osmond and Cowart, 1982) with a general inverse correlation between the A.R. in groundwaters and uranium concentration being found. The latter observation is explained firstly by the loss of uranium from solution to mineral surfaces in the aquifer when reducing conditions are prevalent and secondly by subsequent α -recoil of some surface-adsorbed ^{234}Th to increase the solution $^{234}\text{U}/^{238}\text{U}$ A.R. Just as the aqueous phases take on an A.R. >1.00 , the accompanying solid phases have a resultant A.R. of <1.00 . The weathering of continental rocks to produce soils results in loss of ^{234}U relative to ^{238}U and yields typical A.R. values of ~ 0.9 in soils and ~ 1.3 in runoff waters (Sackett and Cook, 1969). On erosion, soils can adsorb dissolved uranium from runoff with A.R. >1.00 and topsoils of high organic content can show a progressive increase in A.R. from ~ 0.9 to ~ 0.95 or greater (Rosholt et al., 1966). Sackett and Cook (1969) showed high uranium concentrations (5 to 8 ppm) and high A.R. values (1.04 to 1.18) in sediments from the Pettaquamscutt river and postulated that these values might be attributable to the reduction of dissolved U^{6+} to U^{4+} and its uptake into the sediment. By extracting only the surface-adsorbed uranium from sediment particles, using an ammonium carbonate leach, Joshi and Ganguly (1976) found that the A.R. values of these leachates were in the range 1.12 to 1.14, the same as in overlying waters. This finding was shown to be consistent with an adsorption of uranium from the water. This adsorption could be due either to the presence of organic carbon itself or to the uranium reduction in the low Eh conditions commonly associated with it. In contrast, near-equilibrium activities were found in the leached residues.

In/

In rivers, there is a large variability of uranium concentrations, from $0.02 \mu\text{g l}^{-1}$ for the Amazon (Bertine et al., 1970) to $6.6 \mu\text{g l}^{-1}$ for the Ganges (Bhat and Krishnaswami, 1969). The average A.R. values which are generally accepted as being representative of rivers are between 1.20 and 1.30 (although values as high as 2.03 ± 0.08 have been found (Scott, 1982)), these values again reflecting the frequent disequilibrium situation. The higher uranium concentrations found in some rivers have occasionally been partly attributed to anthropogenic activity, particularly to the uranium present in phosphate fertilisers (Spalding and Sackett, 1972), but other rivers with catchment areas of low fertilisation can also show relatively high uranium values (Bhat and Krishnaswami, 1969), contradicting this pollution effect. Furthermore, no definite uranium - phosphate relationship in rivers of cultivated, industrial areas has been found. Mangini et al., (1979) calculated that less than 0.01% of the phosphate from applied fertilisers passes into ground or river waters in a well-fertilised German farming area, the vast majority being retained in the uppermost soil layers. If uranium transport was similar to that for phosphate, then the uranium contamination would amount to less than $0.004 \mu\text{g l}^{-1}$. Mangini et al., (1979) did find that the ground water uranium content was well correlated with HCO_3^- content. This resemblance reflects the dominance in natural waters of the highly soluble anionic uranyl carbonate complexes (Langmuir, 1978). Thus Mangini et al., (1979) suggested that the uranium concentration in surface waters depends on the HCO_3^- concentration in river water and that high HCO_3^- values, rather than fertiliser contamination, is the cause of the high uranium contents sometimes observed. Positive correlations between uranium content and total dissolved solids (T.D.S.) (Bhat and Krishnaswami, 1969; Turekian and Chan, 1971) and the sum of major cations (Borole et al., 1982) have also been found, indicating that the uranium content in rivers is primarily dependent upon the intensity of weathering (Turekian and Cochran, 1978)./

1978). This mutual correlation of HCO_3^- and T.D.S., however, was considered by Scott (1982) to be inevitable since HCO_3^- is the major anion present in most river waters and is therefore expected to correlate with T.D.S. by the constraints of charge balance. The pollutant effect of phosphate fertilisers was studied in detail in the Charente estuary which receives large releases from a phosphate processing plant (Martin et al., 1978a). This effluent, enriched in uranium, increased the soluble uranium concentration in the river from 0.4 ugl^{-1} to 2.0 ugl^{-1} at chlorinities of $\leq 0.03^{\circ}/\text{oo}$, and both uranium and phosphate removal during estuarine mixing was observed. In this case, then, an estuary is acting as a sink for soluble uranium. Most other studies on unpolluted estuaries, however, show that uranium behaves more or less conservatively during mixing (Borole et al., 1977; Martin et al., 1978a; Martin et al., 1978b; Borole et al., 1982; Maeda and Windom, 1982). although at low salinities ($< 10^{\circ}/\text{oo}$) some evidence of uranium removal has been indicated (Borole et al., 1982; Maeda and Windom, 1982). As pointed out by Scott (1982), the quantities of uranium adsorbed on to particulates must be negligible and should make no appreciable difference to the mean riverine uranium input values currently being used for mass balance purposes. The inputs of the stably-dissolved uranium isotopes from rivers to the ocean summate to fluxes which can be determined from estimates of average uranium concentrations in river waters if conservative estuarine behaviour is assumed. Mangini et al., (1979) and Borole et al., (1982) have both calculated a mean riverine uranium concentration of 0.3 ugl^{-1} using different approaches and indicated that the A.R. of river waters should be about 1.2. In a steady-state geochemical mass balance model incorporating a ^{234}U diffusional input of $0.3 \text{ dpm cm}^{-2} \text{ kyr}^{-1}$ from marine sediments, Ku et al., (1977) placed limits on the values of the uranium content and A.R. in river waters using the observed inputs of ^{234}U and ^{238}U and their open ocean values. A range of 0.1 to 0.3 ugl^{-1} for the riverine uranium/

uranium content resulted, with an A.R. of between 1.2 and 1.3. Neglecting the ^{234}U input from sediments yields higher values, for both parameters, of 0.5 ug l^{-1} and 1.3 respectively (Osmond and Cowart, 1976a).

Uranium, however, is transported to the sea not just in surface runoff water and dissolved in groundwater but also in water - transported detrital sediments. The amount transported in surface water is much greater than that in groundwaters and the latter source may be neglected, but the uranium transported by solids is about 5 times that carried in the dissolved state (Osmond and Cowart, 1976a). Rapid deposition of most of this material to sediments on the continental shelf region leads to low particulate concentrations in the sea (average $\sim 100 \text{ ug l}^{-1}$, Chester and Aston, 1976) resulting in the observation (Baturin, 1973; Ku et al., 1977) that $>99.7\%$ of the uranium in sea water is dissolved. The river supply of about $1 \text{ to } 2 \times 10^{10} \text{ g U yr}^{-1}$ to the ocean (Mangini et al., 1979; Bloch, 1980; Borole et al., 1982; Cochran, 1982) can be used to calculate the mean residence time of uranium in the oceans. For a mean uranium concentration of $3.35 \pm 0.20 \text{ ug l}^{-1}$ (Ku et al., 1977) and assuming an ocean volume of $1.37 \times 10^{21} \text{ l}$, the total amount of uranium in the oceans is $(4.59 \pm 0.27) \times 10^{15} \text{ g}$, which, together with the above river supply rate of uranium, yields a residence time of about $2.3 \text{ to } 4.6 \times 10^5 \text{ yrs}$. If the uranium concentration of sea water is to be maintained at a constant value, then the uranium output or removal must balance its input over a period of several of these residence times, under steady-state conditions. Thus, if the area of the world ocean is taken as $3.6 \times 10^{18} \text{ cm}^2$ (Turekian, 1967), a mean uranium deposition rate of $3 \text{ to } 6 \text{ ug cm}^{-2} \text{ kyr}^{-1}$ is required to balance the $1 \text{ to } 2 \times 10^{10} \text{ g yr}^{-1}$ input. A review of the contribution to such a uranium removal rate from various widespread and localised sites has been given in a detailed account by Cochran (1982). It should be realised that the sinks discussed are/

are equally applicable to ^{234}U as to ^{238}U . By far the most significant uranium sink was claimed by Bloch (1980) to be the uptake of uranium by the low temperature weathering of oceanic basalts. A basalt thickness of 1000m was shown to be capable of removing about $1.2 \times 10^{10} \text{ gUyr}^{-1}$, more than 60% of the input value. Removal into the carbonate sediments of the continental shelf and into the anaerobic sediments of the continental shelf and slope, in fjords and anoxic basins, due either to the formation of the relatively insoluble U^{4+} or the adsorption or complexing of uranium with organic matter, has been demonstrated by Veeh (1967), Sackett and Cook (1969), Kolodny and Kaplan (1973) and Mo et al., (1973). A recent uranium oxidation state study (Anderson, 1984) in the Cariaco Trench, an anoxic marine basin with significant concentrations of H_2S , has revealed the virtual absence of U^{4+} thus favouring the adsorption/complexation mechanism for uranium uptake into anaerobic sediments. Veeh et al., (1974) have shown that the organic-rich sediments off South-west Africa, with their high uranium-containing phosphorites, represent an average uranium accumulation rate of $500 \text{ ug cm}^{-2} \text{ kyr}^{-1}$. This value may be locally significant but, as the region constitutes only about 0.01% of the world ocean, the scavenging mechanism does not necessarily represent a globally-important uranium sink. Metalliferous ridge-crest sediments can account for the removal of about $1.4 \times 10^9 \text{ gUyr}^{-1}$ (Bloch, 1980), a value derived from an estimated hydrothermal iron supply rate and an average Fe/U ratio for metalliferous sediments. This flux represents a removal of less than 7% of the input by rivers. Ridge-crest deposits have a $^{234}\text{U}/^{238}\text{U}$ ratio characteristic of sea water (Veeh and Bostrom, 1971), consistent with their incorporation of uranium from sea water by adsorption on to, or coprecipitation with, Fe-Mn oxides. The possible importance of hydrothermal circulation at these ridge crests to the uptake of uranium was highlighted by Cochran (1982) using the evidence of Edmond et al., (1979) that water debouching from hot springs from one such spreading centre is depleted in uranium. Uranium concentrations of up to 500ppm have/

have been found in ridge crest sediments (Lalou and Brichet, 1980). Further work is required, however, to confirm the magnitude of the effect (possible removal of up to 50% of the uranium flux from rivers). Deep-sea clays and silicious oozes play only a minor role in the removal of uranium, being responsible for the uptake of only about $0.04 \text{ ugcm}^{-2} \text{ kyr}^{-1}$ (Krishnaswami, 1976) i.e. about 1% (Cochran, 1982), and $< 2\%$ (Bloch, 1980) of the river uranium input respectively.

1.2 Deep Sea and Nearshore Pore Waters

The pore waters, or interstitial waters, of sediments are the aqueous solutions which occupy the pore spaces between the sedimentary particles or grains which constitute the solid phase. These pore waters represent the most important migration medium for the recycling of diagenetically-produced chemical constituents through the sediments, mainly by slow molecular diffusion. Since the mass ratio of solid to liquid in the sediments is high, chemical changes which may be undetectable in the solid phases can give rise to large signals in the pore waters and so these solutions act as the most sensitive indicators of chemical reactions within the sediments. Thus, by profiling the pore water concentrations of natural constituents with depth in the sediment column, estimates of diffusion can be obtained, and the kinetics and mechanisms of chemical reactions occurring within the sediment can be elucidated. Alteration of the concentrations of pore water constituents by chemical reaction or by complexing with organic or inorganic ligands, can lead to gradients and fluxes of constituents upwards to or downwards from the sediment/sea water interface, factors which can influence the overall geochemical balance within the oceans. The nature and extent of postdepositional changes are most fundamentally determined by the redox potential of the sediment, which in turn depends primarily on the presence of free oxygen or on the amount and type of organic matter present. Other electron acceptors present are either thermodynamically (Froelich et al., 1979) or kinetically (Muller and Mangini, 1980) less favoured. The chemical species determining the actual redox potential are not well-defined, the problems involved in its operational measurements being numerous (Berner, 1971). Eh, as understood in the thermodynamic sense, is usually not directly measurable because many of the species which are involved in important sedimentary redox/

redox reactions (SO_4^{2-} , N_2 , NO_3^- , NH_4^+ , HCO_3^- , CH_4) are not electroactive, i.e. they do not readily accept or donate electrons at the surface of the Pt or Au electrodes used. Most oxidation-reduction reactions in natural waters, which are in a highly dynamic rather than near-equilibrium state, also have a tendency to be much slower than acid-base reactions. Meaningful Eh results are obtained only if reversibly reacting components are present in sufficient concentration and if exchange processes at the electrode surface take place rapidly enough. However, Stumm and Morgan (1981) have discussed extensively the interpretation of measured potentials and the usefulness of pE - pH diagrams, and the Nernst equation, while Whitfield (1974) has discussed some limitations of redox measurements due to coatings on the Pt surface. In any case, it is known that gradual oxidation of deposited organic matter results in the establishment of reducing conditions at depth in a sediment. Since both the amount of organic matter deposited and its rate of burial (sedimentation rate) is greater nearer the continents, on the shelf region, there exists an inverse correlation between the organic carbon content of the surface sediment and the thickness of the oxic zone (Lynn and Bonatti, 1965). This oxic zone thickness can be inferred from a distinct colour change in the sediment core from red/brown to green/grey (depending on lithology), a transition which has been shown to be a marker of the Fe(III) - Fe(II) redox boundary (Lyle, 1983).

It is generally assumed that organic carbon is oxidised continuously in a sediment by a sequence of energy-yielding reactions in which the energy produced per mole of organic matter oxidised decreases. The simplest model of this organic diagenesis assumes that marine organic matter has Redfield composition (Redfield, 1958), i.e. $(\text{CH}_2\text{O})_{106}(\text{NH}_3)_{16}(\text{H}_3\text{PO}_4)$, with the oxidants being utilised to depletion before further oxidation by the next most efficient (free-energy producing) process (Froelich et al., 1979; Stumm/

Stumm and Morgan, 1981). In a closed system, in which the reductant (organic matter) supplies electrons firstly to the lowest unoccupied energy level of the oxidant, the sequence of reactions (Froelich et al., 1979) is utilisation of oxygen in the oxic environment, manganese, iron and nitrate in suboxic environments, and sulphate in anoxic environments. Anaerobic fermentation of organic matter may also occur in a strongly-reducing anoxic environment giving rise to a methanic environment (Berner, 1981). The latter is not too important, however, at the shallow depths reached by corers in the deep sea. The order of nitrate and MnO_2 reduction depends on the stoichiometry of the nitrate reduction reaction (denitrification), the products formed (N_2 alone or N_2 plus NH_3) and also on the MnO_2 phase being reduced. There will usually be overlap, therefore, between the nitrate and manganese reduction zones. These early interpretations are mechanistic and qualitative and are consistent with the shapes of pore water profiles. Further information on the rates of particular reactions is required (Jahnke et al., 1982) to evaluate the magnitude of elemental sinks within the sediments and to estimate concentration gradients near the sediment/water interface. Figure 1.2 shows a schematic representation of the changes in concentration of some of the major redox indicators in pore waters (after Froelich et al., 1979). Sawlan and Murray (1983) have shown that the changes occurring in trace metal diagenesis, in a transect from oxic pelagic red clays through suboxic terrigenous hemipelagic sediments to highly-reducing shelf sediments, is essentially due to the oxidation of organic matter during early diagenesis. For the pore waters studied, Sawlan and Murray (1983) found that manganese and iron were below detection in the oxic red clay sediments where only aerobic respiration was occurring. In the reducing hemipelagic sediments, however, denitification was occurring and manganese and iron reduction to the Mn^{2+} and Fe^{2+} species led to their solubilisation and remobilisation. Stations at which nitrate was being consumed within the top 10 - 15 cm of the core had interstitial manganese gradients which extended closest to the sediment/bottom water interface. In the highly-reducing shelf sediments, sulphate reduction/

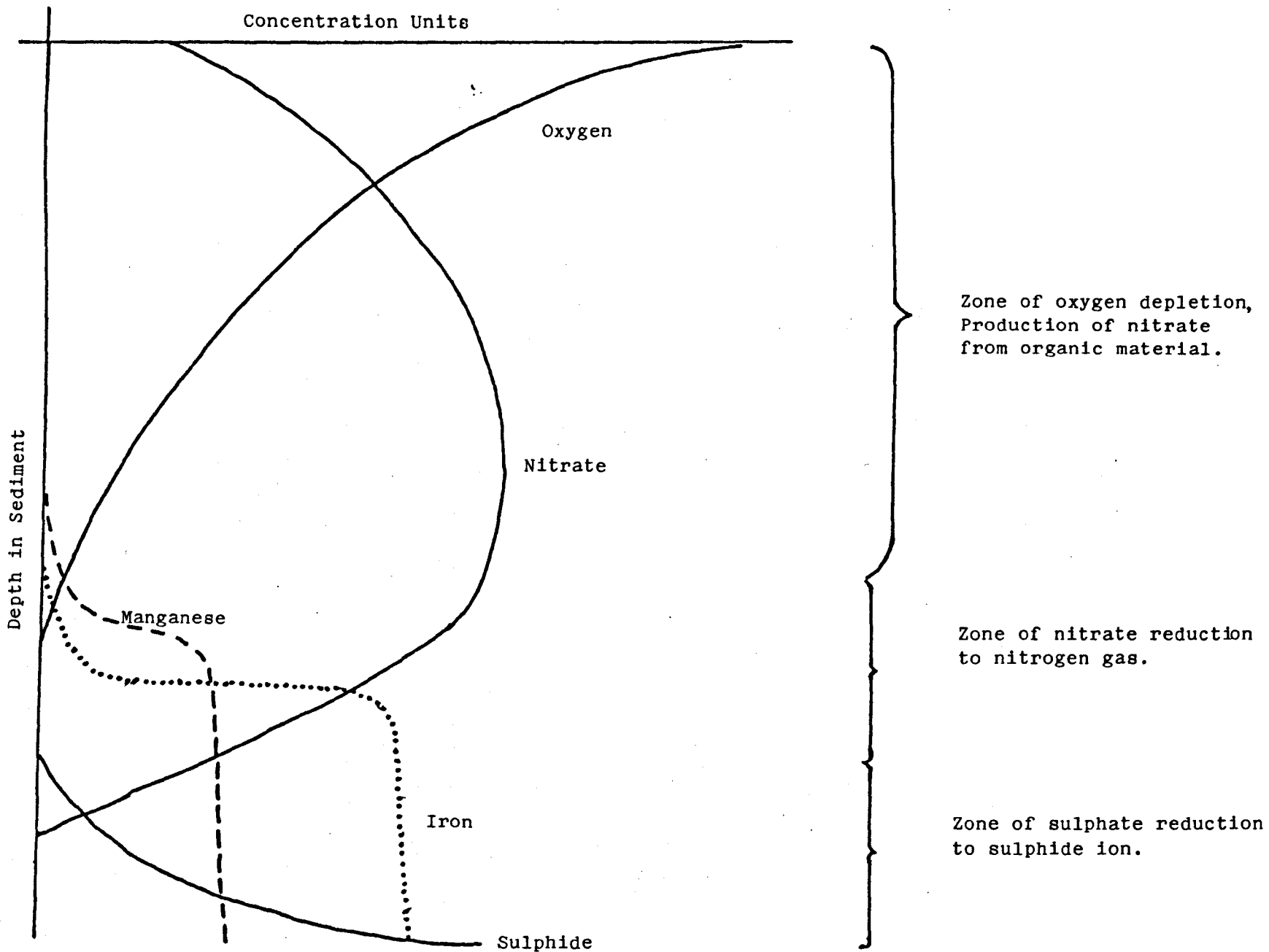


Figure 1.2. Idealised schematic representation of the changes in concentration of some major redox indicators in pore waters. (Arbitrary scales)

reduction was indicated from the high alkalinity values (5 - 14 meqkg⁻¹) reached at depth in contrast to the idealised values of open ocean waters (2.2 to 2.3 meqkg⁻¹ (Broecker and Peng, 1982)). Nitrate was totally consumed in all shelf sediments and high dissolved manganese levels were measured even at the top 0-2cm sampling interval, while the surficial manganese oxidation zone characteristic of the hemipelagic sediments was either confined to a thin layer at the core top or was absent altogether.

Diffusive fluxes across the sediment/sea water interface have been observed both in the deep sea and in nearshore environments for some of the major and trace constituents of sea water, these arising from diagenetic changes in pore water concentrations. Such fluxes have been illustrated for silica (Fanning and Pilson, 1974), trace metals (Elderfield and Hepworth, 1975; Eaton, 1979; Balzer, 1982; Klinkhammer et al., 1982; Sawlan and Murray, 1983) and major elements (Sayles, 1979; Sayles, 1981).

In addition to the aforementioned sediment-water exchange of major and trace metals and nutrients, it has been recognised for a longer time that the naturally-occurring radioactive tracers ²²⁶Ra, ²²⁸Ra and ²²²Rn have distribution patterns in sea water that are consistent with their diffusion from sediments. Support for this idea came from the work of Koczy (1958) who found an increase with depth in the ²²⁶Ra concentration and proposed this isotope as a useful tracer for mixing studies. Such tracer studies have been carried out for ²²⁶Ra (Chung and Craig, 1980), ²²⁸Ra (Moore, 1969) and ²²²Rn (Broecker et al., 1968). In the East Equatorial and North-east Pacific, the ²²⁶Ra increase in the near-bottom waters (Chung et al., 1974; Chung, 1974) reflects a strong input from the sediments, with the flux varying as a function of sediment type. A two orders of magnitude flux variation for ²²⁶Ra, 0.0015 dpm cm⁻² yr⁻¹ (Atlantic) to 0.21 dpm cm⁻² yr⁻¹ (N. Equatorial Pacific) was found by Cochran (1980) using ²²⁶Ra/²³⁰Th disequilibrium patterns in cores, showing a non-linear inverse correlation with the sedimentation rate. If the sedimentation rate is high, then ²²⁶Ra and ²³⁰Th penetrate to greater depths and the radium therefore has a longer path length out/

out of the sediment. Somayajulu and Church (1973) and, more recently, Cochran and Krishnaswami (1980) have produced pore water ^{226}Ra measurements which show that concentrations of up to $14.19 \text{ dpm kg}^{-1}$, a factor of 35 greater than typical bottom-water levels, can be present, a situation which would certainly result in a sediment to sea water flux. Indeed, there is little doubt that ^{226}Ra diffuses upwards, since only about 1% of the ^{226}Ra present in sea water is produced from the parent ^{230}Th . The marked vertical ^{226}Ra gradient in most of the ocean regions studied was interpreted as indicating this isotopes release from interstitial waters in accord with the considerable mobility of Ra^{2+} in chloride containing waters (Levinson et al., 1982), a mobilisation thought to be enhanced by α -recoil on production by decay of its immediate, surface-adsorbed parent, ^{230}Th . This recoil may directly transfer the atom from the sediment solid phase to the aqueous phase (pore water) (Kigoshi, 1971) or render it more susceptible to leaching from its radiation - damaged lattice position (Fleischer and Raabe, 1978).

Decreases in the concentration of ^{228}Ra with height above the sediment/water interface was observed by Sarmiento et al., (1976), a feature analogous to ^{226}Ra , but since its half-life is much shorter (5.75 yrs), its concentration decreases more rapidly to equilibrium with its parent ^{232}Th , which is essentially zero in sea water. Again, both the pore water studies by Somayajulu and Church (1973) and Cochran and Krishnaswami (1980) showed that the ^{228}Ra in the pore water was enriched relative to bottom water. Reported results (Broecker, 1965; Key et al., 1979) indicate that pore water ^{222}Rn concentrations are high (10^2 to 10^4 dpm kg^{-1}) relative to those of ^{226}Ra . This daughter/parent fractionation arises because the α -recoiled ^{222}Rn , not being chemically reactive, is not subjected to the removal processes undergone by ^{226}Ra such as adsorption onto minerals and particles. The ^{222}Rn is then free to diffuse into bottom waters where it produces high $^{222}\text{Rn}/^{226}\text{Ra}$ ratios and mixes vertically in the water/

10.

water column residing there an average of 5.5 days before undergoing radiodecay ($t_{1/2} = 3.824$ days). A near-exponential decrease in ^{222}Rn activity with distance from the seafloor has been shown by Sarmiento et al., (1976).

As far as uranium is concerned, there is a scarcity of reliable data on its pore water concentrations and behaviour, a situation which is attributable to the difficulties involved in sampling, from different sediment depths, the volumes necessary (hundred of ml) for accurate uranium analysis by

α -spectrometry. Indeed it is the ability of fission track analysis to enable uranium analysis of small (≤ 0.1 ml) samples which provided the stimulus for the detailed study here.

Furthermore, it will be shown later (section 3.2) that it is preferable to obtain uranium data from the relatively smaller volumes sampled by an in-situ pore water sampler rather than squeezed core samples.

The earliest studies, by Baturin (1971) and Baturin and Kochenov (1973) on squeezed pore waters from the Atlantic and Pacific oceans and the Black Sea gave an overall range of 1.3 to $650 \text{ ug l}^{-1} \text{ U}$, using a chemical luminescence method. In sediments of different type, the ranges were 1.3 to $650 \text{ ug l}^{-1} \text{ U}$ for the diatomaceous oozes from the Atlantic shelf, 3 to 190 ug l^{-1} for the terrigenous and calcareous oozes from the S.E. Atlantic continental slope, 1.3 to 65 ug l^{-1} for the deep-water Atlantic oozes, 2 - 13 ug l^{-1} for deep water Pacific clays and 2 - 65 ug l^{-1} for Black Sea sediments, indicating that, on average, the uranium contents of interstitial waters are much higher than the typical ocean water value of 3.3 ug l^{-1} (Ku et al., 1977). The authors claimed that the uranium content of the interstitial waters was controlled by the parameters Eh, pH and the U and organic carbon contents of the sediment. The high pore water U contents in the continental shelf pore waters corresponded to very high levels of dissolved organic matter (DOM), an observation which may indicate that part of the enhanced uranium in the pore waters is associated/

associated with some form of DOM, such as colloidal organic matter of fulvic acid type. Kolodny and Kaplan (1973), in their studies on pore water uranium in sediments from an anoxic fjord in the Saanich Inlet, found a range of $4.5 - 120 \text{ ug l}^{-1}$ and illustrated that the amount of uranium dissolved in the pore waters appeared to be a function of (a) the amount of organic matter present in the sediment and (b) the state of reduction of the solid-phase uranium. The authors reasoned that, since the $\text{NH}_2\text{OH.HCl}$ and H_2O_2 - leached authigenic fractions of the sediment had a similar $^{234}\text{U}/^{238}\text{U}$ activity ratio to the interstitial waters themselves, then the uranium concentrations and activity ratios in these waters were a result of their interaction with the co-existing solid phases. If this is the case, and if the solid phase in equilibrium with the interstitial water is a simple U (VI) oxide, then the amount of uranium passing into solution should be a strong function of dissolved CO_2 in the water, a situation expected due to the well-known stability of uranyl-carbonate complexes (Langmuir, 1978). If, on the other hand, the solid phase is a U (IV) compound then the amount of dissolved uranium may strongly depend on the redox potential of the local environment, especially if the Eh is close to that required for U (IV) oxidation to U (VI). From a leaching experiment with Na_2CO_3 and NaOH, on one sample, the authors tentatively proposed that more than half of the authigenic uranium in the studied sediment was associated with organic matter, 50% of which was probably complexed as humates. It was also suggested that since only a small proportion (mean of 24.4%) of the total uranium in the sediment was removed in the first fraction ($\text{NH}_2\text{OH.HCl}$ leach), then it was complexed by organic matter, rather than just adsorbed by it. This suggestion is in accord with the good uranium-organic carbon content correlation found ($r = 0.9$). A possibility not considered by Kolodny and Kaplan (1973) was the increase in phosphate ions expected in the pore waters at the low Eh values encountered, which could compete with carbonate in complexing uranium. In a study/

study of the geochemistry of uranium in the Black Sea, further interstitial uranium data were obtained by Zhorov et al., (1982) using adsorption-colorimetry. Uranium concentrations in squeezed pore waters varied by more than an order of magnitude, from 3.1 to 70 ugl^{-1} as compared with the mean bottom water value of 1.9 ugl^{-1} . The higher uranium concentrations occurred in interstitial waters in zones of active sulphate reduction which were characterised by elevated values of pH and alkalinity. Lower uranium concentrations were present in zones of weak sulphate reduction (low pH and alkalinity) allegedly due to the favourability of formation of the species UO_2CO_3^0 which dominates in carbonate solutions at pH values between 4.5 and 6.5. Thus the maximum adsorption of the uranium on sediments occurs at a pH corresponding to electrical neutrality and minimum solubility of the species UO_2CO_3^0 , which the authors believe is the complex governing the transfer of uranium from the solution to the solid phase.

Somayajulu and Church (1973) analysed a composite pore water sample consisting of equal volumes of waters squeezed from every 20cm of an Eastern Equatorial Pacific core by moderate hydraulic pressing in a teflon squeezer. The authors assayed uranium in the 800 ml sample by α -spectrometry and found a concentration of 1.9 ugl^{-1} and a $\text{U}^{234}/\text{U}^{238}$ isotope activity ratio of 1.19 ± 0.15 , a value which cannot be distinguished from either the equilibrium value of 1.0 or from the value reported for normal sea water, 1.14 ± 0.02 (Ku et al., 1977). Since large uranium concentration gradients have already been observed for uranium in sediment pore waters (see above), the value of such composite sample results is in question, and the large errors involved in such data highlight the need for improved sampling techniques to provide greater pore water volumes from different sediment depths and/or the development of a more sensitive analytical technique. Reported values for uranium in pore waters/

waters from two southern ocean cores, (Dysart and Osmond, 1975a) using a new method of extraction (silica gel as dehydrating agent) revealed greater values than sea water for a pelagic mud (range 11.9 to 21.6 $\mu\text{g l}^{-1}$) and for a silicious ooze (range 1.0 to 6.8 $\mu\text{g l}^{-1}$). The observed initial decreases with depth in the $^{234}\text{U}/^{238}\text{U}$ activity ratio from about 1.44 ± 0.06 to 1.25 ± 0.06 and from about 1.38 ± 0.06 to 1.04 ± 0.04 respectively, were regarded as inconsistent with simple diffusion of ^{234}U upwards and out of the sediment as proposed by Ku (1965). High thorium concentrations in the pore waters, however, ranging from 40 to 199 $\mu\text{g l}^{-1}$ (Dysart and Osmond, 1975b), were over six orders of magnitude greater than that present in ocean water ($6 \times 10^{-5} \mu\text{g l}^{-1}$, Moore, 1981) and about four orders of magnitude greater than found in other deep-sea sediment pore waters (0 to 0.023 $\mu\text{g l}^{-1}$, Cochran and Krishnaswami, 1980). This discrepancy indicates that their silica-gel dehydration technique may have been subject to some contamination by sedimentary particles. Thorium was not detected in the pore waters from cores taken in the Angolan Basin, S.W. Atlantic by Boulad and Michard (1976). All four box cores exhibited a yellow/brown to grey colour change, evidence of a redox barrier, above which the cores were oxic with $\sim 1\%$ organic carbon and below which they were reduced with $\sim 0.6\%$ organic carbon at 25 cm. Uranium was again more abundant in the reducing zones than in the oxidising zones for both sediments and pore waters. The small (40 to 100 ml) samples analysed by α -spectrometry necessitated long counting times of 100 hours. Pore water uranium ranged from 2.7 to 27 $\mu\text{g l}^{-1}$, again demonstrating that higher values than in sea water are found in reducing sediment pore waters, a situation which has some similarity to manganese and iron (Figure 1.2). The $^{234}\text{U}/^{238}\text{U}$ activity ratios were indistinguishable from sea water due to the large errors, but may have been a little greater near the top of the cores. Boulad and Michard (1976) calculated/

calculated that the uranium in the reducing zone of the cores could theoretically just exist in the 4+ oxidation state, by deducing pE limits from oxidation states of the major elements Fe and Mn. In the top oxic zones, where solid phase MnO_2 was abundant with little dissolved Mn, the pE was estimated as greater than or equal to 8 ($\text{Eh} \approx + 1.012\text{v}$). In the reducing zone where iron was reduced and in equilibrium with solid phases, the pE was of the order of -3.6 ($\text{Eh} \approx - 0.454\text{v}$). The electron activity, pE, and the redox potential, Eh, are related (Stumm and Morgan, 1981) by the equation:

$$\text{pE} = \text{Eh}/2.3 \text{RTF}^{-1} \dots\dots\dots(1.2)$$

where R is the gas constant ($8.314 \text{ J}^\circ\text{K}^{-1} \text{ mol}^{-1}$), T is the absolute temperature ($^\circ\text{K}$) and F is the Faraday constant ($9.649 \times 10^4 \text{ Cmol}^{-1}$). At 25°C , RTF^{-1} equals 0.059 V mol^{-1} and at 4°C equals 0.055 V mol^{-1} . Since direct Eh measurements were not performed on the cores described by Boulad and Michard (1976), only quantitative estimates could be obtained by use of pH-Eh- P_{CO_2} diagrams (Garrels and Christ, 1965) and the expression:

$$\text{pE} = 5.18 - \text{pH} - \log \sum \text{CO}_2 + \frac{1}{2} \log \sum \text{U} \dots\dots(1.3)$$

which governs the redox equilibrium in the pH range 6 to 9 between the species $\text{UO}_2(\text{CO}_3)_2^{2-}$ and UO_2 . Uranyl complexes are far more soluble than uranous species. The dominant species present in solution will depend on the Eh/pH conditions, the concentration and availability of complexing ions and the temperature. The carbonate complexes are the most important with the dicarbonate species being the most stable above pH 5 for $\text{P}_{\text{CO}_2} = 10^{-2} \text{ atm}$ (34 mM). As outlined by Kolodny and Kaplan (1973), the UO_2^0 might be immobilised by adsorption onto sedimentary organic matter at low Eh values, while UO_2^{2+} might be mobilised as $\text{UO}_2(\text{CO}_3)_2^{2-}$ by desorption due to the high dissolved $\sum \text{CO}_2$ values. There is little information available at present regarding the importance of organic/

organic versus inorganic uranyl complexes in natural waters in the pH range 4 to 8 mainly because of the lack of thermodynamic data for the uranyl organics. Equilibria of several U(IV) and U(VI) species in the presence of CO_2 in an aqueous environment and Eh/pH diagrams have been given by Halbach et al., (1980). From one of these diagrams (Figure 1.3), for a solution at 1 bar, a uranium concentration of $0.75 \mu\text{g l}^{-1}$ ($10^{-8.5}$ Molar) and ΣCO_2 of 0.32 mM l^{-1} ($10^{-3.5}$ M), the redox potential for the transition from U(VI) to U(IV) is about -90mV at pH 7.4 with corresponding reaction $\text{UO}_2(\text{s}) + 2 \text{HCO}_3^-(\text{aq}) + 2 \text{H}_2\text{O}(\text{l}) = \text{UO}_2(\text{CO}_3)_2(\text{H}_2\text{O})_2^{2-}(\text{aq}) + 2 \text{H}^+(\text{aq}) + 2 \text{e}^-$. The standard $\text{U}^{4+}/\text{UO}_2^{2+}$ oxidation potential, E^0 , with corrections for uranyl-hydroxy complexing was indicated to be $0.273 \pm 0.005 \text{ V}$ at 25°C (Langmuir, 1978) relative to the earlier value of 0.32 - 0.33V (Hostetler and Garrels, 1962) making U(IV) less stable than U(VI) than had previously been assumed. Langmuir (1978) also indicated that the pentavalent uranium species UO_2^+ had a greater stability field than previously thought, and which may be an important species in reduced water of pH 7. Eh values much lower than -0.090V were achieved in the Angolan Basin core, and Boulad and Michard (1976) therefore proposed that the uranium would be preferentially adsorbed in the reducing zone, which would then give rise to soluble complexes with large organic molecules or to very fine suspensions ($< 0.1 \mu\text{m}$) which would be analysed as dissolved uranium in the filtrate from $0.1 \mu\text{m}$ Millipore filtrations. In a laboratory study on the effect of the parameters Eh, pH, adsorptive hydrous ferric oxide solids and kaolinite mineral on the mobility of uranium (Giblin et al., 1981), it was found, using 70 mg l^{-1} uranium solutions which are many orders of magnitude greater than encountered in natural systems, that measured levels of mobile uranium were sometimes greater than those calculated from the predicted concentrations of the equilibrium/

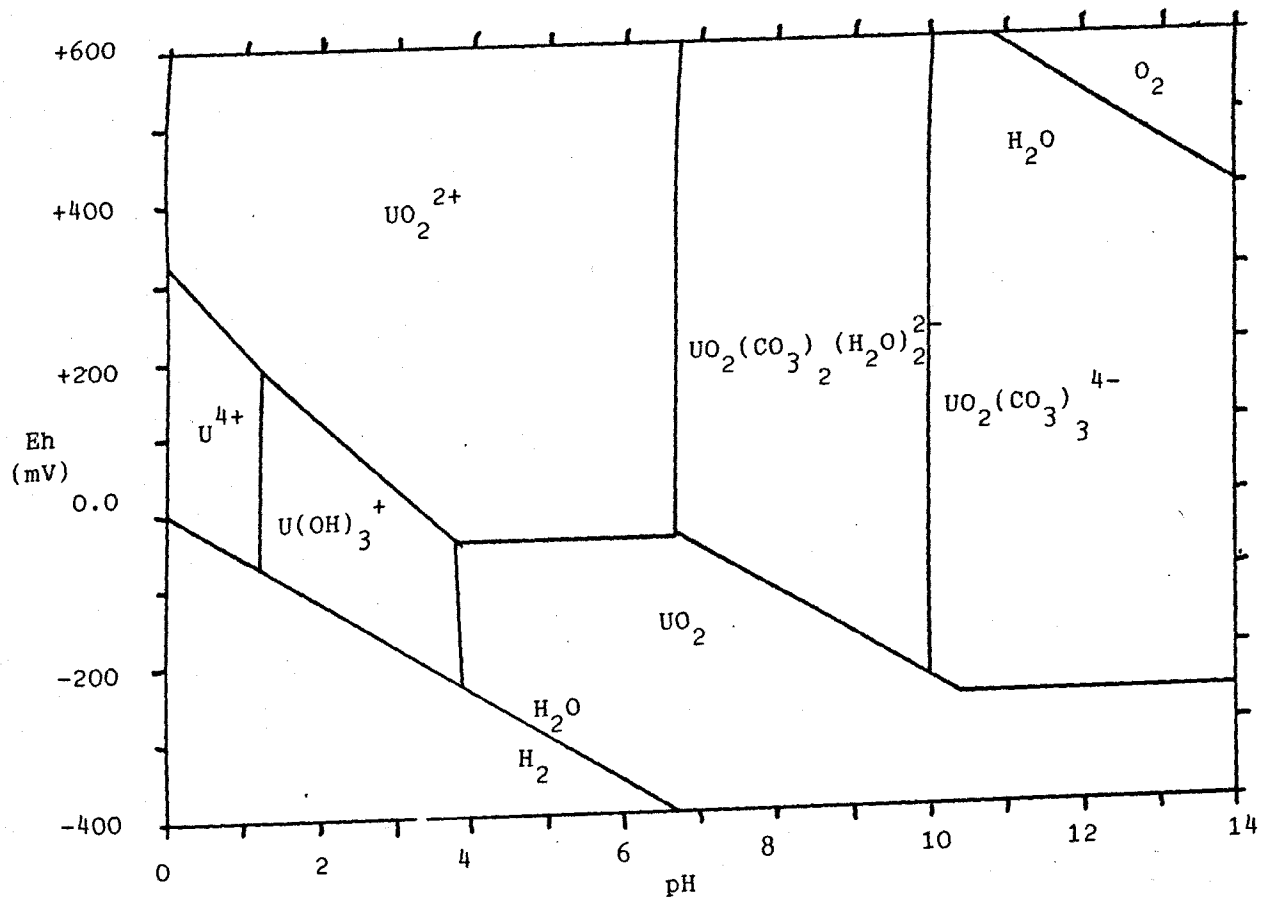


Figure 1.3. Eh-pH diagram of uranium species in the presence of CO₂.
 (T=298K, P= 1bar, U=0.75ugl⁻¹, ΣCO₂ = 0.32mM)

equilibrium species UO_2^{2+} , UO_2OH^+ , U^{4+} , UO_2 and $\text{UO}_2(\text{OH})_2 \cdot \text{H}_2\text{O}$ at specific Eh-pH points. The formation of uranium oxides as mobile colloids (adsorbed on hydrous ferric oxide) in zones where UO_2 is the thermodynamically-stable species can be explained in terms of changes in particle surface charge. The zero point charge (ZPC) of hydrous ferric oxide occurs at around pH 8, below which its surface is positively charged and onto which positively-charged uranium species such as UO_2^{2+} would not adsorb. The presence of CO_2 greatly enhanced this uranium mobility due to the formation of UO_2CO_3^0 , $\text{UO}_2(\text{CO}_3)_2^{2-}$ and $\text{UO}_2(\text{CO}_3)_3^{4-}$ above pH 5, species which, as their negative charge increases, could be more effectively adsorbed by residual bond and electrostatic processes onto hydrous ferric oxide, until uranium mobility decreased at pH 8 and high Eh, where $\text{UO}_2(\text{CO}_3)_3^{4-}$ begins to predominate. It is clear from this laboratory simulation, however, that whatever colloidal or insoluble species are postulated to exist in certain Eh-pH domains, thermodynamic equilibrium models which describe closed systems do not give a complete representation of mobile and immobile uranium in real, open systems which contain large and varied amounts of other inorganic and organic species. These species result in the occurrence of more subtle reactions, giving rise to less abrupt changes in mobility with changes in Eh and pH.

Analyses of 4 core-top waters by Ku et al., (1977) have indicated that the 'pore water component' might have a uranium concentration lower than sea water, while analysis of two pore water samples from a metalliferous ooze showed a possible 10% enrichment over sea water, with values 3.61 ± 0.11 and $3.68 \pm 0.16 \text{ ug l}^{-1}$. The mean of the six analyses was $3.44 \pm 0.25 \text{ ug l}^{-1}$ and as such did not supply definite evidence of a concentration gradient across the sea water/sediment interface. The $^{234}\text{U}/^{238}\text{U}$ activity ratios too, because of the small sample volumes and large counting errors, were not distinguishable from that in sea water, averaging 1.17 ± 0.07 . Much earlier it had been suggested (Ku, 1965) that, based on the deficiency of ^{234}U relative to ^{238}U in deep-sea sediments, ^{234}U was being mobilised by α -recoil from the solid phase into the pore water and was diffusing/

diffusing out of the sediment column at a rate estimated at $0.3 \text{ dpm cm}^{-2} \text{ kyr}^{-1}$. This would show up as a downward-increasing $^{234}\text{U}/^{238}\text{U}$ activity ratio in the pore waters. The precise pore water uranium data obtained by Cochran and Krishnaswami (1980) as a result of combining from successive depths, 500-1000 ml samples from large (50 x 50 x 40cm) box cores, did indeed indicate an enrichment of recoil-produced ^{234}U over ^{238}U in the pore water, with higher ratios (1.17 ± 0.02 to 1.23 ± 0.03 , mean 1.22 ± 0.11) relative to sea water occurring at depths greater than 20cm. The total uranium concentration in the pore waters was relatively constant (mean $2.54 \pm 0.31 \text{ ug kg}^{-1}$) and indicated a ^{238}U depletion of between 11.8% to 30.3% compared with sea water values. The authors took this to imply that these Pacific sediments were acting as a sink for uranium, which diffused into them from overlying sea water, but since all total uranium analyses were performed on samples from depths greater than 10cm, no reasonable uranium flux calculation could be attempted.

In the foregoing discussion, it can be appreciated that a major difficulty arising from the study of pore water chemistry and diagenesis is the perturbations of the physico-chemical pore water system which occur as a result of the sampling and handling procedures employed. The aim of any pore water sampling system, if reliable compositional data are to be acquired, must be to provide samples which are chemically representative of 'in-situ' pore waters, a requirement which calls for an awareness of the errors which can arise due to oxygen contact and temperature and pressure artefacts. Studies have shown that warming of marine sediments prior to pore water extraction can give rise to enrichments of potassium (Mangelsdorf et al., 1969; Bischoff et al., 1970) and silica (Fanning and Pilson, 1971), and depletions in manganese and calcium (Bischoff et al., 1970). These differences are the result of changes/

changes in the ion-exchange selectivity of the sediment as a function of temperature, and so to overcome this effect, sediment must be treated at 'in-situ' temperatures. Any exposure of anoxic marine or estuarine sediments to the atmosphere during sampling and handling of the core can lead to decreased values of ferrous iron, reactive phosphate and silica (Bray et al., 1973; Troup et al., 1974; Loder et al., 1978; Lyons et al., 1979). This was shown from analyses of duplicate samples, manipulated both in air and under N_2 , where the concentrations of Fe (II) and PO_4^{3-} for the air samples were less than those in the unexposed samples, indicating the importance of protecting against oxidation. Small quantities of oxygen present in the filters and trapped in the squeezer units oxidise ferrous to ferric iron. The Fe(III) produced removes inorganic phosphate and silicate from solution either by precipitating PO_4^{3-} as iron phosphate, or by scavenging PO_4^{3-} and SiO_4^{4-} on hydrous ferric oxide by sorption. It is essential also to minimise the storage time of the core prior to squeezing (Bischoff and Ku, 1971) in order to minimise reductions in Ca^{2+} and Fe^{2+} contents of the pore waters. Pressure effects on pore waters have recently been documented (Murray et al., 1980; Emerson et al., 1982; Froelich et al., 1983), and are due to the well-known pressure-dependence of the equilibrium constants in the carbonate system. Thus, when a sediment core is collected from the deep-sea and brought to 1 atmosphere pressure, the pore water must re-equilibrate rapidly, $CaCO_3$ precipitates and the alkalinity measured in the pore water is less than that in samples collected by in-situ sampling devices. If $CaCO_3$ precipitation and therefore the removal of CO_3^{2-} from solution occurs, then the magnitude of this effect should depend on the state of saturation of the pore water under in-situ conditions. If a core which is undersaturated with calcite is being retrieved through the water column, it will become saturated at some particular depth which is less than the total water/

water depth. Thus, the magnitude of the alkalinity change ($[\text{HCO}_3^-] + 2[\text{CO}_3^{2-}]$) due to the pressure change may not be proportional to water depth (Murray et al., 1980) and may prevent the application of a thermodynamic treatment due to a kinetic effect i.e. that equilibrium is not attained before sediment squeezing (Emerson et al., 1982; Jahnke et al., 1982). Emerson et al., (1982) showed by intercalibration of squeezed box core and in-situ sampled pore water results that the pressure decrease effect on the carbonate system appears to depend on the presence of CaCO_3 in the sediments : there was very little evidence for a pressure effect at a silicious ooze site (MANOP site S) presumably because of the lack of CaCO_3 (s) nucleation sites whereas the carbonate system responds to the pressure change in a thermodynamically - predictable way for sediments with low (0.5 - 1.0%) carbonate content (Murray et al., 1980; Emerson et al., 1980). In nearly-pure CaCO_3 sediments (MANOP site C, Emerson et al., 1982) the pressure effect on alkalinity is much greater than predicted from thermodynamic considerations. Similarly, Froelich et al., (1983) observed a related pressure-induced artefact for pore water fluoride, whose values were significantly lower in pelagic red clay, silicious ooze and carbonate ooze box cores than in the bottom water, due, it was proposed, to the formation of a carbonate fluoroapatite. It is evident, then, that care must be exercised prior to pore water extraction and during sample manipulation, with provisions being required for temperature control, for avoidance of contamination and contact with oxygen and, if possible, for the circumvention of pressure effects. The pressure used in the extraction of the interstitial water from cores at depth has been shown to have little effect on salinity at pressures up to 9000psi (Sayles, 1970) and on other constituents before the cores are raised to the surface (Manheim and Sayles, 1974).

Among/

Among the various systems developed for the extraction of pore waters are leaching, centrifugation, liquid/gas displacement, liquid/liquid displacement and low and medium gas-pressure or mechanical-pressure systems (Emery and Rittenberg, 1952; Hartmann, 1965; Powers, 1967; Reeburgh, 1967). Some of these methods can be difficult to control, are slow, or can be inefficient for fine-grained sediments, producing only low-volume pore water samples. High-pressure hydraulic systems are much quicker and can provide large-volume samples with minimal air contact (Kalil and Goldhaber, 1973). A shipboard system, described in section 2.2 was used here for the extraction of pore waters from deep-sea sediments (Ridout, 1981), and included procedures which minimised the above effects of temperature, oxidation and contamination. Pressure effects on certain chemical species, however, could not be avoided during deep-sea core retrieval, but could be evaluated by comparison with the analytical results on samples taken by an in-situ sampler. Estuarine pore waters were collected as described in section 2.3, and were representative of in-situ conditions as they were not subject to large negative pressure differences.

1.3 Aims of the Project

The primary objective of this research was to perfect the fission track analysis technique for sub-nanogram quantities of uranium, particularly with regards to its application to small-volume sediment pore water samples. Reliable pore water data are scarce for this element mainly because of the difficulties involved in collecting and extracting sufficient sample volumes from the sediment such that the samples are chemically representative of in-situ conditions. Much of the experimental work was aimed at optimisation of neutron irradiation times, etching conditions and track counting criteria. Thus, the effects of varying the neutron fluence were studied, as was the variation of etching time and etching temperature. A clear, easily-distinguishable fission track record was of prime importance if automatic track counting was to be successful. Should the technique be shown to be sufficiently accurate and reproducible, the results of subsequent uranium determinations in pore water samples would be examined from a geochemical viewpoint with the help of as many auxiliary data as possible. Thus, attempts might then be made to explain the diagenetic behaviour of uranium from the observed pore water profiles.

Application of the dual fission track/ α -track method to deep-sea sediment geochronology was also to be assessed by comparison of the results with those already obtained by conventional techniques on the same samples and it was hoped that the fission track technique could be applied to the accurate uranium analysis of solid sediment samples.

It was also the intention of the project to illustrate the use of the α -sensitive plastic track detector in an autoradiographic mode and therefore the provision of various types of samples which contained natural or enhanced levels of α -emitting nuclides was planned.

Furthermore/

Furthermore it was thought beneficial that a reasonable portion of the work should involve the study of an aspect of uranium geochemistry by the related but more specialised procedure of radiochemical separation and α -spectrometry. The estuarine behaviour of this element was therefore selected for study and was to be achieved by collecting water samples along the salinity gradients of a number of U.K. estuaries. An assessment of the conservativeness or non-conservativeness of this behaviour was to be performed.

CHAPTER TWO

EXPERIMENTAL METHODS

2.1 Introduction

This chapter describes in some detail the techniques used in sample collection and in development and application of the subsequent particle track and radiochemical methods for the determination of uranium-series nuclides. The relative advantages and disadvantages of the track technique and of the conventional wet radiochemical and α -spectrometric approaches will also be assessed.

In summary, assay of total uranium by the fission-track method involves thermal neutron fission of the isotope ^{235}U which is present with ^{238}U at the known ratio of 1 : 137.88. Comparison of the fission track densities produced in external Lexan polycarbonate detectors between the samples and simultaneously-irradiated standards gives a direct measure of the ^{235}U and hence the ^{238}U content in the sample. It is important that the standards used are similar in chemical composition, otherwise fission track range effects may become important. Thus, glasses from the National Bureau of Standards are used for sediment or soil analysis while gravimetrically-prepared uranium solutions in artificial sea water are used for pore waters. The fission track technique has been successfully applied in the uranium analyses of one deep-sea core, estuarine bottom muds, an evaporite mineral, a series of intercalibration pore waters, eighteen pore water profiles from cores collected at different, geochemically-interesting locations using different coring and pore water sampling methods, and finally to some environmental samples from the vicinity of nuclear installations.

Conventional wet radiochemical analysis of ^{238}U and ^{234}U in aqueous samples involves co-precipitation of the actinides/

actinides and other cations on hydrated ferric oxide and subsequent purification steps including anion-exchange and solvent extraction. Solid samples are completely digested by combinations of concentrated acids and purified as for aqueous samples. ^{232}U is used as internal tracer and as a gravimetric yield monitor. The purified uranium isotopes, ^{238}U , ^{234}U and ^{232}U are electroplated onto a stainless steel disk from an ammonium sulphate electrolyte, which provides a thin source for α -spectrometry. Individual activities are each determined by separation of their characteristic α -particle energies. The potential uses of such isotopes at, or out of, radioactive equilibrium include the determination of conservative or non-conservative behaviour of uranium, geochemical mass balances, their use as a hydrological tracer and in radiometric dating (Ku, 1976; Osmond and Cowart, 1976a; Borole et al., 1982; Broecker and Peng, 1982).

Although it has recently been shown that highly specialised α -particle spectrometry can be achieved with the dielectric track detector CR-39 (Fews and Henshaw, 1982), the α -particle sensitive detector cellulose nitrate (Kodak LR115 Type II) used in this study is restricted to the study of the distribution of α -emitting nuclides (α -autoradiography) and is not considered capable of energy resolution and radionuclide identification. The α -track technique was applied to the deep-sea sediment core 9936K and, as demonstrated by Fisher (1977a, 1978) and Crawford et al., (1982) an estimate of the sedimentation rate determined. Application of the cellulose nitrate (CLN) to pelletised marine particulate matter and soil collected from the Dounreay area, to filtered suspended particulates from the Esk estuary, to a sectioned hydrothermal manganese nodule and to a series of planchets of various electroplated α -emitting nuclides was investigated to assess the presence or otherwise of hot-spots of α -activity and/or the extent of homogeneity of the nuclides. Details of sampling/

sampling locations and sampling methods used in this study will be given in sections 2.2 - 2.5.

To assess the random and systematic errors associated with the fission track analytical procedures for aqueous samples, replicate analyses were performed on standard sea water (I.A.P.S.O. Standard Seawater service) and a pore water intercalibration experiment was conducted in collaboration with Woods Hole Oceanographic Institute. For solid samples, one core (9936K) was analysed by the fission track method and intercalibrated with previous results by α -spectrometry on duplicate samples (Thomson, pers. comm.). In α -spectrometric analyses, solid samples were analysed in duplicate, whenever possible, for their ^{238}U content and $^{234}\text{U}/^{238}\text{U}$ activity ratio. Detector backgrounds were regularly determined over the same counting period as for samples, and reagent blanks were run for both procedures. Analytical-grade reagents were used throughout to minimise these blank contributions.

Since the quantities of radionuclides present for analysis could be as low as $\sim 7.6 \times 10^{10}$ atoms in the case of pore waters (100ul) and $\sim 1.0 \times 10^{16}$ atoms in the case of river, estuarine or sea waters, depending on the volume of sample, precautions had to be taken to avoid cross-contamination. Consequently, small-volume pore water samples were evaporated onto the Lexan polycarbonate detector in a dust-free environment, preferably in a laminar-flow clean hood, since the number of uranium-rich particles in ordinary dust can be considerable. The absence of hot spots (fission stars) showed that such particles were absent. The Lexan itself has a uranium concentration of less than 10^{-10} atom fraction and as such does not constitute a significant contribution to track density. During wet radiochemical operations, glassware and other apparatus (e.g. teflon plating cells) were taken through a rigorous decontamination procedure; firstly they were rinsed in water and soaked at least overnight in $\sim 10\%$ Decon solution, rinsed in distilled water and/

and then soaked in 7 molar nitric acid until required. Suites of estuarine water samples were analysed randomly to prevent the possibility of generating experimentally-derived trends after having been previously filtered and acidified to pH 1 to prevent adsorption of radionuclides onto the container walls.

2.2 Deep Sea Sediments and Pore Waters

All deep-sea pore water samples and sediment cores analysed in this study were collected on various cruises of the N.E.R.C. research vessel R.R.S. Discovery undertaken between 1979 and 1983 for the Institute of Oceanographic Sciences (I.O.S.), Wormley, Surrey with whom this research work is, of course, collaborative. Table 2.1 shows the relevant cruise data for each of the cores examined, while Figure 2.1 shows their location on a world map. The cores were taken either by an I.O.S. 30cm - square box corer (Peters et al., 1980) and a Hydrowerkstätten Kastenlot corer with a 2 metre, 15 cm-square section box barrel, both of which are designed to retrieve samples with minimum disturbance of the sedimentary column. The Kastenlot corer (Figure 2.2) consists of a bronze weight-stand containing up to 1000kg of lead weights, and a 15 x 15 cm square galvanised steel core box of length 2, 4 or 6 metres which can be opened longitudinally in two sections. The core catcher at the bottom of the corer consists of a pair of spring-loaded overlapping doors which can be locked in the open position by means of a pair of trip-levers. A schematic diagram of the box corer in operation is shown in Figure 2.3. The core boxes are opened on deck and the cores subsampled for mineralogical and geochemical studies. Subsamples for pore water extraction are squeezed under hydraulic pressure at low temperatures, in a nitrogen-filled glove bag in an effort to minimise oxidation effects and to provide samples which are as chemically representative as possible of 'in-situ' pore waters. The pore water extraction system is as described by Ridout (1981). Briefly, core samples were collected by inserting a precleaned 4-inch diameter butyric core liner near the centre of a box core and the top deadspace flushed with nitrogen before capping. The samples were transferred to/

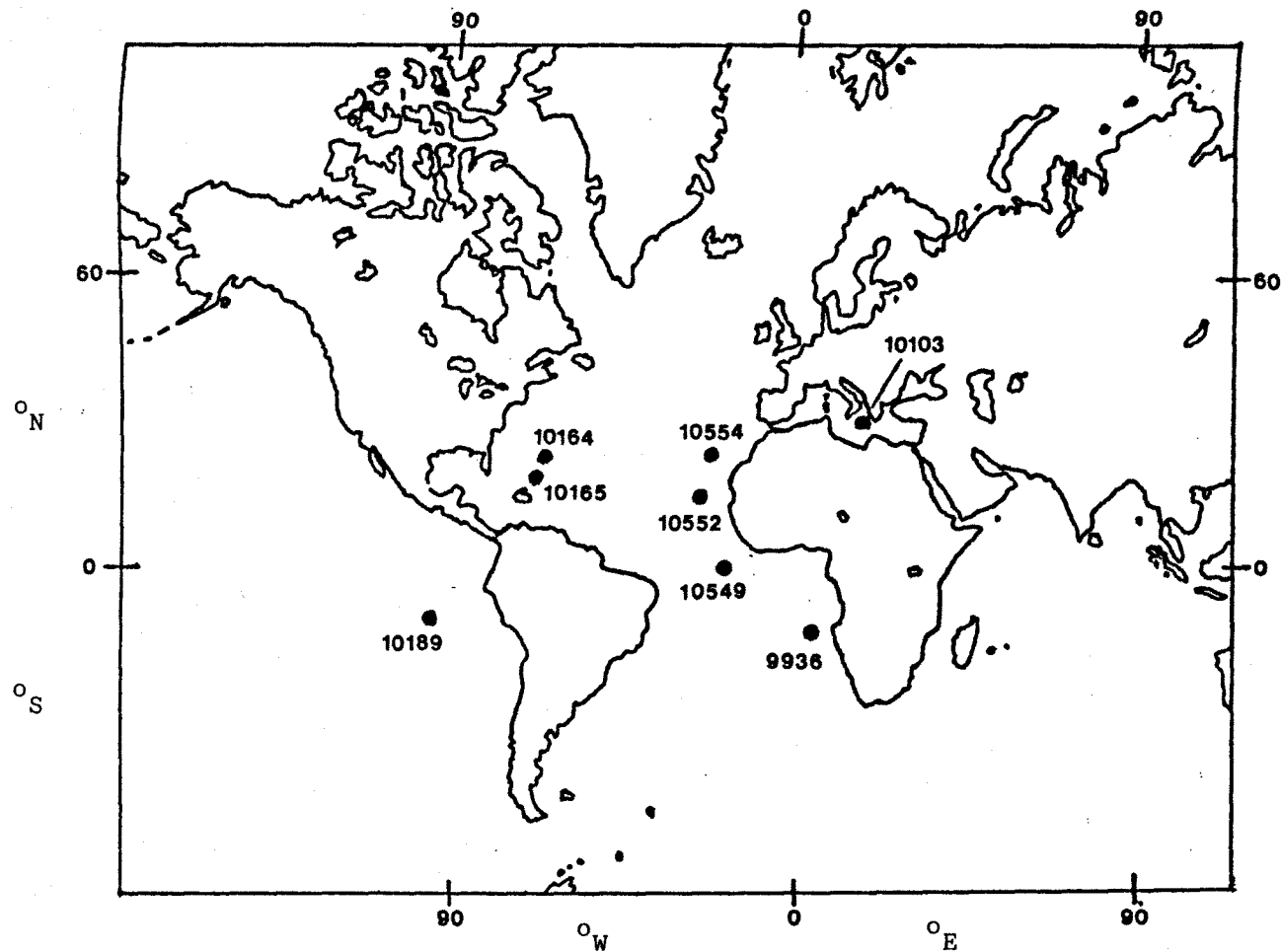


Figure 2.1. Locations of deep-sea cores sampled by R.R.S. Discovery

<u>CRUISE</u>	<u>DATE</u>	<u>LOCATION</u>	<u>LATITUDE/LONGITUDE</u>	<u>WATER DEPTH (m)</u>	<u>SAMPLE</u>
99	18/1/79	Cape Basin	33°42'7"S, 15°39'6" E	3808	78cm Kastenlot core (9936K)
104	17/6/79 -	East Mediterranean	36°09.6'N, 20°28.5'E	2880	62cm Box core(10103 1BX)
	19/7/79	" "	-	2900	61cm Box core(10103 6BX)
		" "	-	2900	74cm Kastenlot core(10103 3K)
108	23/2/80	Nares Abyssal Plain	26°14.0'N, 60°20.7'W	6135	205cm Kastenlot core(10164 1K)
	24/2/80	" " "	26°04.9'N 60°24.7'W	5550	55cm Box core(10164 5BX)
	26/2/80	" " "	23°45.0'N 61°27.5'W	5825	68cm Box core(10165 8BX)
110	1/6/80	East Pacific Ocean	9°58.5'S 102°33.9'W	4445	Box core(10189 4BX)
129	5/6/82	East Atlantic	00°01.9'N 16°10.2'W	3150	200cm Kastenlot core(10549 6K)
	13/6/82	" "	19°23.1'N 29°53.6'W	4683	170cm Kastenlot core(10552 2K)
	13/6/82	" "	19°24.5'N 29°52.7'W	4735	In-situ sampler (10552 #7)
	14/6/82	" "	19°27.3'N 29°53.6'W	4655	41cm Box core(10552 9BX)
	18/6/82	" "	31°29.7'N 24°28.8'W	5370	190cm Kastenlot core(10554 2K)
	18/6/82	" "	31°29.9'N 24°26.1'W	5370	59cm Box core(10554 5BX)
	18/6/82	" "	31°26.6'N 24°26.8'W	5371	In-situ sampler(10554 #12)

TABLE 2.1

Sampling data from all cruises. From Calvert et al., (1979), Kenyon et al., (1980), Culkin et al., (1980), Searle et al., (1980) and Wilson et al., (1982).

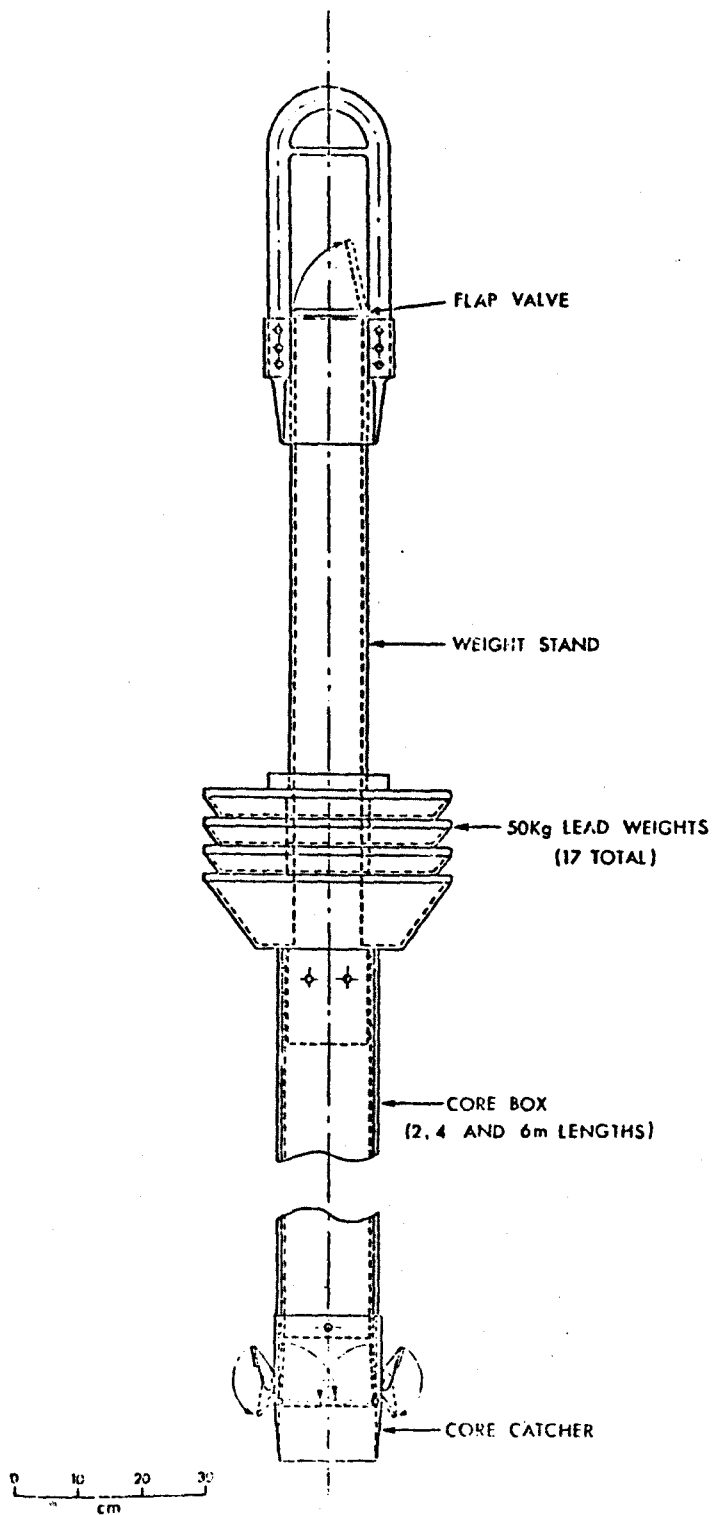
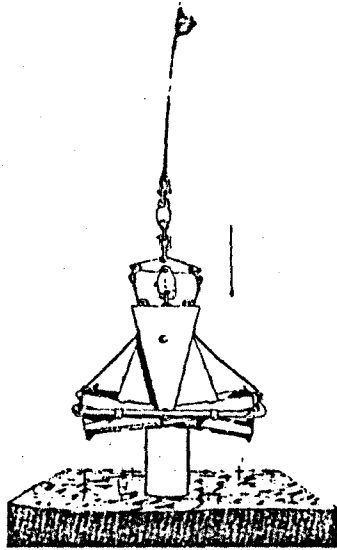
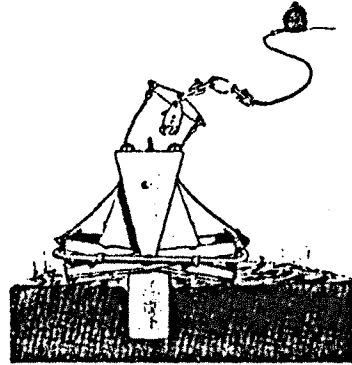


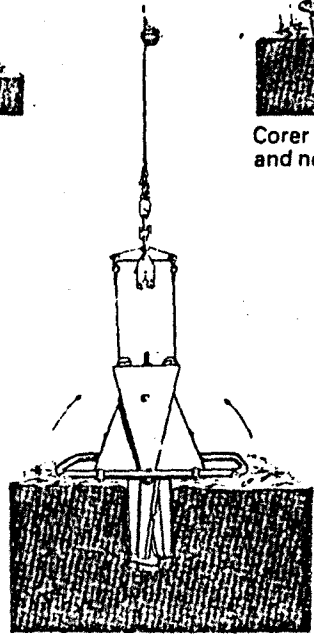
Figure 2.2. Diagram of the Hydrowerkstätten Kastenlot corer.



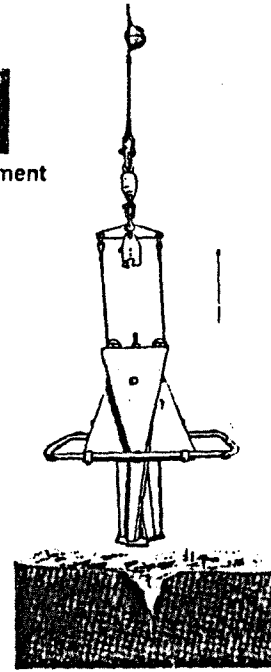
Descent mode with arms open and no-load release set



Corer having penetrated the sediment and no-load release tripped



Partial recovery showing arms having cut through sediment



Recovery

Figure 2.3. Schematic diagram of box corer in operation.

to a cool cabinet at 4°C for storage prior to sectioning. These subcores and the squeezer units were sealed into a large glove bag, its contents flushed with nitrogen and the bag loosely inflated. Subcores were extruded from their liners by a PVC piston and sectioned by a plastic spatula into PVC squeezer units, so constructed that no metal contact with either the sediment or the pore water is allowed. The squeezer units, comprising the cylinder base, cylinder, retaining collar and piston were three-quarters filled for efficient squeezing and positioned on a hydraulic jack in steel frames inside a cool cabinet. After allowing time for the units to come to temperature, each one was pressurised to between 2000 and 4000 psi depending on sediment type. The first few ml of water through the Whatman 542 filter papers incorporated in the base were discarded to flush the dead volume and filter assembly before a 60 ml plastic syringe was inserted into the outlet port. About 100 to 200 ml of sample was collected by squeezing within half an hour, the pressure being maintained at approximately 5 - minute intervals.

Figures 2.4 and 2.5 show schematic diagrams of the I.O.S. Mark II in-situ pore water sampler. It is a modification of the sampler described by Sayles et al., (1976). The sampler consists of a large, spring-operated master cylinder which provides the suction required for sampling, the instrument functioning rather like a large syringe. Instead of toggle valves previously used (Sayles et al., 1976), electromagnetic valves are incorporated, which are triggered when an electro-optical sensor enters the sediment, thus detecting the sea bottom. When this occurs, one of the three valves which is in circuit with a hydraulic ram coupled to a lever bar, is tripped and stops further/

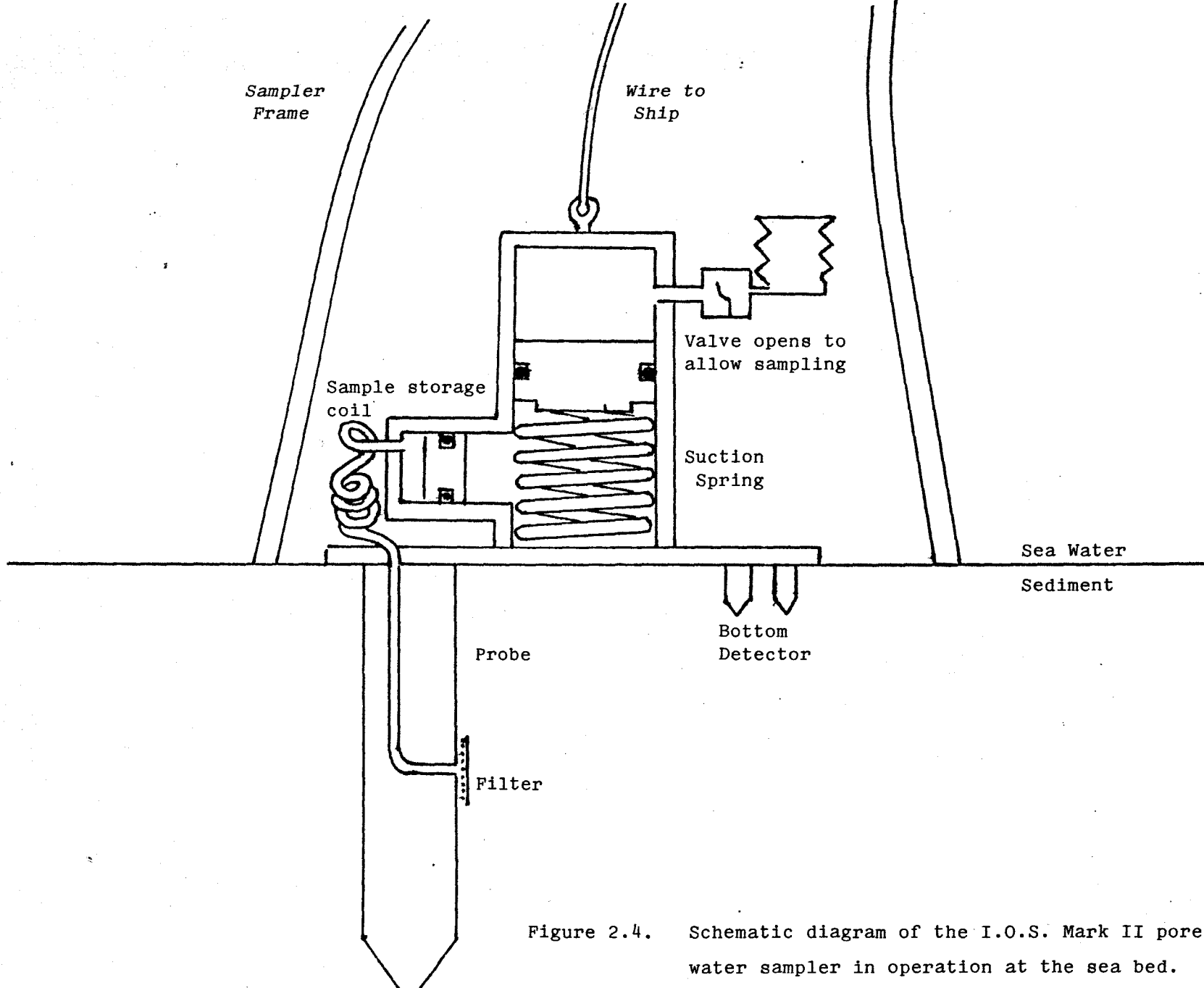


Figure 2.4. Schematic diagram of the I.O.S. Mark II pore water sampler in operation at the sea bed.

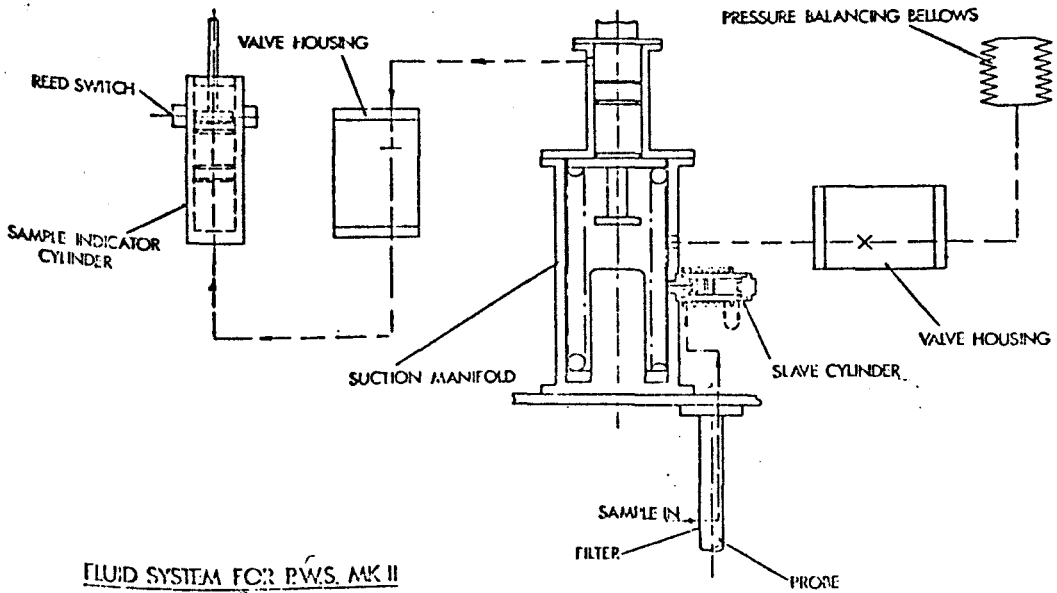
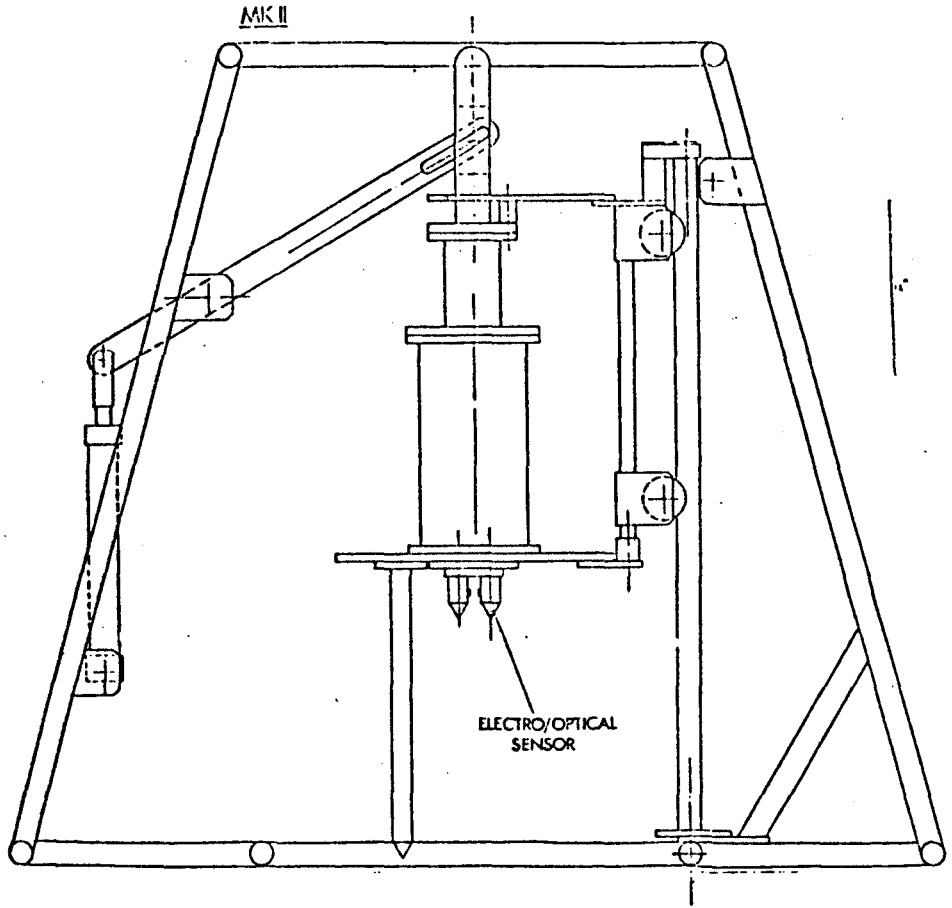
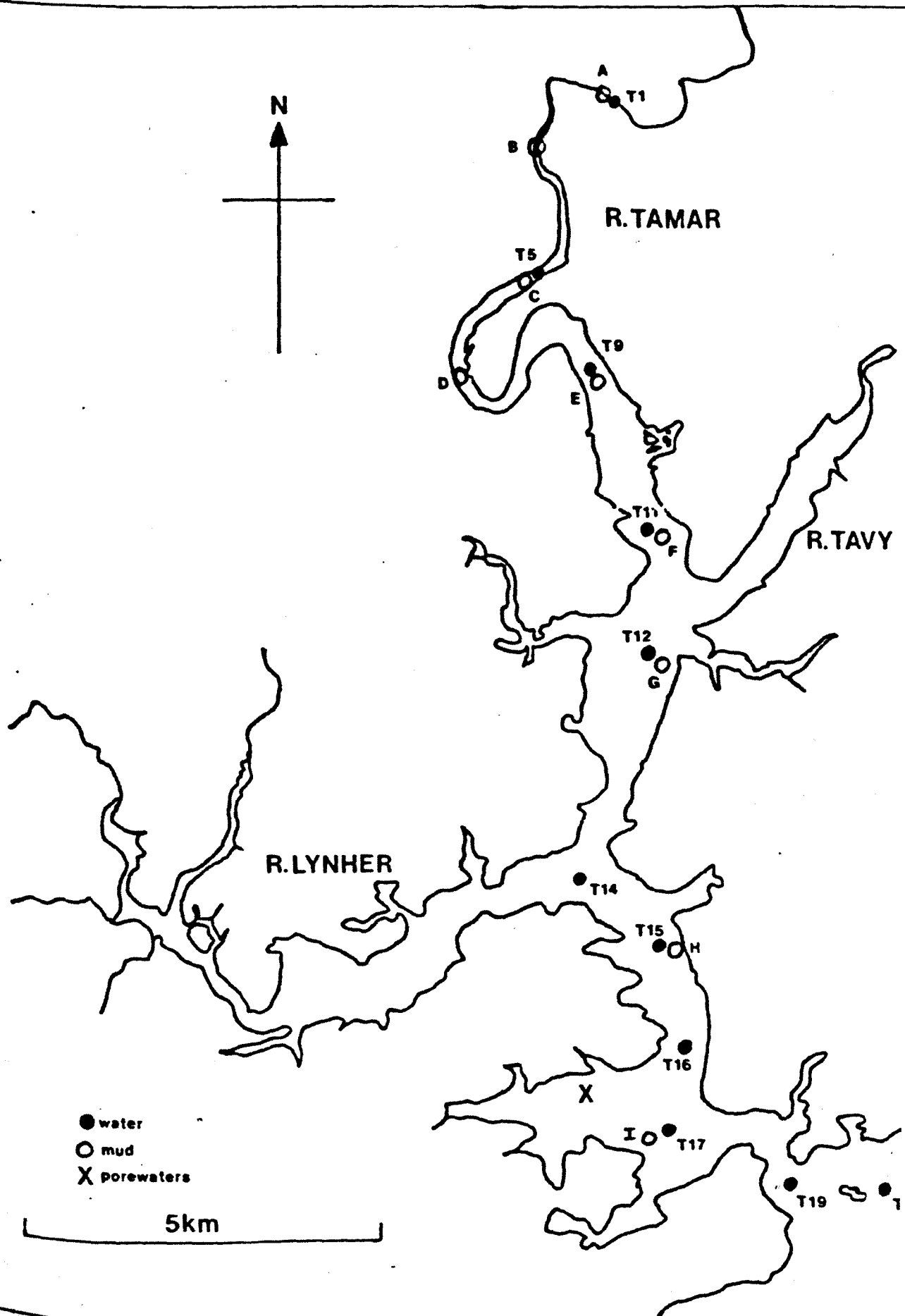


Figure 2.5. Schematic diagram of the I.O.S. Mark II pore water sampler.

further descent of the sampler within its conical frame. The other two valves switch the unit to sampling mode, and samples are taken through filter-containing ports in the two sampling probes or 'harpoons', due to the pressure drop at these ports relative to the adjacent sediment, and are stored in coiled teflon capillary tubing which permits the recovery of uncontaminated pore water samples. Samples are taken at 50 cm and 1 cm above the sediment/sea water interface, and at 2, 3.5, 6.5, 12.5, 24.5 and 45.5 cm below the interface. The ports are concentrated near the sediment/water interface since it is here that the concentration gradients of certain chemical species have been demonstrated by many workers to be steepest, owing to the more intense diagenetic activity there. Examples of such species are trace metals (Klinkhammer, 1980; Klinkhammer et al., 1982), major ions (Sayles, 1979; Sayles, 1981), nutrients (Bender et al., 1977; Froelich et al., 1979; Emerson et al., 1980) and carbonate-system species (Fanning and Pilson, 1971; Emerson et al., 1980; Murray et al., 1980). Sampling is terminated either by a reed switch mounted on a sample indication cylinder, or by a preset clock built in to the electronic circuits.

2.3 Estuarine Pore Waters

All the estuarine pore waters analysed were collected during 1982 at St. Johns lake in the Tamar Estuary, a low-energy, relatively undisturbed site (Clifton and Hamilton, 1979) - position X on figure 2.6. In collaboration with the Earth Sciences Department, University of Leeds, cores were collected under about 5 cm of water at low tide by slowly pushing 25 cm long perspex liners vertically downwards into the mud and sealing the base with a watertight base plate. An undisturbed sediment/water interface, usually with some supernatant water, was thus collected. The cores were kept at 21°C until introduced to a nitrogen-filled, perspex glove box for squeezing (Upstill-Goddard and Alexander, 1982), maintaining a low oxygen level of between 0.2 and 0.0% and a small positive internal pressure. The sediment column was raised into the glove box from below by a scissor-jack through an airtight seal and, after siphoning off any supernatant water, 1 cm increments were sliced off into 250 ml centrifuge bottles and then removed and centrifuged at 10,000 G at 10°C for 30 minutes. The bottles were reintroduced to the glove box and the supernatant pore water drawn off through 2 mm internal diameter silicon rubber tubing into acid-washed subsample bottles using a peristaltic pump with 0.45 µm Millipore filters in-line. Small-volume aliquots of these filtered samples were taken for uranium analysis by the fission-track method.



2.4 Rivers and Estuaries

Three sampling trips were made to the Clyde estuary in 1982 in order to recover water samples for uranium isotope and salinity measurement and bottom sediment for uranium isotopes and organic carbon. In March, 1982, water sampling (~10 litre volumes) at the riverine end of the estuary was achieved by simply lowering a plastic bucket on a rope over the side of each of five Glasgow bridges and transferring to 10 - litre sample bottles. 250 ml subsamples were taken for salinity determination after filtration through 0.45µm Millipore filters with Whatman GF/B prefilters. Salinity measurements were performed on these samples conductimetrically at the Clyde River Purification Board (C.R.P.B.) on an inductive salinometer. Sampling at the sea water end of the estuary was performed from the C.R.P.B. research vessel 'Endrick II' in an attempt to collect a good sea water salinity end-member. The main estuary transect was sampled in May, 1982 on the 'Endrick II' by pumping water from about 6 foot depth during the course of one of C.R.P.B.'s regular 'River Run' surveys. Figure 2.7 shows a map of the area and indicates all the sampling sites.

Bottom mud sampling was achieved using a Craib corer (Craib, 1965) which, via soft-landing and hydraulically-damped sediment-penetration devices, is designed to retain the light, superficial layer of sediment intact. The top two to three centimetres of each core were transferred to self-sealing sample bags.

Samples were collected along a transect of the Tamar estuary, Plymouth on the 15th March, 1982 from the research vessel 'R.L. Gammarus' of the Marine Biological Association (M.B.A.) starting at zero salinity at Calstock and extending seaward to Drake's Island (Figure 2.6) where a maximum salinity of 28.55 was attained. Chlorinity determinations were performed on subsamples at M.B.A. by silver nitrate titration using dichlorofluorescein as indicator. Bottom muds/

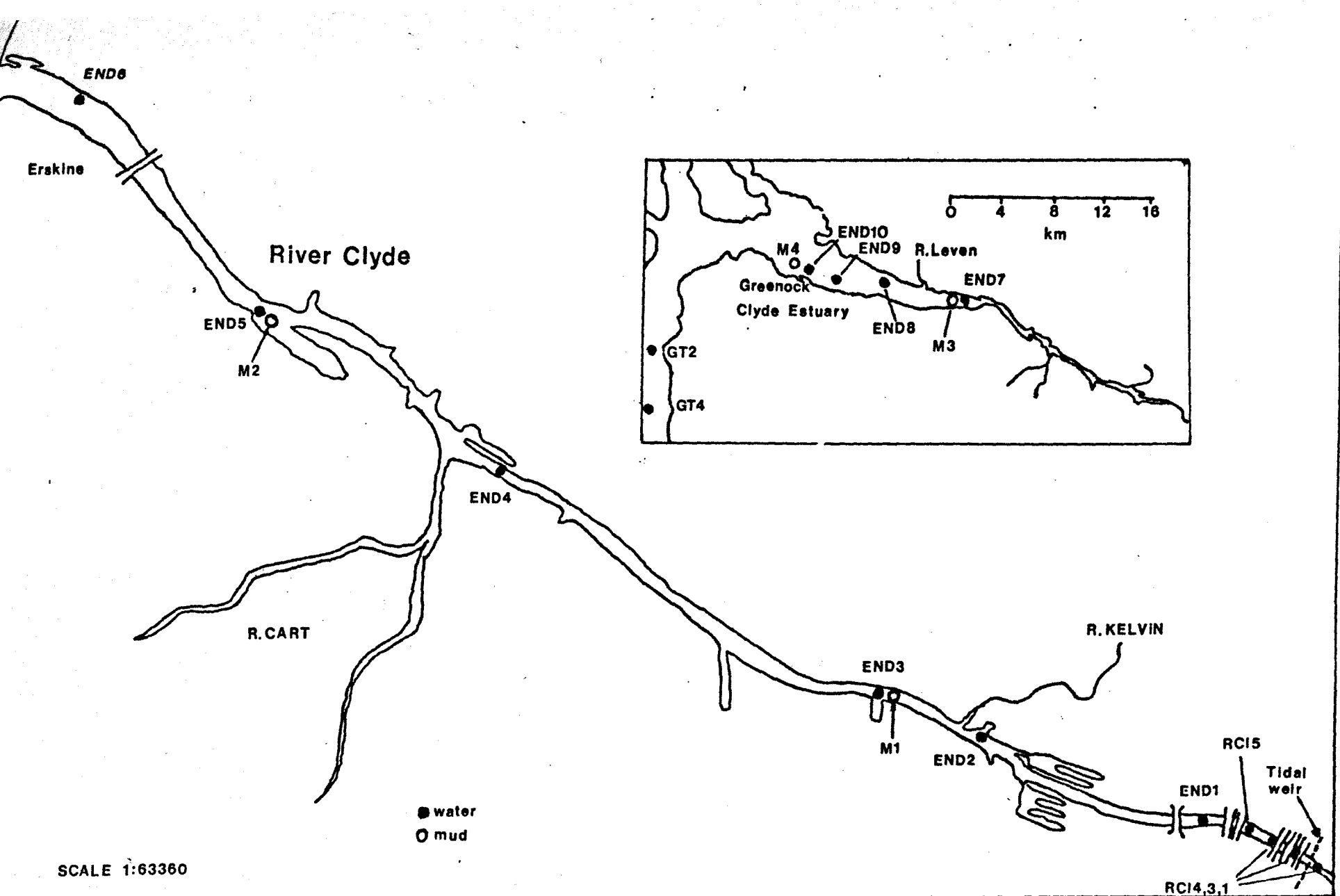


Figure 2.7. Sampling sites in the Clyde estuary

muds were also obtained from shallow waters using a long-handled scoop. These muds were kept in self-sealing sample bags until required.

Figure 2.8 indicates the sampling locations in the Forth river and estuary at which approximately 10-litre surface water samples were taken on 23rd June, 1983 between 2 and 0 hours before high water during one of the Forth River Purification Board's (F.R.P.B.) regular surveys. Particulates from each bulk sample were allowed to settle and were retained. Again 250 ml subsamples were filtered through GF/B prefilters and then through 0.45 μ m Millipore filters. This was considered necessary because the particulate concentrations were visibly high. Salinity determinations were performed at the Institute of Oceanographic Sciences, Surrey, on a Guildline Salinometer against a primary salinity standard.

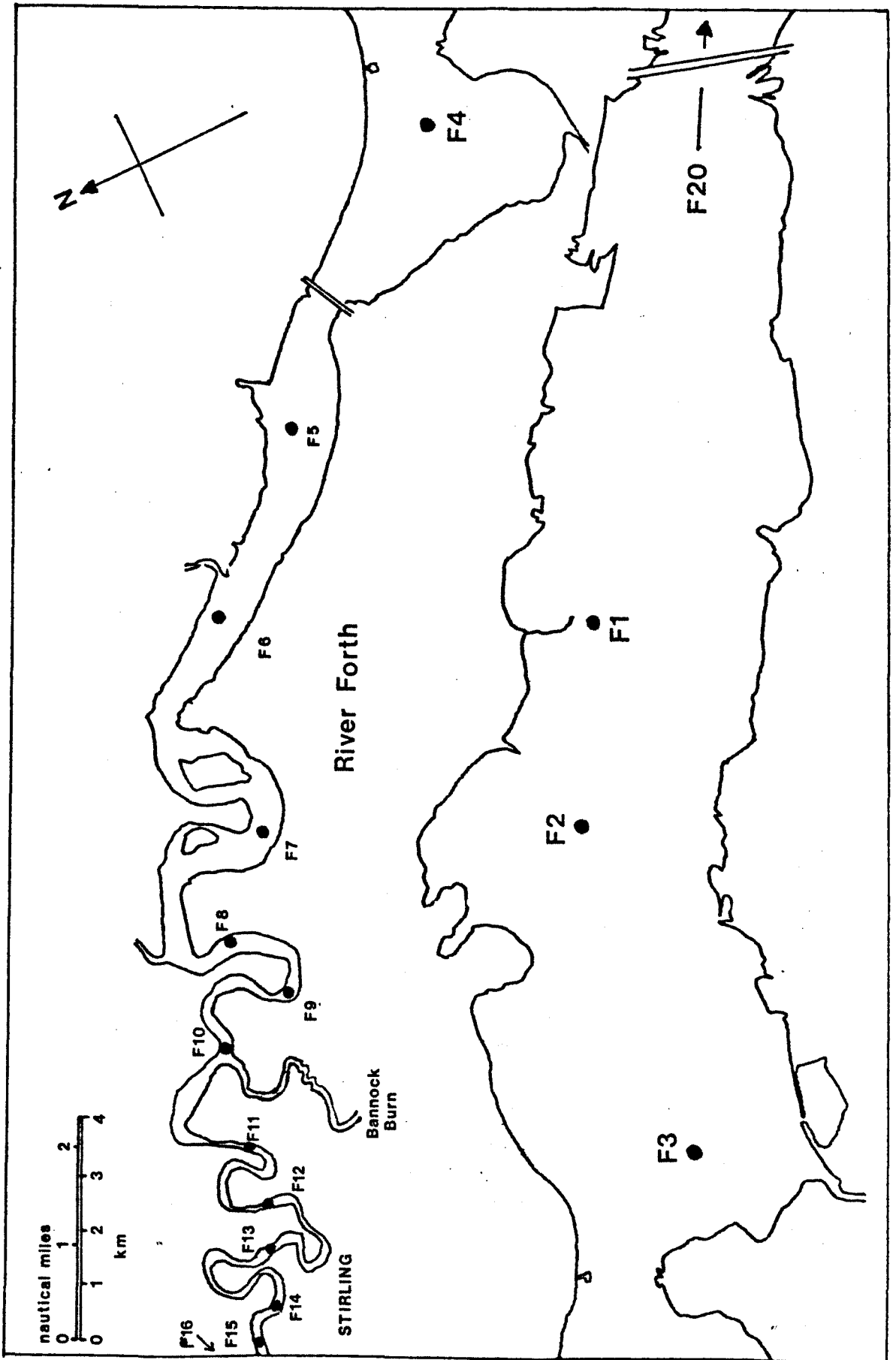


Figure 2.8. Sampling sites in the Forth estuary.

2.5 Particulates from the Vicinity of Nuclear Installations and Miscellaneous Samples

After the gravitational settling of a 10-litre water sample from the Esk estuary, the supernate was filtered through a Whatman GF/B prefilter and then through a Millipore 0.45 μ m filter. This provided a small particulate load on the Millipore filter suitable for α -track analysis. These particulates and the main settled load, were considered to be a possible sink for radionuclides discharged and dispersed from the British Nuclear Fuels plc reprocessing plant at the nearby Windscale (Sellafield) site. The settled particulates were collected for a range of radionuclide analyses.

At Oigin's Geo, about 0.5 km East of the Dounreay Nuclear Power Development Establishment (D.N.P.D.E.) in Caithness, a variety of environmental particulate samples (Table 2.2) was collected from the shoreline on 29th May, 1980 and between 1st - 3rd June, 1981 during a sampling trip associated with an ongoing research contract between D.N.P.D.E. and the University of Glasgow. The samples were analysed by a combination of α and γ -spectrometry and particle track methods.

Miscellaneous samples included a submarine hydrothermal manganese deposit from the south-west Pacific island arc, which was dredged up during a joint New Zealand Oceanographic Institute/Imperial College, London research cruise in May, 1981 (Cronan et al., 1982) and was sectioned and polished by S.A. Moorby (Imperial College) for α -track autoradiography at Glasgow. This α -track technique was also applied to a series of planchets containing one of the electroplated radioisotopes Th, U, Pu and Am, which were provided by various workers in order to assess the degree of homogeneity obtained in the electrodeposition stages of their routine radioanalytical procedures. The planchet submitters were G.T. Cook and J. Toole (University of Glasgow), J. Thomson (I.O.S., Surrey), R. Fukai (I.A.E.A., Monaco) and A. B. Mackenzie (S.U.R.R.C., East Kilbride).

A sample of gypsum was provided by T. M. Leatherland (F.R.P.B.)/

TABLE 2.2

Environmental particulate samples from near Dounreay, Caithness.

<u>SAMPLE NO.</u>	<u>LOCATION</u>	<u>DESCRIPTION</u>
1	Oigins Geo	Dried Scrapings from Rocks(1980)
2	Oigins Geo	Dried Scrapings from Rocks(1981)
3	Oigins Geo	Dried Sea Foam (1980)
4	0 Metres Inland	Sandy Topsoil (1981)
5	50 Metres Inland	Higher Organic Soil (1981)
6	100 Metres Inland	Higher Organic Soil (1981)
7	Offshore	Sandy Marine Sediment (1981)

(F.R.P.B.) for uranium analysis. The gypsum was a waste product generated during the manufacture of phosphates from a high-uranium bearing calcium phosphate ore. The calcium sulphate (gypsum) by-product generated is discharged directly into the Forth Estuary and was considered as a possible source of uranium.

2.6 Fission Track Method

Development of the now commonly-utilised fission track technique (Fisher and Bostrom, 1969; Hashimoto, 1971; Carpenter and Cheek, 1970; Mahajan et al., 1978; Fleischer et al., 1972; Riley, 1981) is described here for the assay of uranium in sediments and sediment pore waters, with particular attention paid to optimisation of both the etching and irradiation parameters. The sample-preparation procedure described for deep-sea sediments was also applied to all other solid samples analysed by the method (e.g. soils, dried sea foam), while that for sea water, deep-sea pore waters and nearshore pore waters could easily be extended to uranium assay of other samples such as river water and human blood (Hamilton, 1970).

Although there is now a myriad of dielectric track detectors available for fission track analysis (Fleischer et al., 1975), Lexan polycarbonate (A.G.Bayer, West Germany) was used throughout the period of research because of its low uranium content, high detection efficiency (Khan and Durrani, 1972; Qaqaish and Besant, 1976; Guo et al., 1981) and proven ability to yield accurate and reproducible results (Crawford, 1982). The polycarbonate plastic is sensitive to heavily-ionising fission fragments and to other massive ions whose energy loss per unit length in the plastic exceeds the critical value of $\sim 4\text{MeV mg}^{-1}\text{cm}^{-2}$ (Fleischer et al., 1965). This critical energy-loss rate, $(dE/dx)_{\text{crit.}}$, results from a rapid drop in track registration efficiency from unity to zero for a fairly narrow range of dE/dx values.

Under a thermal neutron fluence, ^{235}U atoms in samples and standards fission into two asymmetrical, heavily-ionising fragments with concurrent energy release of $\sim 200\text{MeV}$ per fission. Under 2π geometry, one of these fragments typically impinges on the Lexan detector, creating a narrow trail/

trail of radiation damage on an atomic scale. These damage trails are revealed for counting in an ordinary optical microscope or Quantimet 720 automatic image analysing computer (Jesse, 1971; Lycos and Besant, 1976) simply by chemically etching the irradiated plastic in 6 molar NaOH at 45°C for 1 hour in a thermostatically-controlled water bath (FE-type, Grant Instruments Ltd.). The etchant rapidly and preferentially attacks the radiation-damaged material at a faster rate that it removes the surrounding undamaged or bulk matrix, leaving enlarged holes or tracks which mark the site of each individual damaged region. The molarity of the etching solution should be regularly checked to ensure that all samples are etched under the same conditions. Loss of water by evaporation increases the molarity of the NaOH, while absorption of CO₂ from air produces Na₂CO₃, reducing the molarity. The etching process is terminated by immersion of the Lexan initially in a dilute (0.1M) solution of hydrochloric acid at 20°C to remove the NaOH, and then rinsing with distilled water to remove any particles or salt. The Lexan is then dried between lens tissues to reduce static attraction of dust.

2.6.1 Solid Samples

Solid samples are oven-dried at 110°C and ground in a mortar and pestle. They are further homogenised to $\lesssim 50\mu\text{m}$ grain size in an agate ball-mill (15-20 minutes). Thereafter, about 100mg of the sample is accurately weighed, to better than 0.1mg, and is hydraulically pressed in a 13 mm KBr die under 8 ton pressure for 5 minutes, using about 1.0 g of uranium-free cellulose powder as inert binder. This preparation affords a sample which is thicker than the range of fission fragments within it. It is important, too, that the elemental composition of the uranium standard used is not too appreciably/

appreciably different from that of the unknown, since the effective range of the fission fragments increases with increasing atomic number because of the tighter bonding of atomic electrons (Mory et al., 1970). Consequently, glass standards of nominal base composition 72% SiO₂, 12% CaO, 14% Na₂O and 2% Al₂O₃ (SRM 962) were used in this study, their composition being comparable to that of compressed sediment or soil. These standards were obtained from the National Bureau of Standards (Carpenter and Reimer, 1974) and contained 37.38 ± 0.08 ppm uranium, with a ²³⁵U atom percent of 0.2392. This latter figure differs from the natural ²³⁵U abundance of 0.7200 (Hamer and Robbins, 1960) in samples because depleted uranium dopant was used in the glass preparation. A correction for this difference must be applied during uranium analysis. The uranium concentration expressed in weight fraction (ppm) in the unknown is given by

$$U_x = \frac{D_x}{D_s} U_s \frac{I_s}{I_x} \dots \dots \dots (2.1)$$

where U_x and U_s are the uranium contents in ppm of the sample and standard respectively, D_x and D_s are the track densities (cm⁻²) produced in the Lexan by each, and I_x, I_s are their respective ²³⁵U to ²³⁸U isotopic abundance ratios. Background track densities were found to be equivalent to about 0.03 ppm for uranium assay.

Although deep-sea sediment samples generated easily-counted homogeneous fission track distributions, some solid samples, particularly soils and nearshore particulate muds, produced fission stars or 'hotspots' (Figure 2.9) due to the presence of uranium-bearing minerals such as sphene, zircon and mica (Hamilton, 1966, 1980). Although such fission stars preclude quantitative/

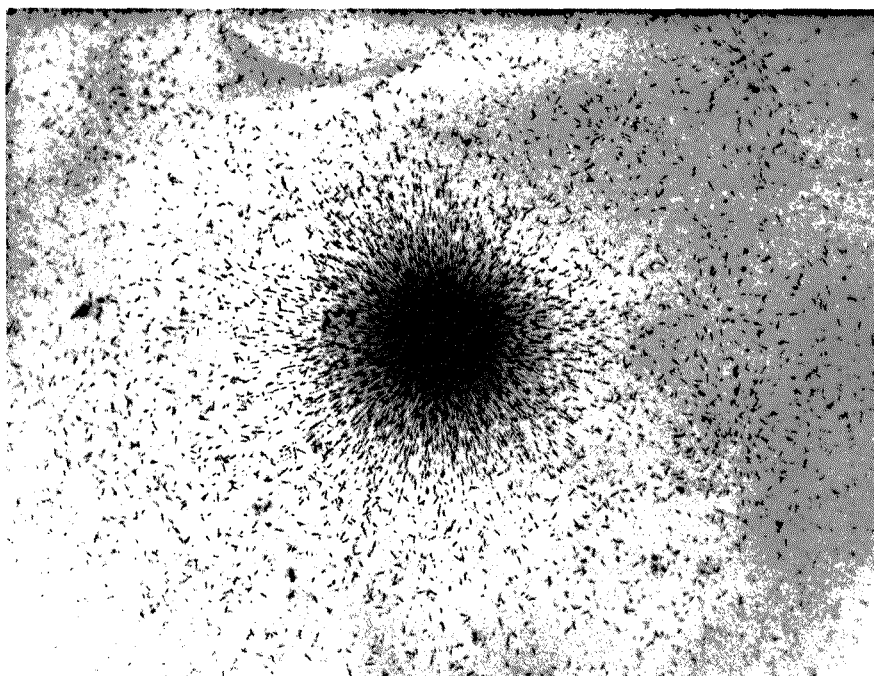


Figure 2.9. Fission star or 'hotspot' from a uranium-bearing mineral in a solid sample.

quantitative track counting, they are useful in uranium distribution studies (Kleeman and Lovering, 1967; Hamilton, 1980) and it is important to be aware of their presence.

2.6.2 Aqueous Samples

The fission track technique was first applied to the determination of uranium in water samples by Fleischer and Lovett (1968) by evaporation of a defined volume onto the track detecting material to leave a thin deposit of non-volatile constituents. After neutron irradiation, the authors found that all the fission tracks had to be counted to eliminate the effects of non-uniformity in their distribution. Since this procedure can become tedious for high track densities, Fleischer and Delaney (1976) described equations applicable to certain regular, non-uniform track distributions such as a constant track density along a circular outside rim, in an effort to avoid total track counting. However, irregular distributions and the presence of fission stars could not be accommodated in the equations. Hashimoto (1971) realised that such heterogeneous track distributions gave erroneous results and used condensed solutions in quartz ampoules for neutron irradiation, with pieces of muscovite mica immersed as the track detector medium. Although homogenous track distributions were achieved, the high uranium content of the mica relative to sea water meant that the uranium in the sea water sample had firstly to be pre-concentrated by aluminium phosphate co-precipitation, and processed to yield just 2 ml of solution. Furthermore, long-term neutron irradiation of sealed solutions is to be avoided because of the high β and γ dose rates induced and of the risk of sample shattering by heat expansion of the solutions.

Geraldo et al., (1979) used a similar wet irradiation method, with polystyrene vials holding about 50 ml of solution. The method involved complete evaporation of 80 ml samples and conversion/

conversion of uranyl carbonate ions to uranyl nitrate before irradiation, again increasing the processing time per sample. Using a standard calibration curve, uranium concentrations in samples were determined with an overall error ranging from 3.3% to 29.0%.

The fission track technique employed in this study, as applied to sea water and pore waters, is an adaptation of the method used by Fleischer and Delaney (1976). No pretreatment of samples is necessary except filtration (0.45 μ m). 100 μ l of pore water or sea water is pipetted onto a piece of Lexan by 5 - 100 μ l variable Eppendorf pipette with a precision of <0.3%. 15 μ l of ethylene glycol is then added as a spreading agent and the mixture is evaporated to dryness in a laminar-flow fumehood under an infra-red lamp. A low-uranium fibre washer is taped round the deposit for protection against abrasion and an identification number impressed on the plastic. The thin, homogeneous deposit of non-volatile seasalt microcrystals is reproducibly produced on the plastic ensuring a homogeneous track distribution (Figure 2.10). After neutron irradiation, the samples and standards are allowed to cool, particularly with respect to decay of the β and γ activities of activation products such as ^{82}Br and ^{24}Na in the seasalt. The taped fibre washers are later removed from the plastic and the seasalt deposit rinsed off with distilled water into a radioactive waste disposal drain. Subsequent chemical etching is identical to that for solid samples. It was found, as noted previously, that without the use of glycol, the salt crystals incorporating most of the uranium tend to concentrate on the outer rim of the deposit (Fleischer and Delaney, 1976; McCorkell and Huang, 1977) resulting in a non-homogeneous track distribution (Figure 2.11). The glycol thus acts as a spreading agent, preventing the formation of this outer rim. The uranium analysis is therefore simplified to one of comparative track density estimation/



Figure 2.10. Homogeneous track distribution from a sea water sample using 15ul ethylene glycol as spreading agent.

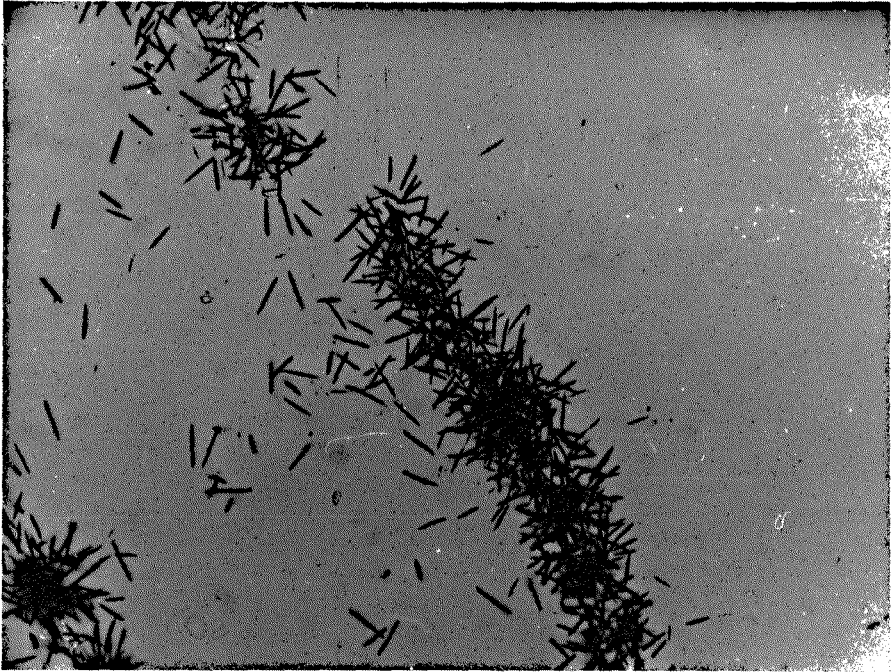


Figure 2.11. Non-homogeneous track distribution from a sea water sample. No spreading agent used.

estimation involving samples and standards and obviates the need for total track counting. With the further observation that fission stars or track-clustering were not in evidence, it could be concluded that aggregates of uranium or of uranium-bearing particulates were absent.

The aqueous uranium standards used in the technique were prepared gravimetrically by dissolving 99.98% pure uranium foil of natural isotopic abundance (Goodfellow Metals, Cambridge) in nitric acid, diluting to the required concentrations in distilled water and adding the appropriate amounts of NaCl, $MgCl_2 \cdot 6H_2O$, Na_2SO_4 , $CaCl_2 \cdot 2H_2O$ and KCl to give the required artificial sea water composition (Lyman and Fleming, 1940). The uranium content of the bulk standard solution was checked by isotope dilution α -spectrometry and a concentration of $14.92 \pm 0.31 \text{ ug ml}^{-1}$ was found, as compared to 15.15 ug ml^{-1} by gravimetric calculation. As shown by Robertson (1968) it is difficult to maintain a known uranium concentration at low levels due to adsorption on container walls. For a sea water solution spiked to 120 ug l^{-1} of uranium it was found (Robertson, 1968) that after 50 days about 20% of the uranium was lost to Pyrex glass surfaces and about 10% to polyethylene surfaces, even with the addition of acid to the sea water. Consequently, the series of uranium artificial sea water standards prepared from the bulk sample were immediately evaporated with ethylene glycol to give multiple standard samples, thus minimising adsorption losses. Pore water samples themselves must also be evaporated as soon as possible after collection, although most samples had been stored either frozen prior to evaporation, thus preventing significant adsorption, or at bottom water temperature (4°C .)

Figure 2.12 shows the linearity obtained between the uranium concentration of the standards and the corresponding track density as observed by the Quantimet. A limitation of the method arises, however, for samples with uranium concentrations greater/

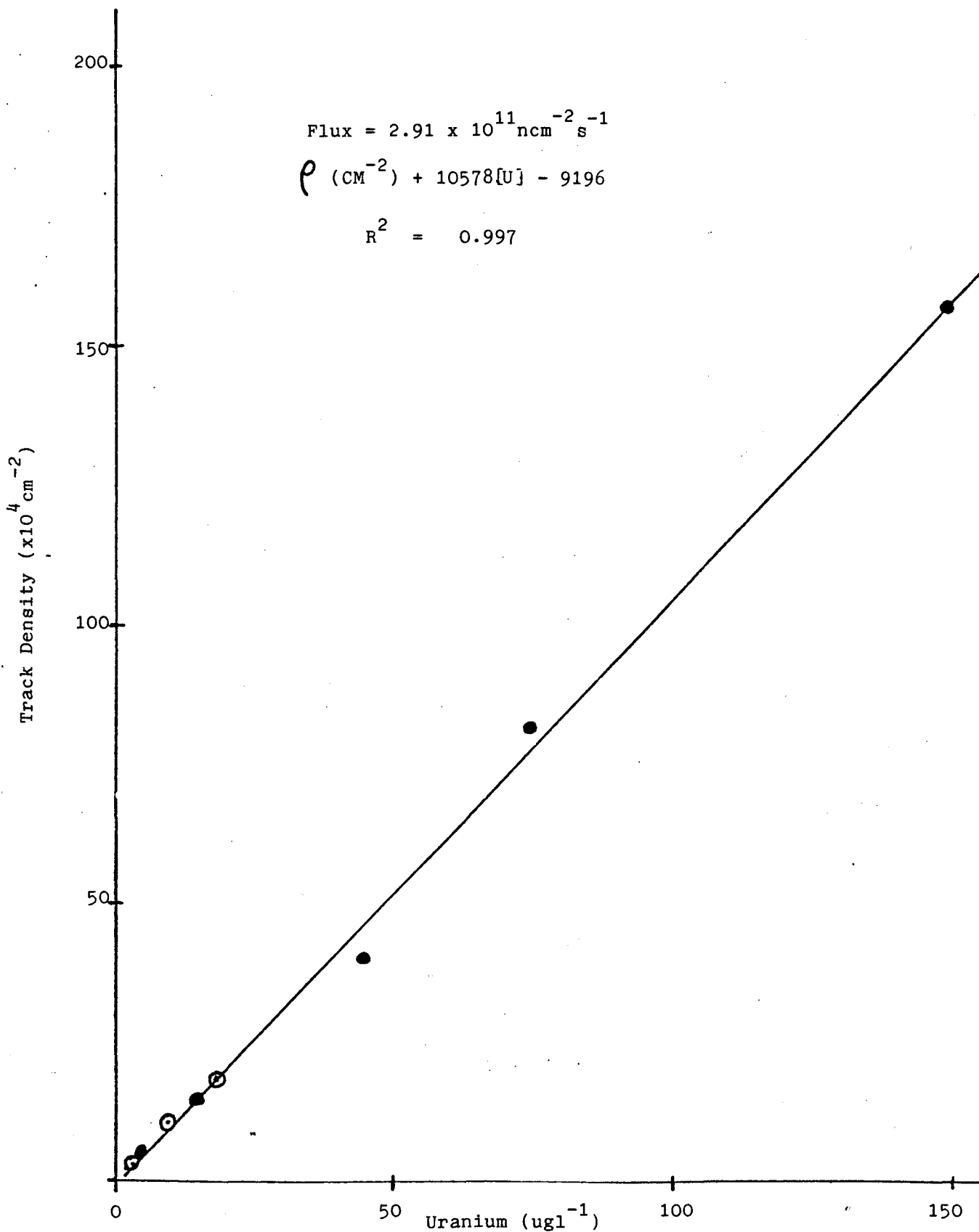


Figure 2.12. Linearity obtained between uranium concentration of standards (●) and samples (⊙) and their corresponding track density observed by the Quantimat

greater than standard F ($149.20 \pm 3.10 \text{ ug l}^{-1}$), since the overlapping of tracks in close proximity to each other, even in the homogeneous distribution, destroys the linear relationship between the total number of tracks or the track density and the uranium concentration. This problem was also encountered by McCorkell and Huang (1977) and Piesch and Weng (1972) in their use of a discharge counter, but to a greater extent since their track widths were much larger. The simple solution to this problem was to re-irradiate such samples, when found, with the appropriate standard(s) in a lower neutron fluence either by shortening the irradiation time or by moving the samples to a lower n-flux position, or both. In a precision check, a series of 10 sea water samples (I.A.P.S.O. Standard Seawater Service) replicates were simultaneously irradiated, and track counting at x 600 magnification under the optical microscope yielded a replicate error of 6.1% (Table 2.3) for a concentration of $\sim 3.3 \text{ ug l}^{-1}$. The intercalibration results for a series of pore water samples provided by J.K. Cochran of Woods Hole Oceanographic Institution are shown in Table 2.4. It is evident that the fission track method used at Glasgow compares favourably with the more established, although more involved, α -spectrometric procedure on which the Woods Hole data are based. Taking the paired differences (Woods Hole - Glasgow) of the results and performing a one-sample t-test (Moroney, 1979), it is found that a 95% confidence interval for the null hypothesis of 'no difference between both sets of results' is (-1.56, 0.10). The calculated t-value of 1.886 does not exceed the critical value of 2.2 given by the 5% probability level for 15 degrees of freedom, and thus we cannot reject the null hypothesis, i.e. it is accepted that there is no difference, on average, between both sets of results. The computed 95% confidence interval above did, however, indicate that there was a slight systematic/

TABLE 2.3

I.O.S. Sea water replicates fission track counts for a 21 hour irradiation in a neutron fluence of $\sim 10^{16}$ ncm⁻²; tracks counted over 50 fields of view (Total Area = 3.348×10^{-2} cm²)

<u>Sample</u>	<u>Total Tracks</u>	<u>Density(cm⁻²)</u>
SW1	1200	35842
SW2	1269	37903
SW3	1335	39874
S"4	1325	39576
SW5	1205	35991
SW6	1187	35467
SW7	1285	38393
SW8	1103	32945
SW9	1268	37877
SW10	1150	34349

Mean count = 1233 ± 76 (6.1%)

TABLE 2.4

Alpha spectrometry/fission track analysis pore water
intercalibration.

<u>Sample</u>	Uranium Concentration (dpm kg ⁻¹)		<u>Ratio</u>
	<u>α-spectrometry(W.H.O.I.)</u>	<u>Fission Track(Glasgow)</u>	
M6348	2.70 ± 0.08	2.40 ± 0.07	0.90
M6505	2.09 ± 0.07	3.50 ± 0.12	1.67
M6506	1.13 ± 0.08	1.18 ± 0.04	1.04
M6748	2.83 ± 0.12	3.74 ± 0.13	1.32
M6749	1.24 ± 0.07	1.21 ± 0.05	0.98
M6750	1.64 ± 0.10	1.62 ± 0.06	0.99
M6629	12.73 ± 0.38	13.16 ± 0.43	1.03
M6630	7.22 ± 0.19	7.32 ± 0.22	1.01
M6631	4.80 ± 0.11	5.83 ± 0.19	1.21
M6632	1.64 ± 0.06	1.94 ± 0.07	1.18
M6635	3.00 ± 0.10	4.32 ± 0.14	1.44
M6368	14.33 ± 0.43	15.01 ± 0.47	1.05
M6493	18.04 ± 0.75	16.58 ± 0.51	0.90
M6495	15.26 ± 0.64	17.82 ± 0.55	1.17
M6618	7.31 ± 0.37	7.14 ± 0.22	0.98
M6445	12.65 ± 0.63	17.99 ± 0.55	1.42

(fission track values were converted to dpm kg⁻¹ from
ugl⁻¹ by the factor 0.741 dpm ²³⁸U/ug ²³⁸U and a sea
water density of 1.025 kg l⁻¹)

systematic error involved, the fission track results being, on average, slightly higher. The Glasgow/Woods Hole ratios lay in the range 0.90 - 1.67 with a mean of 1.14, indicating that the Glasgow samples were about 14% higher on average. This is probably the result of a slight variation in the seasalt deposit diameter when acidified samples are used. Samples M6348 and M6618 were unacidified and show a mean difference of 6.0% which is within the 6.1% analytical precision (1σ) of the method. Blank levels arising from artificial sea water and the Lexan amounted to 0.03 ug l^{-1} equivalent. The relevant equation for uranium determination in aqueous samples is

$$U_x = \frac{D_x}{D_s} U_s \dots\dots\dots(2.2)$$

This is a simplified form of equation 2.1 since here the uranium foil used for the standard is undepleted in ^{235}U , and $I_s = I_x$. A typical sample calculation for uranium in pore water is given in Appendix A.

2.6.3 Track Counting Methods

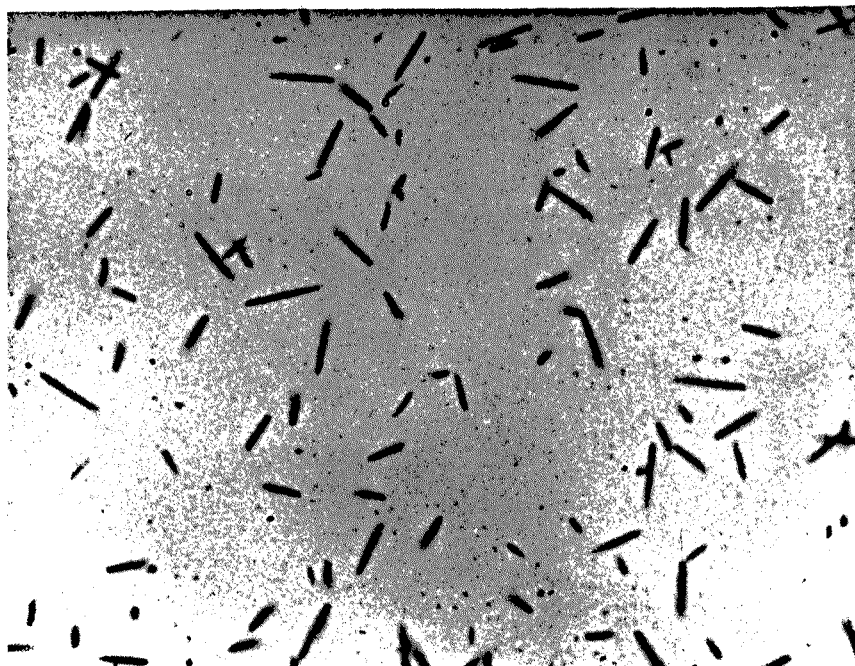
The etched fission tracks from either solid or liquid samples were counted manually under an optical microscope (Olympus Model BHB) at X400 or X600 magnification, fifty random fields of view giving a total counting area of 8.309mm^2 and 3.348mm^2 respectively. If the track density becomes so great that counting the number of tracks per field of view on the optical microscope becomes difficult, then the use of the Quantimet 720 automatic image analyser is required. The Quantimet derives numerical data, in this case fission track counts, from a Vickers M41 Photoplan microscope with an attached Vidicon camera which is connected on-line to a processor with video display screen. By interfacing with a desk-top calculator (Hewlett-Packard 9810A Calculator, Model 10) containing a programmed magnetic card, the derived parameters total count, mean count and 1σ standard deviation are obtained and printed. The area of a field of view at X500 magnification was calibrated using/

using a 2 - 100 um micrometer scale and was found to be $1.397 \times 10^{-4} \text{ cm}^2$. The basic track count parameter can, with appropriate modules, be made subject to variable conditions. For example, only features greater than a certain size can be detected and counted. Since the fission track lengths vary depending on the angle of incidence of the fission fragment in the plastic, a whole range of track dimensions from about 0.5 um diameter for tracks of normal incidence to about 30 um length for tracks near the critical angle of 2.9° (Fleischer et al., 1964) are produced. It is useful, then, to use such a sizing parameter by applying a minimum critical value of ~ 10 picture points length, above which features are detected. The Quantimet is permanently calibrated internally in picture points, one picture point being equal to 0.164 um at X500 magnification. Thus, only tracks greater than ~ 1.64 um are counted. This restriction results in a marked improvement in accuracy, since background imperfections on the Lexan are selectively ignored, as long as the same sizing conditions are applied to both samples and standards. Further discrimination in detection is provided by the Standard Detector module which is based on a lower threshold setting above which everything darker is detected for counting. Since internal reflection of light causes fission tracks to appear as dark rods, only these are counted, provided that there are no large dust particles, etched dislocations or scratches in the fields of view scanned. Although it had previously been considered (Crawford, 1982) that fission tracks viewed under the Quantimet could not be satisfactorily distinguished from background damage and scratches arising from sample contact with the Lexan plastic, various improvements and modifications in the technique enabled the Quantimet system to be utilised successfully: (a) by varying the temperature and time parameters during etching of the Lexan, the background on the plastic can be reduced and the track/

track dimensions controlled. Figures 2.13(a) and 2.13(b) show one field of view of etched tracks from identical sea water samples irradiated at the same position in the Scottish Universities Research Reactor. The lower etching temperature and longer etching time resulted in tracks which are more presentable to the Quantimet. It was therefore decided to etch all Lexan samples at 45°C for 60 minutes in 6M NaOH. Fast neutrons, which constitute a small percentage of the reactor neutron flux used here, can produce tracks by causing nuclei to recoil elastically within the detector (Nishiwaki et al., 1971). This is especially true for protons, which constitute 45% of the Lexan atoms, since they have a higher elastic scattering cross-section and a greater range in the detector. It is these proton recoil tracks which are probably responsible for the background damage. (b) By using a combination of controlled transmitted light intensity with a red filter, the track contrast at the high Quantimet magnifications was sufficiently good for reproducible track counting when a drop of immersion oil was placed between a glass cover-slip and the objective lens. Table 2.5 shows the counts obtained, per field of view, for a high track density standard SRM 962. (c) Preparation of pore water samples as described in section 2.6.2 ensured that there was no abrasion of the plastic by the evaporated seasalt crystals, which had previously occurred when the deposit was sandwiched between two Lexan pieces (Figure 2.14). (d) By conducting a series of experiments at the Research Reactor, the sample irradiation parameters were optimised with regard to the extent of fast neutron damage, track interference from fission products of nuclides other than ^{235}U and the irradiation duration and position. These experiments are described in the following section.

2.6.4 Sample Irradiation

The UTR-300 Scottish Universities Research Reactor,
with/



(a)



(b)

Figure 2.13. Appearance of fission tracks (a) etched at 45°C for 60 minutes (b) etched at 80°C for 20 minutes.

TABLE 2.5

Fission track counts from N.B.S. Standard Glass

SRM - 962 as recorded by the Quantimet - 720

U = 37.38 ± 0.08 ppm.

Each field of view = 1.397×10^{-4} cm².

Neutron Flux = 5.08×10^{11} ncm⁻²s⁻¹.

Irradiation Time = 6 hours.

<u>Total Tracks</u>	<u>Track Density (cm⁻²)</u>
153	1095204
147	1052255
151	1080888
134	959198
146	1045097
143	1023622
140	1002147
143	1023622
130	930565
137	980673
143	1023622
147	1052255
142	1016464
152	1088046
144	1030780
140	1002147
135	966356
134	959198
146	1045097
138	987831

Mean Density = 1016750 ± 41303 cm⁻² (4.1%)

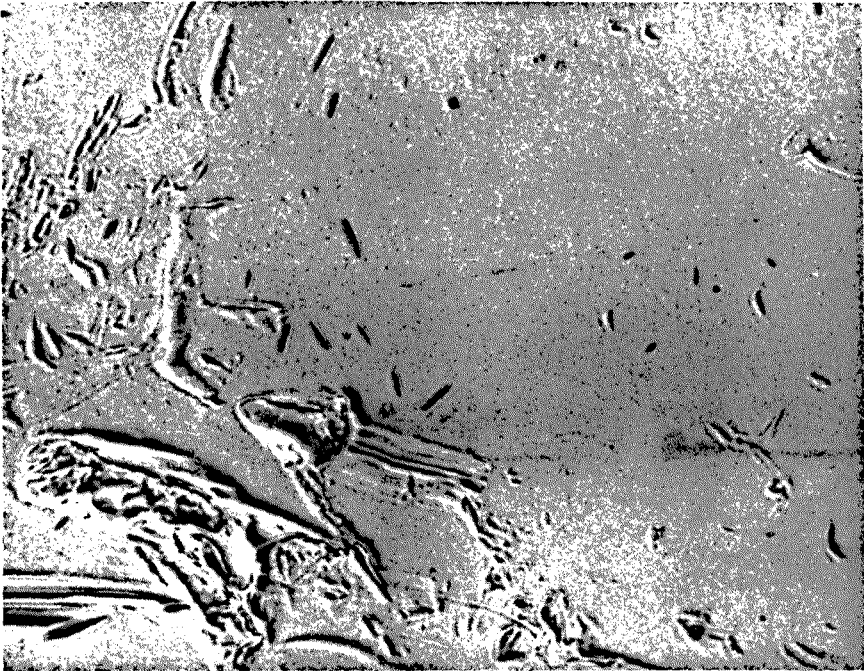
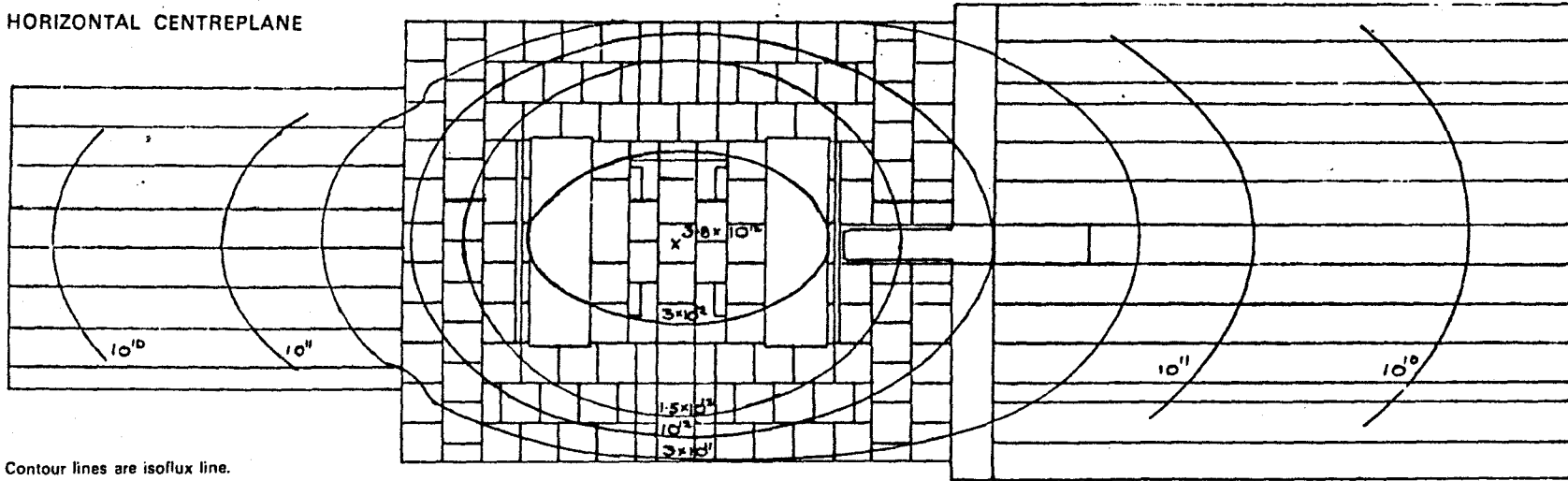


Figure 2.14. Abrasion of Lexan by a sandwiched seasalt deposit.

with its maximum power output of 300 kwatt, houses various neutron irradiation facilities. Amongst these are the Central Vertical Stringer (C.V.S.) which allows access to high-flux irradiation positions in the centre of the reactor core, and a large thermal column abutting against a 4-inch thick lead gamma-ray shield (γ curtain). This thermal column consists of a 6' x 4' x 4' stack of graphite and provides irradiation positions in a well-thermalised flux through 15 4-inch square stringers, access to which is gained by removal of the thermal column door. The C.V.S. irradiation position has a fast neutron component of about 3%, but this does depend critically on actual position between the 2 fuel arrays. Thermal neutron fluxes were determined by the use of Specpure iron flux monitors (Johnson Matthey Chemicals Ltd.), one of which was irradiated within each sample package. The pre-weighed monitors underwent the reaction $^{58}\text{Fe} (n, \gamma) ^{59}\text{Fe}$ and the resulting 1.292 MeV γ -ray emissions were detected on an 80cc Ge(Li) detector, which was efficiency and energy-calibrated using a ^{60}Co standard source. The neutron flux was computed using a Program compiled in Fortran IV (Appendix B). From the results of fluxes for 5 monitors contained in the same 10cm -long package, the mean was found to be $(3.13 \pm 0.44) \times 10^{11} \text{ ncm}^{-2}$, indicating an average flux variation of about 1.4% per cm. In order to find the optimum irradiation position, six packages of identical samples were irradiated at different reactor locations. Each package contained one sediment pellet, five replicate sea water deposits, one flux monitor and a 100 ul, glycol-free deposit of a thorium nitrate standard (thorium concentration $\sim 100\text{ugl}^{-1}$). Figure 2.15 shows the irradiation positions used, and Figure 2.16 shows the measured thermal/

APPROXIMATE NEUTRON-FLUX DISTRIBUTIONS IN THE UTR

HORIZONTAL CENTREPLANE



Contour lines are isoflux line.
Values indicated are thermal flux levels (N/Cm²-Sec) at a reactor power level of 300 KW.

VERTICAL CENTREPLANE

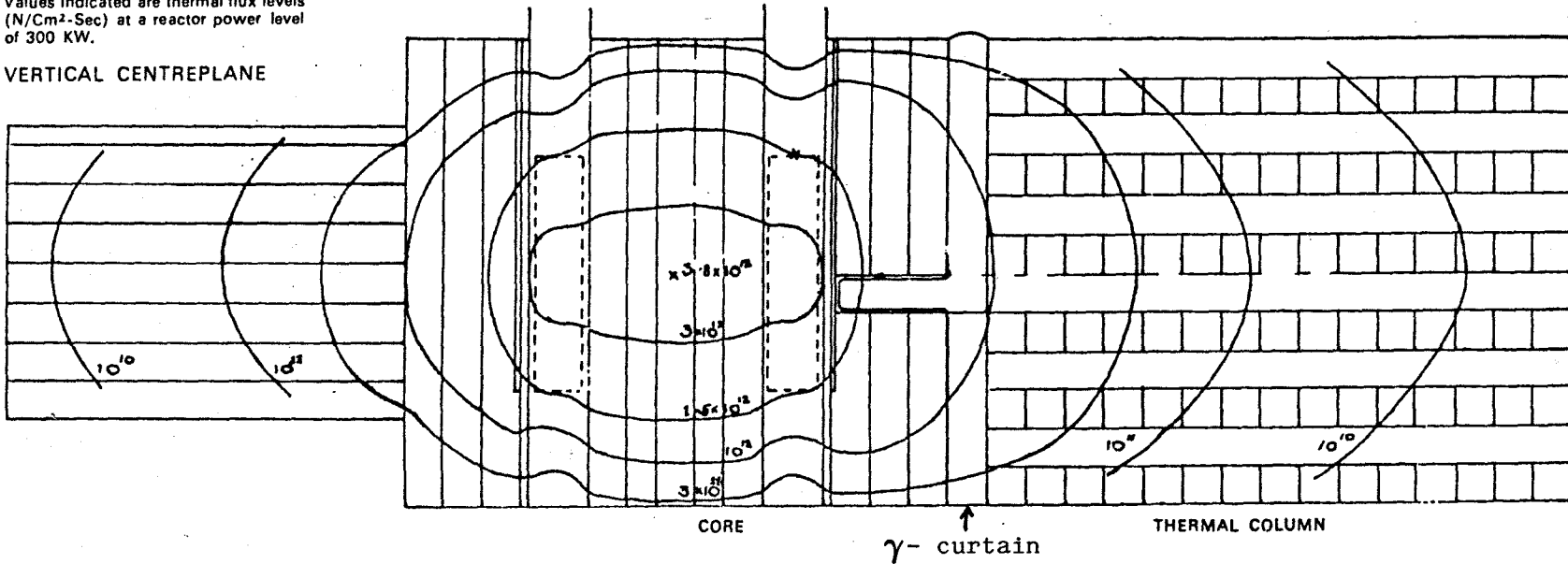


Figure 2.15. The UTR - 300 Research Reactor.

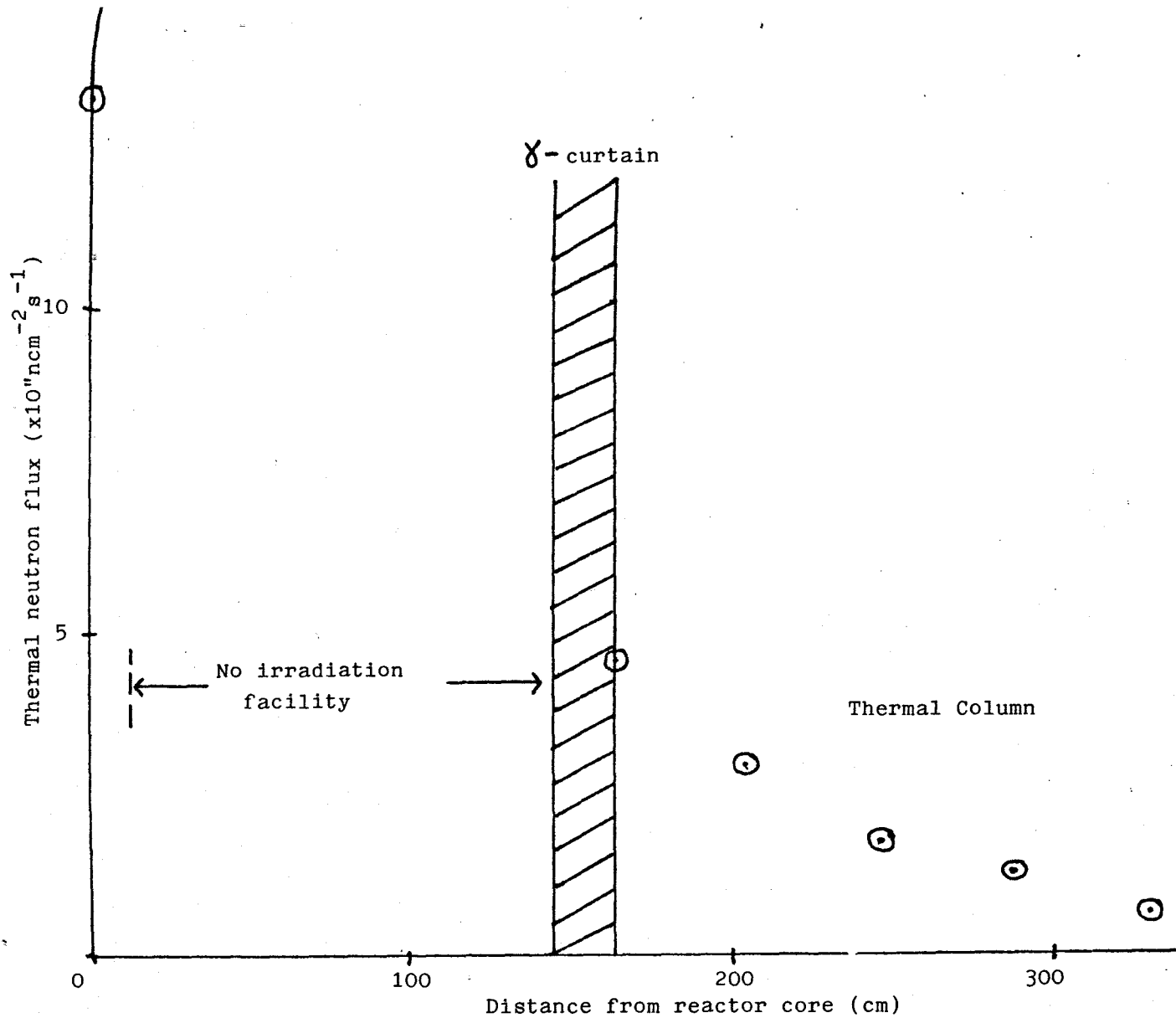


Figure 2.16. Variation of thermal neutron flux with distance from core in the UTR-300 research reactor.

thermal neutron flux plotted against distance in cm from the core. As expected, the flux decreases with distance in an approximately exponential manner. Tracks from the replicate sea water samples were counted, and since the irradiation times for each sample batch varied, the resulting track densities were normalised to the time-integrated flux at the C.V.S. position. It was found that at thermal column position 2 there was an anomalously high track density produced on the plastic for all five sea water samples. Repetition of this experiment, using one pore water deposit of higher uranium content at each position exhibited the same phenomenon (Figure 2.17). Various possible explanations for this effect have been discussed, such as a path or hole in the graphite blocks through which an excess of thermal-neutrons can pass, or the presence of a ^{235}U fission cross-section resonance at the neutron energies found at this position, but all have been subject to uncertainties. Neutron energy profiles, for instance, are not available for the reactor. Further researches by reactor staff into the phenomenon are in progress using a ^{235}U -spike solution and restricting the number of variables. Whatever the cause, the apparent neutron flux per unit distance varies increasingly as this resonance peak is approached, and it was decided that, in routine analyses, samples would be irradiated near the γ -curtain. Here the flux variation was low ($\sim 1.4\% \text{ cm}^{-1}$ as noted previously), the irradiation time required for a neutron fluence of $\sim 2 \times 10^{16} \text{ ncm}^{-2}$ was relatively short (~ 21 hours compared to ~ 93 hours at position 6), and the fast neutron and γ radiation damage was negligible. Figure 2.18 illustrates the background-corrected track interference from ^{232}Th fast fission ($\sigma_{^{232}\text{Th}}(\text{fast}) = 0.078\text{b}$). The total number of tracks were counted over identical areas as for sea water samples to take account of track inhomogeneity, since ethylene/

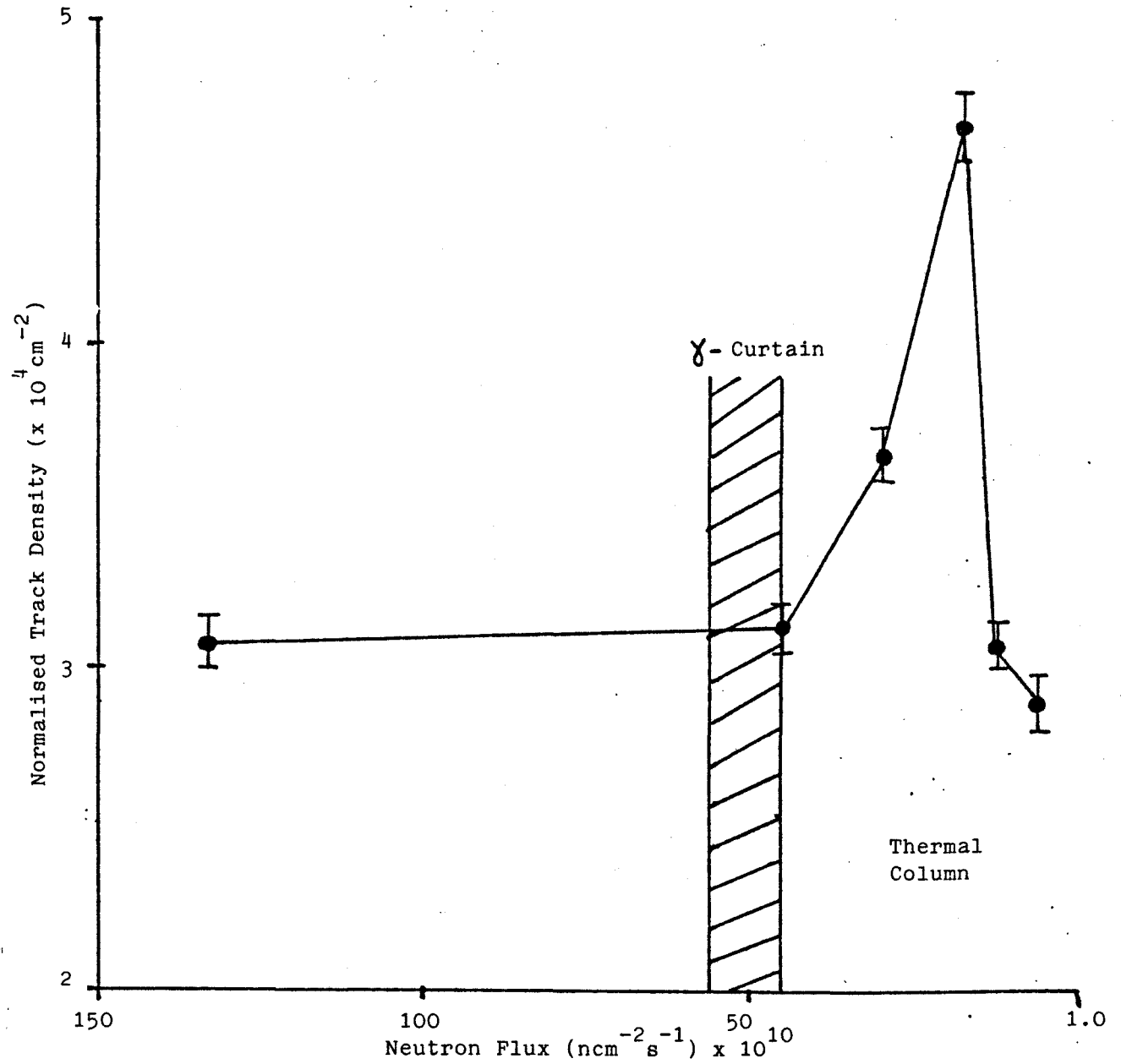


Figure 2.17. Track densities at the various reactor positions, normalised to the integrated flux at the C.V.S. position. Each sample contained $37.68 \pm 1.35 \mu\text{gU}^{-1}$. (1σ counting errors).

ethylene glycol was not used at this time, and track densities were calculated. The track interference from thorium near the γ -curtain even at the high concentrations used ($\sim 100 \text{ugl}^{-1}$) amounted to only 1.6% of the tracks obtained from a typical sea water sample of uranium concentration $\sim 3.3 \text{ugl}^{-1}$ irradiated at the same position. This indicated that, for equal ^{232}Th and ^{238}U concentrations of sea water/pore water, thorium interference would be $\sim 0.05\%$. However, in reality the ^{232}Th content of ocean water is $6 \times 10^{-5} \text{ugl}^{-1}$ (Moore, 1981) and its effect can be neglected, even in sediments or soil samples where the Th/U ratio is ~ 4 . From the sediment irradiation results, a 6 hour irradiation at this same position (flux $\sim 3 \times 10^{11} \text{ncm}^{-2} \text{s}^{-1}$) of a sample with U content of 1 ppm gave a sufficient track density of $\sim 45,000 \text{cm}^{-2}$. ^{238}U fission is also negligible because $\sigma_{^{238}\text{U}}$ (thermal) is $< 5 \times 10^{-4} \text{b}$. Another thermal neutron-fissile nuclide, ^{239}Pu , is present with ^{240}Pu at levels from around 0.2fCi l^{-1} for unfiltered North Sea water (Murray et al., 1978) to around 1pCi l^{-1} in filtered sea water near the Windscale reprocessing plant (Hetherington et al., 1975) and up to 130pCi g^{-1} in intertidal Irish Sea sediments (Aston and Stanners, 1981). ^{239}Pu has a thermal neutron fission cross-section of 742b, which is comparable to that for ^{235}U (579b). However, the track method of analysis is dependent on the mass of a particular fissile species and not on its specific activity. By considering the above cross-sections, the nuclides half-lives ($7.1 \times 10^8 \text{yrs}$ for ^{235}U , $2.44 \times 10^4 \text{yrs}$ for ^{239}Pu) and the constant natural $^{235}\text{U}/^{238}\text{U}$ ratio, a $^{239}\text{Pu}/^{238}\text{U}$ α -activity ratio of 1.17×10^4 is required for an equal probability of fission, a ratio which is not achieved even in the most Pu-active samples studied.

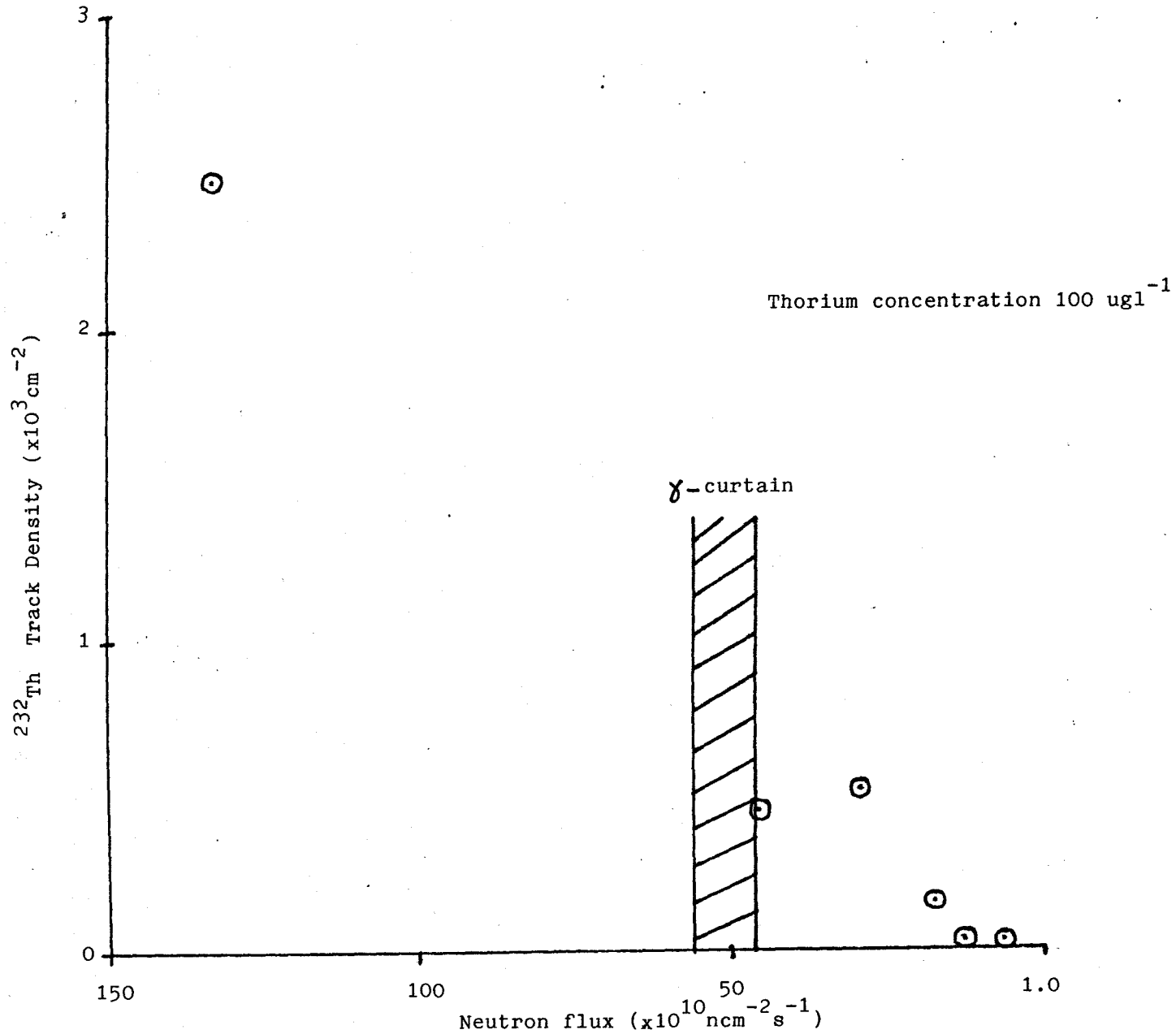


Figure 2.18. Background -corrected track interference from fast fission of ^{232}Th .

2.7 Alpha Track Method

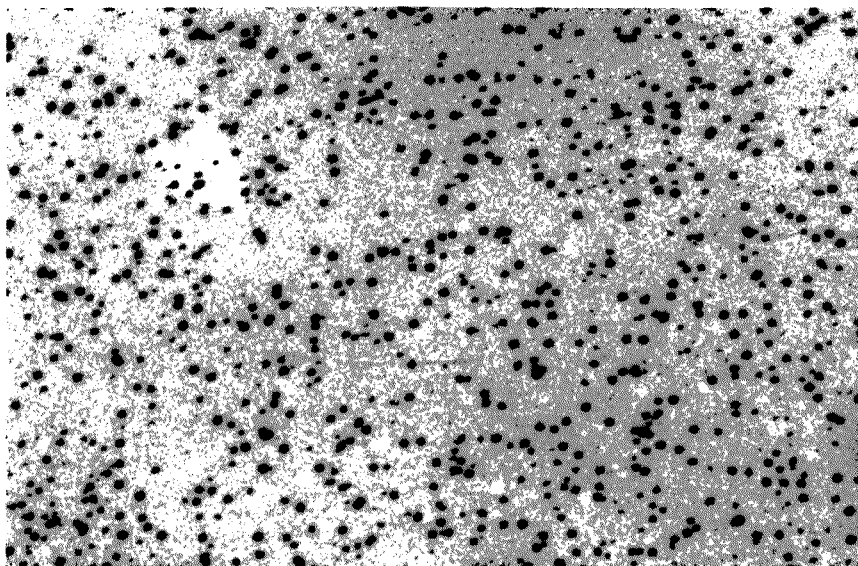
Particle track analysis of environmental alpha-emitting nuclides, either from the three natural decay series or of anthropogenic origin, is a simple and inexpensive technique which offers certain advantages over classical wet radiochemical methods. Very low or high α -activities are detectable since the exposure period of the plastic can be varied from minutes to years. Unlike surface barrier detectors as used in α -spectrometry, the normal availability of the detection system is high, resulting in a high sample turnover rate. However, valuable isotopic data cannot be easily obtained, although Qaquissh and Besant (1976) have shown that reasonable α -energy estimates may be possible by measuring 90° incident α -track diameters or producing range-energy relations after both carefully controlling etching procedures and ensuring bombardment by α -particles of known energy. Indeed, high resolution α -particle spectroscopy has been demonstrated by Fews and Henshaw (1981) using the track detector CR-39, with an energy spread of ~ 35 keV (0.6%) being illustrated for 6 MeV α particles. However, the time and instrumentation needed to measure the required track parameters was not available, and these methods have not yet been proven for real environmental samples.

The nuclear track detector used in this study is the Kodak film LR 115. This medium consists of a thin film (13 μm) of the α -sensitive cellulose nitrate (CLN), strongly coloured red, which is deposited on a thick (100 μm) inert polyester base. The cellulose nitrate is specially treated to increase its response to ionising particles having a sufficiently high linear energy transfer (L.E.T.). The size and extent of the damage region is characterised by the parameter $(dE/dx)_c$, the critical energy loss rate for track formation (Fleischer et al., 1965). The quantity dE/dx in the CLN medium is the specific ionisation and is a function of the energy, charge, and mass of the incident positive ion. Therefore with a knowledge of $(dE/dx)_c$ for a particular detector, it is possible/

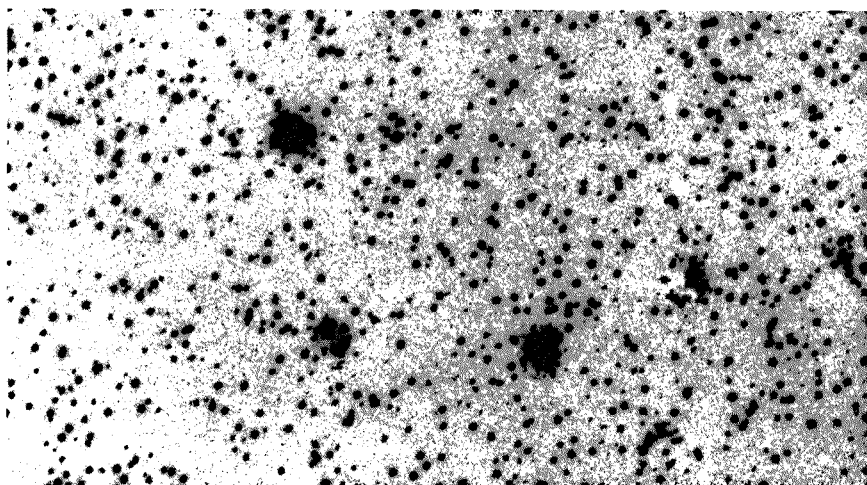
possible to predict which size of charged particle would be registered, and the energy range necessary for track registration. The maximum value of dE/dx of the bombarding nuclei increases with atomic number so that for CLN (or indeed for any other material) there is a lower mass limit for ions which can produce tracks. Consequently, the LR115 films are totally insensitive to X or γ ray photons, electrons or to high-energy protons. They can be used to record the tracks of protons of energy $\lesssim 100\text{keV}$, α -particles of energy $\lesssim 4\text{MeV}$ and heavy ions or fission fragments. In α -track formation, the primary energy-loss mechanism at the high initial α -particle velocities is ionisation and electronic excitation of the CLN molecules. As the energy of the α particle decreases as it progresses along its path, the Coulomb interaction time increases, resulting in an increase in the rate of energy loss. When the particle or positive ion reaches velocities comparable to K-shell electron velocities, the ion starts to pick up electrons from the CLN, until velocities comparable to those of valence electrons are reached. The energy loss mechanism then becomes essentially one of elastic collisions between the particle or ion and the atoms of the detector (a process known as nuclear stopping) rather than one of electronic excitation. Thus the specific ionisation reaches a maximum at low energies or low residual ranges in the CLN, giving rise to tracks whose etched diameter shows a corresponding maximum. It is for this reason that, when recording tracks of α particles whose energies exceed about 4 MeV (for example any good, weightless α -source such as electrodeposited Pu, Am, U or Po isotopes), a deceleration medium such as Al foil or polyester film must be inserted between the sample and the track detector. Hashimoto (1971) observed that electrodeposited ^{241}Am α particles (5.486 MeV) produced well-defined particle tracks only with polyester absorbers of thickness/

thickness 12 μm or greater. Aluminium foils of thickness 4.50 mgcm^{-2} were used in this work for autoradiography, since the range in Al of α particles of the isotopes of interest, from ^{238}U (4.19 MeV) to ^{210}Po (7.45 MeV) are about 5 to 10 mgcm^{-2} Al respectively. Electrodeposited planchet samples of these isotopes, of known total α -activity, were applied to the CLN with inserted Al absorber for a period of time sufficiently long (on the order of days) to produce high-density α -autoradiographs. For thick sources, such as a sediment pellet or manganese nodule, the self-absorption effect obviated the need for Al absorbers, and these samples were merely placed in intimate contact with the CLN by means of a screw-down perspex press. Such unprocessed samples, whether in the form of pellets or thin sections required much longer exposure periods, typically of about 6 to 8 months, because of their lower α -activities. For deep-sea sediment core 9936K, double-sided sediment pellets were prepared. The first side of each was removed after 6 months to test different etching parameters and to obtain an indication of the necessary time to accumulate sufficient tracks. The second sides were removed and etched under the optimised etching conditions. After the appropriate exposure period, the CLN was subjected to an etchant solution of 2.5M NaOH at 60°C for 90 minutes in a thermostatically controlled water bath, etching being stopped by washing in a 1 : 1 mixture of ethanol : distilled water. An initial examination of the plastic under X100 or X400 optical magnification was carried out to affirm successful etching. For electrodeposited radionuclide samples, particularly those of the higher-energy α -emitters, it was considered prudent on occasion to subject the sample to a further 30-minute etch under the same conditions, in order to produce a higher proportion of tracks of greater width and which completely penetrated the sensitive layer. Examination of the track record and semi-quantitative trace counting are easily performed owing to the high contrast between the perforations and the red background, an effect/

effect which can be enhanced by use of a green filter or green light source. Non-quantitative α -autoradiography produces a permanent record of the general distribution of α -activity present on the surface of the sample, which for the samples under study can be homogeneous (Figure 2.19a) or can include hot-spots of activity (Figure 2.19b). Photographs such as those shown are taken on the Olympus BHB Microscope using a Pentax K1000 camera mounted on a Pentax microscope adaptor K. An exposure period of 1 second is used at a magnification of X40, with a green filter which is complementary to the hue of the film. For pelletised sediment, track counting is required, and as in the fission track method, this can be achieved either under a calibrated field-area light microscope or with the Quantimet 720 Automatic Image Analyser. Under the Quantimet, at X100 magnification (field of view = $2.482 \times 10^5 \text{ um}^2$), the α -tracks are counted over 50 random fields of view with the Standard Detector module based on a lower threshold setting, above which all lighter features are detected and counted. Only completely-penetrating tracks are therefore recorded under these conditions. A 13mm diameter pellet constructed from a section of sediment containing 0.76 ppm ^{238}U , 3.89 ppm ^{232}Th and 5.26 dpm g^{-1} of ^{230}Th typically produces a track density of $\sim 4520 \text{ cm}^{-2}$ for a CLN application time of ~ 8 months, background tracks being essentially zero. A typical track distribution after application of a sediment pellet to CLN for 334080 minutes is shown in Figure 2.20, with a typical data set of track counts in Table 2.6. As in the fission track method (section 2.6), a programmable calculator interfaced with the Quantimet prints out the total number of tracks counted, the mean and the 1 σ standard deviation. Replicate analyses of α -tracks produced from a National Bureau of Standards glass (SRM 962) containing 37.38 ppm U and 37.79 ppm Th showed a precision of 5.6% (Crawford, 1982)/



(a)



(b)

Figure 2.19. (a) Homogeneous and (b) heterogeneous alpha track distribution in cellulose nitrate detector.

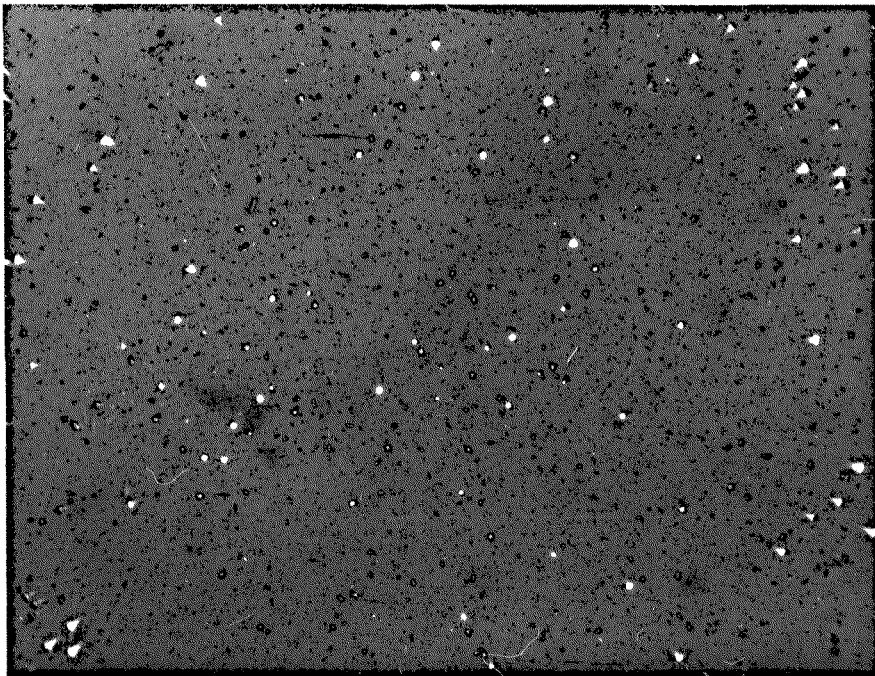


Figure 2.20. Typical alpha track distribution from a 13 mm sediment pellet, application time 8 months.

TABLE 2.6

Typical Quantimet α -track count of a sediment pellet

<u>Field of View</u>	<u>Count</u>	<u>Field of View</u>	<u>Count</u>
1	25	26	25
2	18	27	19
3	22	28	12
4	17	29	34
5	16	30	22
6	13	31	20
7	30	32	18
8	23	33	20
9	21	34	24
10	15	35	21
11	20	36	24
12	17	37	25
13	20	38	31
14	25	39	18
15	18	40	17
16	24	41	18
17	16	42	14
18	23	43	15
19	26	44	21
20	11	45	27
21	22	46	13
22	18	47	21
23	7	48	12
24	27	49	15
25	14	50	15

Mean = 19.68 ± 5.37

1982). The rate R at which α -particle tracks are produced per square centimetre per minute is given by

$$R_{TOT} = C/T \dots \dots \dots (2.3)$$

where T is the CLN - pellet contact time in minutes and C is the track density (cm^{-2}). As a consequence of the incorporation of large amounts of ^{230}Th in deep-sea sediments (Ku, 1976; Osmond, 1979), the above calculation for each section in such a continuous sample, in this case core 9936K, gives rise to a decreasing α -track production rate with depth (Figure 3.1), reflecting $^{230}\text{Th}/^{238}\text{U}$ disequilibrium (Fisher, 1977; Crawford, 1982). In addition, when the results of the α -track (total α 's) and fission track (parent U) analyses are combined, sedimentation rate date consistent with conventional α -particle spectrometry data can be derived (Crawford and Baxter, 1981). The excess α -track density, R_{xs} , is estimated from

$$R_{xs} = R_i - \frac{R_{\infty}}{U_{\infty}} \cdot U_i \dots \dots \dots (2.4)$$

where R_i is the total α -track density for sample i , U_i is the fission-track uranium content in ppm of the same sample and U_{∞} is the uranium concentration at a depth sufficiently great that all excess α -activity is assumed to have decayed back into secular equilibrium with the uranium parents, and R_{∞} is the corresponding α -track density. The error on R_{xs} is determined as shown in appendix A. Sedimentation rate calculation of a pelagic core by the f/ α track and ^{230}Th excess methods is discussed in section 3.1, and the relative merits and deficiencies of each approach is compared.

2.8 Alpha Spectrometry

In order to gain a broader understanding of the marine geochemistry of uranium, it is advantageous to study the well-documented isotopic disequilibrium (see, for example, Osmond and Cowart, 1976) between the two uranium isotopes ^{238}U and ^{234}U , which exists in both aqueous and solid samples. Therefore, since uranium is transported through rivers and estuaries into the oceans and other water basins, controlling the input of the geochemical mass balance (Bloch, 1980), isotopic analyses of river and estuary water samples, muds and, in one case, particulates were performed by α -spectrometry. The analytical methods used for the simultaneous determination of ^{238}U and ^{234}U in both the aqueous and solid samples collected are described here.

2.8.1 Aqueous Samples

All estuarine water samples are filtered through GF/B grade glass microfibre filters under suction. These filters have very high loading capacity and have to be renewed only infrequently. The oven-dried filters are retained for calculation of turbidity, or, if the turbidity is noticeably high, the particulates are allowed to settle and the supernate filtered. In the latter case, the turbidity is calculated as the sum of the dried, settled particulates and the weight on the filters for the same sample. The filtrate is then acidified to $\sim\text{pH } 1$ with 10 ml concentrated HNO_3 to prevent bacterial growth. Five to ten litres of sample, the higher volumes being taken for samples of salinity less than about 10‰, are thoroughly equilibrated with an aliquot of $^{232}\text{U}/^{228}\text{Th}$ tracer and about 50mg of Fe carrier. This carrier is prepared by dissolving ferric chloride hexahydrate in 8 molar HCl and extracting the iron into 8M HCl - saturated di-isopropyl ether (DIPE). Ferric ion is back-extracted into 500 ml distilled water and 5 ml of this solution ($\sim 10\text{mg Fe ml}^{-1}$) taken as Fe (III) carrier. The sample is stirred and evaporated overnight on a hotplate to a volume of ~ 2 litres and carbonate-free ammonia solution added to a pH of about 7 - 8 when hydrated ferric oxide flocs, on which the uranium isotopes and other actinides are adsorbed, become apparent. It is essential that no carbonate ions are present in solution as the uranium forms a carbonate complex/

complex which remains in solution (Urry, 1941; Langmuir, 1978). The gelatinous precipitate is allowed to settle in the warm solution and the supernate decanted off and discarded. The precipitate is transferred with water washings to a 40 ml centrifuge tube and centrifuged on a bench centrifuge for ~5 minutes. It is then washed with 20 ml 0.05 Molar ammonia solution and the washings and supernate discarded. 5 ml of concentrated HCl is added together with 5 ml of 8 molar HCl to dissolve the precipitate. This solution is transferred, with ~10ml 8 molar HCl washings, to a previously prepared anion exchange column (column I). The column consists of a 10 cm X 0.9 cm i.d. glass tubing with a number 2 porosity glass frit at the lower end and a 100 ml reservoir bulb at the top. It is filled to a depth of 5 cm with Bio-rad AG1-X8 anion exchange resin (100-200 mesh) in the chloride form, which had previously been expanded in distilled water, and is preconditioned with 2 x 20 ml portions of 8 molar HCl prior to use. The strongly basic anion exchange resin consists of quaternary ammonium functional groups. Since strong anionic complexes of the uranyl and ferric ions such as $\text{UO}_2\text{Cl}_4^{2-}$ and FeCl_4^- are formed in aqueous hydrochloric acid solutions, separation of these elements from any other metals can be obtained. The adsorption of uranium and iron increases rapidly with increasing molarity of the HCl, the distribution coefficient for uranium being ~1 with 1 molar and $\sim 10^3$ for molarities ≥ 8 (Korkisch, 1969). Thorium, which does not form an anionic complex in an aqueous hydrochloric acid medium (Kraus et al., 1956), passes through the column. However protactinium (Kraus and Moore, 1950) polonium and plutonium if present (Wish, 1959; Talvitie, 1971; Ballestra et al., 1978) will closely follow the uranium behaviour.

After loading the sample, the column is washed with 30 ml 8 molar HCl, and, since thorium is not to be determined, the eluate is discarded. The iron and uranium are eluted from the column/

column with 50 ml of 0.2 molar HCl into a 250 ml beaker, a procedure which leaves many co-adsorbed transition metals such as Zn and Bi still adsorbed on the column. The eluate is evaporated to dryness on a hotplate, and the black anhydrous residue taken up in 25 ml 8 molar HCl. The solution is then quantitatively transferred to a 100 ml separating funnel and shaken with the same volume of 8 molar HCl - saturated di-isopropyl ether (DIPE). The bulk of the iron is extracted into the organic phase by ion-pair formation between the protonated extractant cation and FeCl_4^- , while uranium remains in the aqueous phase. The lower aqueous phase is withdrawn into a 250 ml beaker and a 5 ml 8 molar HCl washing of the ether combined with it. The DIPE extraction is repeated and the aqueous layer brought to near dryness on a hotplate. The sample is wet washed by repeated addition of 5 ml concentrated HNO_3 and evaporation to near-dryness. It can become difficult to dissolve the residue completely in nitric acid if the solution is evaporated to complete dryness (Sill, 1974) because of the formation of a refractory oxide. Six ml of 7 molar HNO_3 is added to the beaker and the contents transferred with 3 ml 7M HNO_3 washings to a second Bio-rad AG1-X8 anion exchange column (column II). This column, identical in design to that of column I, consists of a 14 cm resin bed, preconditioned with 2 x 50 ml 7 molar HNO_3 washings. In aqueous HNO_3 solutions, the uranium complex anion is only weakly adsorbed on the anion exchange resin, the distribution coefficient, K_D , being between 12 and 16 (Korkisch, 1969) for a HNO_3 molarity of 7. However, since iron has an even smaller K_D value in this nitric acid medium, further and essentially complete purification of uranium from iron can be achieved by controlled, slow washing of the sample through the column with 7 molar nitric acid. Therefore, after the 6 ml of sample plus 3 ml washings have been loaded onto column II, a further 20 ml of 7 molar HNO_3 is loaded by dropping funnel/

funnel at a flow rate of ~ 2 ml per minute. The purified uranium is then eluted with 50 ml 0.2 molar HCl into a 50 ml beaker and 1 ml of concentrated H_2SO_4 added. The solution is evaporated to fumes of SO_3 , before which a yellow colour is observed due to organic residues from the column. The solution is allowed to cool, 5 ml concentrated HNO_3 added and the organics oxidised by again taking to fumes of SO_3 . The solution is then allowed to cool. For subsequent α -spectrometric analysis of the sample, the method of choice for source preparation from the many suitable techniques reviewed by Yaffe (1962) and Lally (1982), is electrodeposition. Ideally, the source should have a monatomic layer of the radionuclides of interest, with no intervening foreign material between source and detector to produce α attenuation. This situation is closely met by the electrodeposition method which affords the thin, uniform and nearly weightless sample mounts required for high resolution of the α -energies. The procedure used here is based on the work of Talvitie (1972) in which the sample is fumed with H_2SO_4 (preventing premature hydrolysis of the actinides) and an ammonium sulphate electrolyte prepared. If electrolytes containing chloride are used, chlorine evolution will result in the etching of the platinum anode and stainless steel cathode unless an organic acid such as oxalic acid is added (Puphal and Olsen, 1972), and both the Pt and Fe will redeposit along with the actinides, resulting in a degraded α -spectrum (Kressin, 1977).

To the cooled, concentrated sulphuric acid solution containing the purified uranium isotopes, 5 ml of distilled water and 2 - 3 drops of thymol blue indicator are added. The pH is then adjusted to 2.0 (using Whatman BDH pH1 - 4 narrow range indicator papers) by addition of concentrated ammonia. The ammonia liquor should be silica-free, or vapour used, to prevent formation during electrolysis of flocs/

flocs which could adsorb the actinides present (Talvitie, 1972). The resulting ammonium sulphate electrolyte is quantitatively transferred with 5 ml distilled water washings to an assembled electrodeposition cell. The cell (Figure 2.21) is similar in design to that used by Thomson (pers.comm.). It consists of a brass base containing a water coolant jacket, spade-clip attachment for the cathode and a shallow recess for holding the planchet. The planchets (Nuclear Supplies) are 2.5 cm diameter, mechanically-polished stainless steel, which come provided with a protective screen to prevent scratching or contamination before use. The brass screw-down collar holds the teflon chimney and forces a watertight seal between the teflon and the planchet when tightened. The teflon cell incorporates two small exhaust holes near the top to allow escape of hydrogen during the plating procedure. The anode consists of 0.75 mm diameter platinum wire, partially enclosed in glass, the last 10 cm of which is wound into a coil. The rubber 'O'-ring is positioned round the sleeve so that when the anode and teflon cap are inserted into the cell, the anode-cathode distance is 0.5 cm. The total capacity of the assembled cell is 17.5 ml and the plating area is 1.77 cm^2 . Electrolyses were performed without stirring, using a Coutant LQ100/30 power supply capable of providing 0-30V and 0-1A. A current of 1 amp (current density 0.57 Acm^{-2}) is passed through the cell for 3 hours and the temperature maintained at $\sim 60^\circ \text{C}$ by use of the water jacket. A voltage reading of between 8 and 9V indicated that the electrical resistance of the ammonium sulphate electrolyte was $\sim 8 \Omega$ for the 0.5 cm anode-cathode spacing, which compares favourably with other electrolytes; for example (Kressin, 1977) a $\text{NaHSO}_4 - \text{Na}_2\text{SO}_4$ electrolyte with a resistance of 18Ω for a 180-minute, 0.39 Acm^{-2} plating and a 5 mm electrode-planchet spacing resulted in evaporation of up to 25% of the electrolyte solution. When electrolysis is complete, 2 ml of concentrated NH_3 is added via one of the exhaust holes/

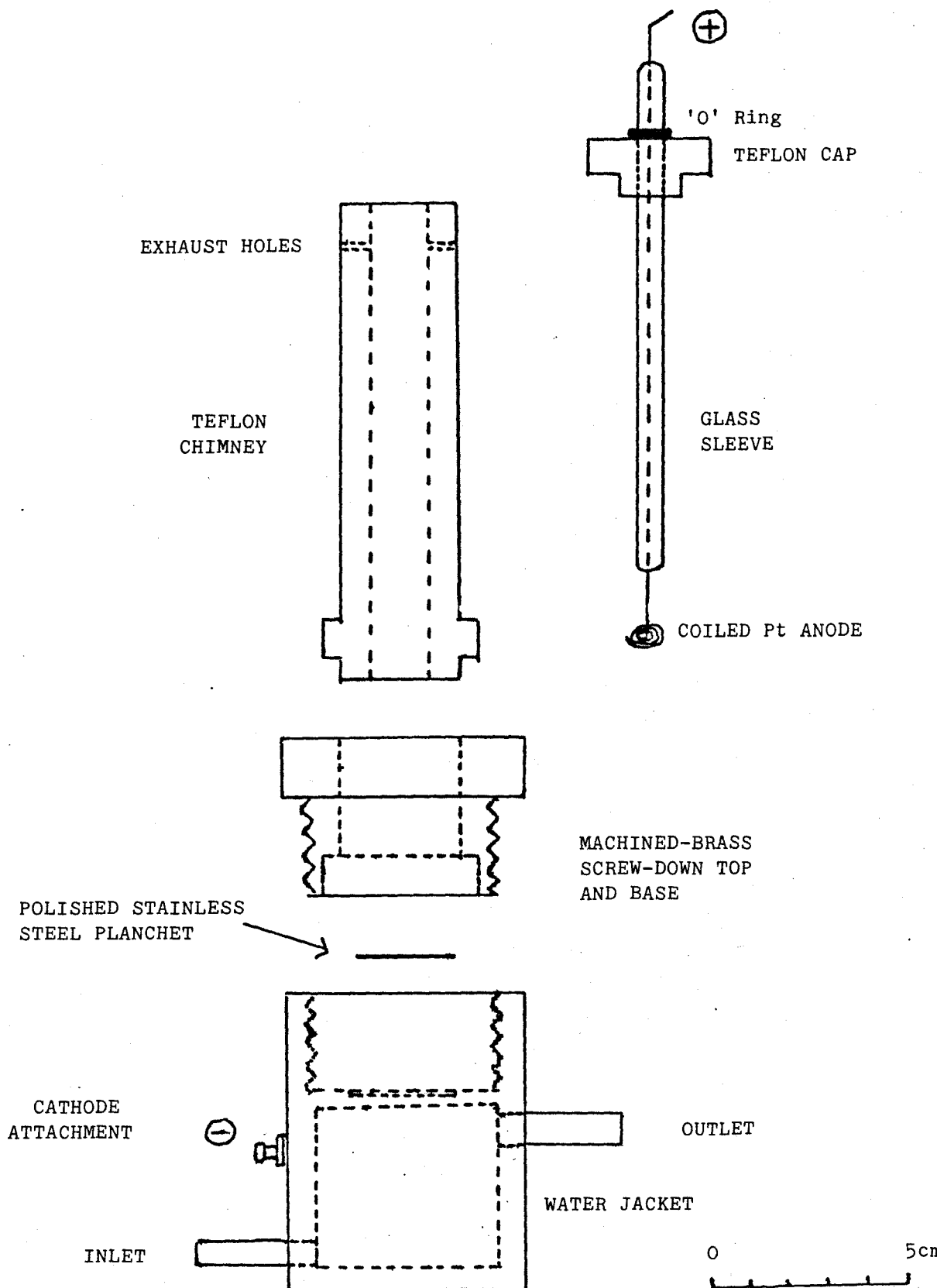


FIGURE 2.21. Electrodeposition cell, dismantled.
Total capacity 17.5 ml with anode inserted.

holes and the plating left for 1 minute. After removing the Pt anode, the current is switched off and the electrolyte discarded. The cell is rinsed with ~2ml distilled water and the planchet removed and rinsed in methylated spirits, made to pH8 with dilute NH_4OH . It is then heated on a hotplate at 200 to 250°C to remove volatile Po isotopes. Higher temperatures oxidise the planchet surface and result in poorer resolution. From subsequent α -autoradiography (section 3.5) using cellulose nitrate plastic, it was observed that the activity was deposited homogeneously on the planchet. The sample is then ready for counting in an α -spectrometer system.

2.8.2 Solid Samples

Collected estuarine mud samples and particulate matter are dried overnight in an oven at 110°C and these and other dry solid samples are broken up individually in a mortar and pestle to a small particle size. Thereafter they are further homogenised and powdered in an agate ball mill for 15 minutes. About 5g of sample is weighed accurately to better than 0.0001g into a silica crucible and ashed overnight in a muffle furnace at 500°C. Suspended particulates from the Clyde and Tamar estuaries, with total sample weights ranging only from 0.1218 to 0.3974g and from 0.0498 to 0.2450g respectively, were not analysed for uranium isotopes, since it was estimated that an error of up to 20% would result for the $^{234}\text{U}/^{238}\text{U}$ activity ratio, assuming 100% chemical efficiency and a uranium content of ~1.5 ppm (Borole et al., 1982). This level of precision was considered unsatisfactory since sample activity ratios were unlikely to vary outside this $\pm 20\%$ range. For the Forth estuary samples, which had by far the greatest turbidity at time of sampling, the total weight of suspended particulate matter ranged from 0.2354 to 1.868g and it was decided to pool the high-salinity samples (low turbidity) together and low-salinity/

salinity samples (high turbidity) together for dissolution and uranium analysis. Ashing in a muffle furnace at 500°C decomposes the organic matter present in the sample. Rapid reweighing of the silica crucible and ashed samples gives the % loss on ignition, which can be approximated as the % organic carbon. The sample is then carefully and quantitatively transferred to a 250 ml teflon beaker and moistened with a few drops of distilled water. An aliquot of ^{232}U tracer is added, equal in activity to about twice the expected ^{238}U content, followed by 50 ml of 8 molar HCl. The solution is then heated to near-dryness to ensure, as far as possible at this stage, the equilibration of tracer and leached isotopes on which all such spike methods depend. 25 ml of concentrated HNO_3 is added and the solution covered, and heated to $\sim 80^{\circ}\text{C}$ for 2 hours, during which time brown NO_2 fumes are evolved. Since acid leaches have been shown to release around 33% (mainly authigenic) of the total uranium from sediments (Rona and Emiliani, 1969; Mo et al., 1971), the balance of uranium must be incorporated within the lattice matrix of the minerals present and so complete dissolution of the silicates and any refractory clay minerals must be effected. Thus, 25 ml of HF (40% w/v) is added and the solution evaporated to small volume with release of volatile SiF_4 . The solution is clear at this stage and if a gelatinous precipitate remains equal volumes of HF (40% w/v) and concentrated HNO_3 are added and the mixture boiled. After again taking to near dryness, the residue is leached with 25 ml 8 molar HCl and heated to remove any HF and HNO_3 . Following filtration of the solution, a fine black powder sometimes remains on the filter paper, being less than 0.1% of the original sample weight. Microanalysis of this powder gave 95.9% C, 1% N, 0% H, suggesting that it might be coal dust. The filtrate is stirred, boiled down to ~ 10 ml and 50 ml distilled water added. Addition of concentrated CO_2 -free ammonia precipitates the hydrous oxides of the iron and aluminium/

aluminium carriers naturally-present and the actinides are scavenged on these. The solution is cooled, transferred to a 250 ml linear polyethylene centrifuge bottle and the precipitate centrifuged down at 2000 r.p.m. for ~20 minutes. The supernate is decanted off and 10 ml concentrated HCl, followed by 10 ml of 8 molar HCl, added to dissolve the precipitate. After DIPE extraction of the bulk of the iron, the anion-exchange purification on Bio-rad AG-1X8 resin is identical to the procedure used for aqueous samples, unless plutonium isotopes are known to be present. This was certainly the case for the samples taken from the vicinity of the Dounreay Nuclear Power Development Establishment in Caithness, where the $^{239,240}\text{Pu}$ activities reached about 40 pCi g^{-1} (Cook et al., 1984). Mackenzie and Scott (1982) found $^{239,240}\text{Pu}$ concentrations of 0.03 pCi g^{-1} in the intertidal surface sediment in the River Clyde, values which can constitute a significant interfering α -activity contribution, since the main α energies of ^{239}Pu and ^{240}Pu (5.157 and 5.168 MeV respectively), are close to those of the added ^{232}U tracer (5.320 MeV (68.6%) and 5.263 MeV (31.2%)). This interference is particularly bad for thick sources in which the α -spectrum peaks have low-energy tails. The activity contributions from plutonium isotopes in water samples are not so important, since the levels rapidly fall northwards to fCi l^{-1} level in the Irish Sea (Murray et al., 1978).

The method for plutonium-uranium separation is that described by Lally and Eakins (1978). Although the authors were interested in the Pu fraction, the eluate from their first anion-exchange column can easily be assayed for U. The sample solution containing the Pu and U isotopes is loaded, as before, onto an 8 molar HCl-conditioned, 5 cm deep bed of Bio-rad AG-1X8 (100-200 mesh) anion exchange resin. 8 molar HCl washing removes rare earths, thorium and radium isotopes; a subsequent 100 ml 7 molar HNO_3 washing removes iron, uranium and polonium isotopes, while plutonium remains on the column, capable of being removed only/

only by reduction to the non-adsorbed Pu^{3+} species by eluting with, for example, 1.2 molar HCl - 0.6% H_2O_2 (Talvitie, 1971) or 11.1 molar HCl - 0.2 molar HI (Lally and Eakins, 1978). For samples with known high Pu concentrations, the nitric acid eluate is converted back to the chloride form and the above steps repeated to purify the uranium further from plutonium. The nitric acid eluate is taken to near-dryness, converted to chloride form and purified further from iron by 8 molar HCl/DIPE extraction, being subsequently processed as for water samples. In order to quantify the extent of $\text{U} - \text{Pu}$ separation using the above method, 1 ml aliquots of $^{232}\text{U}/^{228}\text{Th}$ (11.94 dpm) and ^{242}Pu (8.92 dpm) spike solutions were combined and taken through the procedure with ~ 50 mg Fe carrier. Only one initial 5 cm column was used. Integration of the counts under both the ^{242}Pu peak and the ^{232}U peak indicated a separation efficiency of 97.84%. Assuming a 1π geometry factor, and neglecting backscatter and self-absorption (Faires. and Boswell, 1981), recoveries of uranium from aqueous samples ranged from 8.5 to 63.9% (mean 30.4%) and for solid samples from 10.4 to 61.0% (mean 33.8%). Where possible, solid samples were analysed in duplicate.

2.8.3 α - Spectrometry - Theory and Instrumentation

All radiation detectors, including the solid state dielectrics discussed in sections 2.6 and 2.7, work on the principle that the detected radiation gives up some or all of its energy to the medium of the detector either by primary or secondary ionisation processes. In α -spectrometry, the silicon surface barrier detector, housed in a high vacuum chamber to reduce air scatter, is used to detect the α -radiation from the electrodeposited uranium sources. In the silicon semiconductor, the energy gap between the valence band and the conducting band is 1.1eV, a value which results in minimal occupation of the conduction band by thermally-excited electrons. n-type impurities present in the Si donate electrons to the conduction band, while p-type impurities accept electrons from the/

the valance band, thus if n - and p-type materials in contact are subjected to a bias voltage such that is is positive to the n-type material, the free charge carriers are drawn away from both sides of the n-p junction to leave a depletion layer with almost no charge carriers. Such a junction is prepared by allowing a thin surface of a high purity n-type silicon wafer to oxidise (p-type layer). A thin gold film of uniform thickness ($\sim 40 \text{ ugcm}^{-2}$) is then vacuum-deposited on this p-type surface to act as a contact, while a thin layer of aluminium ($\sim 40 \text{ ugcm}^{-2}$) provides the contact for the rear n-type face (Goulding and Stone, 1970). Under these conditions, current flow through the device is highly limited since neither the n or p regions can supply carriers of appropriate sign. When an α -particle enters the detector, ionisation occurs and electrons are excited into the conduction band. Electron-hole pairs are thus produced in the Si, with an energy-loss rate of 3.6 eV per pair per α -particle, which are swept rapidly towards the electrodes under the applied electric field. Provided that the depth of the depleted or sensitive region is greater than the range of α -particles of interest and that electron-hole recombination does not occur, then the charge collected is proportional to the energy of the incident α -particle. Ancillary electronic equipment consists of a preamplifier which does some amplifying and pulse shaping, but its chief purpose is to match the small-voltage output pulses from the high-impedance cables between it and the detector, into low-impedance cables. The preamplifier also transfers the bias voltage to the detector from the bias voltage supply unit. Further pulse shaping and amplification is performed by the main amplifier which incorporates a linear gain control, set so that the largest pulses do not overload the amplifier. A biased amplifier accepts the shaped output pulses from the main amplifier (still proportional to the incident α -energy) and provides expansion of any selected portion/

portion of the total spectral range for the analysis of a region of interest; the pulses are fed to a pulse height analyser, which sorts them according to their amplitude, and an analogue-to-digital converter (ADC) gives out a digital signal proportional to the pulse height. During counting, the multichannel analyser (MCA) accumulates a spectrum of the number of particles of a particular energy (channel contents) versus particle energy (channel number).

In this work, four Ortec silicon/gold surface barrier detectors (EG and G Ortec Instruments) of active area 300mm^2 and minimum depletion depth $100\ \mu\text{m}$ were used. Bias voltage was provided by two Ortec Model 428 dual voltage supplies through four preamplifiers (2 x Ortec Model 125, 2 x Ortec Model 142B). The detector output signals were fed through twin pulse-shaping spectroscopy amplifiers (Ortec Model 471) and twin bias amplifiers (Ortec Model 408A) into the quarters of a 204.2 channel ADC of a multichannel analyser (Canberra Series 80 MCA - version 2).

Since sample count rates amounted to only a few counts per minute, low detector background and low blank contributions were desirable for the long counting times used (~ 48 hours). For the four detectors, background count rates in the ^{238}U , ^{234}U and ^{232}U peak regions are shown in table 2.7 for the dates indicated. No evidence of background increase due to detector contamination by recoil nuclides (Sill, 1970) was evident for the ^{238}U or ^{234}U regions, but there were significant increases in the ^{232}U spike region, due probably to ^{228}Th recoil atoms on the detector face, or to ^{210}Po (alpha energy 5.305 MeV) transferred from sample mounts. Reagent blanks, using 5 ml of the Fe (III) carrier solution, were run and the blank contribution found to contribute $0.01\ \text{dpm } ^{238}\text{U}$ and $0.03\ \text{dpm } ^{234}\text{U}$; corresponding to from 3.6 and 11.6% respectively of the lowest/

TABLE 2.7

Detector Backgrounds. Activity in counts per hour.

Date: 4/10/82.

<u>Detector</u>	<u>^{238}U Region</u>	<u>^{234}U Region</u>	<u>^{232}U Region</u>
1	0.02	0.02	0.02
2	0.04	0.32	0.21
3	0.15	0.15	0.10
4	0.08	0.19	0.51

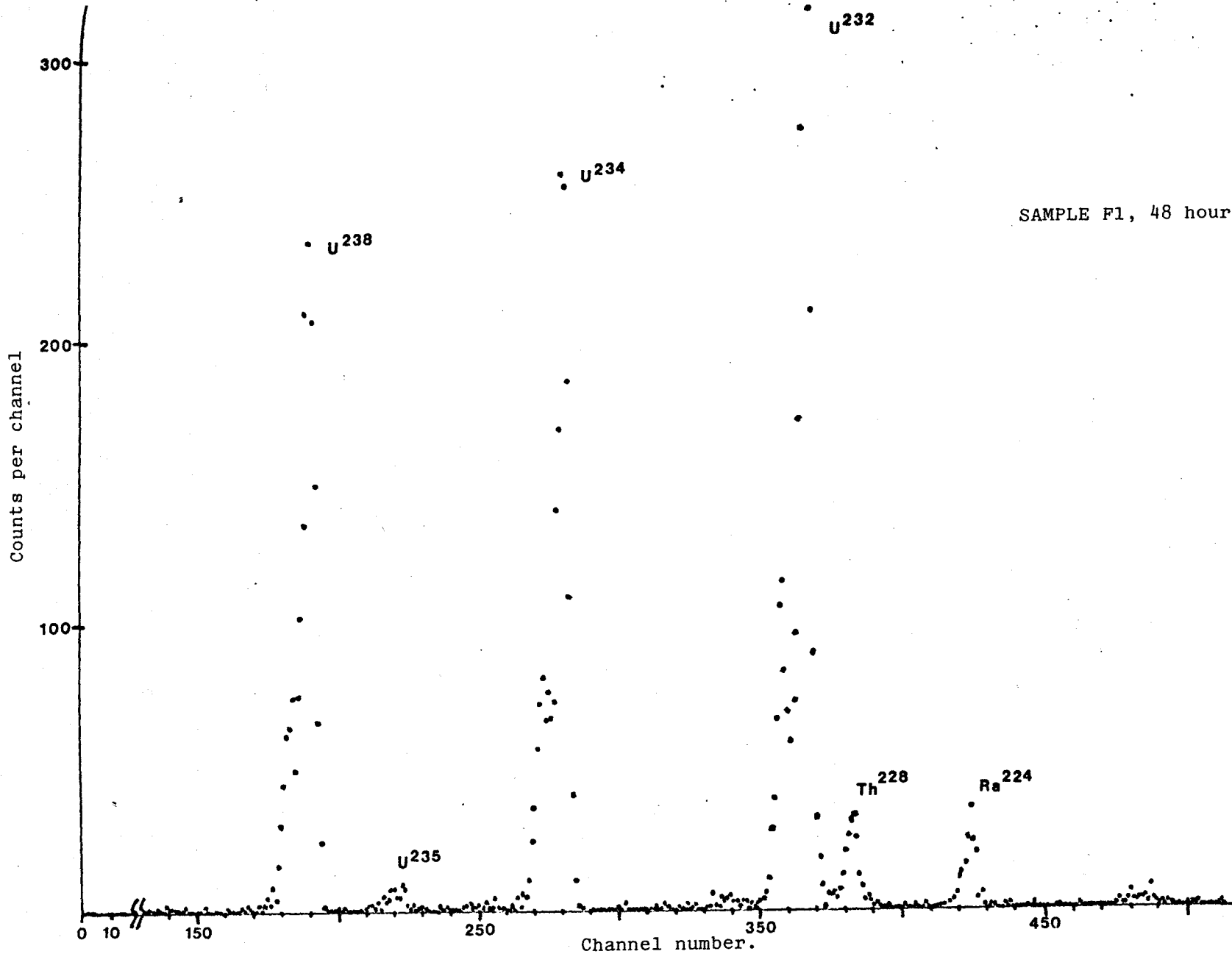
Date: 20/7/83

<u>Detector</u>	<u>^{238}U Region</u>	<u>^{234}U Region</u>	<u>^{232}U Region</u>
1	0.02	0.00	0.19
2	0.08	0.10	0.27
3	0.10	0.08	0.77
4	0.02	0.19	1.02

lowest uranium content sample analysed, to 0.08 and 0.21% respectively of the highest uranium sample. Both the blank and detector backgrounds were subtracted from the peak integrals and net counts used to give absolute concentrations and isotope ratios of ^{238}U and ^{234}U . Appendix C shows a Fortran IV program compiled to calculate the ^{238}U content and $^{234}\text{U}/^{238}\text{U}$ activity ratio of water samples in dpm l^{-1} . A conversion factor of $1.343 \text{ ug/dpm}^{238}\text{U}$ is used to give concentrations in $\text{ug l}^{-1} \text{ }^{238}\text{U}$. Figure 2.22 shows a typical sample spectrum, with ^{238}U (97% 4.196 MeV, 23% 4.149 MeV), ^{234}U (72% 4.774 MeV, 28% 4.723 MeV) and ^{232}U (69% 5.321 MeV, 31% 5.264 MeV) peaks clearly resolved (data from Lederer and Shirley, 1978). This particular spectrum was obtained from a source which was recounted 3 months after electroplating, and therefore shows ingrowth of the uranium spike daughters ^{228}Th ($t_{\frac{1}{2}}$ 1.91 yrs, E_{α} 5.421 MeV) and ^{224}Ra ($t_{\frac{1}{2}}$ 3.665 d, E_{α} 5.686 MeV). Since samples were normally counted within 1 week of plating, the daughter peaks were not usually observed. As can be seen, the resolution (26 keV) with a 7 - 8 mm source-detector clearance is sufficiently good to show doublets for each nuclide, although a smaller source-detector distance will have a greater detection efficiency but at the expense of resolution. The spectral region can be energy-calibrated to check for electronic drift or α -degradation by using a three-standard source (Radiochemical Centre, Amersham, code AMR22) containing ^{241}Am , ^{244}Cm and ^{239}Pu nuclides of combined activity $2.99 \times 10^4 \text{ dpm}$, determined in a 2π proportional counter.

2.8.4 Spike Solutions

Throughout the project, three different spike solutions were obtained. The first, an aged $^{232}\text{U}/^{238}\text{Th}$ solution was originally obtained from the Lamont-Doherty Geological Observatory, Columbia University, New York, uranium purification having been carried out in January, 1950. The spike had a ^{232}U activity of 5.4 dpm ml^{-1} in August, 1968, and an alpha contribution from ^{233}U , equal to/



SAMPLE F1, 48 hour count.

Figure 2.22. Typical alpha spectrum. Ingrowth of ^{232}U daughters shown by recounting sample after a storage period of about 3 months.

to 2.2% of the ^{232}U activity, falling in the ^{234}U peak region (Thomson, 1972). These values were decay-corrected on 16th November, 1982 to 4.72 dpm ml^{-1} and 2.5% respectively. Duplicate water samples were analysed, one using this Lamont spike and the other with one of the well-characterised Harwell spikes (discussed below) to determine whether adsorption of spike on the container walls had occurred over the long time period since its last use. Since both results agreed within error ($2.33 \pm 0.11 \text{ ug l}^{-1}$ and $2.25 \pm 0.07 \text{ ug l}^{-1}$), it was assumed that the Lamont spike was good and could be used as and when required. 2.5% of the ^{232}U peak must, however, be subtracted from the ^{234}U peak due to the ^{233}U impurity.

The other two ^{232}U spikes were recent solutions from Harwell. A limited amount of the first spike (provided by A. B. Mackenzie, Scottish Universities Research and Reactor Centre, East Kilbride) had an activity of $11.94 \pm 0.12 \text{ dpm g}^{-1}$ on 12th May, 1982. The second (provided by J. Thomson, Institute of Oceanographic Sciences, Surrey) had an activity of 33.5 dpm ml^{-1} ^{232}U on 30th April, 1980, corrected to $32.79 \text{ dpm ml}^{-1}$ on 19th July, 1983.

CHAPTER THREE

This chapter presents and analyses the particle track and α -spectrometric data obtained by the methods outlined in sections 2.6, 2.7 and 2.8. For the sake of clarity, the different applications of the fission track, α -track and wet radiochemical techniques will be discussed individually in separate sections.

3.1 Particle Track Dating of Deep-Sea Core 9936K

The particle track analogue of the conventional ^{230}Th dating technique (Ku, 1976; Osmond, 1979) can be applied usefully to deep-sea sediments. Both methods rely on the well-known isotopic disequilibrium situation which results from the preferential hydrolysis and particulate scavenging of Th over U isotopes. ^{230}Th , formed continuously by decay of its conservative parent ^{234}U in sea water, is thus quantitatively removed (Moore and Sackett, 1964) on settling particulate matter, and accumulates on the sea-floor as unsupported, or excess, ^{230}Th . Subsequent parent-unsupported decay with a half-life of 7.52×10^4 yrs occurs in the sediment column, the specific ^{230}Th activity decreasing with depth (time). Since the total ^{230}Th content of a sediment is the sum of this excess contribution and of a ^{234}U -supported component, both U and Th isotopic analyses must be performed. The development of analytical methods to measure ^{230}Th directly (Isaac and Picciotto, 1953; Goldberg and Koide, 1958) provided proof of $^{226}\text{Ra}/^{230}\text{Th}$ disequilibrium in surface sediments. In the absence of diffusion, the ^{226}Ra concentration of a continuous deep-sea core would increase with depth until it reaches equilibrium with ^{230}Th , then decrease from its peak concentration with the half-life of the ^{230}Th parent until secular equilibrium with ^{234}U is attained. The use of ^{226}Ra as an index of excess ^{230}Th as assumed by Urry (1942, 1948, 1949) for the dating of several cores was brought into/

into question by Kroll (1953, 1954) who found an erratic ^{226}Ra distribution in most of the cores studied, with secondary maxima and minima, suggesting Ra migration. Such diffusion was subsequently proven by Cochran and Krishnaswami (1980) and in model ^{226}Ra profiles by Kadko (1980). The current state of refinement of the ^{230}Th dating technique is exemplified by Thomson (1982) who describes a fusion method for total sample dissolution before separate U and Th α -activity determination, and variations of the method for use on different sediment types. In contrast, the particle track analysis (P.T.A.) method uses the measured depth-related trends in fission and α -particle damage track densities produced in the plastic detector films (sections 2.6 and 2.7) as indicators of uranium isotope and total ^{230}Th profiles respectively (Fisher, 1978; Crawford, 1982). The applicability of the track technique to the analogous ^{210}Pb dating of rapidly-accumulating nearshore or lacustrine sediments has also been demonstrated (Baxter et al., 1981).

Tables 3.1 and 3.2 display all the particle track and relevant radiochemical data respectively for core 9936K. In table 3.1, R_{TOT} is the total α -track production rate calculated using equation 2.3 and a sediment pellet : CLN plastic application time of 341280 minutes. R_{XS} is the excess α -track production rate calculated from equation 2.4 using a mean R_{∞}/U_{∞} value of $0.0110 \text{ Tcm}^{-2} \text{ min}^{-1} \text{ ppmU}^{-1}$ to correct for α -emitters in secular equilibrium with ^{238}U and ^{232}Th . In table 3.2, subtraction of the ^{234}U -supported ^{230}Th activity from the total ^{230}Th levels produces the ^{230}Th excess values down the core. Figure 3.1 shows the variation in R_{TOT} with depth, reaching maximum levels of up to $0.0237 \text{ Tcm}^{-2} \text{ min}^{-1}$ between about 5 and 15 cm and steadily declining beyond 20 cm to $\sim 0.0070 \text{ Tcm}^{-2} \text{ min}^{-1}$. Examination of the ratios of ^{230}Th to ^{234}U (Table 3.2) indicates that decay of ^{230}Th excess to equilibrium is still not achieved at 68cm. This type of profile is interpreted as reflecting the radioactive decay with depth predominantly of the unsupported ^{230}Th and of its ingrown α -daughters ^{226}Ra through ^{210}Po .

The/

TABLE 3.1

Particle Track data for core 9936K

Depth (cm)	R_{TOT} ($Tcm^{-2} min^{-1}$)	U(ppm)	R_{xs} ($Tcm^{-2} min^{-1}$)	% $CaCO_3$
0 - 2	0.0077 \pm 0.0003	0.73 \pm 0.03	-	74.35
2 - 4	0.0078 \pm 0.0004	0.61 \pm 0.03	-	75.92
4 - 6	0.0225 \pm 0.0007	0.72 \pm 0.03	0.0146 \pm 0.0014	76.39
6 - 8	0.0144 \pm 0.0003	0.51 \pm 0.02	0.0088 \pm 0.0011	76.90
10 - 12	0.0213 \pm 0.0007	0.54 \pm 0.02	0.0154 \pm 0.0015	77.73
12 - 14	0.0186 \pm 0.0006	0.56 \pm 0.02	0.0124 \pm 0.0014	77.02
14 - 16	0.0237 \pm 0.0007	0.48 \pm 0.02	0.0185 \pm 0.0013	73.66
16 - 18	0.0125 \pm 0.0005	0.73 \pm 0.03	0.0045 \pm 0.0016	71.28
18 - 20	0.0130 \pm 0.0005	0.69 \pm 0.03	0.0054 \pm 0.0016	71.91
20 - 22	0.0158 \pm 0.0006	0.79 \pm 0.03	0.0072 \pm 0.0014	71.61
26 - 28	0.0132 \pm 0.0005	0.78 \pm 0.03	0.0047 \pm 0.0017	66.45
28 - 30	-	0.73 \pm 0.03	-	68.12
32 - 34	-	0.75 \pm 0.03	-	66.73
38 - 40	-	0.77 \pm 0.03	-	69.36
42 - 44	0.0090 \pm 0.0004	0.59 \pm 0.03	0.0025 \pm 0.0015	74.53
46 - 48	-	0.49 \pm 0.02	-	73.18
48 - 50	0.0085 \pm 0.0004	0.60 \pm 0.03	0.0020 \pm 0.0015	71.93
52 - 54	0.0079 \pm 0.0004	0.72 \pm 0.03	-	71.12
54 - 56	-	0.77 \pm 0.03	-	71.20
56 - 58	-	0.66 \pm 0.03	-	70.19
58 - 60	-	1.01 \pm 0.04	-	65.04
60 - 62	0.0066 \pm 0.0003	0.89 \pm 0.03	-	63.36

TABLE 3.2

 α -spectrometric data for core 9936K

Depth cm	U ppm	$\frac{^{234}\text{U}}{^{238}\text{U}}$ activity ratio	^{230}Th dpm/g	^{234}U dpm/g	^{230}Th dpm/g ^{excess}
2 - 4	0.60 \pm 0.02	0.99 \pm 0.05	11.0 \pm 0.2	0.44 \pm 0.02	10.6 \pm 0.2
10 --12	-	-	8.91 \pm 0.17	-	(8.5 \pm 0.2)
14 - 16	0.66 \pm 0.02	1.60 \pm 0.05	8.25 \pm 0.17	0.52 \pm 0.02	7.7 \pm 0.2
18 - 20	-	-	6.31 \pm 0.15	-	(5.9 \pm 0.2)
26 - 28	0.76 \pm 0.03	1.05 \pm 0.06	5.26 \pm 0.10	0.59 \pm 0.03	4.7 \pm 0.1
32 - 34	0.83 \pm 0.04	0.93 \pm 0.06	5.44 \pm 0.13	0.57 \pm 0.03	4.9 \pm 0.1
38 - 40	0.77 \pm 0.05	0.80 \pm 0.07	4.75 \pm 0.11	0.46 \pm 0.03	4.3 \pm 0.1
46 - 48	0.63 \pm 0.03	0.96 \pm 0.06	4.67 \pm 0.07	0.45 \pm 0.03	4.2 \pm 0.1
52 - 54	0.77 \pm 0.03	0.93 \pm 0.04	2.87 \pm 0.06	0.53 \pm 0.02	2.34 \pm 0.06
66 - 68	0.91 \pm 0.04	0.89 \pm 0.05	2.20 \pm 0.05	0.60 \pm 0.03	1.60 \pm 0.06

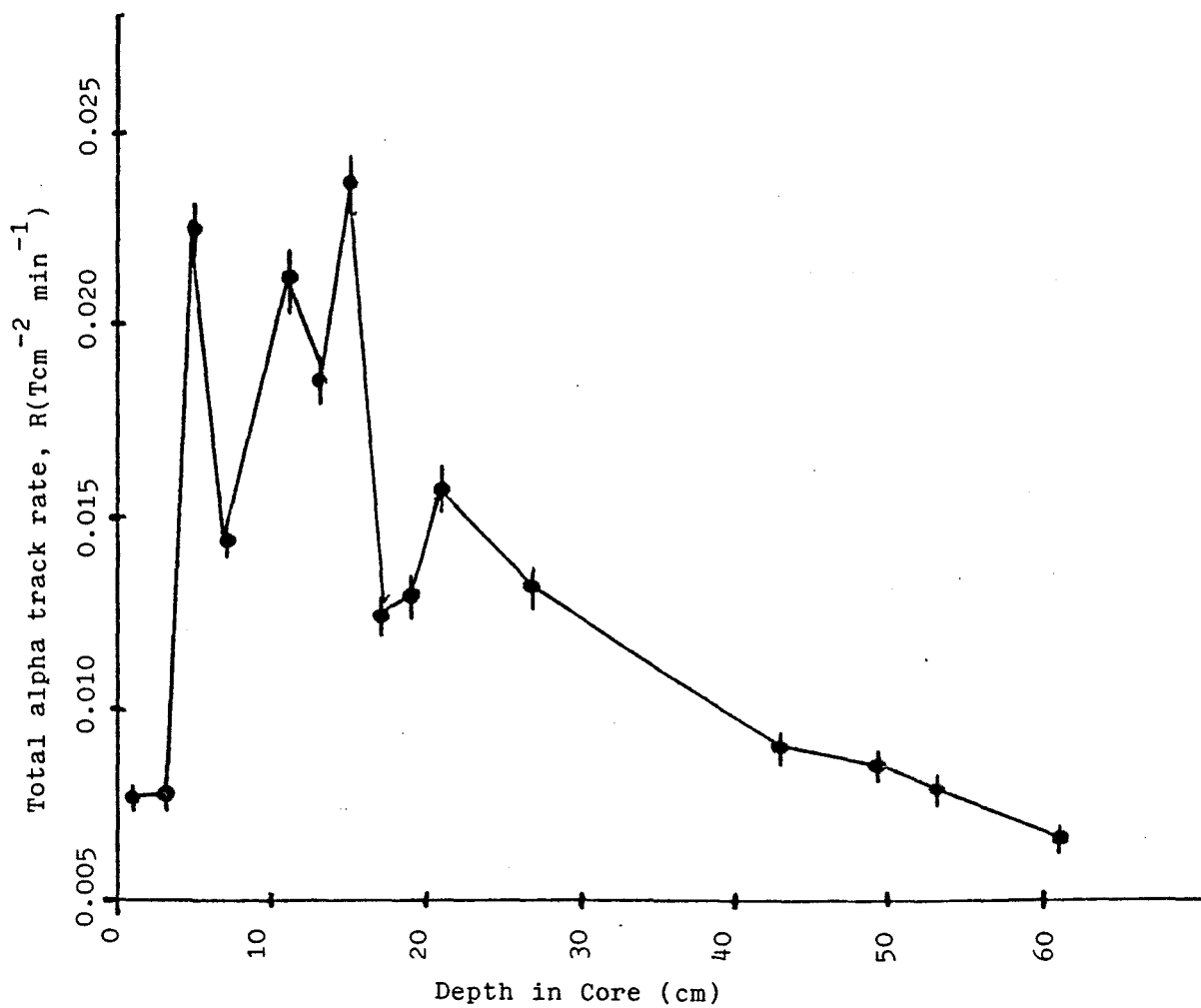


Figure 3.1. Depth profile of total alpha track rate in core 9936K.

The apparent loss of α -activity in the top 3 or 4 cm of the core (Figure 3.1) is calculated as $\sim 65\%$ using equation 2.4 and an extrapolated R_{xs} value of $0.0160 \text{ Tcm}^{-2} \text{ min}^{-1}$ at 2-4 cm depth from figure 3.3a. This loss is explicable in terms of outward diffusion and loss from the sediment of a fraction of the Ra and Rn isotopes with a consequent loss of their short-lived daughters. Using the data in table 3.2 for the 2-4 cm section, it is possible to estimate the total activity from all α -isotopes, and to calculate the maximum possible % loss in α -activity due to Ra plus daughter diffusion. The total

α -inventory at 3 cm depth is as follows:-

^{238}U (0.44 dpmg^{-1}) plus 7 α -daughters at equilibrium	$= 3.52 \text{ dpmg}^{-1}$
^{238}Th (0.70 dpmg^{-1}) plus 5 α -daughters at equilibrium	$= 4.20 \text{ dpmg}^{-1}$
$^{230}\text{Th}_{xs}$ (10.6 dpmg^{-1}) plus 5 α -daughters at equilibrium	$= 63.60 \text{ dpmg}^{-1}$
$^{231}\text{Pa}_{xs}$ (0.86 dpmg^{-1}) plus 5 α -daughters at equilibrium	$= 5.16 \text{ dpmg}^{-1}$
Total α -activity	$= 76.48 \text{ dpmg}^{-1}$

Here, it is assumed that (a) The α -activity contribution of ^{235}U and its equilibrium daughters is negligible, (b) from the estimated sedimentation rate (0.26 cm kyr^{-1}), the age of the sediment at 3cm is 11,538 yrs and ^{226}Ra ($t_{1/2}$ 1622 yrs) and its daughters have therefore grown into secular equilibrium with $^{230}\text{Th}_{xs}$, (c) the $^{230}\text{Th}_{xs}/^{231}\text{Pa}_{xs}$ surface ratio equals the theoretical value of 10.8 (Krishnaswami and Cochran, 1978) and increases to 12.25 at 3cm depth. If it is further assumed that all the Ra and Rn daughters from the surface-adsorbed, authigenic nuclides ^{230}Th and ^{231}Pa are lost from the sediment core and that their short-lived daughters decay in-situ before CLN plastic application, then the maximum loss in α -activity equals $5(10.6 \text{ dpmg}^{-1}) + 4(0.86 \text{ dpmg}^{-1}) = 56.44 \text{ dpmg}^{-1}$, or $\sim 74\%$. The low total α -activity observed near the surface of the core is therefore attributed to the loss of such mobile radionuclides. From Figure 3.3b, it can be seen that ^{230}Th activity decreases fairly regularly/

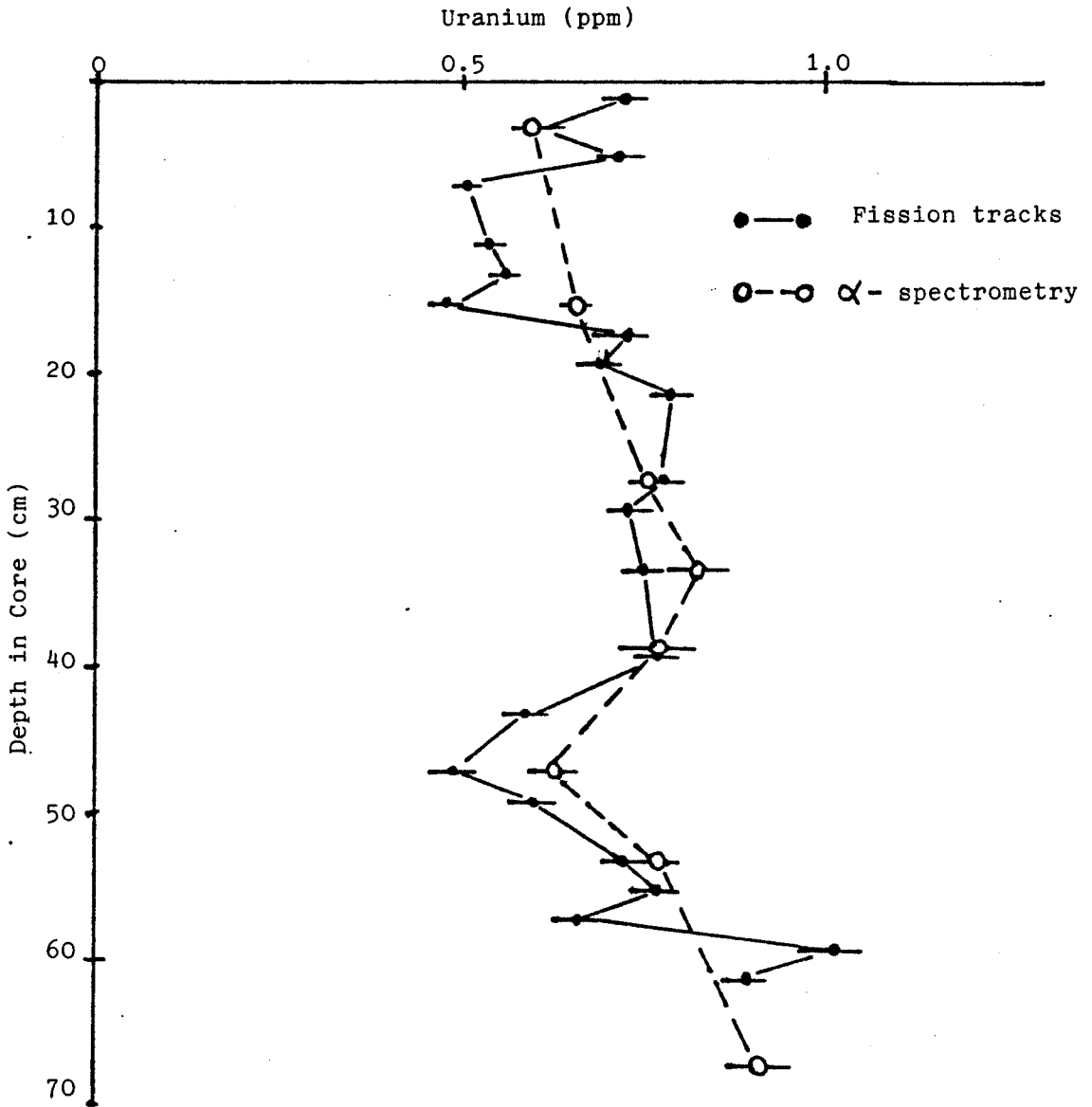


Figure 3.2. Depth profiles of uranium levels in core 9936K from both fission track and alpha spectrometry techniques.

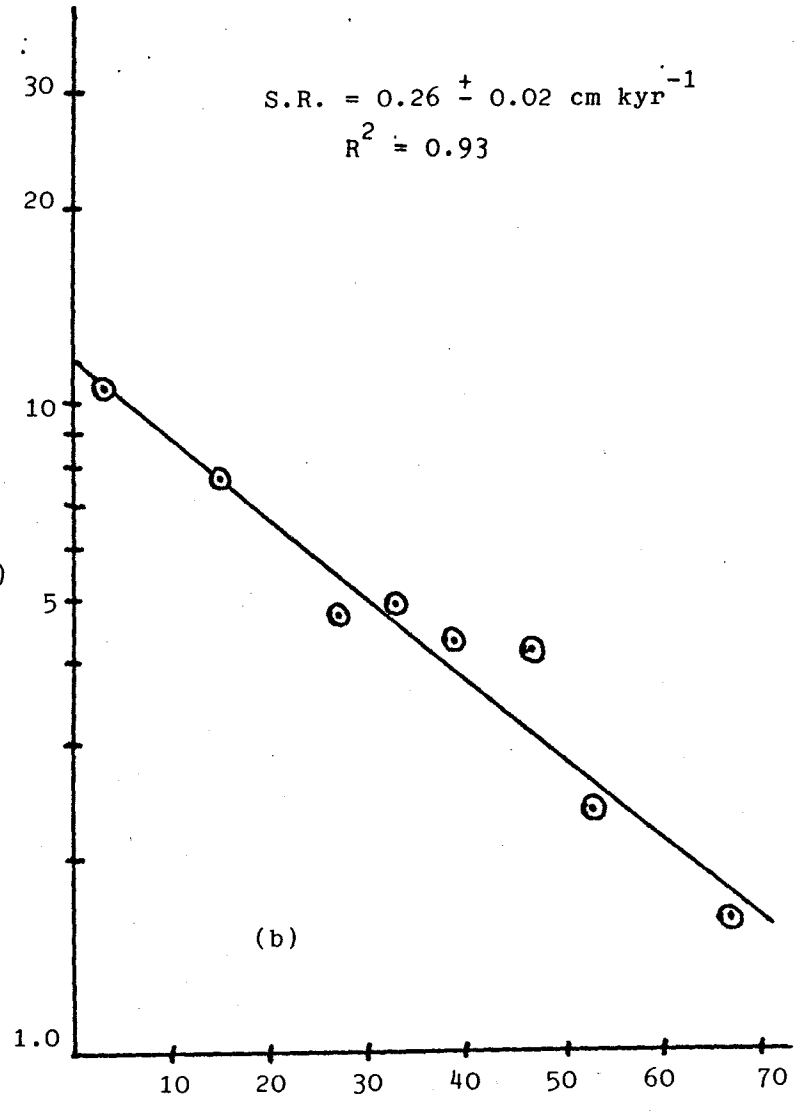
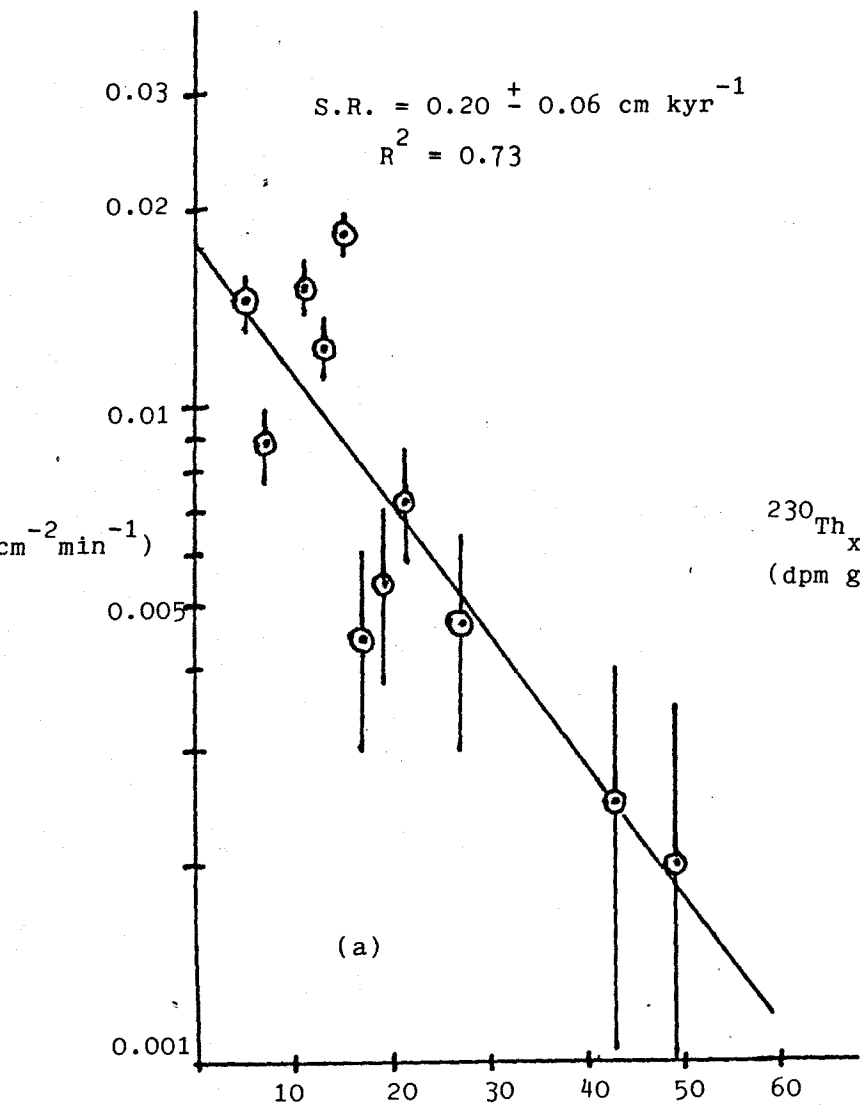


Figure 3.3. Depth profiles of (a) excess alpha track rate and (b) unsupported ^{230}Th activity in core 9936K.

regularly, providing evidence for its non-mobility. Cochran and Krishnaswami (1980) have found solid-phase $^{226}\text{Ra}/^{230}\text{Th}$ ratios of ~ 0.3 at the top of N. Equatorial Pacific cores, suggesting that at least 70% of the ^{226}Ra atoms produced are lost from the sediment and diffuse out of the core, while $^{228}\text{Th}/^{232}\text{Th}$ ratios less than 1.0 also suggest that ^{228}Ra is being lost. $^{210}\text{Pb}/^{226}\text{Ra}$ ratios from 1.70 ± 0.08 to 1.81 ± 0.07 in the top 1 cm of these same cores suggest that ^{210}Pb (and consequently also ^{210}Po) returns from the water column to the sediment (Nozaki et al., 1977) to contribute to the total α -activity.

Figure 3.2 displays the uranium content of the core as determined by both analytical methods, and shows good agreement. In the fission track technique, which had previously been shown to be an accurate one for the determination of uranium in sediments (Rydell and Fisher, 1977), equation 2.1 is used for the uranium determination, with I_s/I_x equal to 0.33. The uranium concentrations observed here, (mean value for whole core = 0.68 ppm) lie at the low end of the range found for pelagic sediments. For example, Bertine et al., (1970), using a fission-track method, found values of 0.25 to 7.09 ppm U for non-reducing pelagic sediments, while Mo et al., (1973) using the delayed neutron counting method reported levels of between 0.57 to 4.3 ppm U for sediments from open marine basins having highly-variable calcium carbonate concentrations (1 - 86%). In pelagic sediments, the calcareous plankton material (coccoliths and foraminifera) can usually be regarded as diluting material of low-uranium content. Ku (1965) determined that coccoliths have less than 0.1 ppmU and foraminifera have 0.015 ppm. Holmes et al., (1968) measured U values in foraminifera as 0.13 ± 0.08 ppm in the Drake Passage, and 0.11 ± 0.44 ppm in the South Pacific. Bertine et al., (1970) extrapolated the uranium concentration of clay/ CaCO_3 sediment mixtures to the pure CaCO_3 end member to yield a value of/

of 0.08 ppm. More recently, Delaney and Boyle (1983), analysing carefully-cleaned samples, found a maximum concentration of lattice-bound U of 0.023 ppm. Thus there seems to be discrimination against the incorporation of uranium into skeletal calcitic calcareous structures (excluding aragonitic types which have more U). Blanchard and Oakes (1965) found ratios of U/Ca in skeletal material to U/Ca in sea water to be usually below 0.1, and that calcitic molluscan shells show more discrimination than aragonitic types by a mean factor of about 7. A plot of the uranium and % CaCO₃ data for the calcareous ooze core 9936K is shown in Figure 3.4. The core contains high (63 - 78%) calcium carbonate concentrations composed predominantly of carbonate shells and foraminiferal tests, but the narrow range of CaCO₃ values is not conducive to providing a pronounced U-CaCO₃ inverse correlation. The linear correlation with equation $U(\text{ppm}) = 2.27 - 0.022 \text{ CaCO}_3(\%)$ implies by extrapolation that the U concentration of pure CaCO₃ is 0.06 ± 0.49 ppm, in reasonable agreement with the above values given the low (0.5) correlation coefficient.

In the determination of the sedimentation rate by the decay of ²³⁰Th excess or of α -track rate excess with depth, the initial (surficial) activity C_0 and that at depth x cm, C_x , are related by the equation

$$C_x = C_0 \exp(-\lambda x/S) \dots\dots\dots(3.1)$$

where λ is the decay constant of ²³⁰Th and S is the sedimentation rate in cm per unit time down to depth x . Rewriting equation 3.1 in the form

$$\ln C_x = (-\lambda/S)x + \ln C_0 \dots\dots\dots(3.2)$$

indicates that a plot of $\ln C_x$ against x should afford a straight line whose slope yields the sedimentation rate, S . This has been done for the R_{xs} and ²³⁰Th excess data (Figure 3.3) giving sedimentation rates of 0.20 ± 0.06 cm kyr⁻¹ and 0.26 ± 0.02 cm kyr⁻¹ respectively from the least-squares regression lines, a satisfactory agreement given the non-specific nature of the P.T.A. α -detection process, and the characteristic migratory behaviour of certain α -emitters/

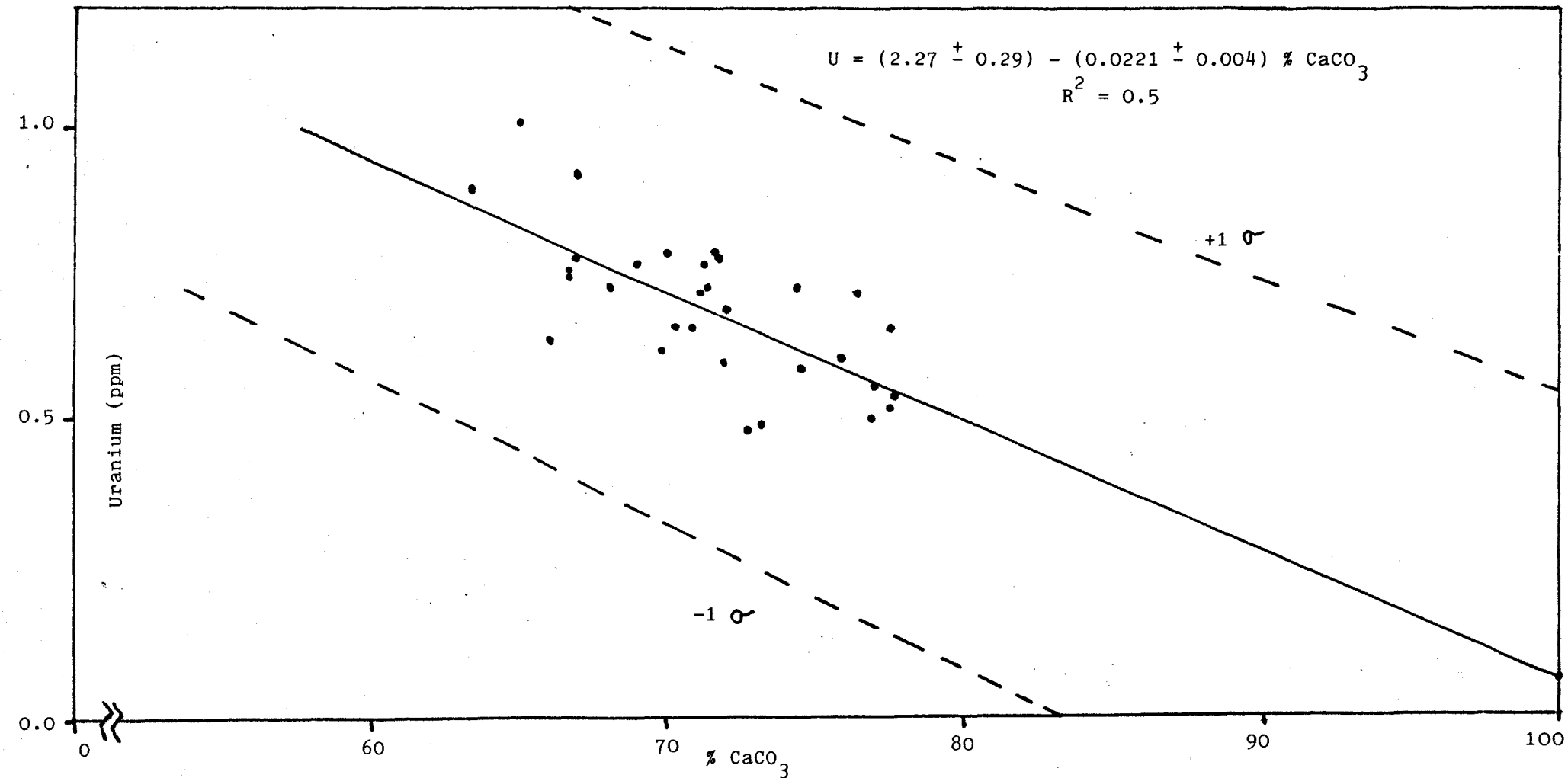


Figure 3.4. Plot of uranium against calcium carbonate content for core 9936K

emitters as outlined previously. A greater regression coefficient, R^2 , implies a greater likelihood of uniformity in the deposition of both ^{230}Th and total sediment over the time period to depth x cm. Non-linear plots of ^{230}Th excess against depth could be explained if the initial concentration of ^{230}Th depositing varied with time. The likely cause of such a variation is a change in the bulk sediment settling rate, since the long U oceanic residence time (10^5 to 10^6 yrs) combined with the short ^{230}Th residence time (~ 100 yrs) favours a constant ^{230}Th precipitation (Ku, 1976). The chemical scavenging of Th isotopes in the deep sea occurs by a reversible exchange process (Bacon and Anderson, 1983) whose rate is fast compared with the rate of removal of particulate matter. Another cause of deviation from linearity could be a result of rapid influx of material from the continental slope, possibly by turbidity currents. The location of core 9936K, near the bottom of the South African continental slope, means that the sediments here are vulnerable to such influxes, and examination of Figure 3.3b suggests that between ~ 30 and 50 cm, a change in slope of the excess ^{230}Th profile might be present. Co-incident with this is a textural and colour change in the core itself (0 - 28 cm brown, 28 - 52 cm grey). The decrease in slope of excess ^{230}Th at these depths is consistent with the higher rate of sedimentation which would result if bottom currents or gentle density currents were transporting fine sediment to the area. The presence of sediment laminae over vast areas of the abyssal plains are due to frequent bottom-hugging, gentle density currents (Davies and Gorsline, 1976). Fine-grained turbidites, separated by thin pelagic units alternating from oozes to pelagic clays have been found off the North West coast of Africa on the Madeira Abyssal Plain (Weaver and Kuijpers, 1983). Assuming the presence of such a turbidite unit within core 9936K, then this feature highlights a limitation of the P.T.A. method i.e. that of being unable to identify such details due to the scatter in the data (Figure 3.3a), although the data points are,/

are, admittedly, poorly-spaced around the region of interest.

The observed agreement between the 2 techniques in the estimation of sedimentation rate is within analytical error for core 9936K, and for other cores subjected to similar analyses (Fisher, 1978; Crawford, 1982). The data here formed part of a collaborative study (Crawford et al., 1984) which showed that the sensitivity of the P.T.A. method was poorer than that of the conventional method due to the non-specific nature of the α -particle detection process, a shortcoming which results in consistently larger errors on the derived sedimentation rates for pelagic cores. In contrast, the high analytical precision, down to 2% (Ku, 1976) for $^{230}\text{Th}_{\text{excess}}$ assay using α -particle spectrometry gives more precise rates, although large scattering in the data can be exhibited, especially in cores of varied lithology, resulting in greater uncertainty in rate estimates. Often, the more laborious radiochemical technique leads to sedimentation rates being calculated on the basis of few but good analytical data, whereas the more rapid and simple P.T.A. method, if used in an initial screening mode or used complementary to the conventional $^{230}\text{Th}_{\text{excess}}$ method, could yield more detailed, if less precise α -profiles for cores. The results shown here indicate that the track technique is accurate, comparable in performance with and simpler and more rapid than the conventional method. If the initial period of α -track accumulation is neglected and access to a reactor is available, then the α -track and fission track analyses require about 2 and 1 hours per 0.1g sample respectively, enabling a whole core of, say, 30 samples to be analysed by the P.T.A. procedure in under 4 man-days. This is to be compared with a turnover rate of about 1 man-day per 1.5 to 2g sample by radiochemistry and α -spectrometry (Thomson, 1982). It is evident, however, that because of equilibrium-disequilibrium uncertainties within the natural series nuclides in sediment cores, the radiochemical method is the more valuable one for α -analyses since it measures specifically the isotopic activities of interest. Nevertheless/

Nevertheless, very good agreement between the particle track and radiochemical methods is found (Figure 3.2) for the uranium analyses, and so the fission track method would seem to offer unlimited potential.

3.2 Uranium in pore waters of deep-sea sediments

The following results of porewater uranium analyses, obtained by the fission track method described in section 2.6.2, are presented in non-chronological order so that the earliest uranium profiles obtained can be discussed in the light of important evidence of a pressure effect revealed in the latter stages of this study. This evidence of a sampling artefact comes from a comparison of the uranium data in squeezed Kastenlot and box core pore waters with those from in-situ samples pore waters (Toole et al., 1984). Table 3.3 shows the pore water uranium and alkalinity results for station 10552 on the Cape Verde abyssal plain. The calcareous marl/ooze sediments here consist of 36 - 78% CaCO_3 and are oxic down the whole length of the deepest core (1.7 metres). The dissolved oxygen contents, measured by a headspace analysis technique (Sorenson and Wilson, 1984), indicate the presence of free oxygen falling from 66% of bottom water values just below the interface to 43% at 1.7m, and that by extrapolation of this profile, the sediment may be oxic to ~ 10 metres. Manheim and Sayles (1974) observed that in slowly-deposited pelagic oozes with a high water content, there was little evidence of diagenesis and alteration and little change in pore fluid composition. From a study of the decomposition rates of metabolizable organic carbon in oxic silicious and calcareous ooze sediments, Muller and Mangini (1980) found large rate constants which reflected the higher efficiency of organic matter decomposition under oxygenated conditions and explained the prevailing oxic conditions of biogenic oozes and clays at depths beyond 1 metre. A sedimentation rate threshold of between 1 and 4 cm kyr^{-1} was suggested below which the chemical environment remains/

TABLE 3.3

Pore water uranium and alkalinity data for station

10552 (Cape Verde Abyssal plain) ($\pm 1\sigma$ error)Box Core 9Bx : $19^{\circ} 27'N 29^{\circ} 54'W$, In situ sampler #7: $19^{\circ} 25'N 29^{\circ} 53'W$
4655m 4735m

Depth(cm)	Uranium ($\mu g l^{-1}$)	Alkalinity ($meq l^{-1}$)	Depth(cm)	Uranium ($\mu g l^{-1}$)	Alkalinity ($meq l^{-1}$)
0 - 2.5	2.14 ± 0.09	-	-50	3.38 ± 0.12	2.32
5 - 7.5	2.04 ± 0.09	-	- 1	3.41 ± 0.13	2.34
10 -12.5	1.99 ± 0.08	-	2	3.48 ± 0.13	2.49
15 -17.5	1.72 ± 0.08	-	3.5	2.90 ± 0.11	2.35
20 -24	1.77 ± 0.08	-	6.5	3.16 ± 0.12	2.55
28 -32	1.50 ± 0.07	-	12.5	3.28 ± 0.12	2.58
32-37	1.48 ± 0.07	-	24.5	2.74 ± 0.11	2.62
			45.5	4.04 ± 0.14	2.74

Kastenlot Core 2K : $19^{\circ} 23'N 29^{\circ} 54'W$, 4683m

Depth (cm)	Uranium ($\mu g l^{-1}$)	Alkalinity ($meq l^{-1}$)
8 - 13	1.75 ± 0.08	1.99
26 - 31	1.57 ± 0.07	1.81
44 - 49	2.25 ± 0.09	1.91
57 - 62	1.57 ± 0.07	2.03
67 - 73	1.29 ± 0.06	2.09
84 - 89	1.20 ± 0.06	2.11
103 - 108	1.38 ± 0.06	2.09
119 - 124	1.85 ± 0.08	1.90
132 - 137	1.03 ± 0.05	2.36
145 - 150	1.28 ± 0.06	2.12
163 - 168	1.92 ± 0.08	2.09

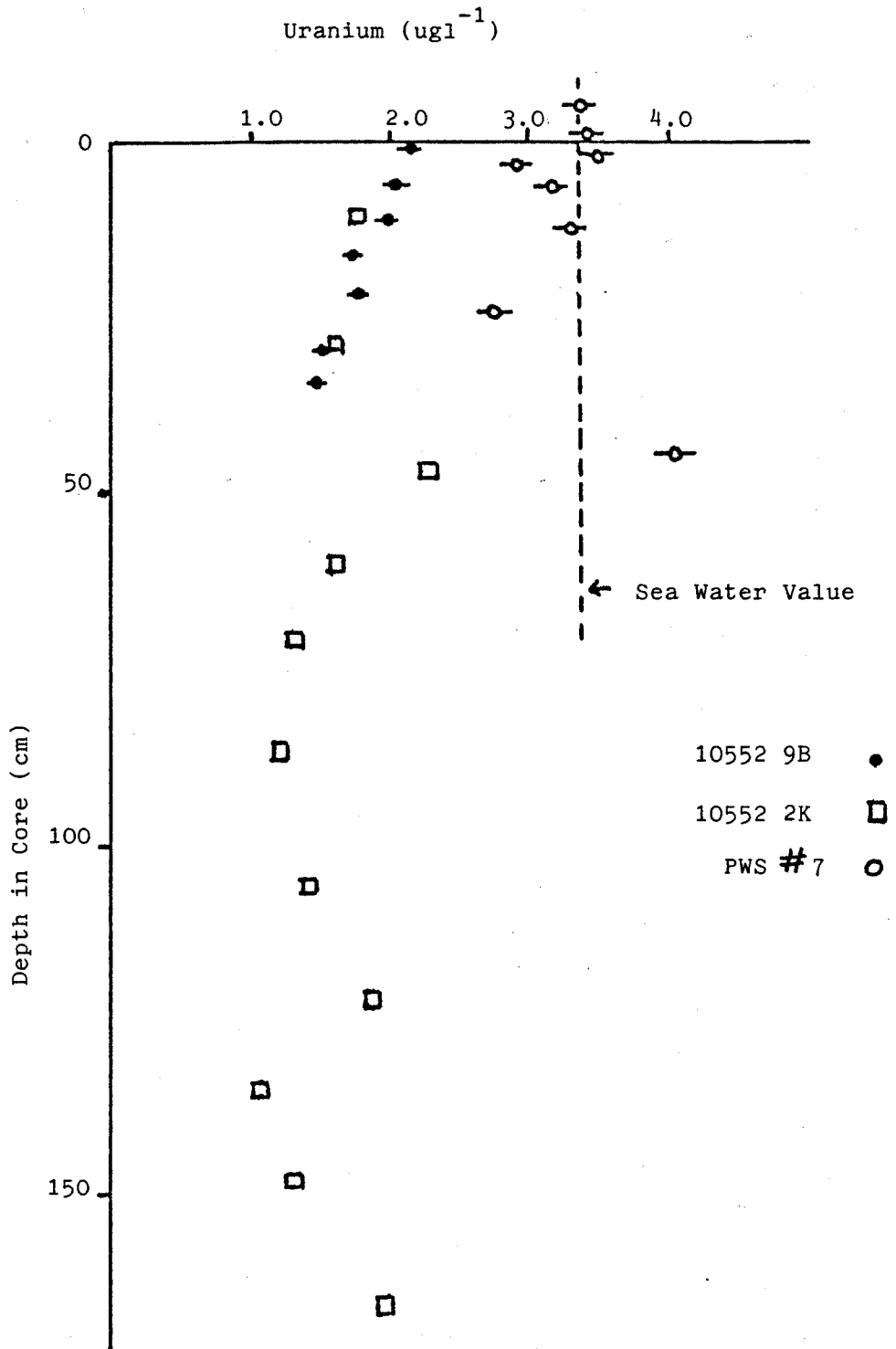


Figure 3.5. Uranium concentrations in the pore waters of cores from the Cape Verde abyssal plain.

Alkalinity (meq kg⁻¹)

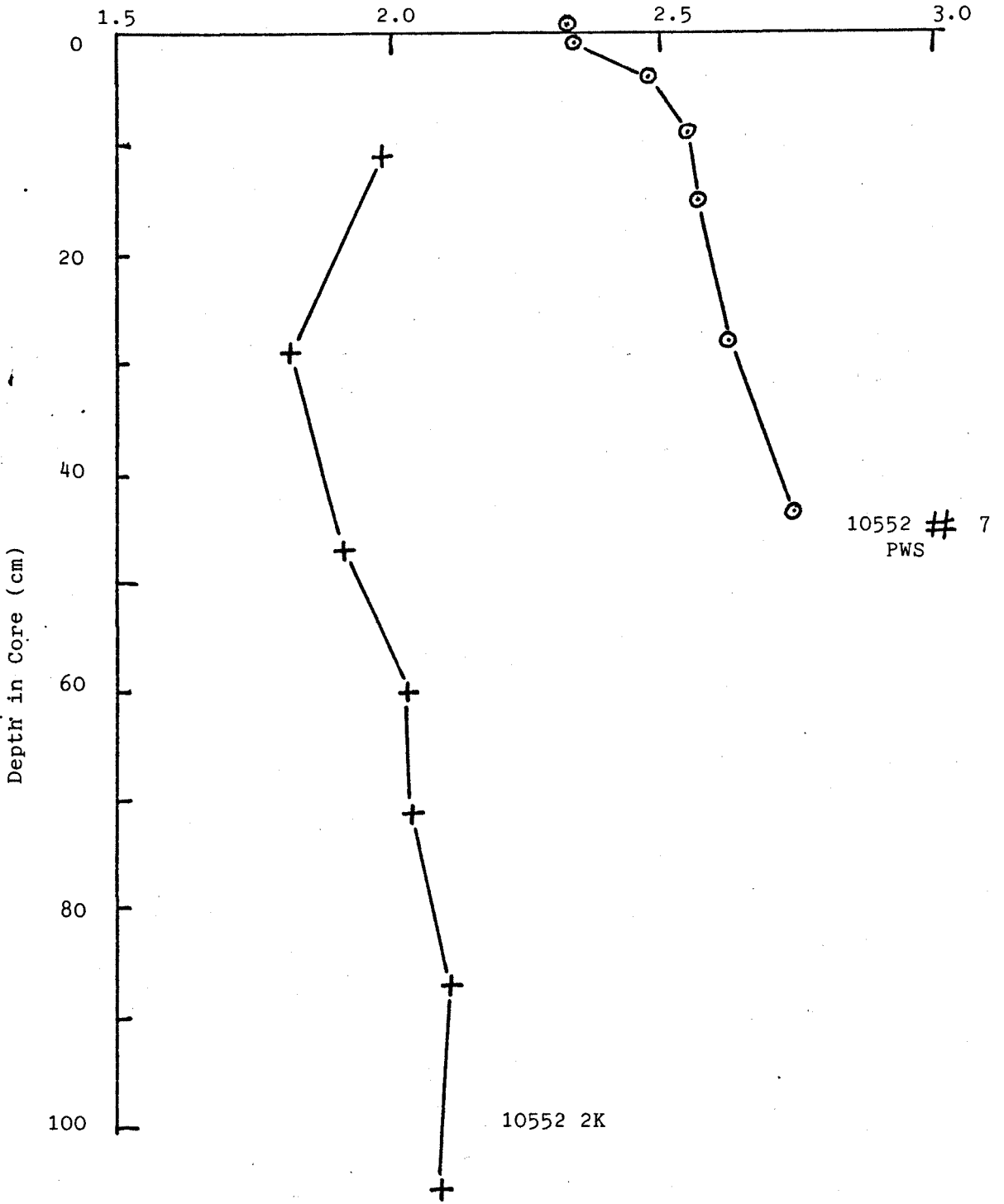
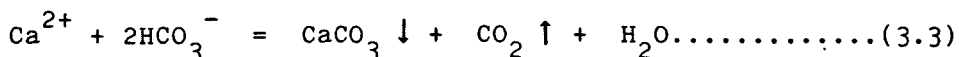


Figure 3.6. Alkalinity in the pore waters of cores from Cape Verde abyssal plain.

remains oxic in pelagic regions of moderate productivity. Thus, since ^{230}Th excess dating of cores from station 10552 showed them to be accumulating slowly at a rate of about 0.4 cm kyr^{-1} , these oxic sediments were not expected to show any dramatic changes in pore water constituents (Grundmanis and Murray, 1982). No dissolved manganese was found at any depth in the cores. Although there was good agreement between the levels of silicate and phosphate for the box core, Kastenlot core and in-situ sampler at this station, there was a systematic difference in both the alkalinity and uranium content between the profiles from the corers and that from the in-situ pore water device (Table 3.3 and Figures 3.5 and 3.6). Over the depth range 0-49 cm, the core samples (combining both box and Kasten) have a mean uranium content of $1.82 \pm 0.03 \text{ ug l}^{-1}$, while the in-situ samples (2 - 45.5 cm) have a mean value of $3.27 \pm 0.05 \text{ ug l}^{-1}$, a reduction of 44%. For alkalinity, over a similar depth range (6.5 - 49 cm), a mean reduction of 27% in the squeezed samples relative to the pore water sampler is evident. The two in-situ bottom water samples give an average uranium concentration of $3.40 \pm 0.09 \text{ ug l}^{-1}$ for bottom water, in agreement with the accepted value of $3.35 \pm 0.2 \text{ ug l}^{-1}$, with the pore waters below showing essentially conservative uranium behaviour with depth in this carbonate sediment. The loss of alkalinity from corer pore waters during recovery (Emerson et al., 1980; Murray et al., 1980; Sayles, 1981; Emerson et al., 1982; Jahnke et al., 1982) is believed to be due to CaCO_3 precipitation and the removal of bicarbonate ions from solution as can be seen from the carbonate equilibrium :



and the relationship :

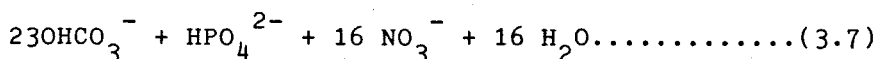
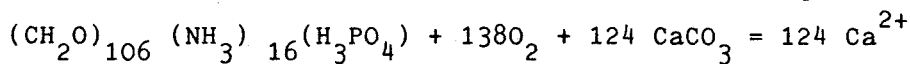
$$\text{Alkalinity} = [\text{HCO}_3^-] + 2[\text{CO}_3^{2-}] \dots \dots \dots (3.4)$$

When the concentration of B(OH)_4^- is neglected and other proton acceptors OH^- , PO_4^{3-} and S;O(OH)_3^- are also not considered.

The degassing (loss of CO_2) from the core as it is recovered from the high-pressure deep waters displaces the equilibrium (equation 3.3) to the right, thus lowering the alkalinity.

In/

In solutions such as sea water which have substantial carbonate alkalinities, uranyl carbonate complexes predominate (Langmuir, 1978; Morse et al., 1984) and it is reasonable to assume that the UO_2^{2+} can adsorb initially from solution onto sediment surfaces due to the formation of hydroxy-carbonate precipitates or even just simple calcium carbonate. Morse et al., (1984) have reported rapid sorption of uranyl ion onto carbonate mineral solids, although only when the concentration of uranyl ion approached that of the carbonate alkalinity, values which are orders of magnitude in excess of natural soluble uranium levels. If a simple co-precipitate is formed consisting of occluded uranyl ions in a calcium carbonate lattice, then this and the much larger concentration of CO_3^{2-}/HCO_3^- (μM) over uranium ($10^{-2}\mu M$) might explain the greater percentage decrease in uranium than in alkalinity, if it is assumed that every dissolved uranium species exists as $UO_2(CO_3)_2^{2-}$. This process can be considered analogous to calcite or aragonite deposition in fresh water which generally occurs by CO_2 loss from groundwater, here uranium is corecipitated along with other dissolved trace elements such as Mg, Sr, Ra and Ac, or indeed analogous to the biogenic precipitation of carbonate minerals in sea water, a process which also incorporates uranium (Gascoyne, 1982). Murray et al., (1980) observed the systematic alkalinity decrease in a core containing essentially no $CaCO_3$, indicating that this need not be present as a nucleating surface for precipitation to occur on core retrieval. An attempt made by the authors to correct for the effect on alkalinity via thermodynamic considerations of the carbonate system was later shown not to be generally applicable (Emerson et al., 1982; Jahnke et al., 1982). The increase in alkalinity from 2.32 to 2.74 meq l^{-1} with depth in core 10552 (in-situ samples, Table 3.3) is a result of aerobic oxidation of organic matter in the presence of $CaCO_3$ which can be represented by the idealised stoichiometric equation (Sayles, 1981)



where the Redfield C : N : P ratio for the material oxidised is assumed/

assumed (Jahnke et al., 1982). There was little evidence of denitrification at station 10552, with NO_3^- increasing irregularly from 35uM at the surface to 60uM at 166 cm depth. Phosphate remained roughly constant at a low level of about 1.2uM in the Kasten core 10552 2K indicating the absence of anoxic decomposition of P-containing organic matter.

It would appear from the above discussion, therefore, that there is no alternative to in-situ pore water sampling of deep-sea cores (from depths greater than 500 metres (Murray et al., 1980)) if reliable pore water alkalinity and uranium results are to be obtained. This conclusion is confirmed on examination of uranium data obtained from squeezed cores taken from the Nares abyssal plain and the Bauer basin (stations 10164 and 10189 respectively). Table 3.4 and Figures 3.8(a) and (b) show the squeezed pore water uranium results in two box cores from the Nares abyssal plain stations in the Caribbean. In core 10164 5Bx, pore water uranium values decrease slightly from 2.82 to 1.83 ugl^{-1} in the 30cm depth sampled, with a mean value of $2.29 \pm 0.05 \text{ ugl}^{-1}$. In core 10165 8Bx, the decrease is from 3.20 to 1.44 ugl^{-1} U (mean $2.20 \pm 0.25 \text{ ugl}^{-1}$) over the same depth range. Excess ^{230}Th dating of core 10164 5Bx gives a low sedimentation rate of about 0.6 cm kyr^{-1} . Both of these cores are low in CaCO_3 (< 1 %) since they lie below the carbonate compensation depth (CCD) of about 5 to 5.5 km in this area (Berger, 1976; Biscaye et al., 1976). At the CCD, the rate of supply of calcareous shells equals the rate of their dissolution, and the underlying sediments contain only a few per cent of carbonate. All the pore waters sampled gave indications of an oxic or very mildly reducing environment. Thus, little dissolved Mn^{2+} was found in the box cores, namely from 5 to 35 ugl^{-1} for 10164 5Bx down to 50 cm, and less than 60 ugl^{-1} for 10165 8Bx down to 45 cm, and suggesting that these two cores remained oxic. Further evidence for this assumption comes from the iodate/iodide profiles, iodate to iodide interconversion occurring at a depth of $\sim 30\text{cm}$ in core 10164 5Bx and at 45cm in 10165 8Bx. If this iodate-iodide couple is/

TABLE 3.4

Uranium concentration in pore waters from stations 10164 and 10165 (Nares Abyssal Plain).

Box Core 5B : $26^{\circ} 12'N$ $60^{\circ} 25'W$, 5613m.

<u>Depth (cm)</u>	<u>Uranium ($\mu g l^{-1}$)</u>
0 - 5	2.82 ± 0.14
5 - 10	2.45 ± 0.13
10 - 15	2.25 ± 0.12
15 - 20	2.25 ± 0.12
20 - 25	1.83 ± 0.11
25 - 30	2.11 ± 0.12

Box Core 8B : $23^{\circ} 45'N$ $61^{\circ} 27' W$, 5825m.

<u>Depth (cm)</u>	<u>Uranium ($\mu g l^{-1}$)</u>
0 - 5	3.20 ± 0.15
5 - 10	2.65 ± 0.14
10 - 15	2.22 ± 0.12
15 - 20	1.72 ± 0.11
20 - 25	1.95 ± 0.11
25 - 30	1.44 ± 0.10

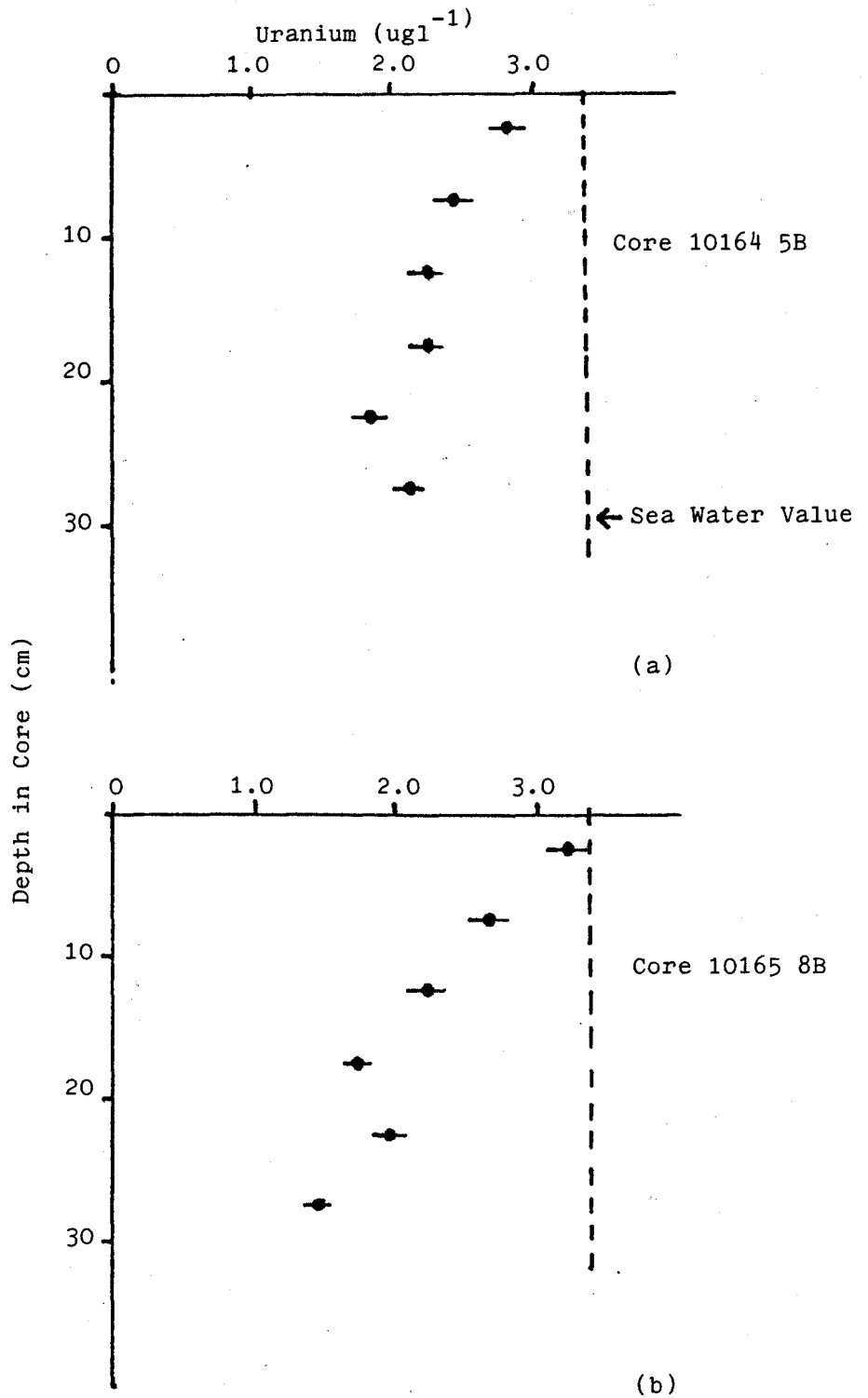


Figure 3.7. Uranium concentration in the pore waters of cores from the Nares abyssal plain

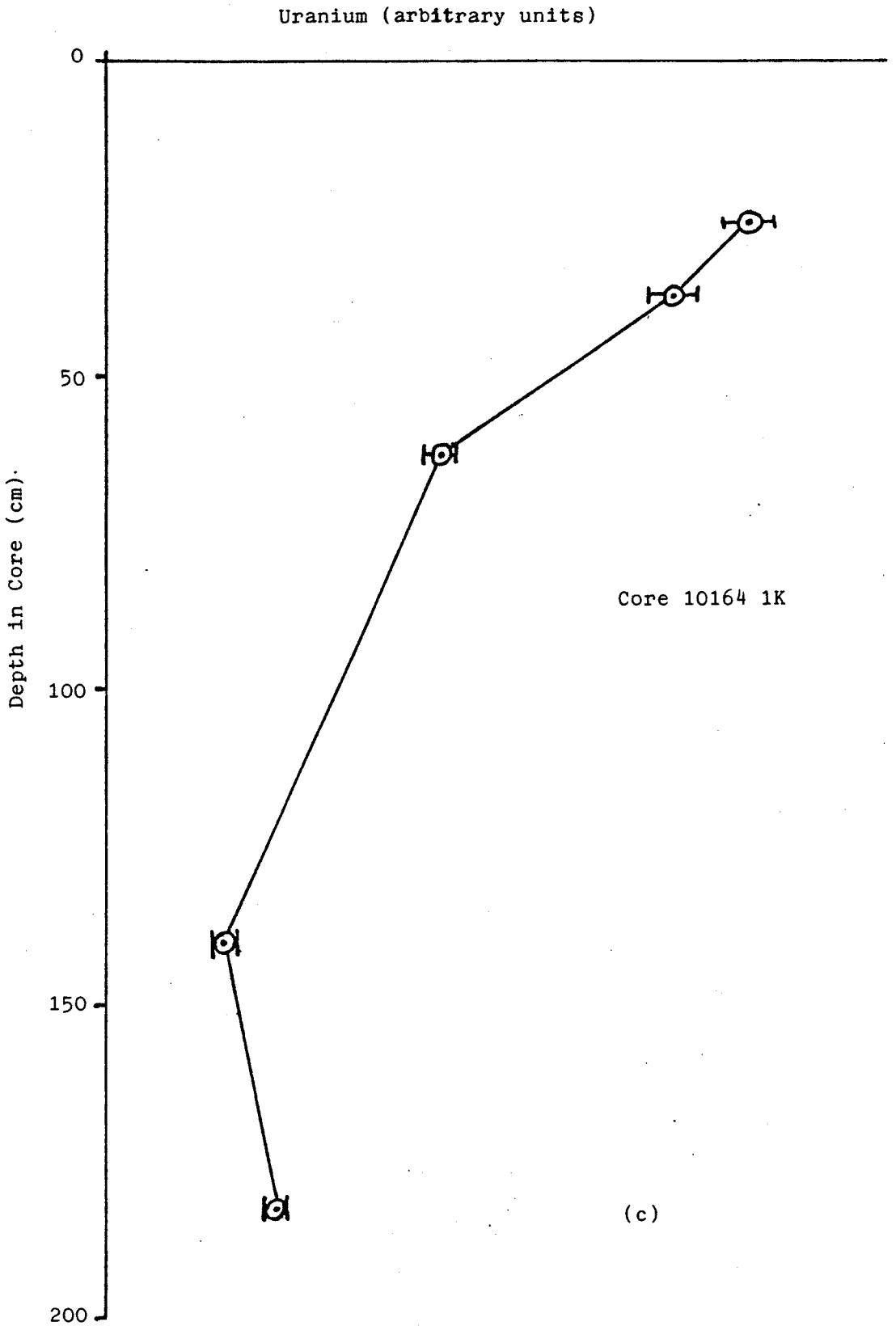


Figure 3.7 (contd.)

is considered as an Eh indicator with a value of + 1.42v (pE10.5, Liss et al., 1973), then the former core might be regarded as slightly more reducing. Although diagenetic activity in these Nares abyssal plain cores was not intense, classic concentration profiles of increasing silicate and phosphate and the presence of a manganese solid phase spike (Froelich et al., 1979) at ~20cm indicated that diagenesis was occurring to some degree. The geochemical evidence, however, points to the pore water in the two box cores remaining oxic and if, as observed for core 10552 #7, the uranium concentration in the pore water should remain roughly constant at the sea water value of $3.35 \pm 0.20 \text{ ug l}^{-1}$ (Ku et al., 1977), then the pressure effect was again evident in these low-carbonate cores, with mean uranium decreases of 30.6% and 33.3% for 10164 5Bx and 10165 8Bx respectively. Higher pore water uranium levels characteristic of strongly reducing sediments as noted earlier (section 1.2) were, of course, not observed. One other Caribbean core for which squeezed pore waters were analysed for uranium was the Kastenlot core 10164 1K, sampled to a depth of ~2 metres. Only five pore water samples were available, and these were the first to be assayed by the fission track technique. Unfortunately the precautions required to guard against uranium adsorption on container walls as mentioned in section 2.6.2 were not followed at this time and it is thought that the prepared uranium standards had a lower concentration than the nominal value, thus giving rise to pore water uranium levels which were too high (equation 2.2) by an unknown factor. With this in mind, examination of the systematically elevated data in Figure 3.7c indicates that the uranium concentration in the pore water for the upper two samples declines in a manner consistent with the two box cores, and removal onto the sediment at greater depths. The Kasten core was indeed quite similar in redox status to the box cores, to depths of about 50 cm but became more reducing at greater depths. It is probable, therefore, that the pore water uranium values should be similar to the two box cores above about 50 cm, exhibiting the pressure effect. The core showed iodate/iodide interconversion at a depth of 60 cm, and manganese mobilisation occurring at about 80 cm underlying a solid-phase Mn spike at 40 cm. A calcareous organic-rich/

rich turbidite is present between 50 and 150 cm in this core. This is reflected by the presence of large excesses of ^{230}Th at 51, 105 and 185 cm, and by a fivefold increase in the solid CaO concentration below 50 cm over the pelagic clay baseline above. Below 50 cm a non-steady state pattern of organic matter diagenesis was also evident, with the slopes of dissolved silicate, manganese and total iodine all approaching a constant positive value with depth rather than zero. Twice as much phosphate and silicate was apparent in the pore waters of the Kasten core relative to the two box cores, corresponding to the greater diagenetic activity associated with the higher, variable organic content of the turbidite (0.13 to 0.67%). As compared to uranium-organic carbon correlations found in sediments by Mo et al., (1972), Kolodny and Kaplan (1973) and Mangini and Dominik (1979), a moderate correlation ($r^2 = 0.67$) was observed here, which resulted in a variable solid-phase uranium content (2.2 to 4.0 ppm) over the whole depth range, but in uranium values identical to 10164 5Bx above 50 cm. The apparent uptake of uranium from the pore waters at depth onto the solid phase may actually be a manifestation of uranium enrichment in the turbidite prior to its emplacement. However, this feature has been discussed by Yamada and Tsunogai (1984) for a reducing core from the Bering Sea. The authors suggested that uranium diffuses from sea water through the pore waters of a surface oxidising sediment layer, to be precipitated in the deep reducing layer. The pore water uranium profiles found here, at station 10164, are consistent with this. Pore water uranium data from the other oxic sediment core, 10189 4Bx from the Bauer basin (see Figure 2.1), is shown in Table 3.5 and Figure 3.8. Also included is the phosphate content of the pore waters which are elevated relative to those found in natural sea water ($\sim 1.2\mu\text{M}$). The Bauer deep lies/

TABLE 3.5

Uranium and phosphate concentrations in pore waters
from station 10189 (Bauer Basin).

Box Core 4B : 9° 58'S 102° 34'W, 4445m.

<u>Depth</u>	<u>Uranium (ugl⁻¹)</u>	<u>Phosphate (uM)</u>
0 - 5	2.73 ± 0.15	3.21
5 - 8	2.55 ± 0.14	3.66
8 - 11	2.46 ± 0.14	3.00
11 - 14	2.32 ± 0.13	3.15
14 - 17	2.49 ± 0.14	3.24
17 - 20	2.35 ± 0.13	2.85
20 - 23	2.20 ± 0.13	2.91
23 - 26	2.79 ± 0.15	2.97
26 - 29	2.57 ± 0.14	3.00
29 - 32	3.22 ± 0.16	9.63
35 - 39	2.09 ± 0.12	3.21
42 - 45	2.41 ± 0.13	3.79
50 - 53	3.11 ± 0.16	34.20
58 - 61	2.53 ± 0.14	3.27
64 - 67	3.06 ± 0.16	6.51

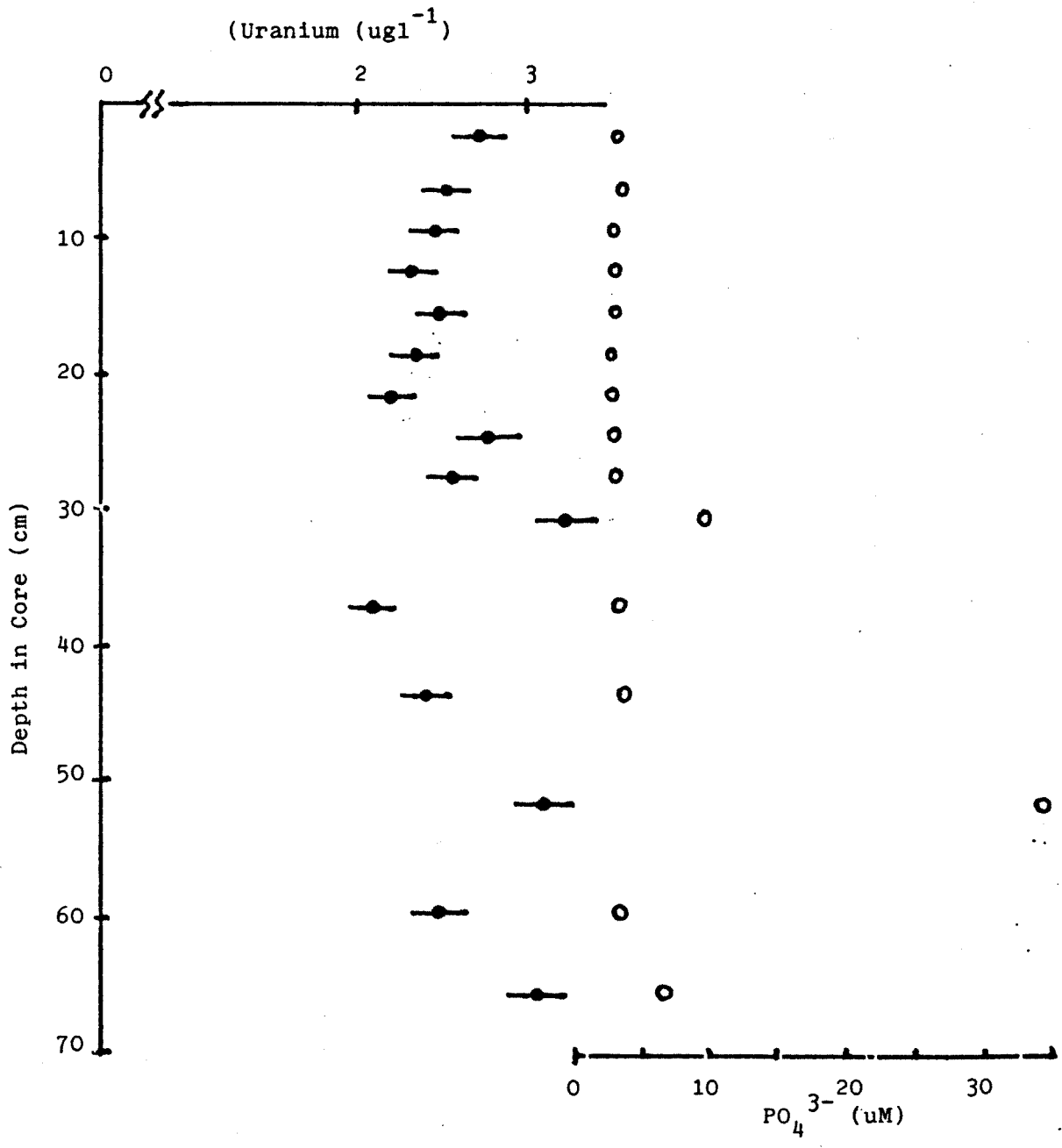


Figure 3.8. Uranium and phosphate concentrations in the pore waters from core 10189 4B in the Bauer basin

lies between the East Pacific Rise (EPR) and the extinct Galapagos Rise, and contains low carbonate concentrations of 1.2 to 1.6%, an abundance of fish teeth, high concentrations of metals (Fe, Mn, Ni) and zeolites (e.g. Phillipsite) which are all due to the precipitation of metal-rich, volcanically-derived hydrogenous phases into the slowly-accumulating sediments (Dymond and Veeh, 1975). From observed $^{234}\text{U}/^{238}\text{U}$ ratios of 1.00 ± 0.02 to 1.04 ± 0.02 , it was concluded (Dymond and Veeh, 1975) that there was little uranium uptake from sea water, unlike the EPR sediments which showed higher activity ratios due to higher uranium accumulation rates there resulting from the precipitation of hydrothermal solutions by the reaction of sea water with cooling basalt lava. Bischoff and Sayles (1972) have shown, in a sampling transect across the Bauer deep and the EPR, that the Eh environment of all the sediments is between +100 and +200 MV. This mildly reducing environment showed no significant sulphate depletion from bottom-water values, and the most metalliferous cores in the Deep had amongst the lowest levels of dissolved manganese ($\lesssim 55 \mu\text{M}$). In core 10189, the solid-phase MnO (3.62 wt. %), Fe_2O_3 (14.0 wt.%) and P_2O_5 (0.61 wt.%) signified enrichments relative to average ocean sediment (0.41, 4.89 and 0.16 wt. % respectively, Chester and Aston, 1976) and had very similar profiles indicating EPR crest volcanic activity as their common origin. Examination of the pore water uranium profile (Figure 3.8) shows again the pressure artefact of core retrieval and squeezing, with the uranium values down to 23 cm depth averaging $2.44 \pm 0.05 \text{ ug l}^{-1}$, indicating a depletion of 26% relative to sea water concentration. Below 23 cm the uranium concentration varies irregularly with depth between 2.09 and 3.22 ug l^{-1}

a/

a feature which may be related to the increased dissolved phosphate levels at 30 cm and 51 cm. The importance of phosphate complexes of uranium, particularly the species $\text{UO}_2(\text{HPO}_4)_2^{2-}$, was recognised by Langmuir (1978) and Dongarra and Langmuir (1980). Indeed, the presence of only $1\mu\text{M PO}_4^{3-}$ will displace the stability field of carbonate complexes to pH 7.5 or greater (Tripathi, 1979).

In all the previous cores discussed, the geochemical data available have indicated either oxic or mildly reducing environments, with essentially conservative pore water uranium behaviour. The uranium data for the squeezed pore waters were assumed to be subject to a pressure artefact and were translated as lower pore water values relative to sea water. However, to ensure that this is indeed the case, samples from the in-situ pore water sampler must be examined for each individual core. In the following discussion, all the deep-sea cores have anoxia at depth and show concomitant elevations in their pore water uranium contents.

Station 10554 east of the Great Meteor seamount on the Madeira abyssal plain (Table 2.1, Figure 2.1) is the only other station where comparative corer and in-situ data are available. Table 3.6 shows the uranium and alkalinity results in the pore waters squeezed from the box core 10554 5B and the Kasten core 10554 2K, together with the in-situ sampler data 10554 #12 PWS. Straightforward intercomparison of the profiles, however, is not possible here, since the composition of the cores taken only a few miles apart is variable, with pelagic sedimentation being interrupted sporadically by deposition of fine-grained, calcareous distal turbidites (Weaver and Kuijpers, 1983) whose possible source areas are the North-west African continental slope and the slopes of the Madeira and Canary archipelagos. The box core, about 60 cm long, showed a decreasing dissolved O_2 profile, falling to less than 10% air saturation at 30 cm and to zero at 40 cm./

TABLE 3.6

Uranium and alkalinity data for station 10554

(Madeira abyssal plain - Great Meteor seamount) ($\pm 1\sigma$ error)Box Core 5B : $31^{\circ}30'N$ $24^{\circ}26'W$,
5370m.In situ sampler #12: $31^{\circ}27'N$ $24^{\circ}27'W$,
5371m

<u>Depth(cm)</u>	<u>Uranium</u> <u>($\mu g l^{-1}$)</u>	<u>Alkalinity</u> <u>($meq l^{-1}$)</u>	<u>Depth(cm)</u>	<u>Uranium</u> <u>($\mu g l^{-1}$)</u>	<u>Alkalinity</u> <u>($meq l^{-1}$)</u>
0 - 2	2.75 \pm 0.10	1.89	- 50	3.78 \pm 0.13	2.25
2 - 4	2.48 \pm 0.09	-	- 1	2.37 \pm 0.08	2.33
4 - 6	2.44 \pm 0.09	1.81	2	4.96 \pm 0.17	2.63
6 - 8	3.03 \pm 0.11	-	3.5	5.36 \pm 0.18	2.51
8 - 10	2.23 \pm 0.08	1.80	6.5	6.43 \pm 0.24	2.79
12 - 14.5	2.20 \pm 0.08	-	12.5	8.76 \pm 0.31	2.92
14.5 - 17	3.37 \pm 0.12	1.92	24.5	8.69 \pm 0.31	3.03
17 - 19.5	2.24 \pm 0.08	-			
19.5 - 22	2.20 \pm 0.09	1.85			
22 - 24.5	2.22 \pm 0.09	-			
24.5 - 27	2.31 \pm 0.09	2.04			
27 - 29.5	1.66 \pm 0.07	-			

Kastenlot Core 2K : $31^{\circ}30'N$ $24^{\circ}29'W$, 5370m

<u>Depth(cm)</u>	<u>Uranium</u> <u>($\mu g l^{-1}$)</u>	<u>Alkalinity</u> <u>($meq l^{-1}$)</u>
21 - 26	14.63 \pm 0.48	1.93
35 - 40	10.84 \pm 0.37	2.43
53 - 58	10.92 \pm 0.37	2.50
76 - 81	11.34 \pm 0.38	2.55
95 - 100	8.20 \pm 0.29	-
113 - 118	7.60 \pm 0.28	2.59
138 - 143	4.45 \pm 0.18	2.48
157 - 162	5.63 \pm 0.22	-
184 - 189	4.75 \pm 0.19	2.27

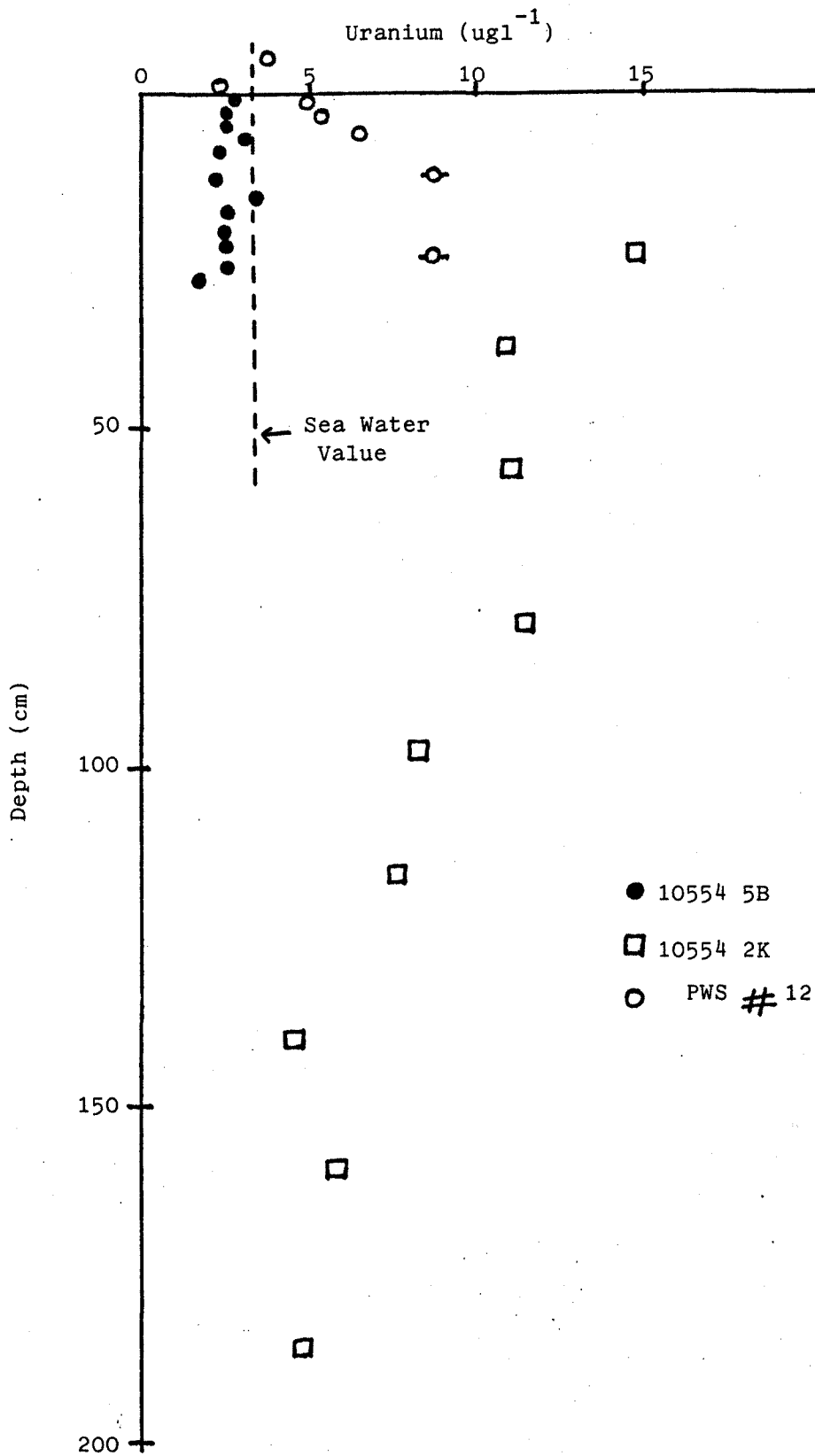


Figure 3.9. Uranium concentrations in the pore waters of cores from the Madeira abyssal plain.

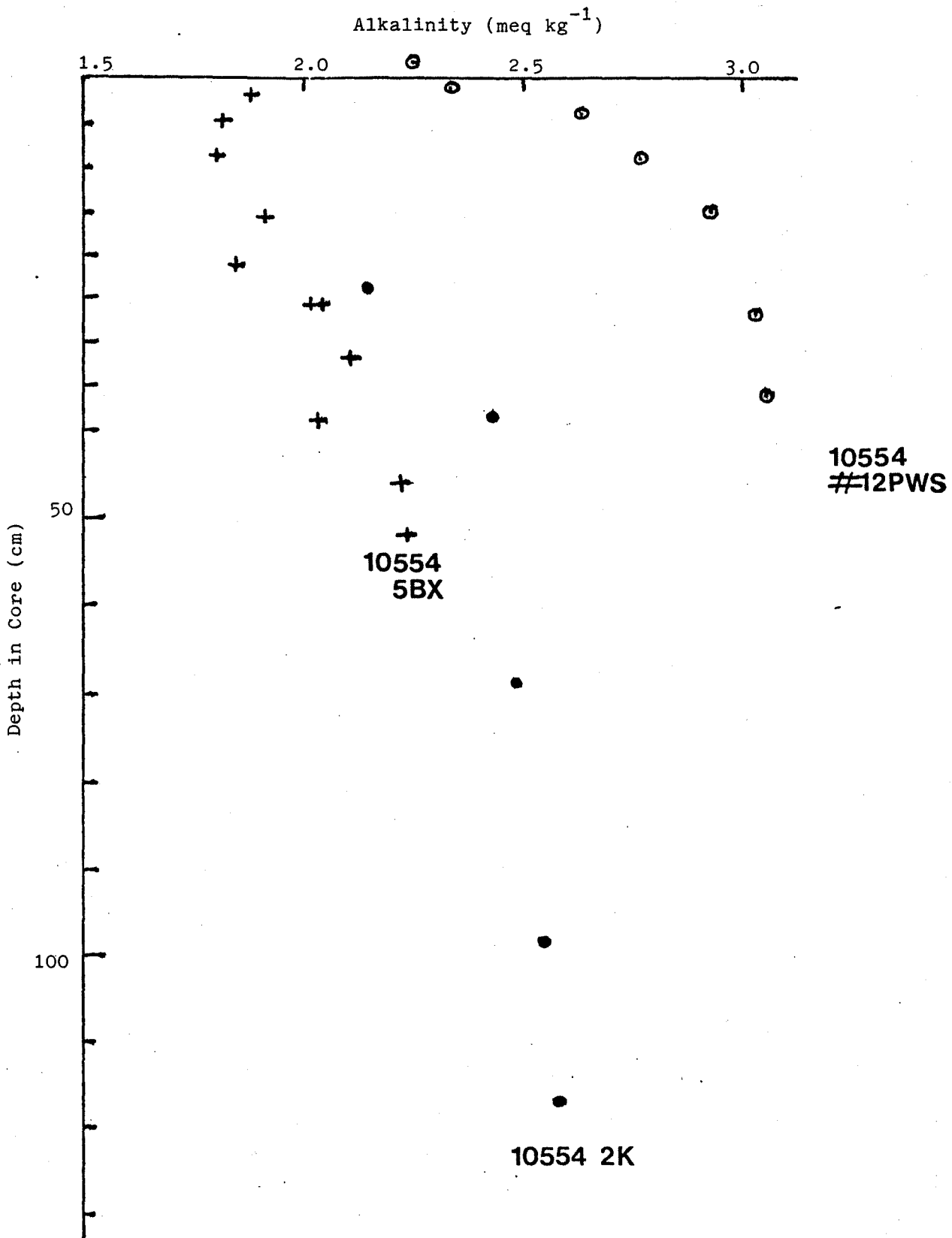


Figure 3.10, Alkalinity in the pore waters of cores from the Madeira abyssal plain.

40 cm (Sorensen et al., 1984). Further evidence of reducing conditions was complete denitification by 40 cm (Sorensen et al., 1984) and manganese release. Dissolved silicate increased to about 5 times and dissolved phosphate to about 2.5 times their bottom-water values by this depth. From Figure 3.10, the alkalinity pressure effect was again observed for the box and Kasten cores, with a mean decrease in alkalinity of 31.7% over the depth range 0 - 29.5 cm relative to the in-situ samples. Only the uranium content of the box core, however, showed a corresponding 26.3% mean decrease from the sea water value. Solid phase analysis of the box core showed high uranium values between 31 and 52 cm (range 3.59 to 9.77 ppm, mean = 6.75 ppm), with anoxic conditions here coincident with a 20 cm thick green layer, the lower part of a turbidite. This layer was also present in a nearby Kasten core (10554 11K) and had a mean organic carbon content of ~1.5% as compared to 0.17% for the overlying and underlying calcereous ooze, and a mean CaCO_3 content of 23.7%, as compared to a mean 55.2% CaCO_3 for the overlying and underlying ooze. The observation that the pore water uranium values in the box core are depressed at all depths down to 29.5 cm was surprising with a high uranium, high organic carbon turbidite layer below 31 cm. It would perhaps have been expected that the upward diffusion of solubilised uranium, with this anoxic layer as source, would register as a gradient, positive downwards, in the pore waters as was observed in the PWS data (Figure 3.9). That the pressure effect alone cannot be responsible for suppressing such a gradient is shown by the results for core 10554 2K (Figure 3.9). Here, the pressure effect is operative (depressed alkalinity, Figure 3.10), yet the pore water uranium associated with the grey-green anoxic turbidite at 35 cm and beyond is enhanced. The explanation for these low pore water uranium values above the turbidite may lie in a combination of two effects. The pressure effect in oxic, low-organic carbon sediment/

sediment (0.17% for 10554 5B overlying ooze) could depress pore water uranium, but as observed by Suess (1970), reduced, high-organic carbon sediment (1.5% in the turbidite here) may contain sufficient dissolved organic matter (DOM) to adsorb onto and saturate carbonate mineral surfaces, thus inhibiting calcium carbonate precipitation, a suggestion also made by Berner et al., (1970). Since plutonium and uranium are both actinide elements of variable oxidation state and may behave similarly in sediments, it is of relevance to consider the work of Pillai et al., (1982) on plutonium. These authors demonstrated that Pu can be present in sea water in association with high molecular weight organic compounds and that at levels of 20 mg DOM l⁻¹, values easily attained and often exceeded in marine pore waters (Nissenbaum et al., 1971; Nissenbaum et al., 1972; Krom and Sholkovitz, 1977; Lyons et al., 1979; Barcelona, 1980; Elderfield, 1981), the solubility of Pu in waste effluent was increased by a factor of 5. Such solubilisation was apparently higher, by a factor of about 26, in the presence of carbonates/bicarbonates. The amount of Pu released from sediments by sea water containing excess organic matter (20mg l⁻¹) and added carbonate (140 mg l⁻¹) was less than 3.5%. Under reducing conditions, however, simulated by bubbling H₂S gas through a sediment/sea water slurry, the Pu release was enhanced to 60%.

The maximum pore water uranium of 14.63 ug l⁻¹ at the 21 - 26 cm depth interval in core 10554 2K could be due to an Eh boundary change within the sediment, where a high solid-phase uranium content is in contact with oxic pore water, resulting in oxidation of organic matter and release of bound uranium. This effect is similar to that observed in a groundwater redox barrier (Cowart, 1980), and in a brown clay sediment from the/

the North East Atlantic (Colley et al., 1984), wherein a downward-advancing oxidation front released and mobilised uranium from the organic matter of a turbidite. It is assumed that there would be an upward flux of uranium within the pore waters for the Kasten core here, as well as the observed downward flux (Figure 3.9) which seems to be concave downwards indicating some uranium uptake by the reduced sediment below. In contrast to the conservative in-situ uranium values found in the oxic pore waters of core 10552 (Table 3.3), the in-situ sampler uranium profile here (Table 3.6) was enhanced over the sea water value. The two overlying water samples gave a mean uranium concentration of $3.08 \pm 0.08 \text{ ug l}^{-1}$. The dissolved O_2 profile for this core (10554 #12) was similar to that of the box core (10554 5B), decreasing with depth. The enhanced uranium levels probably had as their source the grey-green turbidite described earlier, whose top surface was assumed to lie about 12.5 cm below the sediment : water interface at the site of the PWS drop. Taking the uppermost four pore water uranium data points, a concentration gradient of $3.63 \times 10^{-4} \text{ ug U cm}^{-4}$ was indicated. Fick's first law of diffusion (Lerman, 1979) states that

$$F_u = -D_u \frac{dc_u}{dx} \dots\dots\dots(3.6)$$

where F_u is the flux of solute U in $\text{g cm}^{-2} \text{ yr}^{-1}$, D_u is its effective diffusion coefficient in $\text{cm}^2 \text{ yr}^{-1}$ and dc_u/dx is the concentration gradient of solute U in g cm^{-4} . The formal relationship between the diffusion coefficient in free solution, D_o , equal to $134 \text{ cm}^2 \text{ yr}^{-1}$ for the uranyl ion (Li and Gregory, 1974) and the bulk sediment or effective diffusion coefficient D_u , can be expressed as

$$D_u = D_o \phi^2 \dots\dots\dots(3.7)$$

where ϕ is the volume fraction of sediment occupied by water (porosity) and $0 \leq \phi \leq 1$. If deposition is slow, then the porosity of a sediment tends to be low since the expulsion of pore water keeps pace/

pace with pressure loading. In box cores porosity values are usually \pm 15% of the mean showing an exponential decrease with depth. Measurements of wet/dry ratios on core 10554 5B showed a constant porosity in the top 27 cm of 0.440 \pm 0.003, giving an effective diffusion coefficient D_U of $26\text{cm}^2\text{yr}^{-1}$ in the sediment at this station. This is in good agreement with the value used by Ku et al., (1977) of $30\text{cm}^2\text{yr}^{-1}$. From equation 3.6, assuming transport of uranium as the uranyl ion, an upward flux of $0.94 \times 10^{-8} \text{g cm}^{-2}\text{yr}^{-1}$ ($7.0 \text{dpm cm}^{-2}\text{kyr}^{-1}$) is calculated. If it is supposed that the source of uranium for this flux was a turbidite identical to that found in core 10554 5B, i.e. 21 cm thick with a mean uranium content of 6.75 ppm, and if a mean density of 2.5g cm^{-3} is assumed, then the total uranium inventory in this band was 354.5ug cm^{-2} (262.5dpm cm^{-2}) and so this flux of $7.0 \text{dpm cm}^{-2}\text{kyr}^{-1}$ could be maintained for 37,500 yrs in both directions and therefore for 18,750 yrs upwards if diffusion away from the band is considered symmetrical. The calculated uranium flux above is more than an order of magnitude greater than the flux of ^{234}U from deep-sea sediments ($0.3 \text{dpm cm}^{-2}\text{yr}^{-1}$) calculated by Ku (1965) based on the deficiency of ^{234}U with respect to ^{238}U in the solid phase. If one considers that the $^{234}\text{U}/^{238}\text{U}$ activity ratio in reducing sediment pore waters would be > 1.14 (see, for example, Cochran and Krishnaswami, 1980) then the actual ^{234}U flux (in activity units) from core 10554 # 12 would be even greater, indicating the importance of such reducing sediments in the geochemical balance of uranium isotopes in the ocean. Using only solid-phase uranium data, Yamada and Tsunogai (1984) came to the conclusion that reducing sediments from the Bering Sea were acting as a sink for uranium. Both of these considerations, reducing sediments acting as a uranium source or sink, would place either lower or higher limits respectively on the riverine uranium concentrations and activity ratios required in any steady-state model (Ku et al., 1977). The above picture of uranium solubilisation by some organic or inorganic species within a high organic turbidite unit, with subsequent migration away from the/

the pore water maximum concentration does not, unfortunately, explain the uranium profile obtained from core 10549 6K, shown in Figure 3.11. This core contained a glacial sediment section deeper than 50 cm ($\sim 70\%$ CaCO_3 , $\sim 0.6\%$ organic C) above which lay a postglacial carbonate ooze (75 - 85% CaCO_3 , $\sim 0.2\%$ organic C). ^{14}C dating gave sedimentation rates of 8.3 cm kyr^{-1} and 3.2 cm kyr^{-1} for these layers respectively. Where the change in accumulation rate occurred, there was a noticeable green colour from 49 cm to the bottom, corresponding to the Fe(III)/Fe(II) redox boundary according to Lyle (1983). Dissolved O_2 dropped to its minimum value at $\sim 50\text{cm}$, just above which lay a solid-phase manganese spike, with manganese reduction and mobilisation in the pore waters below. The glacial sediment contains elevated uranium contents (mean concentration $4.50 \pm 0.11 \text{ ppm}$ from 64 to 136 cm) as compared to that for the postglacial carbonate ooze (mean concentration $0.37 \pm 0.02 \text{ ppm}$ from 0 to 51 cm). The pore water uranium concentration also increased dramatically from 1.13 ug l^{-1} to 8.51 ug l^{-1} at 51 cm, to a maximum of 85 ug l^{-1} at 65 cm within the suboxic zone (Figure 3.11). It was evident from the increased pore water phosphate concentration and alkalinity concentration (although only one datum point) that organic matter combustion was proceeding in the suboxic glacial layer, with the pore water uranium and alkalinity showing a possible correlation. This would be in accord with Kolodny and Kaplan's (1973) idea of high $\sum \text{CO}_2$ levels solubilising adsorbed or complexed or reduced uranium from the solid phase. However, this suggestion here must be qualified when it is expected that the pressure effect would occur in this deep-sea core. Down to 45 cm in core 10549 6K, the pore water uranium content decreased linearly from $2.89 \pm 0.11 \text{ ug l}^{-1}$ to $1.13 \pm 0.06 \text{ ug l}^{-1}$ (mean $1.98 \pm 0.04 \text{ ug l}^{-1}$) suggesting a 40% mean reduction in the oxic, carbonate-rich layer relative to sea water. Again, the proposed explanation for high pore water uranium in the glacial sediment below is oxidation or combustion of the relatively high organic matter ($\sim 0.6\%$) and concurrent solubilisation of some adsorbed or complexed (authigenic) uranium. The observed linear uranium decrease from sea/

TABLE 3.7

Uranium, alkalinity and phosphate data for station
10549 (East Atlantic) ($\pm 1\sigma$ error)

Kastenlot Core 6K : $00^{\circ} 01.9'N 16^{\circ} 10.2'W$, 3150m.

<u>Depth (cm)</u>	<u>Uranium ($\mu\text{g l}^{-1}$)</u>	<u>Alkalinity (meq l^{-1})</u>	<u>Phosphate (μM)</u>
12	2.89 \pm 0.11	2.67	1.5
19	2.56 \pm 0.10	-	0.5
27	2.29 \pm 0.10	2.51	0.2
33	1.68 \pm 0.08	-	0.2
39	1.34 \pm 0.06	2.51	0.1
45	1.13 \pm 0.06	-	0.3
51	8.51 \pm 0.33	2.34	1.7
58	72.92 \pm 2.56	-	4.7
65	84.99 \pm 2.93	2.88	5.8
72	47.05 \pm 1.76	2.40	6.8

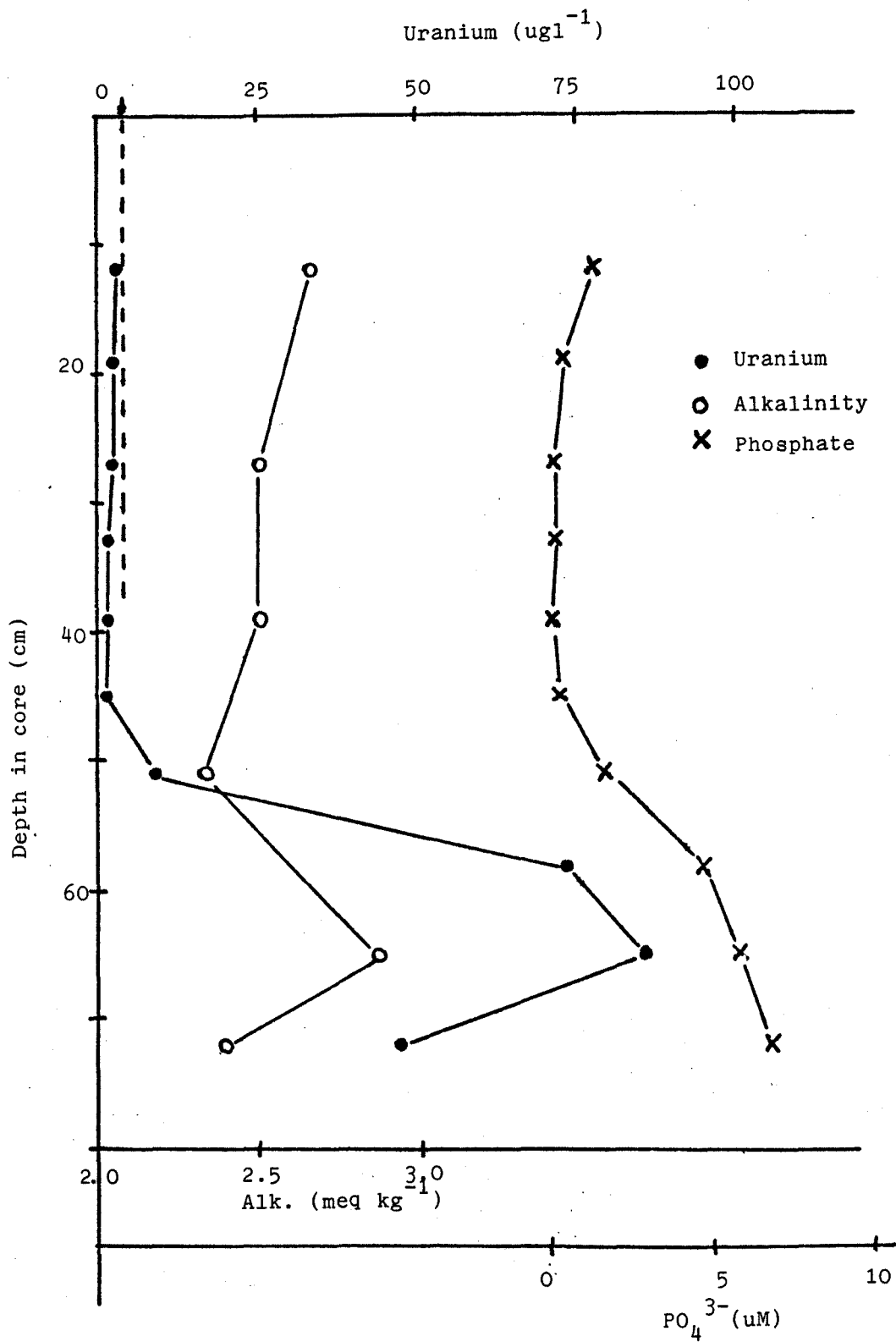


Figure 3.11. Uranium, alkalinity and phosphate in the pore waters of eastern Atlantic core 10549 6K.

sea water value to a low value of 1.13 ug l^{-1} seems to represent a sink for uranium, if the upper values in this core are not a reflection of the pressure artefact. As noted previously, such a sink has already been found by Yamada and Tsunogai (1984) in a reducing core from the Bering sea. If uranium mobilisation is via organic complexation, then the pressure effect cannot be the reason for the absence of a downward-increasing profile to peak levels at depth in both this core and core 10554 5B (discussed earlier). More mystifying is the fact that such a profile was observed for the in-situ samples from this station (10554). Colley et al., (1984) have illustrated the downward-mobilisation of uranium in a core off the North West coast of Africa. From the solid-phase uranium data for this core, it was proposed that oxygen diffusion downwards into a turbidite layer progressively oxidised some of the combustible organic material, evidenced by a depression in the organic carbon content at the top of the turbidite, which released uranium to the pore waters, evidenced by a solid-phase uranium depression in the same sediment layer. About two-thirds of this remobilised uranium diffused downwards to be fixed again, giving rise to a uranium solid-phase spike at the base of the turbidite, with the other 30% assumed to have diffused upwards and out of the sediment column (Colley et al., 1984). A strange pore water profile is implied to pump uranium in the downwards direction preferentially, but unfortunately pore water data were not available. Looking again at core 10549 6K, if we assume similar porosities to 10554 5B i.e. a mean water content of 58.2%, then in 1 kg of sediment there are 582 g of pore water and 418 g of sediment. For a mean uranium content of 4.50 ppm in the glacial sediment layer, this amount of sediment contains a total of 1881 ug of uranium which is in contact with the 582 g (568 ml) of pore water. To achieve the maximum observed pore water concentration of 85 ug l^{-1} , equal to an enhancement of $\sim 82 \text{ ug l}^{-1}$ over the sea water value, the desorption of 46.6 ug of uranium from the solid phase by whatever method (released with oxidised organic matter, solubilised by organic complex formation, remobilised by the sharp redox change accompanying anoxia, or by higher carbonate values) is required, an amount/

amount equal to only $\sim 2.5\%$.

Core 10549 could be considered analogous to the high-organic carbon, sapropel-layered sediments found in confined, periodically stagnant basins such as the Ionian Sea in the Eastern Mediterranean region (Mangini and Dominik, 1979, Thomson, 1982) or to the sediments of deep-water basins with static cyclic circulation zones (Baturin, 1973) both of which show large enrichments of uranium. Uranium concentrations of up to 50 ppm and organic carbon up to 7.2% together with a correlation between the uranium and organic matter content have been reported for Late Quaternary sapropels from the Mediterranean Ridge (Mangini and Dominik, 1979). The formation of the sapropel layers was suggested by Rossignol-Strick et al., (1982) to be a result of Nile river flooding, which spread a low-density, low-salinity discharge over the sea surface, resulting in the establishment of a steep vertical salinity gradient. The stable stratification triggered by this salinity and density gradient prevented thermohaline convection and resulted in the depletion of oxygen at depth and the formation of the sapropel due to the creation of a reducing environment. The increased erosion resulting from the flooding of the Nile supplied excess nutrients to the water column, producing a greater bacterial supply to the sediment and giving rise to the anoxic conditions which kills off the benthic community, preserving the organic carbon for the sapropel. The study of one such sapropel layer in detail by Mangini and Dominik (1979) led to the conclusion that uranium incorporation was indeed by authigenic deposition ($^{234}\text{U}/^{238}\text{U}$ activity ratios around 1.15 for young sapropels less than $\sim 25,000$ yrs) and was later confirmed by Thomson (1982). A half-closed system for uranium isotopes was proposed, however, for older sapropels of 130,000 yrs in a particular layer which exhibited uranium activity ratios close to unity for the middle sections with the highest uranium content, but remarkably higher ratios of up to 1.19 ± 0.04 in the sections underneath and above. The expected $^{234}\text{U}/^{238}\text{U}$ activity ratio for a sapropel layer of this age would be 1.10. This was explained by the half-closed system/

system in which only the ^{234}U produced in-situ by radioactive decay of ^{238}U , which eventually replaces the originally deposited ^{234}U , is able to move. Such ^{234}U production would be greatest in the highest uranium-containing sections of the sapropel layer, and this ^{234}U would diffuse along the produced concentration slope to yield the given activity ratios, and would eventually be lost from the layer. However, if the total uranium and $^{234}\text{U}/^{238}\text{U}$ ratios are used, it can be shown that the 'total' $^{234}\text{U}/^{238}\text{U}$ ratio of the whole sapropel band is 1.10, a value equal to the expected ratio for a band of such an age, indicating very little escape, if any, even of ^{234}U . Modelling of this diffusion process (Mangini and Dominik, 1979) gave a diffusion constant, D_u , of between 10^{-11} and $10^{-12} \text{ cm}^2 \text{ s}^{-1}$, about 5 to 6 orders of magnitude lower than that for uranium in oxic sediment pore water (Ku et al., 1977), indicating that the ^{234}U has only a very small chance to diffuse freely, spending most of its lifetime adsorbed on particles in the sapropel, probably as $^{234}\text{U}^{4+}$ given the high reducing conditions present. If the D_u value of $10^{-12} \text{ cm}^2 \text{ s}^{-1}$ (relevant for all isotopes of uranium) is used for the uranium present in the glacial layer of core 10549 6K, which is also under reducing conditions, then with the data at depths 45 cm and 65 cm from Table 3.7 giving a concentration gradient of $4.19 \times 10^{-3} \text{ ug cm}^{-4}$, an upward uranium flux of only $4.19 \times 10^{-15} \text{ ug cm}^{-2} \text{ s}^{-1}$ is calculated from equation 3.6. Such a low flux should not (and from Figure 3.11 does not appear to) give rise to an increase in the uranium content in the overlying pore waters, even considering that, from ^{14}C dating of the neighbouring core 10549 1K, the glacial layer has had $\sim 13,000$ yrs in which to do so. Viewed another way, a breakthrough time for diffusional transport through a sediment can be defined (Thomson, 1978) as

$$t = Z^2 / D_u \dots\dots\dots(3.8)$$

where Z is the barrier thickness in cm and D_u is the diffusion coefficient in $\text{cm}^2 \text{ s}^{-1}$. The time required for the uranium in the pore water below 45 cm to break through just 5 cm to 40 cm depth using equation 3.8 and the above D_u value of $10^{-12} \text{ cm}^2 \text{ s}^{-1}$, is 7.96×10^5 yrs. Although this treatment is rather simplistic, the result/

result shows that a negligible amount of uranium would be expected to diffuse upwards in the pore waters of this reduced sediment. Squeezed pore waters taken from two box cores and one Kasten core from Hellenic Trench sediments in the Eastern Mediterranean were analysed for uranium and the results are shown in Table 3.8. All three cores contained 30 cm calcareous ooze overlying sapropel layers of various thicknesses and overall sedimentation rates (Thomson, 1982), due to the complex physiography which controls sediment redistribution in this vicinity (Stanley, 1978). The sapropels have low concentrations of manganese, consistent with the behaviour of this element under anoxic conditions, enrichments of Cr, Cu, Mo, Ni and Zn due to organic matter or sulphide association (Calvert, 1976; Sutherland et al., 1984) and very high concentrations of uranium in both the sediment and pore waters. The pore water uranium data for the three cores 10103 1B, 6B and 3K are given in Table 3.8 and are plotted in Figures 3.12 to 3.14 respectively.

A number of workers have found metal-organic associations in marine sediments and pore waters, and have shown that high molecular weight humic and fulvic acids and their dissolved precursors including degraded planktonic cellular material, amino acids and carbohydrates are most important for metal complexing (Nissenbaum and Kaplan, 1972; Nissenbaum and Swaine, 1976; Krom and Sholkovitz, 1977; Krom and Sholkovitz, 1978; Lyons et al., 1979; Elderfield, 1981). The various types of dissolved organic matter (DOM) in pore waters are higher than in the overlying water (Henrichs and Farrington, 1979; Lyons et al., 1979), stay about constant in oxic cores (Krom and Sholkovitz, 1977; Henrichs and Farrington, 1979) but become further enriched with depth in anoxic layers (Krom and Sholkovitz, 1977; Henrichs and Farrington, 1979; Lyons et al., 1979; Barcelona, 1980; Elderfield, 1981) In short-term laboratory tank experiments, too, a large increase with depth of dissolved organic carbon in the pore water, from 1 to 10 mg l⁻¹ has been observed (Sholkovitz et al., 1983) indicating that/

TABLE 3.8

Uranium data for station 10103 (East Mediterranean)

Box Core 1B : $36^{\circ}09.6'N$, $20^{\circ}28.5'E$, 2880m.

<u>Depth (cm)</u>	<u>Uranium ($\mu g l^{-1}$)</u>
0 - 5	8.84 \pm 0.33
5 - 10	5.04 \pm 0.22
10 - 16	4.96 \pm 0.21
19 - 22	5.13 \pm 0.22
22 - 25	3.76 \pm 0.18
25 - 28	3.90 \pm 0.18
28 - 33	20.27 \pm 0.64
33 - 38	10.84 \pm 0.38
38 - 43	16.45 \pm 0.53

Box Core 6B : $36^{\circ}N$ $20^{\circ}E$, 2900m.

<u>Depth (cm)</u>	<u>Uranium ($\mu g l^{-1}$)</u>
0 - 6	3.85 \pm 0.18
10 - 16	3.52 \pm 0.17
24 - 29	34.87 \pm 1.16

Kastenlot Core 3K : $36^{\circ}N$ $20^{\circ}E$, 2900m.

<u>Depth (cm)</u>	<u>Uranium ($\mu g l^{-1}$)</u>
0 - 5	3.38 \pm 0.14
8 - 13	4.36 \pm 0.18
16 - 20	3.24 \pm 0.13
21 - 26	3.90 \pm 0.15
27 - 32	37.68 \pm 1.35
35 - 40	361.27 \pm 4.22
44 - 49	99.21 \pm 2.84
54 - 59	68.46 \pm 2.11

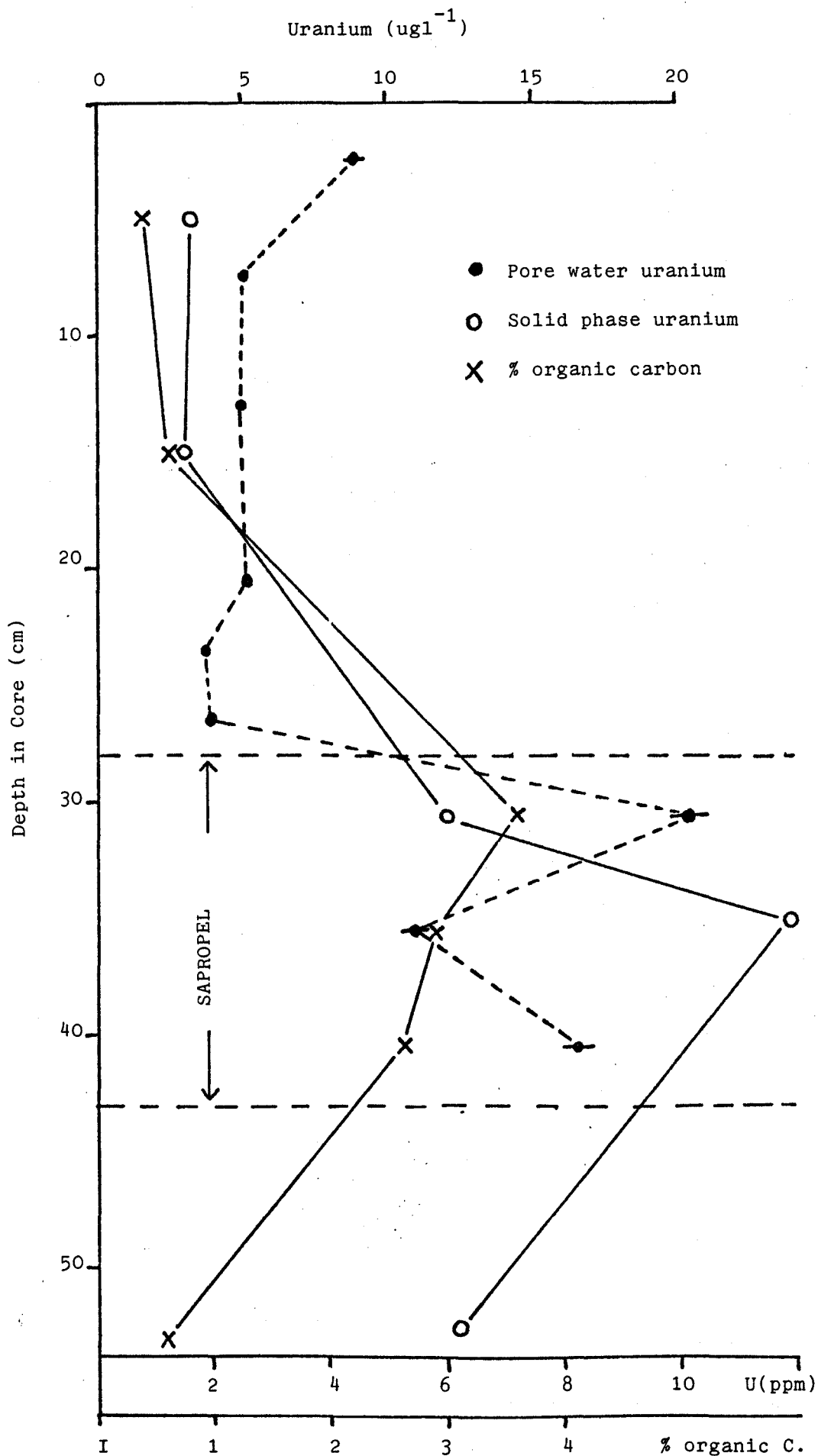


Figure 3.12. Pore water uranium and solid-phase uranium and organic carbon in east Mediterranean core 10103 1B.

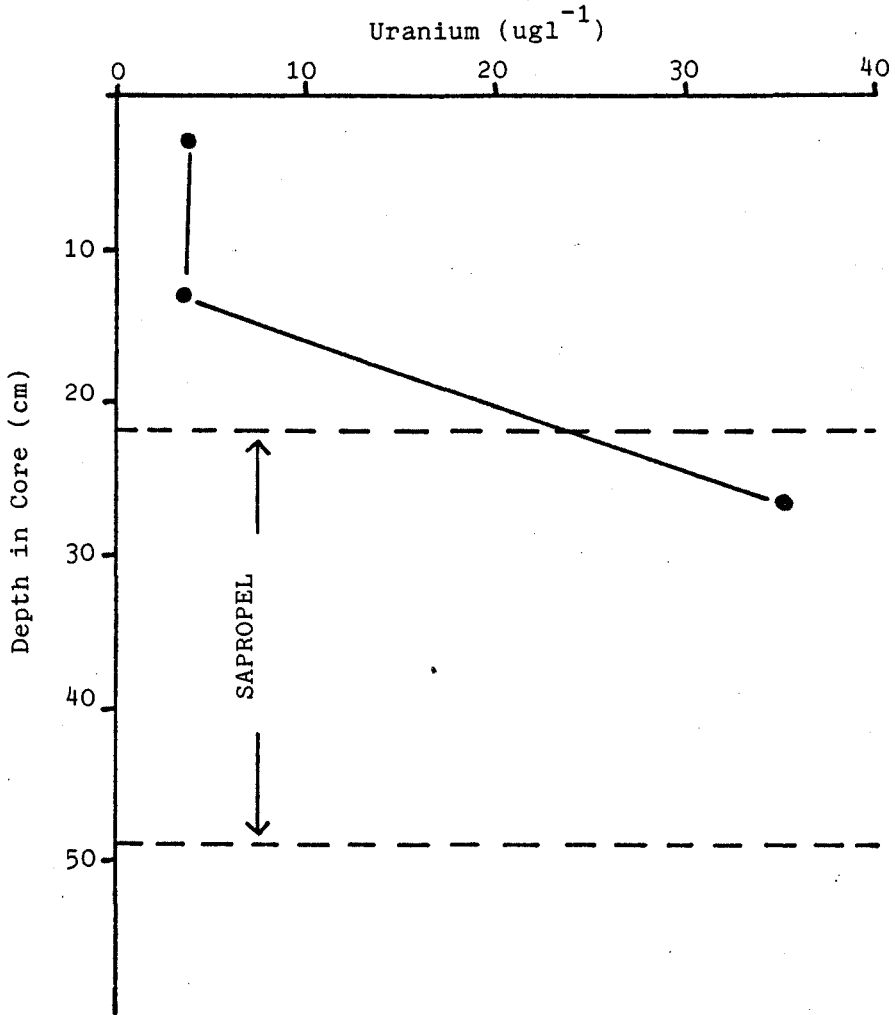


Figure 3.13. Pore water uranium in east Mediterranean core 10103 6B.

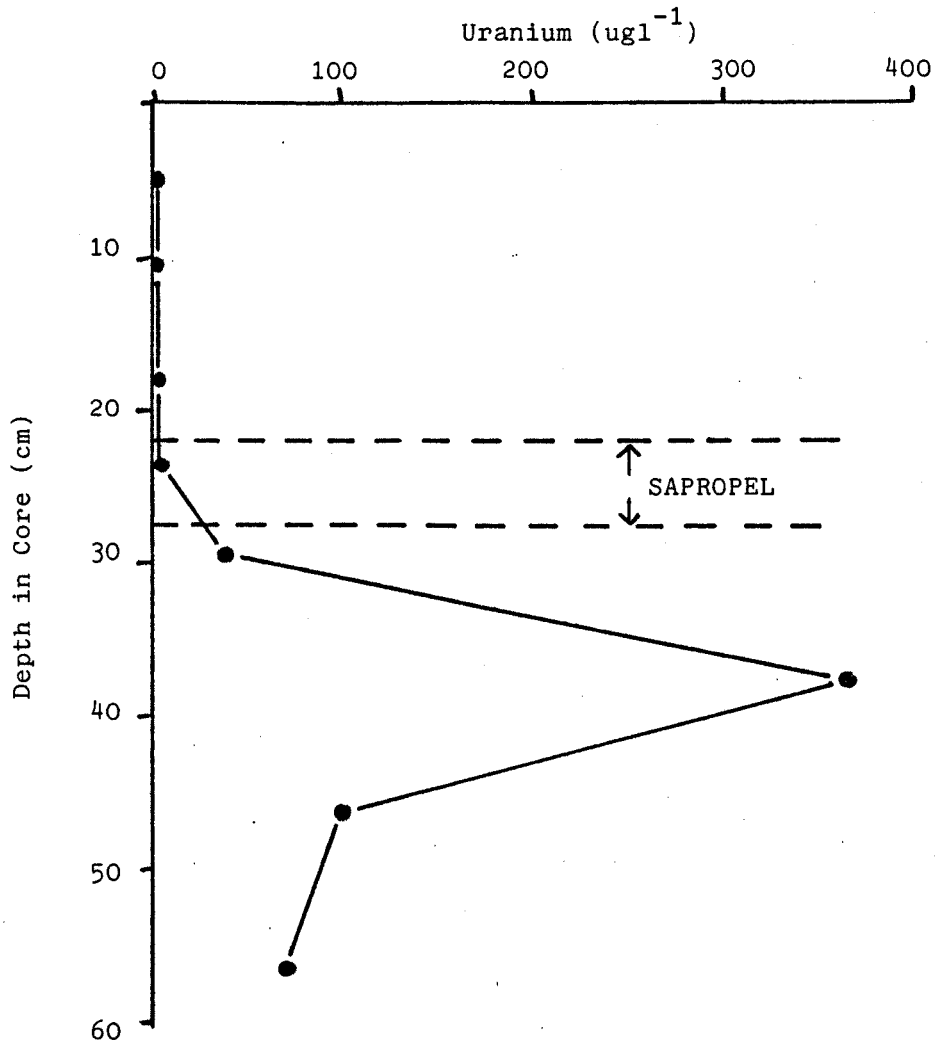


Figure 3.14. Pore water uranium in east Mediterranean core 10103 3K.

that the diagenetic reactions occurring in sediments, as were simulated here, are adding organic matter to the pore waters. The data of these authors tend to confirm the pathway of humification (Nissenbaum et al., 1971; Nissenbaum and Kaplan, 1972) where marine humic acids can be formed in-situ from autochthonous material (degradation products of plankton) and are not necessarily allochthonous (transported from the continent). Since marine humates have a rather constant $\delta^{13}\text{C}$ value of -20 to -22%, whereas $\delta^{13}\text{C}$ of soil humic acid is related to its plant source material and ranges from -25 to -26%, the organic material in the eastern Mediterranean sapropels with its carbon isotopic signature of -20% was distinctly of marine origin. Marine humic and fulvic substances can comprise up to 70% of the organic matter in recent sediments (Nissenbaum and Kaplan, 1972) and the major products of their oxidation are aliphatic, benzenecarboxylic and phenolic acids which, together with the more abundant heterocyclic structures found in the marine humics relative to terrestrial humics (Nissenbaum and Swaine, 1976) could be the important species involved in the bonding or complexing of metals in the sediments and pore waters. Data from laboratory and field experiments have shown that humic acids and fulvic acids are important in the geochemistry of uranium. The binding of tracer level UO_2^{2+} to a soil humic acid was interpreted (Shanbhag and Choppin, 1981) as involving one or two carboxylate groups, and it was shown that at pH6, if the concentration of CO_3^{2-} was low enough ($\sim 10^{-7}\text{M}$) and that of the humate high enough ($\approx 10^{-4}\text{M}$), then the uranyl ion would be complexed predominantly by humate. Uranium was almost completely removed as a uranyl-organic anion from a CO_3^{2-} solution by anion exchange resins in a < 1000 m.wt. filtrate (Bloomfield et al., 1973) indicating the formation of a small molecular weight uranium complex which was more stable than the carbonate. Such cation exchange properties of humic or fulvic acids are responsible for the/

the observed geochemical enrichment of uranium in, for example, lignites (Szalay, 1964), peat bogs (Halbach et al., 1980) and reducing sediments (Kolodny and Kaplan, 1973). The latter authors found high levels of DOM up to 66mMl^{-1} in the reducing pore waters of Saanich Inlet and it is reasonable to assume that, due to the greater organic matter deposition at the time of sapropel formation, the pore waters at the sapropel horizons in the cores from Station 10103 will have much greater concentrations of DOM. Nevertheless, there might not be any statistically significant correlation between the concentration of organic carbon in the sediment and its concentration in the pore water (Nissenbaum et al., 1972). It is this DOM and the known uranium-organic matter correlation which is believed to be responsible here for the enhanced pore water uranium values for the three 10103 cores (Table 3.8). From Figures 3.12 to 3.14 it is observed that only in the two box cores do the high uranium concentrations lie within the sapropel bands, the massive peak of $\sim 360\text{ugl}^{-1}$ for 10103 3K lying below this core's sapropel band. The reason for this downward displacement phenomenon is not clear, but as discussed by Crawford (1982), the siting of a rapid Eh change or the draining of pore water on gravity coring were possible explanations. The coincidence of the pore water uranium peaks and sapropel bands in the other two profiles, in which the sediment was sampled by square box corer and therefore not subjected to severe disruption by penetration, favours the second of these explanations. The mean pore water uranium values in the top carbonate ooze sections of cores 10103 3K and 6B are similar to the sea water value being 3.72 ± 0.08 and $3.69 \pm 0.18\text{ugl}^{-1}$ respectively, and thus do not show the expected decrease due to the pressure effect. This may be due to a small systematic error in the uranium standard calibration, or to the fact that these cores were recovered from water depths less than 3000 m which could mean that any pressure artefact on alkalinity and uranium would be smaller than observed previously for deep-sea cores (26-44% uranium decrease relative to sea water in depths ranging from 3250 to 5600 metres), pressure being proportional to depth.

For/

For core 10103 1B, however, the main carbonate ooze pore water uranium value of $5.27 \pm 0.21 \text{ ug l}^{-1}$ is certainly greater than in sea water, an observation that is difficult to reconcile with the data from the other two cores. The sedimentation rate for the ooze section is about 4 cm kyr^{-1} from ^{14}C data, while for the sapropel, $^{230}\text{Th}_{\text{excess}}$ data, based on water column supply considerations, yields a sedimentation rate of 3.1 cm kyr^{-1} (Thomson, 1982) a value not greatly dissimilar to the mean long term rate (Mangini and Dominik, 1979). The typically high sedimentation rate for the ooze and its low organic carbon content (mean 0.26%) prevents significant uranium uptake from sea water, as signalled by the solid phase uranium $^{234}\text{U}/^{238}\text{U}$ activity ratio of 0.99. In contrast to this is the ratio of 1.13 and the 3% organic carbon in the sapropel, levels which provide the necessary uranium and the DOM for enhancement of uranium in the pore waters. Levels above sea water are thus not expected in the carbonate ooze and their observation here, at values too large to be due to a small systematic error, could be a result of contamination of the pore water with sediment particles during the core squeezing process. A small amount of particulates was present in at least one of the top 6 pore water samples (19-22 cm) in 10103 1B as shown by a slight brown colouration in the sample vial. A possible argument against this, however, was the absence of fission track stars.

Auxiliary geochemical data for the cores 10103 3K and 10103 6B are not available, but it is considered that the processes of organic complexation in the sapropel pore waters are operative, giving the uranium peak concentrations of 361 and 35 ug l^{-1} respectively, values which lie well within the range of reported levels as high as 260 ug l^{-1} for Atlantic sediments and 650 ug l^{-1} for Black Sea sediments (Baturin and Kochenov, 1973). As was observed in the East Atlantic cores 10554 5B and 10549 6K (but not, mysteriously, at 10554 #12 PWS), diffusion upwards to the sea water value at the surface from high uranium sources at depth does not occur probably for the same reasons, i.e. a very low effective diffusion coefficient of 10^{-11} to $10^{-12} \text{ cm}^2 \text{ s}^{-1}$ in a high organic, reduced environment (Mangini and Dominik, 1979).

3.3. Estuarine pore waters

Rapidly-accumulating nearshore deposits are usually oxygen-deficient and more organic material is available for postdepositional reactions in these than in pelagic environments. These differences reflect the higher rate of primary organic production at the ocean margins and the more rapid burial and preservation of material by the land-derived sediment influx. Generally, anoxic conditions form below a thin oxidised surface layer and show a low redox potential following diagenesis. The organic fraction comprises about 5% of the Hudson river estuary sediment (McCrone, 1967), 5.8% for a basin core from Loch Duich (Krom and Sholkovitz, 1977) and up to about 29% found here for the bottom muds of the Clyde estuary (section 3.4), although this latter figure probably arises from heavy sewage pollution. Because of the rapid burial of such relatively high concentrations of organic material, it is utilised by bacteria and other microorganisms within the sediments with the result that oxygen becomes depleted in the pore waters and production of H_2S by sulphate-reducing bacteria leads to reducing conditions. The thickness of the upper oxidised layer is evidently a function of the total rate of accumulation of the sediment and decreases in thickness shorewards, becoming anoxic below only the top 0.5 to 20 mm of the sediments studied here at St. Johns Lake in the Tamar estuary (Upstill-Goddard and Alexander, 1982), and can disappear altogether to give rise to H_2S - rich bottom waters as found in some fjords, some upwelling areas and restricted bays. Investigations into the isotopic composition of organic carbon from nearshore, estuarine and marine sediments (Sackett and Thompson, 1963; Nissenbaum and Kaplan, 1972) revealed an enrichment of ^{13}C in marine samples as compared to terrestrial values, with the estuarine samples tending to be intermediate and exhibiting considerable variation, but nevertheless indicating that in estuaries the terrestrial organic matter contribution is dominant. Gardner and Menzel (1974), using phenolic aldehydes/

aldehydes as indicators, suggested that the greatest deposition of terrestrially-derived organic material occurred where the terrestrial humic material rapidly precipitated - at the interface between fresh water and sea water (Sholkovitz, 1976). Thus the nature of the organic material in estuarine sediments will be substantially different from that in the foregoing discussion on deep-sea sediments, a situation which might lead to a difference in the behaviour of uranium in the pore waters if organo-uranyl complexes are invoked. Specifically, it might explain partly why uranium is enriched in the anoxic pore waters of deep-sea sediments, and, as shown in the following discussion, is depleted in anoxic/suboxic layers of estuarine sediment pore waters. The anodic character of the humic content of river water DOM enables them to interact at least with trace metal cations, forming complex linkages of various kinds by ion-exchange, surface adsorption and chelation, and according to Reuter and Perdue (1977), the stability of these heavy metal-humic complexes in natural waters is higher than that of corresponding inorganic-metal complexes.

The pore water uranium contents of the anoxic estuarine sediments carefully collected in the Tamar estuary (see section 2.3) were analyzed by the fission track method (section 2.6.2) and are shown in Table 3.9 and plotted in Figures 3.15 to 3.17. For core 075, some of the samples analyzed had been acidified to pH1 including 3 duplicates. It was observed from these duplicates that there was a systematic difference between the uranium results for the acidified and non-acidified pore water samples. As previously pointed out in the intercomparison exercise with the Woods Hole Oceanographic Institution (section 2.6.2), this discrepancy is the result of the more difficult homogeneous deposition of the acidified samples, in this case giving salt deposits of slightly greater diameter than normal and leading to slightly lower fission track densities and hence lower uranium concentrations. The mean values of these three duplicate samples are plotted amongst the rest of the uranium data for core 075 (Figure 3.17). A blank sample taken through the pore water squeezing and filtering procedure contained only $0.05 \pm 0.01 \text{ ug l}^{-1}$ of uranium. The dissolved Fe/

TABLE 3.9

Pore water uranium data for cores from the Tamar estuary
(St. John's Lake). ($\pm 1\sigma$ error)

Core 053 (pH1)		Core 075 (pH1)	
Depth (cm)	Uranium ($\mu\text{g l}^{-1}$)	Depth (cm)	Uranium ($\mu\text{g l}^{-1}$)
0 - 1	2.90 \pm 0.07	1 - 2	1.57 \pm 0.03
2 - 3	0.81 \pm 0.04	3 - 4	0.25 \pm 0.09
10 - 11	1.48 \pm 0.05	4 - 5	0.30 \pm 0.08
15 - 16	5.63 \pm 0.28	5 - 6	0.31 \pm 0.08
		6 - 7	0.64 \pm 0.05
		7 - 8	0.37 \pm 0.07
		11 - 12	0.59 \pm 0.05

Core 054 (pH7)		Core 075 (pH7)	
Depth (cm)	Uranium ($\mu\text{g l}^{-1}$)	Depth (cm)	Uranium ($\mu\text{g l}^{-1}$)
0 - 1	3.28 \pm 0.11	2 - 3	0.36 \pm 0.03
1 - 2	0.63 \pm 0.03	5 - 6	0.45 \pm 0.03
3 - 4	0.56 \pm 0.03	7 - 8	0.61 \pm 0.03
4 - 5	0.72 \pm 0.03	10 - 11	0.67 \pm 0.03
8 - 9	0.63 \pm 0.03	11 - 12	0.69 \pm 0.03
9 - 10	0.50 \pm 0.03	12 - 13	0.63 \pm 0.03
14 - 15	0.66 \pm 0.03	13 - 14	0.74 \pm 0.03
15 - 16	1.34 \pm 0.06	15 - 16	1.44 \pm 0.05
17 - 18	1.48 \pm 0.06	16 - 17	1.51 \pm 0.05
18 - 19	1.27 \pm 0.06	18 - 19	1.76 \pm 0.06
20 - 21	1.27 \pm 0.06		

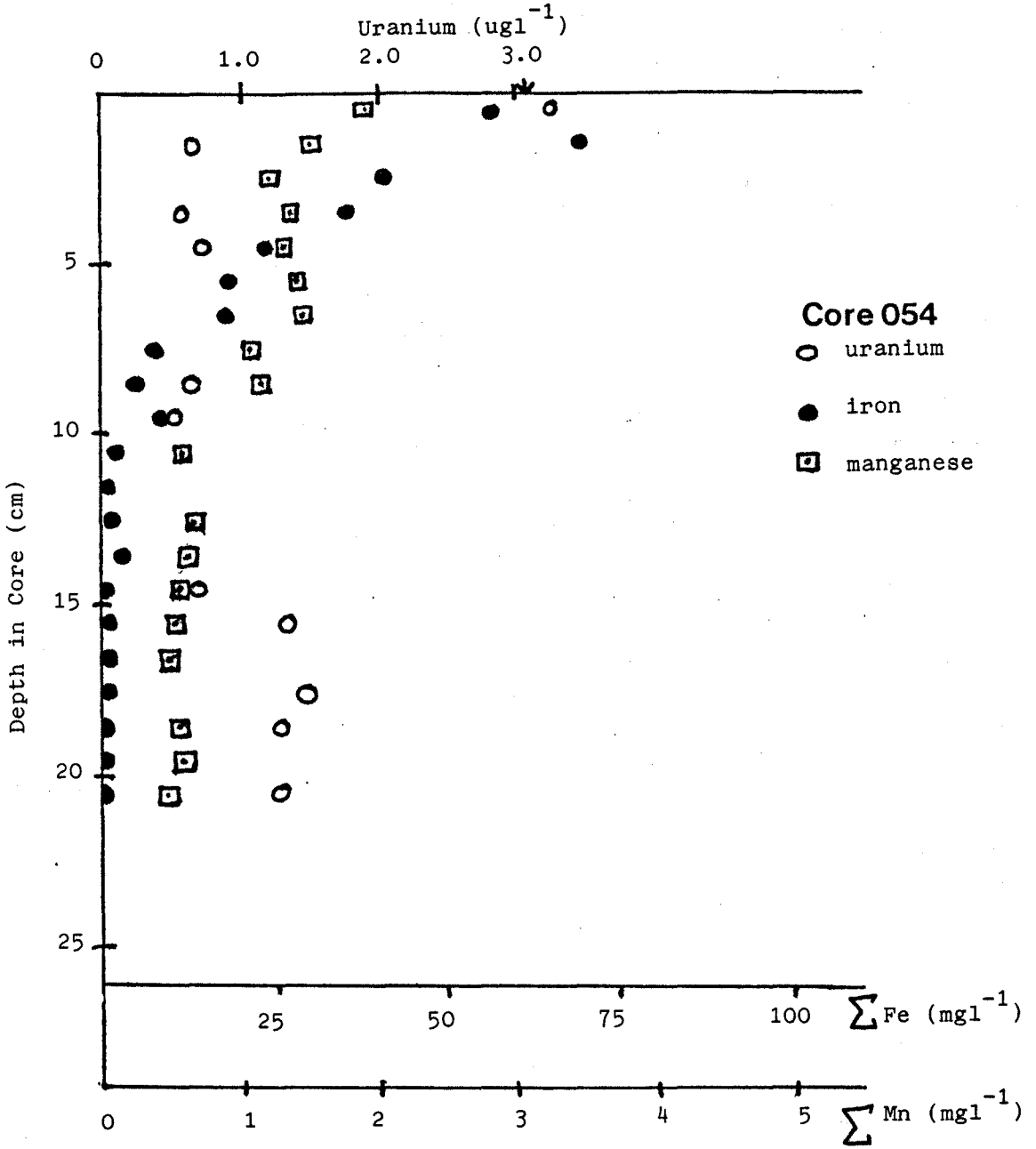


Figure 3.15. Pore water uranium, iron and manganese in core O54 from the Tamar estuary.

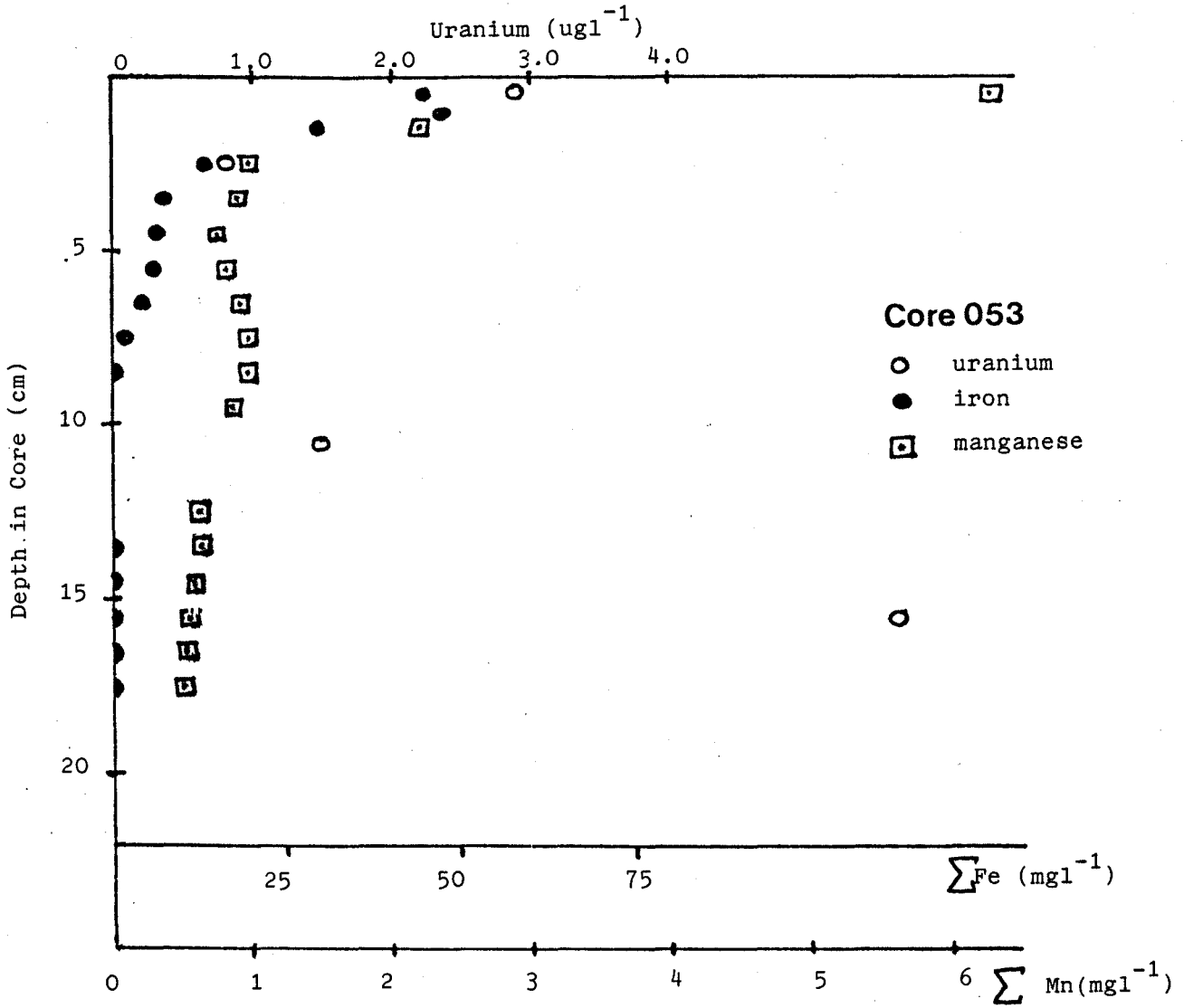


Figure 3.16. Pore water uranium, iron and manganese in core 053 from the Tamar estuary.

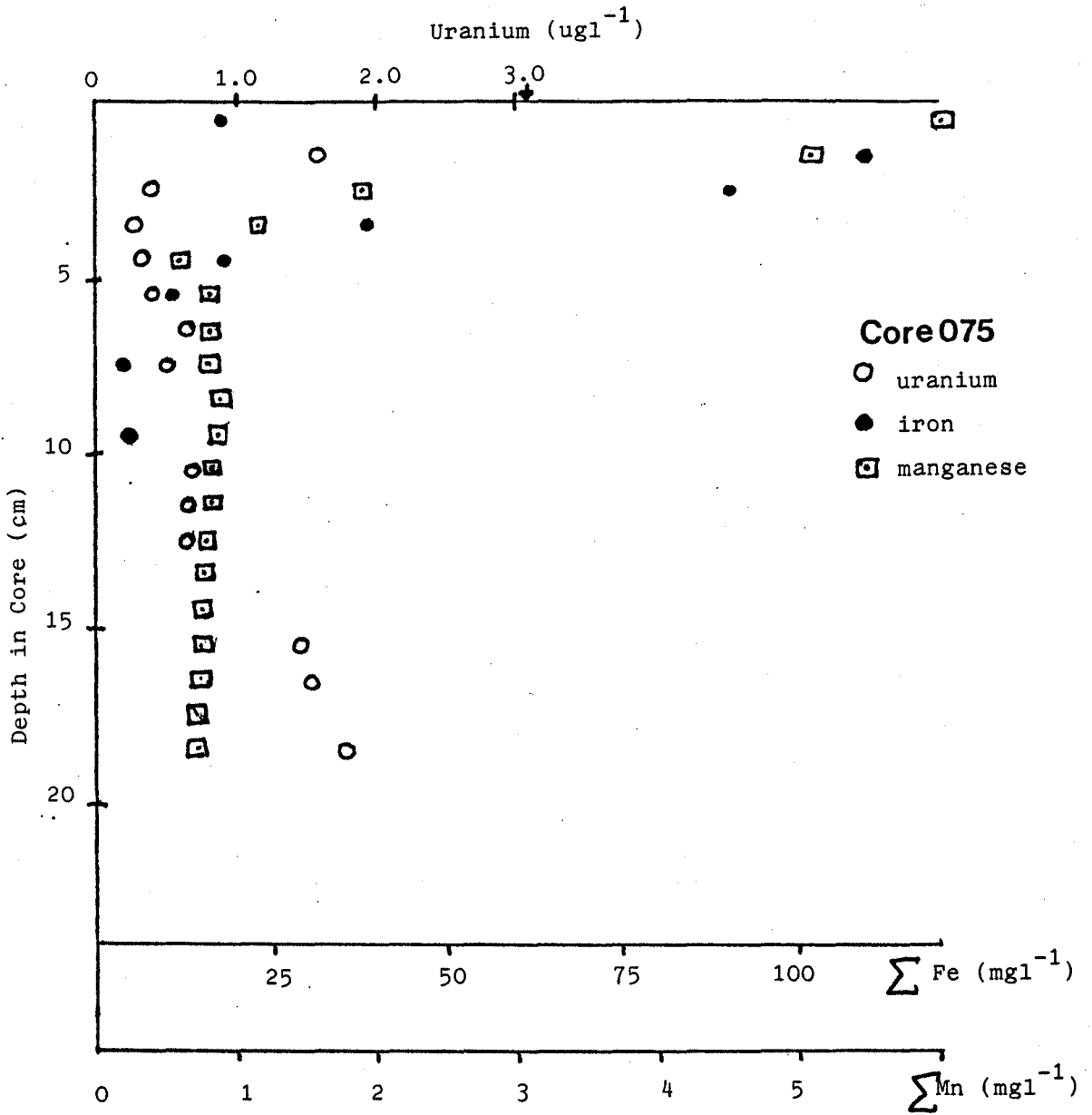


Figure 3.17. Pore water uranium, iron and manganese in core 075 from the Tamar estuary.

Fe and Mn values (Alexander, 1984) are also plotted in Figures 3.15 to 3.17. The uranium concentrations consistently showed a decrease from a surface value of around 3.0 ug l^{-1} , a value expected assuming an overlying water salinity similar to the measured pore water salinity of around 32‰ in the Tamar Estuary (section 3.4). It remained roughly constant between 0.25 and 0.81 ug l^{-1} until a depth of 15 cm was reached, then increased abruptly by x 2.2 to x 4.9. Similar profiles for uranium have been found by Cochran (pers. comm.) in box cores from Buzzards Bay, where the concentration of uranium in the top 3 cm section had decreased to about half the overlying sea water value and then increased by a factor of about 4 beyond 30 cm depth. Also, in laboratory tank experiments with dredged and sieved Buzzards Bay sediment, Cochran (pers. comm.) noticed a reduction in the uranium content of the overlying water and pore water with time, and proposed that uranium was being reduced in these sediments and removed from solution. The only Eh values available for the Tamar cores, those measured on core 053 by placing an Eh electrode onto the top of each sediment slice as it was extruded into a N_2 -filled glove bag (Alexander, 1984), showed a sharp decrease from + 32.2 mV at 0-1 cm to - 117 mV at 1-2 cm, with the lowest value of -140.4mV at 3-4 cm. The Eh value at the greatest depth measured, 7-8 cm, was - 110.6mV, thus showing evidence of a possible increase in Eh with depth. A decrease in Eh with depth is common in nearshore sediments, but the sharpness of the decrease and the minimum value reached can vary widely (Presley and Trefry, 1980), possibly a function of the difficulties involved in its measurement. The profiles of other pore water species showed that decomposition of organic matter was indeed occurring in these sediments (Upstill-Goddard, 1984; Alexander, 1984). Steady increases in NH_3 from about 0 to 900 μM over $\sim 20\text{cm}$, in phosphate from about 50 to 150 μM and in silicate from about 30 to 500 μM were observed. If thermodynamic considerations are used to evaluate when the oxidised species present in the sediment-water environment are reduced with falling Eh, the order $\text{O}_2 > \text{NO}_3^-$, $\text{MnO}_2 > \text{Fe}_2\text{O}_3 > \text{SO}_4^{2-}$ is found (Froelich et al., 1979; Lyle, 1983; Sawlan and Murray, 1983) but overlap does occur depending on, for/

for example, stoichiometry of reaction. Since sulphate can only be reduced below an Eh of about - 150 mV, no large decreases in pore water sulphate was expected in the Tamar cores, with their minimum Eh of - 140mV, and indeed none was observed, with levels remaining steady at ~25mM. Highly anoxic conditions were therefore not attained in these cores, as also shown by alkalinity measurements which increased with depth from 4.36mM at 1 cm to only 9.04 mM at 13 cm in one core from St. John's Lake in the Tamar. This is to be compared to alkalinity values of over 30 mM attained in more reducing cores up-river (Upstill-Goddard, 1984), to values of 20 mM l⁻¹ at 12 cm in tank experiments (Sholkovitz et al., 1983) and to values of over 70mM l⁻¹ in anoxic marine sediments (Berner et al., 1970). These high alkalinity values are predominantly the result of a progressive bacterial reduction of sulphate which, as mentioned previously, does not occur here. For the trace metals Fe and Mn, pore water concentrations are often several orders of magnitude greater than in oxic overlying water (Elderfield and Hepworth, 1975), and steep concentration gradients such as those observed in Figures 3.15, 3.16 and 3.17 are typical (Calvert and Price, 1972). Here, a thin layer of oxic sediment overlies a suboxic layer with maximum metal remobilisation occurring near the +/- Eh interface due to the reductive solubilisation of the adsorbed manganese or iron and its subsequent cycle of upward diffusion, fixation, reburial and reduction. It appeared from the decrease in pore water metal content with depth that Mn was being reduced before Fe with uranium perhaps in between (Figures 3.15 to 3.17) although the sharp redoxcline makes it difficult to tell. The negative pore water Mn and Fe gradients observed below their peak concentrations may be explained by the precipitation of their carbonates as suggested for Mn by Robbins and Callendar (1975). The decrease in pore water uranium levels is presumed to be due to the formation and fixation of insoluble UO₂, the thermodynamically-stable species (Figure 1.3) at the existing Eh levels, - 110 to -140mV, and pH levels, 7.1 to 7.3 (Halbach et al., 1980). In order to propose/

propose a cause for the uranium increase at depth, the basin sediments of Loch Duich (Krom and Sholkovitz, 1977) are considered, sediments which are rich in organic matter (5.8%) and contain a thin oxic surface layer. The decrease in sulphate concentration to zero and accumulations of titration alkalinity, phosphate and sulphide were characteristic of chemical changes that have been observed in estuaries (Berner et al., 1970). Although sulphate reduction was not occurring in the top ~ 20 cm of the Tamar cores, reduction deeper in the cores cannot be ruled out. Ultrafiltration measurements on the Loch Duich pore waters indicated that the concentration of the low molecular weight organics in the DOC remained approximately constant ($10 \pm 2.4 \text{ mgCl}^{-1}$) for both oxic and anoxic cores and were at least partly autochthonous since their concentration was twice that in the overlying water. The ultrafiltration retentate from anoxic cores, however, showed that the observed, approximately linear increase in DOC accumulation from about 10 mg l^{-1} to about 70 mg l^{-1} beyond 70 cm was due almost entirely to the accumulation of high molecular weight (HMW) organic matter. There was also some suggestion of a greater rate of accumulation below 55 cm which coincided with the boundary between the sulphate reducing and methane producing zones. Although little sulphate depletion occurred in the Tamar cores, and hence little sulphide would be produced, in the depths sampled, it is probable that the Eh would decrease beyond 20 cm to levels below -150 mV , not upturn as can be observed in certain circumstances (Presley et al., 1972; Kolodny and Kaplan, 1973), and allow conditions analogous to those described above to develop. Thus we may be seeing the top zone of enhanced uranium concentration below 15 cm (Figures 3.15 to 3.17) due to its complexing and solubilisation by autochthonous HMW organic matter. Stabilisation of trace metals in pore water by HMW organic materials has already been shown (Elderfield and Hepworth, 1975; Krom and Sholkovitz, 1978), although their insoluble sulphides may keep their concentration down, assuming that the solubility product is the controlling factor.

3.4 Uranium in Rivers and Estuaries

Section 1.1 has described the chemical weathering and mobilisation of uranium nuclides from rocks and soils and their transport to, and behaviour in, the marine environment. Complex chemical interactions between rivers and the ocean can modify the supply of many elements to the latter reservoir (Sholkovitz, 1976). Here, the variations in concentration of dissolved uranium along the salinity gradients of several estuaries are examined in order to assess its conservative or nonconservative behaviour. Precipitation of dissolved organic matter and iron and manganese hydroxides can all occur during the mixing of river water with sea water (Sholkovitz, 1976; Boyle et al., 1977) and these substrates may adsorb dissolved elements from solution. Clay particles and hydroxides are flocculated by the inorganic salts of sea water, a process which can be promoted by a greater particle concentration (Dyer, 1972). A change in the surface charge of $\text{Fe}(\text{OH})_3$ from positive below pH7 to negative at higher pH's (Balustrieri and Murray, 1978) is partly responsible for this flocculation. Shen et al., (1983), for example, observed that plutonium underwent rapid coagulation under simulated estuarine conditions, with a strong correlation between the amount of coagulation of dissolved plutonium, humic acids and iron. The increase in dissolved salts as mixing of river and sea water progresses may cause a marked desorption of some elements adsorbed on the surfaces of river sediment or particulate matter e.g. Ra and Ba (Li and Chan, 1979). For uranium in particular, the large influence of salinity on the pH and the carbonate systems, giving rise to a pH minimum at a specific mixing ratio (Mook and Koene, 1975), and the strong association between hydrous ferric oxide and adsorbed uranium (Langmuir, 1978; Giblin et al., 1981), could be competing processes affecting the behaviour of uranium in an estuary.

Studies/

Studies by various workers on the uranium nuclides in the estuarine mixing zone have yielded conflicting and inconclusive results. Conservative behaviour has been reported by Borole et al., (1977), Martin and Meybeck (1978) and Martin et al., (1978a,b) while various removal processes particularly at low salinities have been suggested to operate on uranium (Martin et al., 1978a,b; Turekian and Cochran, 1978; Borole et al., 1982; Maeda and Windom, 1982). Martin and Meybeck (1978) have cited evidence of preferential leaching or desorption of ^{234}U from suspended sediments during mixing at the head of the Zaire estuary and they attributed this to the well-known physico-chemical mechanisms of α -recoil and preferential leaching (see section 1.1).

The conservative or nonconservative properties of uranium using salinity tie-lines, will be more profitably examined in estuaries where there is a single riverine end-member in order to prevent unwanted scatter in the dissolved uranium data. The spatial, temporal and chemical variability found in estuaries has been discussed by Elderfield (1978) who outlined factors such as highly variable river discharge, multiplicity of inputs and fluxes of dissolved species at the water-sediment interface, which can influence the speciation and concentration of uranium.

The three main river-estuarine systems selected for this study were the Clyde on the west coast of Scotland (Figure 2.7), and the Tamar at Plymouth in the south of England (Figure 2.6) and the Forth on the eastern Scottish coast (Figure 2.8). Uranium concentrations and isotopic activity ratios were measured on filtered water samples by isotope dilution α -spectrometry described in section 2.8. The results for the individual river-estuarine systems will be discussed in sequence, with the methodological approach gone into in more detail in the Clyde example.

The/

The Clyde estuary above Greenock (Figure 2.7) occupies a drowned river valley which now has a shipping channel maintained by regular dredging to a mean depth of about 10 metres. Between Greenock and Erskine there are large areas of mudflats exposed at low tide but, above Erskine, the estuary is much narrower and is largely confined between man-made banks, with no appreciable intertidal area (Mackay and Leatherland, 1976). The Clyde Basin has a catchment area of $\sim 2600 \text{ km}^2$ which in addition to the River Clyde itself includes those of two major tributaries, the Kelvin and the Carts. The second major catchment emptying into the estuary is that of Loch Lomond (785 km^2) via the River Leven which has previously been shown to have a uranium concentration of 0.13 ug l^{-1} (Conlan et al., 1969). The drainage area rocks of the River Clyde are composed mainly of Upper Palaeozoic Lavas, Upper and Lower Old Red Sandstone and Carboniferous sequences (Natural Environment Research Council, 1974; Swan, 1978). As in most rivers, the daily average volume of fresh water entering the estuary from the River Clyde varies considerably during a typical year. The 99% and 1% exceedence levels, which are surpassed during most years, are about 8 and $270 \text{ m}^3 \text{ s}^{-1}$ respectively. Such variable fresh water flow affects the salinity structure, retention time and the operation of storm water overflows at sewage works. The Clyde has a fairly pronounced salt wedge (Mackay and Leatherland, 1976), and is regarded as being very different in this respect from most other estuaries around the British coast which generally exhibit a greater degree of vertical mixing. Further complications arise due to the input of large amounts of mixed domestic and industrial wastes mainly from two sewage disposal works at $\sim 7 \text{ km}$ and 14 km from the tidal weir and, through numerous outfalls, from the towns lower down the estuary. The much greater volume of water available at the lower estuary to dilute these effluents results in a minimal effect/

effect on dissolved oxygen. However, the total biological oxygen demand (BOD) loading received by the upper estuary is greater than it can sustain during periods of low river flow, and so considerable portions of it can become anoxic for several months every summer.

The dissolved uranium data for the Clyde estuary are given in Table 3.10. The concentration in river water at the time of sampling just beyond the tidal weir was $0.155 \pm 0.005 \text{ ug l}^{-1}$ and increased linearly with salinity to $2.78 \pm 0.10 \text{ ug l}^{-1}$ at the most seaward sample, with a correlation coefficient of 0.994. Reported uranium concentrations in surface waters range from < 0.01 to $> 100 \text{ ug l}^{-1}$ (Osmond and Cowart, 1976), with concentrations presumably reflecting the geological composition of the drainage basins. The uranium content depends on such factors as contact time with the uranium-bearing horizon, uranium content of the horizon, amount of evaporation and availability of complexing ions (Gascoyne, 1982). Values for river waters range from 0.02 ug l^{-1} for the Amazon (Bertine et al., 1970) to 6.6 ug l^{-1} for the Ganges (Scott, 1982). Seasonal variations by a factor of 2 or 3 in the uranium concentrations of individual rivers have also been observed (Scott, 1982). Concentrations of dissolved uranium have been shown to exhibit a strong positive correlation with total major cations (Borole et al., 1982) and HCO_3^- (Mangini et al., 1979; Borole et al., 1982) suggesting that the release of uranium isotopes to these waters is controlled by the intensity of weathering of the source rocks. However, some of the higher uranium levels reported have been attributed to its release from phosphate fertilizers applied to the land (Spalding and Sackett, 1972; Sackett and Cook, 1969; Martin et al., 1978a), however Mangini et al., (1979) have indicated that very little if any uranium from fertilizer phosphate reaches the rivers, being adsorbed on the uppermost soil layers. The variation in the ^{238}U concentration with salinity in the Clyde is shown in Figure/

TABLE 3.10

Uranium concentrations and activity ratios in the Clyde estuary ($\pm 1\sigma$ error).

<u>Sample Code</u>	<u>Salinity (‰)</u>	<u>Uranium ($\mu\text{g l}^{-1}$)</u>	<u>$^{234}\text{U}/^{238}\text{U}$</u>
RC11	0.0	0.155 \pm 0.005	1.63 \pm 0.06
RC13	0.1	0.149 \pm 0.007	1.68 \pm 0.10
RC14	0.5	0.173 \pm 0.011	1.45 \pm 0.11
RC15	1.0	0.172 \pm 0.008	1.47 \pm 0.08
END 1	3.6	0.41 \pm 0.02	1.46 \pm 0.06
END 2	5.0	0.56 \pm 0.02	1.29 \pm 0.04
END 3	8.0	0.84 \pm 0.03	1.22 \pm 0.07
END 4	11.5	1.02 \pm 0.04	1.19 \pm 0.06
END 5	14.5	1.37 \pm 0.05	1.19 \pm 0.05
END 6	17.1	1.47 \pm 0.07	1.24 \pm 0.06
END 7	19.7	1.52 \pm 0.11	1.27 \pm 0.10
END 8	25.8	2.34 \pm 0.09	1.12 \pm 0.05
END 9	29.8	2.70 \pm 0.11	1.20 \pm 0.05
END 10	30.2	2.52 \pm 0.14	1.20 \pm 0.07
GT 2	30.25	2.54 \pm 0.08	1.16 \pm 0.03
GT 4	31.00	2.63 \pm 0.10	1.13 \pm 0.04
GT 6	31.85	2.78 \pm 0.10	1.10 \pm 0.04

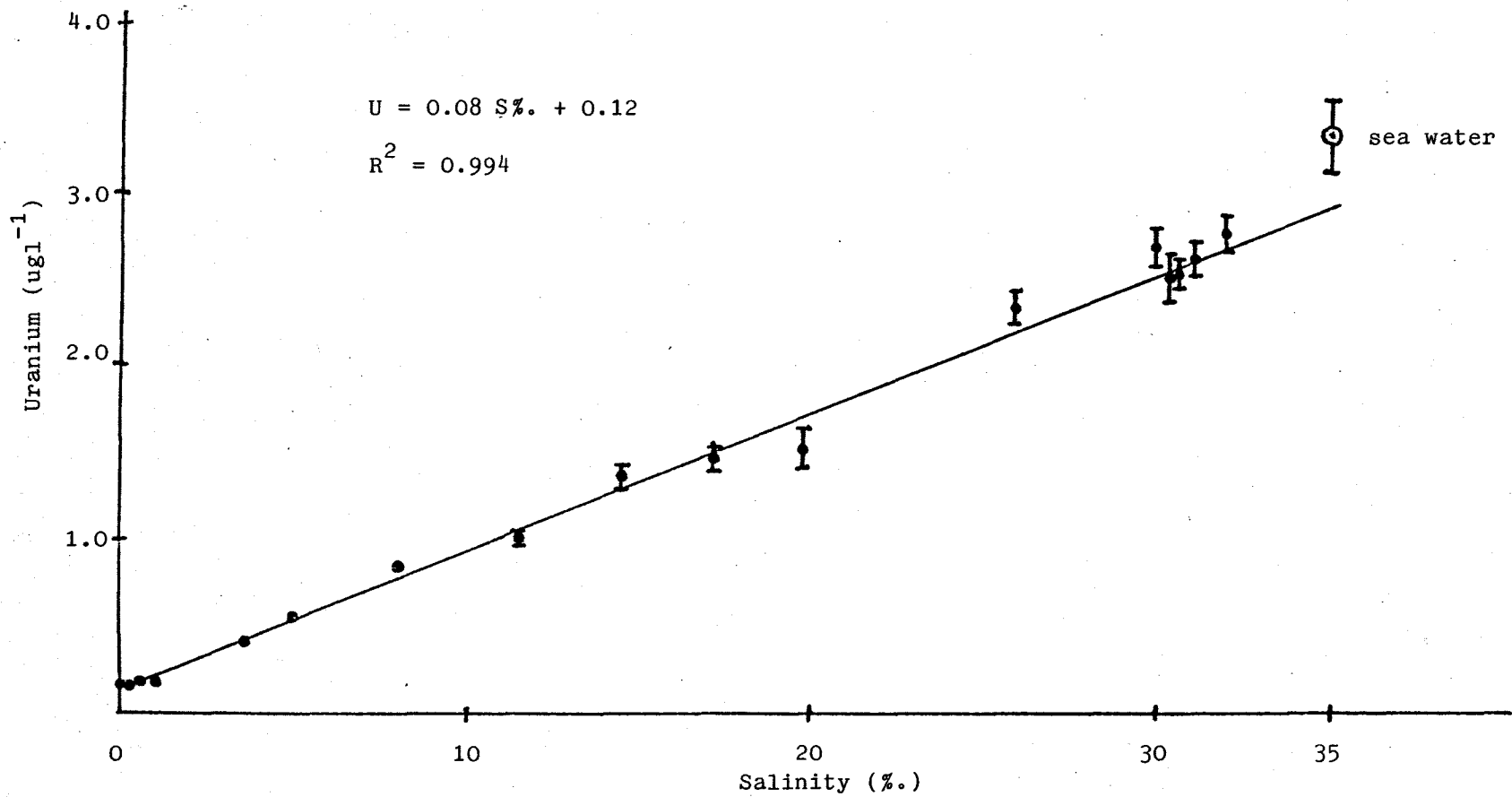


Figure 3.18. Variation in uranium concentration with salinity in the waters of the Clyde estuary.

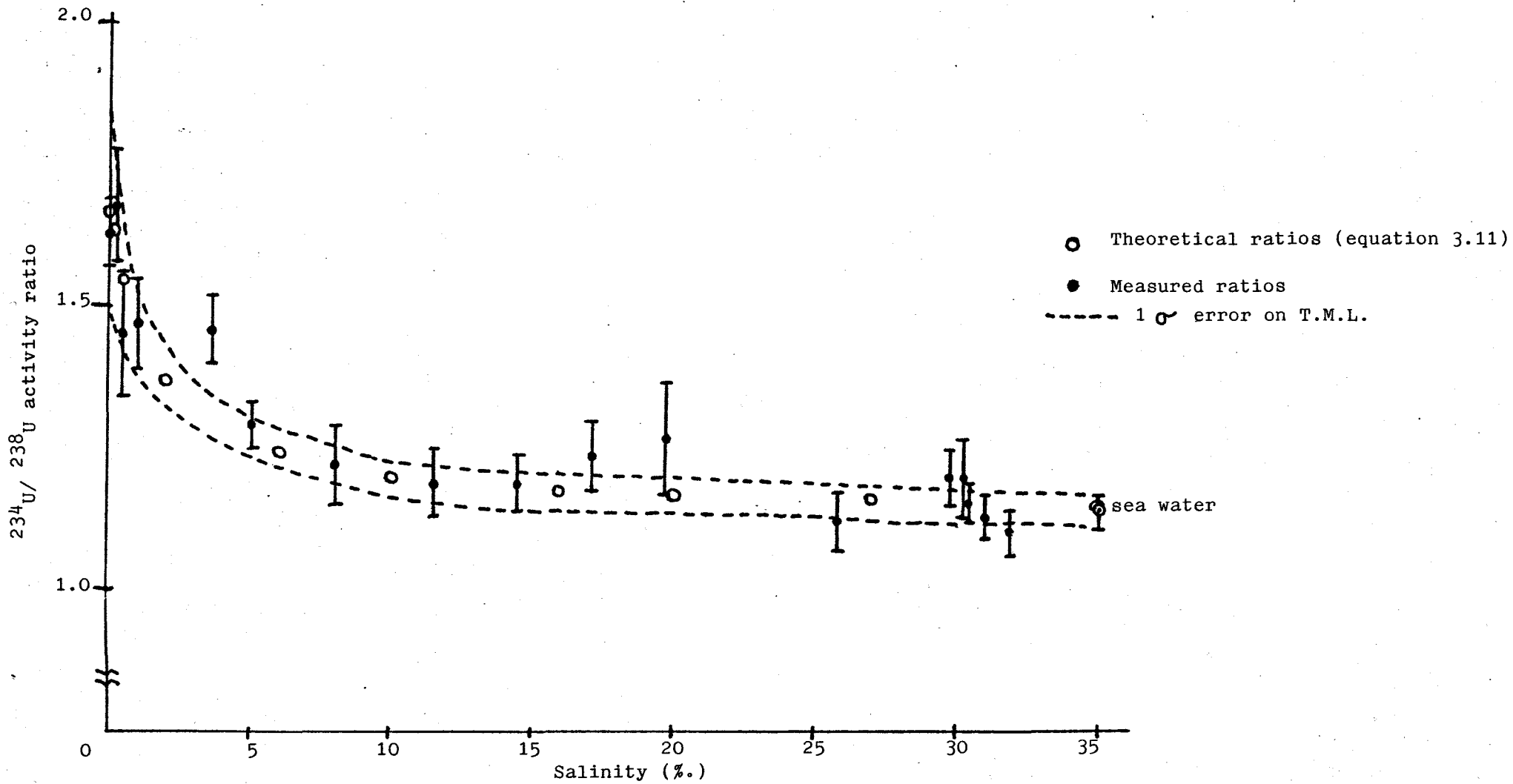


Figure 3.19. Variation in the $^{234}\text{U}/^{238}\text{U}$ activity ratio with salinity in the waters of the Clyde estuary.

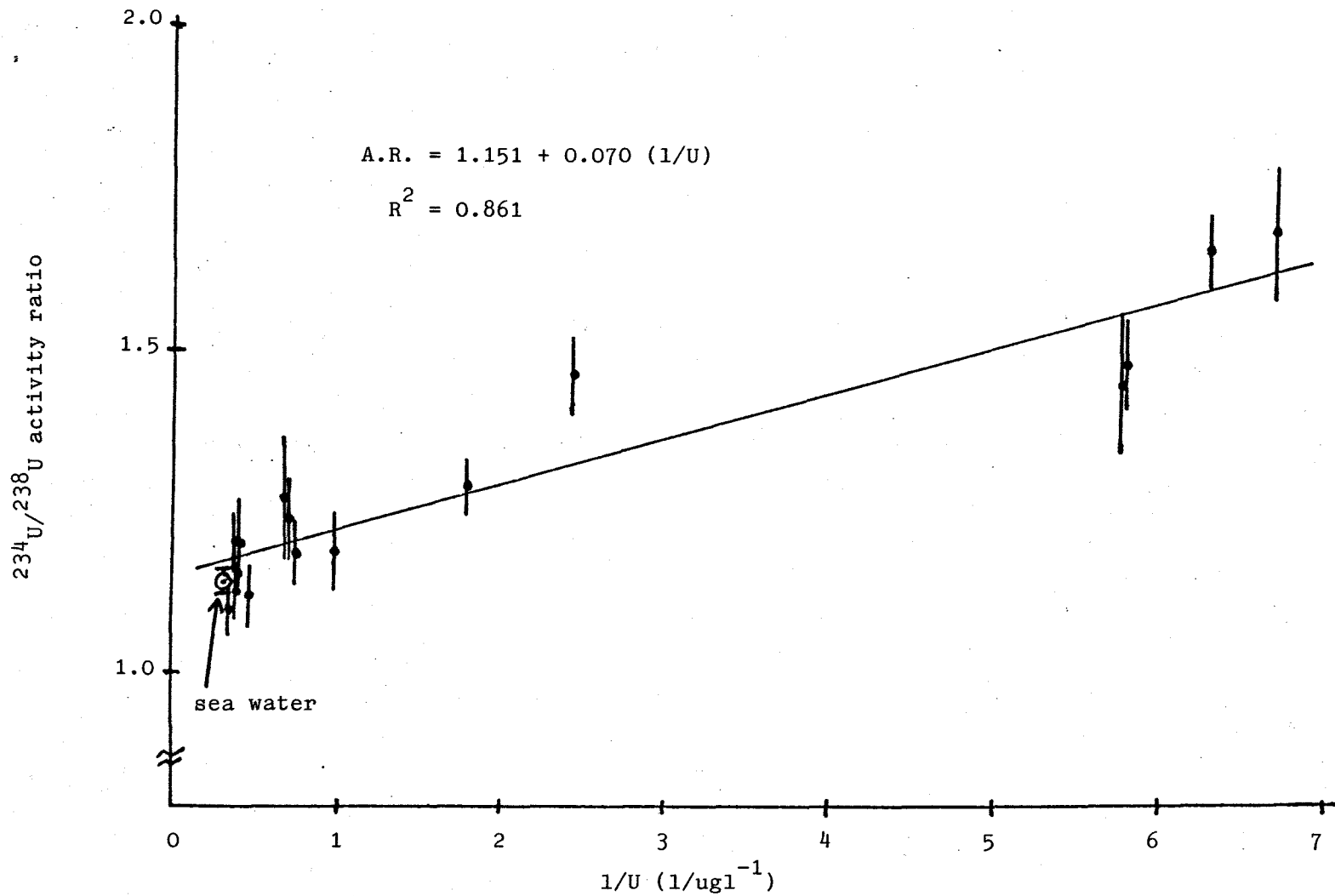


Figure 3.20. Plot of A.R. against $1/U$ as an indication of the conservativeness of mixing of the fresh and saline water end-members in the Clyde estuary.

Figure 3.18 together with the regression equation. The interpretation of such mixing curves, where points over the whole salinity range fall around the theoretical dilution line, with no systematic trend away from the line, is that conservative behaviour is indicated for the element concerned (Liss, 1976). It is most direct to use a dissolved constituent of known or assumed conservative behaviour, whose concentration is characteristic of the oceanic component, as a tracer of the degree of mixing of river and sea waters. Although salinity is not defined in rivers, it is more convenient to use it as an index of mixing since the levels of total river salts are sufficiently low in most instances to make the uncertainty introduced negligible (Boyle et al., 1974). In order to establish non-conservative behaviour the data points must be on a curve which cannot be split into straight-line segments, which would indicate simple physical mixing of a number of inputs to the estuary. This is clearly not possible here. Sample END 7 with a uranium content of $1.52 \pm 0.11 \text{ ug l}^{-1}$ is the nearest sampling point to the River Leven tributary (lying just within 2σ of the regression line). This tributary has been shown to have a similar mean volume flow (in $\text{m}^3 \text{ s}^{-1}$) to the Clyde River (Clyde River Purification Board, 1971 - 1978) and if a uranium content of 0.13 ug l^{-1} as found in Loch Lomond (Conlan et al., 1969) is assumed, then mixing with estuarine water of uranium content of 1.47 ug l^{-1} (sample END 6) would result in a concentration of $< 1 \text{ ug l}^{-1}$. Therefore it can be assumed that, at the time of sampling, the effect of mixing of these two inputs on the uranium concentration was small, and that the uranium-salinity plot does indicate conservative behaviour for uranium within the estuary. Conservative behaviour was also observed for ^{226}Ra and ^{137}Cs in this estuary (Mackenzie, 1977) but, in the case of ^{226}Ra , a sample taken near the mouth of the River Leven showed a 30% depletion below the radium-salinity regression line and indicated that dilution by water of low Ra content was occurring. It is possible that sample END 7/

END 7 may reflect a similar but much smaller effect for uranium, but the experimental uncertainties are too large to be definitive on this point. Inspection of Figure 3.18 shows that the best-fit line does not meet the constant open ocean uranium value of $3.35 \pm 0.20 \text{ ug l}^{-1}$ (2σ) and suggests that a slight amount of uranium removal is occurring outside the estuary, recognising that, at high salinity values, the contribution of riverine uranium (and of other elements more abundant in sea water than in river water) is negligible in comparison with the ocean water contribution. The continued dumping of sewage and industrial sludge in the deep water south of Garroch Head off the Isle of Bute, and the discharges to both the upper estuary and the Ayrshire coast via local authority sewers, may result in the diagenetic formation of suboxic or reducing sediments in the Firth of Clyde, conditions required for the formation of manganese nodules which are found north of the Cumbraes (Natural Environment Research Council, 1974). However, manganese nodules can be formed without uranium fixation since a lower Eh is necessary for the latter. Two sites in the Clyde Sea Area studied by Smith-Briggs (1983) were completely anoxic because of the high oxygen demands imposed by pollutant dumping operations. Radiocaesium measurements (Baxter et al., 1979) have indicated that 90% of the water in the area is of Irish Sea origin with 9% contribution from the Atlantic and 1% fresh water, so that large areas of bottom sediment are available for stripping of uranium from the water column. Removal of uranium in inshore or shelf sediments was postulated by Koczy (1963) in order to explain the lower uranium contents of deep-sea sediments relative to continental sediments. Veeh's (1967) results on uranium deposition from the ocean seemed to bear this out. This would make the uranium content of sea water dependent on the distribution and character of the shelf sediments. Aller and Cochran (1976) have found evidence for uranium uptake in the sediments of Long Island Sound where anoxic conditions/

conditions exist below a few cm of oxic sediment underlying an oxygenated water column. Cores from this area have an increasing uranium content with depth and Aller and Cochran (1976) took this to imply that uranium was being taken up in the lower anoxic sections. Several reports indicate that nearshore waters are highly variable in uranium concentration. Most of the nearshore samples analysed by Blanchard and Oakes (1965) exhibited lower uranium concentrations than sea water with a range of 0.98 to 6.37 ugl^{-1} (mean 2.24 ugl^{-1}). Blanchard (1965) reported uranium levels in the Merrimack estuary of 1.31 and 1.46 ugl^{-1} for samples with salinities of 28.6 and 29.5%, respectively and six other coastal marine samples with salinities from 24.41 to 32.23% had uranium concentrations between 0.98 and 1.90 ugl^{-1} , indicating that some process capable of removing $\sim 50\%$ of the dissolved uranium was operative. Bhat et al., (1969) found uranium values of 1.6 to 2.8 dpml^{-1} (2 - 3.7 ugl^{-1}) for near-coastal waters in the Arabian Sea with salinities of 34.1 to 36.5%. All these low uranium values for nearshore waters might therefore be related to uranium removal processes. However, unequivocal supporting evidence for such removal processes occurring in the Firth of Clyde or Irish Sea is lacking.

The $^{234}\text{U}/^{238}\text{U}$ activity ratios in the Clyde samples are given in Table 3.10 and their variation with salinity is shown in Figure 3.19. The ratios decrease from a river water value of 1.63 ± 0.06 to a seaward end-member value of 1.10 ± 0.04 , and follow closely the theoretical mixing line (TML). This line is calculated for each estuary using the equation (Borole et al., 1977) :

$$R_{\text{mix}} = \frac{x\text{CswRsw} + (1 - x) \text{CrwRrw}}{x\text{Csw} + (1 - x) \text{Crw}} \dots\dots\dots(3.9)$$

where x is the fraction of sea water at any point between pure end-members deduced from the salinity of these end-members (0.0% for/

for pure river water and 35.0% for sea water), C is the concentration of ^{238}U , R is the $^{234}\text{U}/^{238}\text{U}$ activity ratio (A.R) and the subscripts rw,sw and mix refer to river water, sea water and mixture respectively. The rapid decrease towards a roughly constant value shows that the riverine A.R. is swamped early in the mixing series by the contribution from the seaward A.R. The data points for the Clyde A.R.'s (Figure 3.19) confirm that the uranium isotopes behave conservatively in this estuary. Figure 3.20 shows another representation of the data, with the A.R. being plotted against the reciprocal of concentration. A linear relationship between these two variables points to conservative mixing between two water types (Osmond and Cowart, 1976), in this case sea water with a relatively high uranium concentration and low A.R. mixing with low-uranium, high-A.R. river water. Although there is some scatter in the data, it too suggests that mixing is conservative, but care should be exercised when making such deductions from a plot of this kind since the errors on the data points can be quite large, and here are up to $\sim 8\%$ (1σ).

Apart from the water samples discussed above, bottom muds were also analysed for uranium. Analyses of suspended material would have permitted assessment of, for example, the fraction of the total uranium being transported in the dissolved phase, but the low turbidities ($< 40\text{mg/l}$, Figure 3.23) observed in the surface samples collected during the main sampling transect precluded this. Table 3.11 presents the uranium data for the mud samples. It has previously been reported (Natural Environment Research Council, 1974) that the bottom sediments in the Clyde estuary are predominantly generated by influxing riverborne material (87.5%), with the rest being equally provided by solid sewage discharge and dredging spillage. They consist of fine silt, slowly increasing in particle size in the dredging channel between Glasgow and the Cart rivers. Fine sand is found before the River Leven is reached, becoming coarser with distance downstream. From Table 3.11, the uranium/

TABLE 3.11

Uranium concentrations and activity ratios in Clyde muds
($\pm 1\sigma$ error).

<u>Sample</u>	<u>Uranium (ppm)</u>	<u>$^{234}\text{U}/^{238}\text{U}$</u>	<u>LOI(%)</u>
M1	2.50 \pm 0.11	1.08 \pm 0.05	28.67
M2	2.48 \pm 0.15	1.05 \pm 0.06	15.95
M3	1.58 \pm 0.11	1.04 \pm 0.07	6.10

For sample positions see Figure 2.7.

uranium contents of the mud samples M1 and M2 are seen to be identical within error, being about 2.5ppm (about equal to the mean coastal abundance) while the other sample, M3, had a lower concentration of 1.58 ppm, probably reflecting the gradual transition from fine silt to sand since quartz is low in uranium (Hamilton, 1966). Attempts to take a Craib core sample at station M4 (Figure 2.7) were unsuccessful because the corer could not penetrate the sandy sediment. McKay(1983) found by particle size analysis and X.R.D. that a nearby site off Greenock had 70% of its material $> 20\mu\text{m}$ diameter (sandy texture), being predominantly quartz. The 2.8% organic carbon present was concentrated in the $< 20\mu\text{m}$ fraction, and only 1.23% CaCO_3 was present, indicating the general absence of skeletal planktonic remains.

The high LOI (loss on ignition, 500°C) for M1 and M2 are due predominantly to the high organic content of the muds which is a result of the sewage inputs along the narrow upper stretches of the estuary.

The weathering and leaching of rocks gives rise to runoff waters with $^{234}\text{U}/^{238}\text{U}$ A.R.s greater than 1.00 and soils would be expected to have an A.R. < 1.00 . Any subsequent erosion or river transportation of these soils may allow adsorption of uranium from runoff waters under certain conditions and result in a progressive change in A.R. from ~ 0.90 to ~ 0.95 in river muds (Sackett and Cook, 1969). Scott (1968), however, has shown that the distribution of uranium isotopes varies with both sediment size fraction and geographical location and noted that the factors responsible for the isotope ratios of soils and their derivative sediments were difficult to determine due to complex variability in the weathering process. Most river sediments for which uranium isotopes have been analysed have A.R.s between 0.90 and 1.0, with an average of about 0.95 (Scott, 1982). Nevertheless the A.R. values for the Clyde muds, 1.04 to 1.08, are in agreement with values > 1.00 found for/

for sediments from two rivers (Scott, 1968) and for surface soil profiles (Rosholt et al., 1966). These were explained (Rosholt et al., 1966) by the leaching of uranium with A.R. > 1.00 from the lower portions of the soil profile (the B and C horizons) and its transportation to the surface layers where humus may provide a reducing condition for uranium accumulation. According to Osmond and Cowart (1976), the inverse correlation between suspended solid loading and its A.R. observed for some suspended sediment could be interpreted to mean that, at low loading, only A horizon (high $^{234}\text{U}/^{238}\text{U}$ activity ratio) soil is eroded, but at higher sediment loads, B horizon soil is being removed. Thus it is not necessary to propose uranium removal from the estuarine waters in order to explain the higher than expected activity ratios found in the bottom muds.

The Tamar estuary flows over geological formations of Devonian and Carboniferous slates, shales and grits. Its two main tributaries, the rivers Tavy and Lynher flow over these same formations but the Tavy rises among the peat bogs overlying the Dartmoor granite whereas the Lynher runs for most of its length over Carboniferous Rocks (Hartley and Spooner, 1938). The Tamar itself is tidal to $\sim 30\text{km}$, and there are a number of sewage outlets discharging from both banks. These banks and the bed of the estuary consist wholly of soft muds and there are considerable extents of intertidal mudflats bordering the river channel. From cores taken in the lower estuary (Butler and Tibbitts, 1972) the muds generally consist of a $\sim 1\text{cm}$ oxic surface layer composed of flocculant brown material, a lower brown and black mixed layer, and a third, entirely black layer with metal sulphides present. The suspended matter in the estuary rises after heavy rain and concentrations of up to 101 mg l^{-1} have been recorded. From salinity data and isohaline plots (Milne, 1938) vertical salinity differences ranged from 2% at high water to only $\sim 9\%$ at low water in one transect (near T12 on Figure 2.6) indicating good vertical mixing. Salinity stratification increases in the up-river direction, however, and may become considerable during winter spate.

The/

TABLE 3.12

Uranium concentrations and activity ratios in the Tamar estuary ($\pm 1\sigma$ error).

<u>Sample code</u>	<u>Salinity (‰)</u>	<u>Uranium ($\mu\text{g l}^{-1}$)</u>	<u>$^{234}\text{U}/^{238}\text{U}$</u>
T1	0.0	0.041 \pm 0.003	0.95 \pm 0.10
T5	0.0	0.040 \pm 0.006	1.44 \pm 0.36
T9	2.65	0.23 \pm 0.01	1.27 \pm 0.09
T11	5.95	0.59 \pm 0.03	1.10 \pm 0.06
T12	14.05	1.33 \pm 0.07	1.11 \pm 0.07
T15	15.14	1.57 \pm 0.06	1.12 \pm 0.05
T16	19.00	1.67 \pm 0.07	1.18 \pm 0.05
T14	20.29	1.92 \pm 0.10	1.15 \pm 0.06
T17	23.90	2.25 \pm 0.07	1.17 \pm 0.04
T19	26.67	2.69 \pm 0.15	1.06 \pm 0.06
T20	28.55	2.83 \pm 0.10	1.12 \pm 0.04

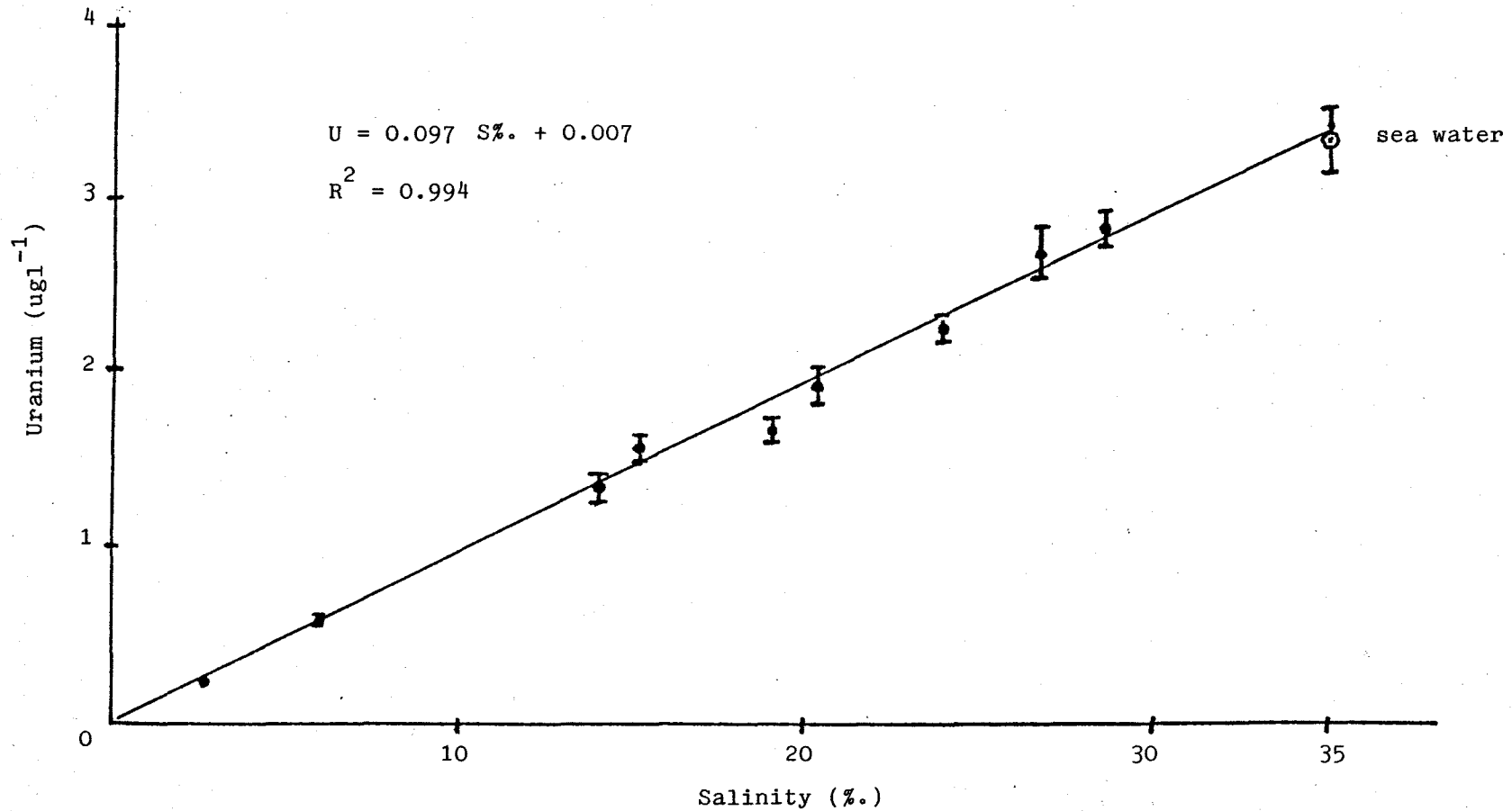


Figure 3.21. Variation in uranium concentration with salinity in the waters of the Tamar estuary.

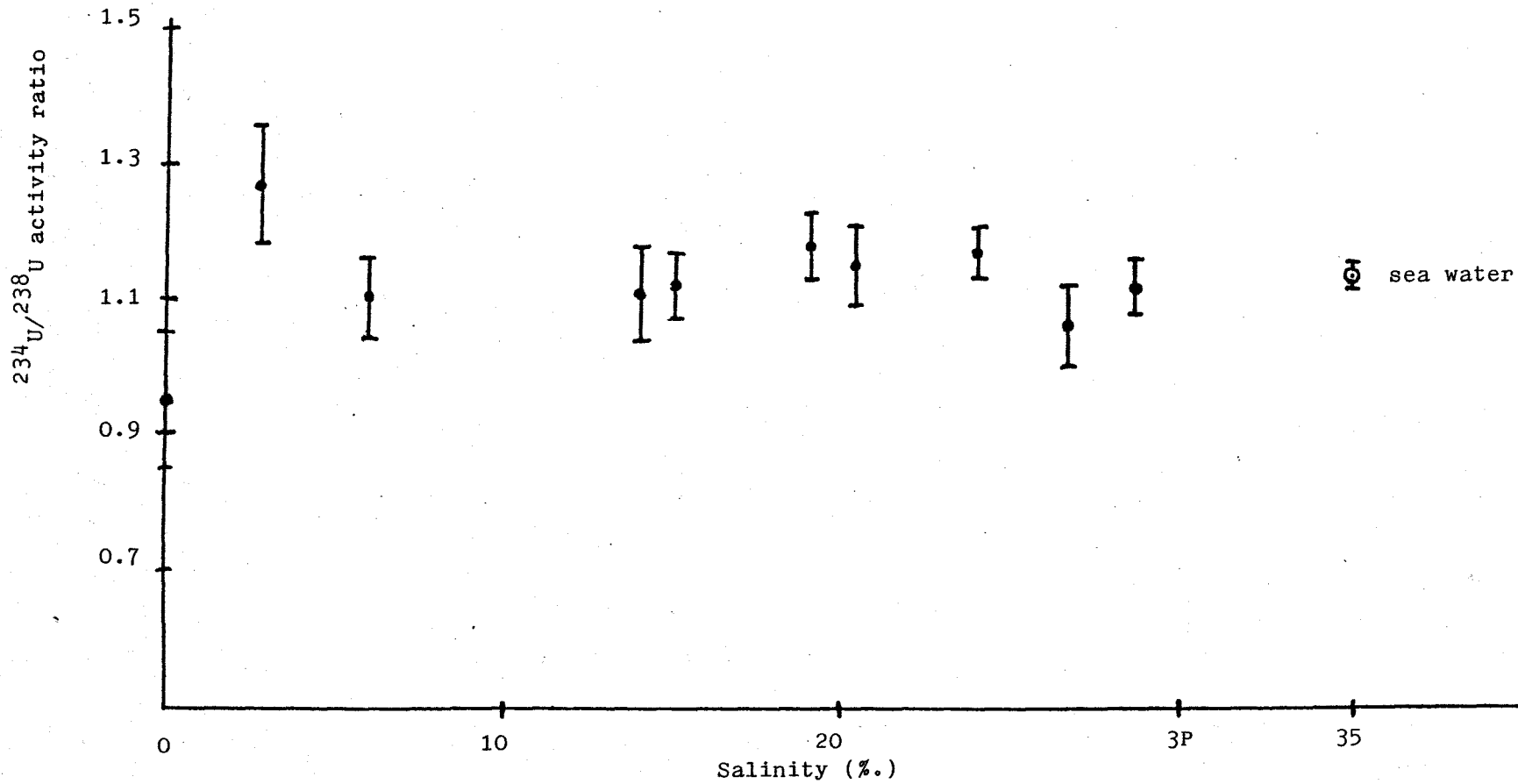


Figure 3.22. Variation in the $^{234}\text{U}/^{238}\text{U}$ activity ratio with salinity in the waters of the Tamar estuary.

The uranium results for the Tamar estuary waters and muds are presented in Tables 3.12 and 3.13 respectively. The uranium concentration was 0.04 ug l^{-1} in the river end-member and increased linearly with salinity to 2.83 ug l^{-1} at 29‰ with a correlation coefficient of 0.994 (Figure 3.21). In contrast to the Clyde estuary, the uranium-salinity plot for the Tamar did meet the open ocean end-member concentration of $3.35 \pm 0.20 \text{ ug l}^{-1}$, giving clear evidence of conservative uranium behaviour and indicating that, because of the much smaller continental shelf area lying between the Tamar (relative to the Clyde) and the open ocean Atlantic waters, either no uranium removal processes were occurring or, more probably, that their magnitude was imperceptible. The Tavy and Lynher tributaries might conceivably have an effect on the uranium concentration of samples T12 and T14 respectively, but Figure 3.21 shows that these samples do not deviate from the mixing line. This in turn indicates that the uranium content or U/S‰ ratios in these rivers are not too different from their values in the Tamar river itself. Again, insufficient quantities of suspended material were present for uranium assay, turbidities being $< 25 \text{ mg l}^{-1}$ at the time of sampling (see Figure 3.23). The $^{234}\text{U}/^{238}\text{U}$ A.R.s (Table 3.12) are plotted in Figure 3.22 except that for sample T5, which is considered to be statistically unreliable since the number of counts under the ^{234}U and ^{238}U peak regions in the α -spectrum were both less than 100 over the standard counting period. The A.R. for sample T1 is plotted on the figure, although it too had low net counts of 209 and 220 respectively under these peak regions. The low A.R. for T1 (0.95 ± 0.10) is within error of values for fresh waters found by Bhat and Krishnaswami (1969) and Martin et al., (1978b). The latter authors discerned a definite increase in the A.R. from fresh water to low salinity waters at the head of the tropical Zaire estuary, suggesting a preferential leaching of ^{234}U . This, they thought, was due to the increase in content of anions such as Cl^- and CO_3^{2-} which occurs during the initial mixing of river water and sea water with which the radiogenically and physico-chemically produced $^{234}\text{U}^{6+}$ cation (existing as UO_2^{2+}) forms stable complexes (see section 1.1). In contrast, Borole et al., (1982), in common with/

with most other workers on other rivers, find A.R.s of between 1.12 and 1.67 for the Narbada river and its tributaries. The paucity of the A.R. data at low uranium concentrations in the Tamar and the similarity in their values at higher uranium concentrations do not make the results here amenable to interpretation via a $^{234}\text{U}/^{238}\text{U}$ versus A.R. plot. From Figure 3.22, however, it does look as though the A.R. might decrease initially before it converges to the sea water end-member value (1.14) implying conservative behaviour for ^{234}U as well as for ^{238}U .

The mud samples collected near the banks of the river Tamar (Figure 2.6) show total uranium concentrations ranging from about 3 to 4 ppm (Table 3.13). These analyses were performed by the fission track technique and thus isotopic activity ratios were not determined. Samples A to E inclusive, taken at the narrower upper stretches of the river, showed similar uranium contents with a mean of 3.89 ± 0.09 ppm. The next three samples F, G and H showed lower values with a mean of 3.07 ± 0.08 ppm. It should be noted that the former 5 samples were scraped up and were black in colour reflecting their reduced state, while the other four samples, F to I, obtained from the boat's anchor, were light brown and were probably mainly from the top oxidised portion of the sediment (Butler and Tibbitts, 1972) which would be expected to increase in thickness as the estuary is traversed seawards. Without A.R. measurements on these muds, the source of their relatively high uranium contents could not be determined unequivocally. Total uranium values of between 2.15 to 3.7 ppm were found by Martin et al., (1978a) for bottom sediments in the Charente estuary and showed a tendency for their uranium content to decrease from fresh water to low-salinity areas, a feature also observed in the suspended sediment. The A.R.s in these samples (Martin et al., 1978a) were all < 1.00 and therefore typical of a terrigenous source.

The third estuary to be examined was the Forth estuary (Figure 2.8) which has a tidal limit 6 or 7km upstream from Stirling bridge and extends eastwards into the Firth of Forth past Edinburgh and out into the North Sea.

The/

TABLE 3.13

Uranium concentration in the muds from the Tamar estuary,
as determined by fission track analysis ($\pm 1\sigma$ error).

<u>Sample</u>	<u>Uranium (ppm)</u>
A	3.78 \pm 0.09
B	3.95 \pm 0.09
C	4.07 \pm 0.10
D	3.71 \pm 0.09
E	3.94 \pm 0.09
F	3.11 \pm 0.08
G	3.01 \pm 0.08
H	3.08 \pm 0.08
I	3.44 \pm 0.08

For sample positions see Figure 2.6.

The principal geological formations of the drainage area of the Forth are Scottish Carboniferous limestones and Lower Old Red Sandstone, with lesser outcrops of Productive coal measures and Upper Old Red Sandstone (Geological map of Great Britain, Sheet 1). From limited studies of cores taken by the Forth River Purification Board, the bottom sediments are aerobic with oxic surface layers of 2 to 3 cm, at least in the lower estuary up to Kincardine bridge (between samples F4 and F5, Figure 2.8). The salinity structure corresponds to a typically well-mixed estuary, but under certain unusual hydrographic conditions it can have a partially-mixed structure (Leatherland, pers. comm.). Sampling was carried out during a period of unsettled weather following a 2 month interval of stable, dry conditions (Forth River Purification Board, 1982). Surface water samples were taken between 2 and 0 hours before high water, a slack period with weak tidal streams in the range 1.0 to 1.5 m s^{-1} . The suspended solids ranged from about 4.7 to 187 mg l^{-1} , with values at low salinities substantially greater than those observed for either the Clyde or the Tamar (Figure 3.23). The region of maximum turbidity generally moves with the tide : landwards with flood and seawards with ebb. If sampling had been carried out 2 or 3 hours earlier or later than high water, very much higher levels of suspended solids would have been encountered. This is because much of the solids content of the water literally drops out during the high and low water slack periods, only to be picked up and resuspended when the tide turns and starts to flow strongly again. Levels of suspended solids up to 6160 mg l^{-1} have been recorded during tidal cycle surveys when the tide is running strongly (Leatherland, pers. comm.). The jump in turbidity to a value of 84.4 mg l^{-1} at station F10 was probably due to the influx of material from the Bannock Burn (Figure 2.8), whose mean annual volume flow is only about 6% of that for the river Forth measured upstream beyond Stirling. All dissolved phosphate - salinity plots derived from water quality surveys in this estuary show some sort of phosphate removal and the dissolved phosphate data on samples collected synchronously with those studied here showed/

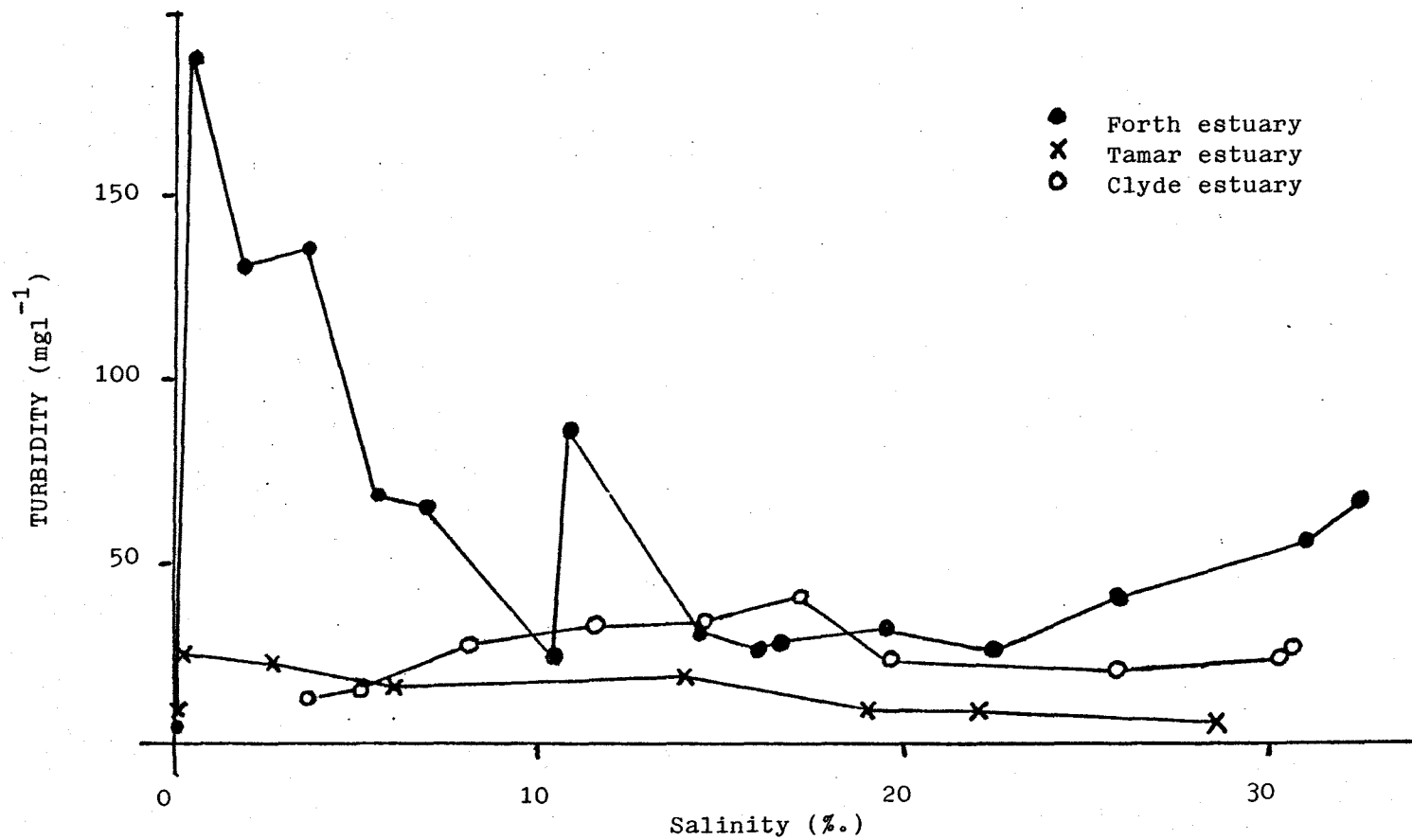


Figure 3.23. Concentration of suspended solids (turbidities) at time of sampling in three U.K. estuaries.

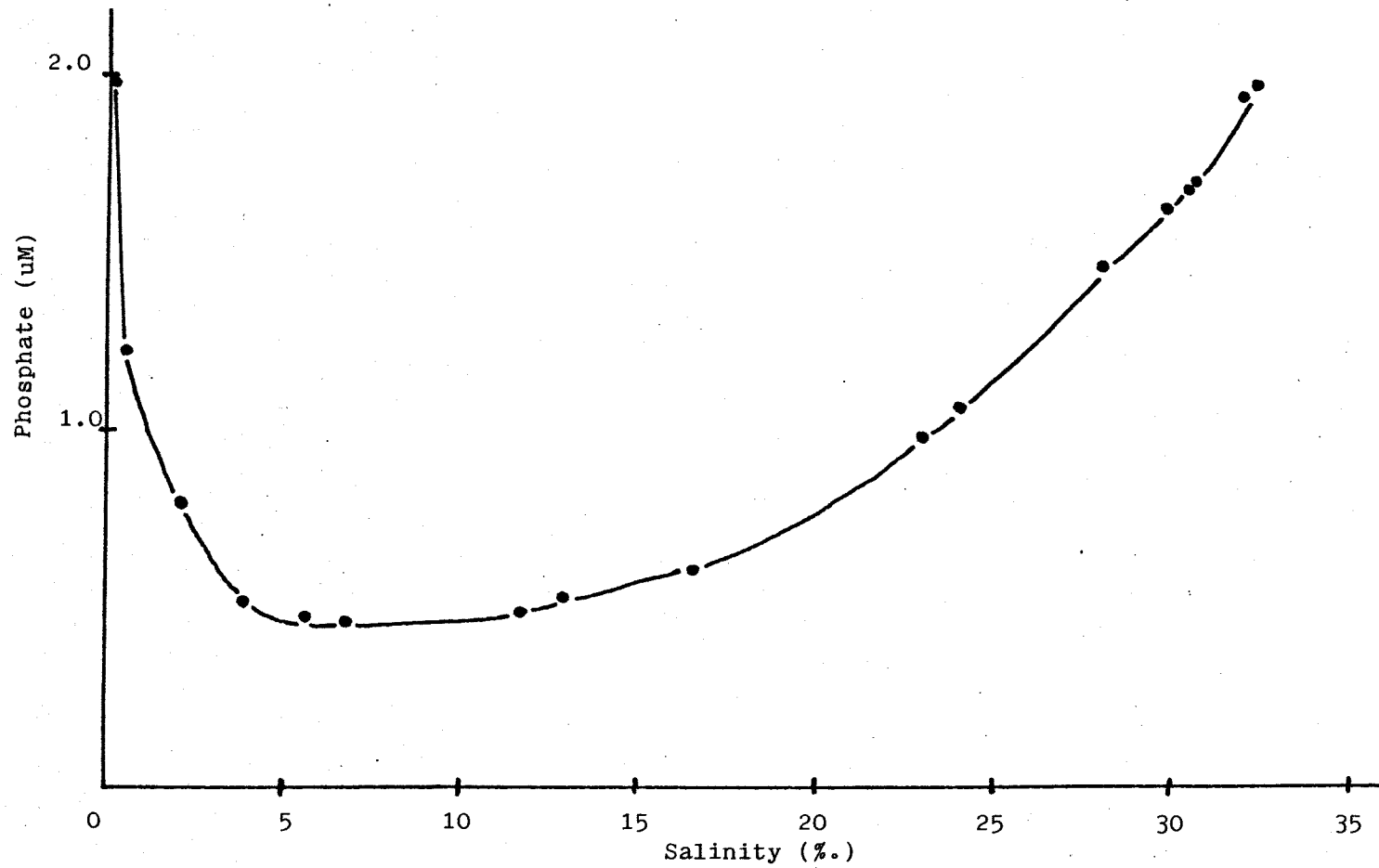


Figure 3.24. Variation in phosphate concentration with salinity in the waters of the Forth estuary.

showed that phosphate removal was occurring (Figure 3.24) with approximately 75% removed before a salinity of 4‰ was reached. In such plots, sewage inputs along the estuary show up as high phosphate contents which affect only one station, implying that removal of phosphate must be fairly rapid (Leatherland, pers. comm.). The similar phosphate concentrations for the fresh and sea water end-members (Figure 3.24) are coincidental and atypical. The sea water value is generally lower than the fresh water one. Because of the exceptionally poor light penetration in the upper estuary, it is very unlikely that the removal process is due to phytoplankton. The removal mechanism is usually regarded as one of adsorption of phosphate from solution onto the solid phase, so that the amount removed will depend on the concentration of phosphate in the water and the area of solid available for adsorption. The optimum pH for phosphate adsorption shows a broad maximum in the range 3 - 7 where the dissolved species will be H_2PO_4^- (Kester and Pytkowicz, 1967). At pH 8, sea water has ~87% of the phosphorus in solution as HPO_4^{2-} with ~1% as H_2PO_4^- , implying that in an estuary where characteristically low pH water mixes with sea water of pH ~8, the efficiency of removal will be greater in the fresh water than in the saline part of the estuary (Liss, 1976).

The uranium results for the Forth estuary, which are thought to be connected with the above chemisorptive removal process, are given in Table 3.14. In Figure 3.25 a degree of uranium removal at low salinities can be discerned, coincident with the high turbidities here (Figure 3.23). The high concentrations of dissolved solids facilitate solid-solution chemical interactions. This could explain the resultant uranium removal, with possible enhancement by flocculation of dissolved organic and inorganic matter (Sholkovitz, 1976) and iron-bearing colloids (Boyle et al., 1977), processes which occur during the mixing of river water and sea water. According to Dongarra and Langmuir (1980), a typical natural water with $p\text{CO}_2 = 10^{-2.5}$ atm., uranium concentration 10^{-8} M ($2.4\mu\text{g l}^{-1}$) and $\sum\text{PO}_4^{3-} = 1\mu\text{M}$ would have $\text{UO}_2[\text{HPO}_4]_2^{2-}$ as the dominant uranium species between pH 4 and 7.5, within which range the pH values of/

TABLE 3.14

Uranium concentrations and activity ratios in the Forth
estuary ($\pm 1\sigma$ error)

<u>Sample code</u>	<u>Salinity(‰)</u>	<u>Uranium(ugl⁻¹)</u>	<u>²³⁴U/²³⁸U</u>	<u>²³⁴U(ug-equiv.l⁻¹)</u>
F16	0.065	0.089 \pm 0.006	1.50 \pm 0.13	0.13 \pm 0.01
F15	0.406	0.070 \pm 0.007*	0.91 \pm 0.13*	0.06 \pm 0.01*
F14	1.77	0.12 \pm 0.01	1.34 \pm 0.17	0.16 \pm 0.02
F13	3.62	0.16 \pm 0.01	1.27 \pm 0.12	0.21 \pm 0.03
F12	5.46	0.23 \pm 0.01	1.24 \pm 0.10	0.29 \pm 0.03
F11	6.82	0.35 \pm 0.02	1.28 \pm 0.09	0.45 \pm 0.04
F10	10.57	0.86 \pm 0.03	1.12 \pm 0.05	0.96 \pm 0.05
F9	10.40	0.97 \pm 0.06	1.16 \pm 0.07	1.13 \pm 0.10
F8	14.39	1.45 \pm 0.08	1.08 \pm 0.07	1.57 \pm 0.13
F7	15.97	1.48 \pm 0.04	1.18 \pm 0.04	1.75 \pm 0.11
F6	16.63	1.73 \pm 0.06	1.15 \pm 0.05	1.99 \pm 0.11
F5	19.49	2.07 \pm 0.11	1.17 \pm 0.07	2.42 \pm 0.19
F4	22.38	2.23 \pm 0.07	1.15 \pm 0.04	2.56 \pm 0.12
F3	25.80	2.69 \pm 0.07	1.11 \pm 0.04	2.99 \pm 0.13
F2	30.89	2.90 \pm 0.12	1.18 \pm 0.05	3.42 \pm 0.20
F1	32.40	3.12 \pm 0.08	1.19 \pm 0.03	3.71 \pm 0.13
F20	33.20	3.53 \pm 0.11	1.12 \pm 0.03	3.95 \pm 0.16

(* - Less than 100 counts under ²³⁴U and ²³⁸U peak regions.)

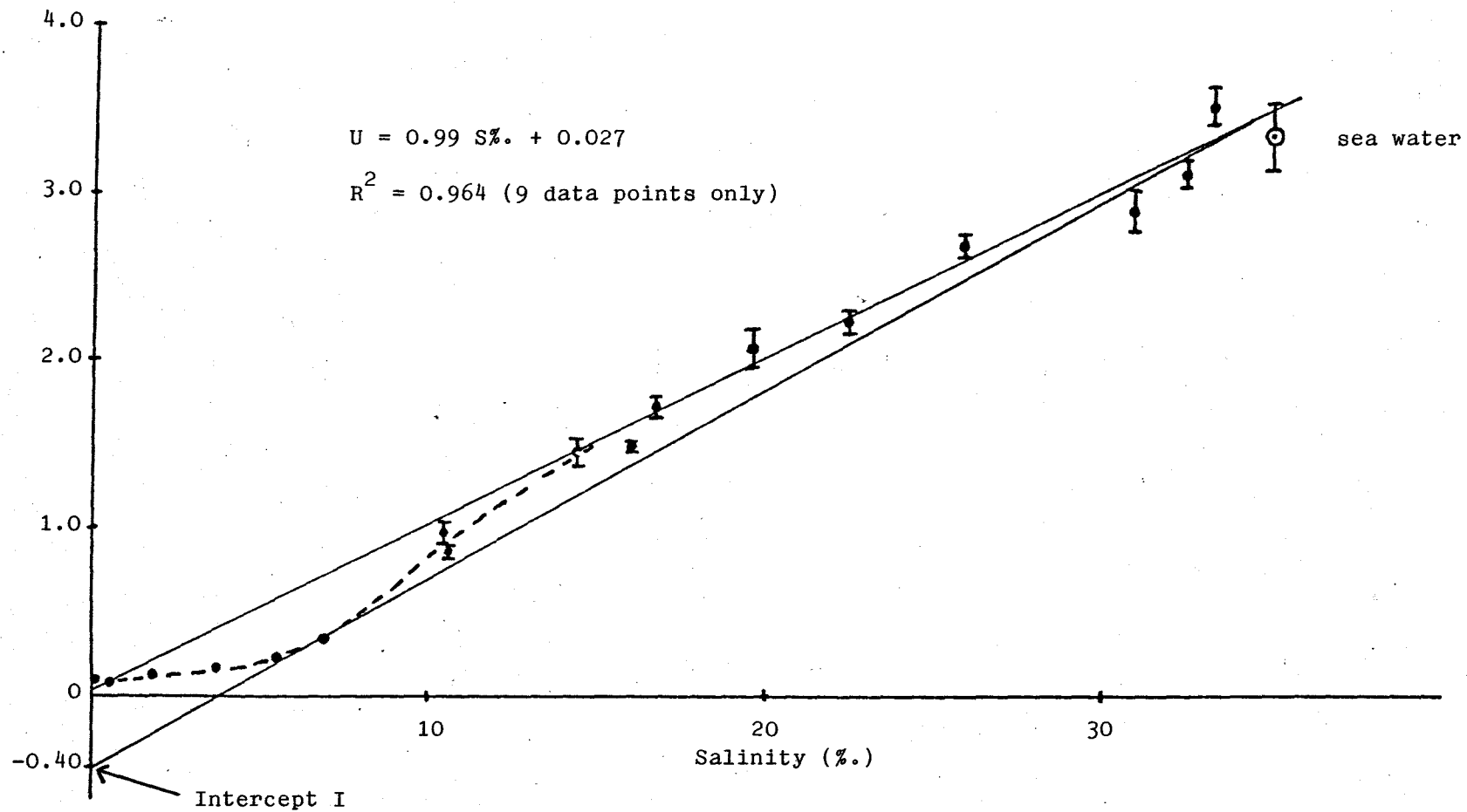


Figure 3.25. Variation in uranium concentration with salinity in the waters of the Forth estuary.

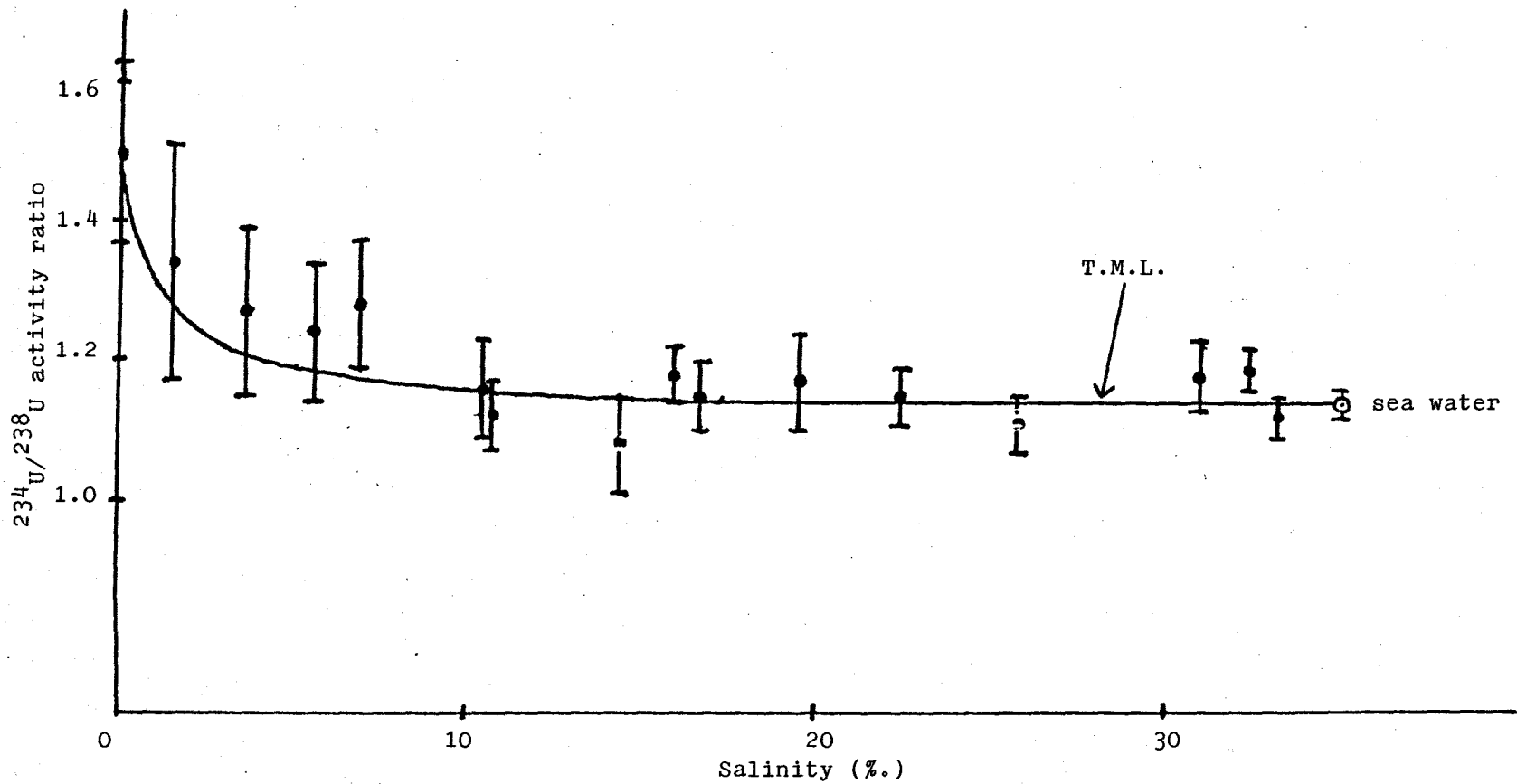


Figure 3.26. Variation in the $^{234}\text{U}/^{238}\text{U}$ activity ratio with salinity in the waters of the Forth estuary.

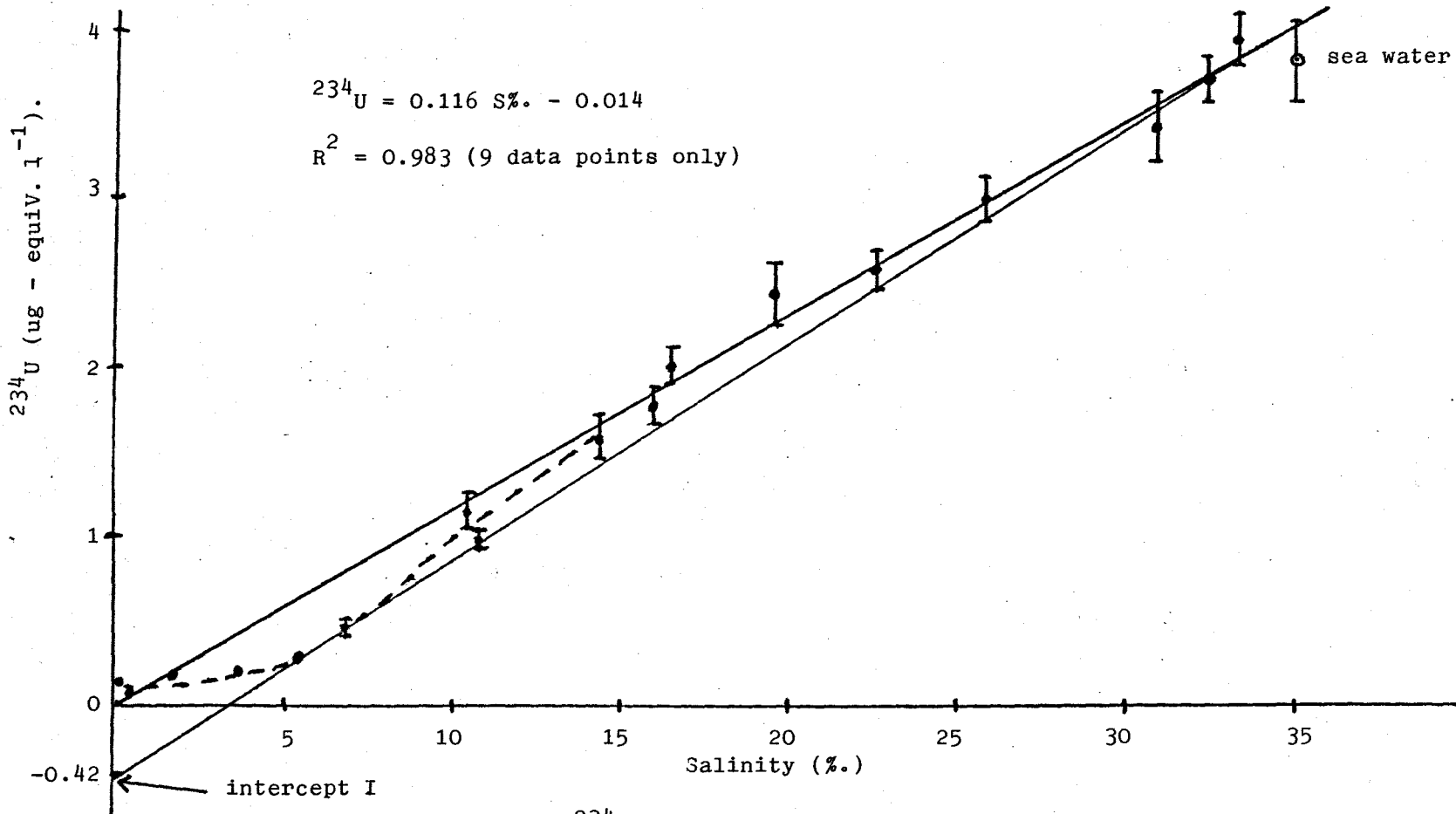


Figure 3.27. Variation in the ^{234}U concentration with salinity in the waters of the Forth estuary.

of the river Forth lie (Forth River Purification Board, 1982). Thus, since uranium can complex strongly with phosphate, it could be removed in concert with it. Martin et al., (1978a) noted a similar removal of uranium in the Charente estuary which had been polluted with orthophosphate originating from fertilizer processing unlike above where the phosphate was sewage-derived. In the Charente, below 4% salinity, effluent from a calcium fluorophosphate processing plant artificially increased the phosphate content to $\sim 18\mu\text{M}$ (as compared to $< 2\mu\text{M}$ in the Forth) and increased the uranium content from 0.4 to $2\mu\text{g l}^{-1}$. Both elements, phosphorus and uranium, showed non-conservative behaviour via removal processes during estuarine mixing.

Examination of Figure 3.25 indicates that there might be a change of curvature from negative to positive, in the uranium profile, with the inflexion point at $\sim 10\%$ salinity. Thus there is not a clear linear increase in concentration between the sample showing the maximum percentage deviation from the regression line (sample F12) and the extrapolated sea water end-member ($3.50\mu\text{g l}^{-1}$ at 35%). This feature would suggest a reversible process, with some desorption of uranium from particulates on increasing salinity due to exchange with other ions as the ionic strength increases. The regression line in Figure 3.25 was calculated using the upper 9 data points only, since the other uranium points signified removal and would have skewed the line if included. With $R^2 = 0.964$, uranium appeared to show conservative behaviour at the lower end of the Forth estuary. The removal rate of uranium can be calculated by the approach of Li and Chan (1979) and Maeda and Windom (1982), in which the lower straight-line segment of the mixing curve (Figure 3.25) defines an intercept I on the ordinate. This intercept is given by

$$I = U_r + \frac{R_u}{Q_r} \dots\dots\dots(3.10)$$

where U_r is the dissolved uranium concentration of the river water end-member ($0.089\mu\text{g l}^{-1}$), Q_r is the rate of river discharge ($2.764\text{ m}^3\text{ s}^{-1}$ mean value for June 1982 in the Forth) and R_u is the removal rate or release rate of uranium from particulates/sediment depending on whether R_u is negative or positive respectively. For an I value of $-0.40\mu\text{g l}^{-1}$ (or mgUm^{-3}), the uranium removal rate/

rate was calculated from equation 3.10 as 1.4 mg s^{-1} or $4.4 \times 10^4 \text{ gy}^{-1}$. The total riverine uranium input to the oceans of between 1 and $2 \times 10^{10} \text{ g yr}^{-1}$ was calculated assuming a world mean river/uranium concentration of 0.3 to 0.6 ug l^{-1} (Cochran, 1982) and a total river water flux of $0.35 \times 10^{20} \text{ g yr}^{-1}$ (Livingstone, 1963). Therefore the above removal process amounts to only 2 to $4 \times 10^{-2}\%$ of this total world uranium input value and as such does not constitute a significant removal process. It is likely, however, that the above calculated removal rate would be temporally variable, depending on such factors as runoff rate, tide, river uranium concentration, and would be highly sensitive to uncertainties in the intercept value I , especially during periods of large river discharges (Q_r).

Figure 3.26 shows the change in A.R. with salinity and from this it would appear that the results follow the TML (Equation 3.9) quite well within the uncertainty of the data. However, when the total uranium concentration ($99.27\% \text{ }^{238}\text{U}$) and $^{234}\text{U}/^{238}\text{U}$ activity ratio for each sample are used to calculate the absolute ^{234}U concentration, these absolute values (Figure 3.27) show that a similar removal rate of $1.5 \text{ mg-equiv. s}^{-1}$ ($4.7 \times 10^4 \text{ g - equiv. yr}^{-1}$) is also operative on ^{234}U . Here, $I = -0.42 \text{ ug-equiv. }^{234}\text{U l}^{-1}$, $^{234}\text{U}_r$ is $0.13 \text{ ug-equiv. }^{234}\text{U l}^{-1}$, and again only the upper 9 data points are used to define the regression line, giving $R^2 = 0.983$. Since uranium concentrations in this work are reported in mass units per volume (e.g. ug l^{-1}) for ^{238}U , and since the concentration by weight of ^{234}U is about four orders of magnitude less, the ^{234}U values above are given in equivalent concentration units, i.e. the concentration of ^{238}U that would be equivalent in activity to the ^{234}U present (Osmond and Cowart, 1976). An alternative is to quote both uranium isotope concentrations in dpm l^{-1} . Taking both the calculated R_u values for ^{234}U and ^{238}U , the activity ratio of the uranium removed from the upper estuary would be in the region of 1.07 ($1.5/1.4$), although subject to large errors due to uncertainties in I values and Q_r levels. Nevertheless it was considered/

considered worthwhile that, since turbidities were high and ample particulate matter was available for precise uranium analysis, the isotopic activities of the suspended matter should be investigated to see if it showed an A.R. signature compatible with this uptake of uranium. Borole et al., (1982) found A.R.s in the suspended phases of the Narbada estuary to be between 1.01 ± 0.02 and 1.06 ± 0.02 (mean 1.03), samples which had been settled out from waters with dissolved A.R.s of between 1.14 ± 0.02 and 1.35 ± 0.02 (mean 1.25). These solid phase A.R.s did not exhibit any systematic variation with salinity, ruling out any major adsorption/desorption processes, ^{234}U and ^{238}U both behaving conservatively. The small excess of ^{234}U in the suspended phases, however, was not explained. The non-conservative uranium behaviour found by Martin et al., (1978a) in the Charente estuary did not show such ^{234}U enhancement in the suspended matter, with A.R.s between 0.91 ± 0.09 and 1.01 ± 0.02 (mean 0.95). The particulate matter from the Forth estuary was here allowed to settle and was oven-dried at 110°C . These samples which came from waters showing uranium removal, F10 to F15 inclusive, were combined to yield a 6.24 g composite sample (A), while the others, F1 to F8 yielded a 2.78 g composite (B). Ashing at 500°C gave, respectively, LOI values of 18.7% and 21.0% due to oxidation of organic and carbonate carbon. Alpha-spectrometry gave at total uranium content of 4.10 ± 0.09 ppm and an A.R. of 1.00 ± 0.02 for sample A, and 3.06 ± 0.06 ppm and 1.00 ± 0.03 for sample B. Thus, there was no definitive evidence for uptake of uranium with an A.R. of ~ 1.07 , but the higher total uranium (^{238}U), and higher ^{234}U content (implied by the solid-phase A.R. of 1.00) of the particulates from the lower-salinity samples could be compatible with uptake of uranium of A.R. >1.00 if the particulate input had an expected original ratio <1.00 (Sackett and Cook, 1969) and vice-versa. It should be noted that the mean uranium distribution coefficient (ratio of specific activity on the solid phase to that in solution) for sample A is 1.37×10^7 while that for sample B is 1.38×10^6 . This decrease in K_D could partly be a manifestation of the uranium adsorption on the sample A composites, although, for a constant particulate/

particulate uranium concentration along an estuary, the natural increase in soluble uranium content seawards by ~ 2 orders of magnitude would easily account for the 1 order of magnitude decrease in K_D .

As a final indication of the conservative behaviour of uranium in sea water and in estuaries with low dissolved solids, a plot of uranium versus salinity was constructed from the 3 studied estuaries except for (i) 8 samples (Forth F9 to F16) for which uranium removal was observed, and (ii) a further 8 samples with salinities $< 5\%$. in which the salt content is not well-defined. Figure 3.28 under regression analysis gives a U/S% ratio of $(9.53 \pm 0.84) \times 10^{-8} \text{ gg}^{-1}$ for the salinity range 5.0 - 33.2%. This is in excellent agreement with the values of Turekian and Chan (1971) : $(9.21 \pm 0.04) \times 10^{-8} \text{ gg}^{-1}$, salinity range 33.50 - 34.68%. and of Ku et al., (1977) : $(9.34 \pm 0.56) \times 10^{-8} \text{ gg}^{-1}$, salinity range 30.3 - 36.2%..

The results in this section add to the substantial body of data on the uranium concentration and activity ratio of river water (see Scott (1982) for summary) and may be used in a recalculation of the mean value of riverine uranium and its A.R. for mass balance purposes. The mean uranium contents and A.R.'s for the three estuaries are, respectively, 0.12 ugl^{-1} and 1.37 ± 0.09 . These can be compared to the weighted mean values of 0.22 ugl^{-1} and 1.20 ± 0.06 calculated from some major and minor world rivers (Borole et al., 1982). The data provided here can also be applied to the steady-state model of Ku et al., (1977). These authors derived an equation which could set limits on the mean uranium concentration of world rivers (U_r) and on the diffusional flux (in $\text{dpm cm}^{-2} \text{ kyr}^{-1}$) of ^{234}U from deep-sea sediments (I_s). Assuming that ^{238}U input to the ocean comes mainly from rivers and that ^{234}U input comes from two sources, rivers and sediments, then after Ku et al., (1977),

$$0.05/U_r + 1.14 = A_r + I_s / 7.35 U_r \dots\dots\dots(3.11)$$

where A_r is the $^{234}\text{U}/^{238}\text{U}$ activity ratio in rivers, and the left hand side of the equation is the oceanic activity ratio due to riverine input, calculated from the following known parameters : river discharge rate (1 yr^{-1}), ocean volume (l), uranium concentration/

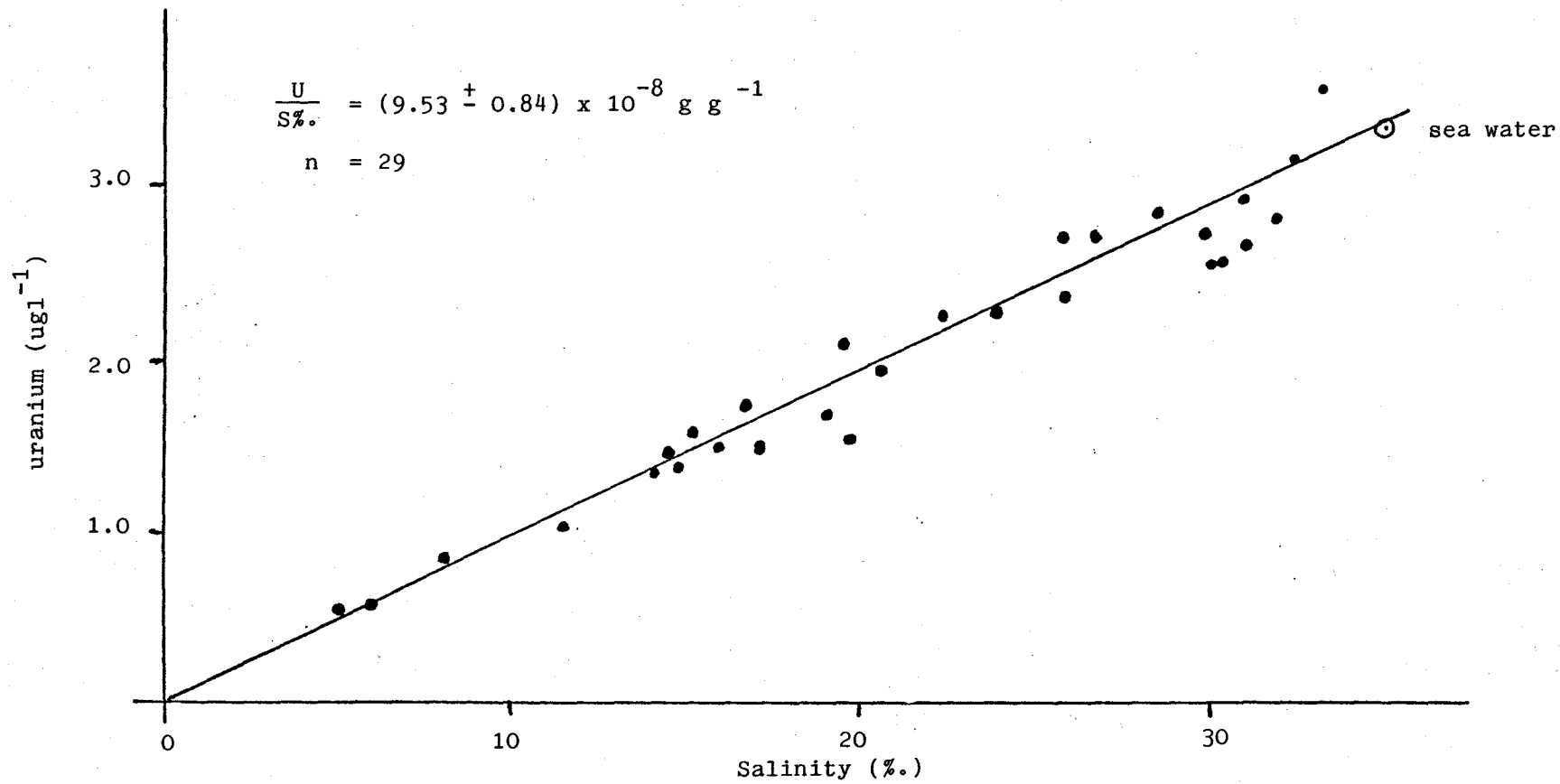


Figure 3.28. Uranium - salinity relationship for all three U.K. estuaries

concentration in the ocean (3.3 ug l^{-1}) and its activity ratio. Since losses of ^{234}U have been observed from most pelagic clays (Ku, 1965), then $I_S \geq 0$, otherwise ^{234}U would be depositing in preference to ^{238}U . In addition, since the A.R. of river water (A_r) is greater than the sea water value of 1.14, then from equation 3.11, I_S must be < 0.37 .

If, from Tables 3.10, 3.12 and 3.14, the U_r and A_r values for the Clyde, Tamar and Forth rivers are taken as, respectively, 0.15 ug l^{-1} and 1.65, 0.04 ug l^{-1} and 1.44, 0.09 ug l^{-1} and 1.50 then I_S values of -0.19, 0.28 and $0.13 \text{ dpm cm}^{-2} \text{ kyr}^{-1}$ are generated from the above equation. This indicates that the data for the latter two of the three rivers compares favourably with the predicted model I_S values, and that the combination of relatively higher uranium concentration and A.R. in the Clyde river leads to an I_S value which is too low, implying preferential ^{234}U deposition. However, world rivers show a considerable spread in their uranium concentration and each will have a characteristic, although sometimes temporally variable (Scott, 1982) A.R. value. Thus, values of I_S which lie outside the predicted limits of 0 to $0.37 \text{ dpm cm}^{-2} \text{ kyr}^{-1}$ are bound to be found. It is the world mean A_r and U_r river input values which will provide the ultimate test for the model.

3.5 Further applications of Particle Track Analysis

The P.T.A. technique can be used to map out areas of α -radioactivity, i.e. in an autoradiographic mode, and it is shown here how useful information is obtained from the permanent track records resulting from the application of CLN to the samples described in section 2.5. The α -track records are discussed in the light of data obtained on the same samples by other analytical techniques (fission track analysis, wet radiochemistry, γ -analysis etc.), when such data are available.

The particulates in a 30.15% salinity water sample from the Esk estuary were allowed to settle and the supernate filtered firstly through a Whatman GF/B filter (nominal pore size 1.0um) and collected in a 0.45 um millipore filter. The millipore filter containing the 0.45 - 1.0 um particles was then applied to CLN for a period of 44 days. After etching (see section 2.7), a number of areas of intense α -radioactivity could clearly be identified (Figures 3.29 and 3.30). These 'hot particles' are similar to those found by Hamilton and Clifton (1980) and Hamilton (1981) in resuspended sediment of the Esk, and are believed to be derived from the authorised discharge of radioactive effluent into the Irish Sea by the British Nuclear Fuels Limited (B.N.F.L.) reprocessing plant at Sellafield, some 10 km north of the estuary. Hamilton (1981) found by acid leaching of the particles that Pu and Am radionuclides were always present, with Cm nuclides occasionally present, but less than one in four of all the particles studied contained any uranium. No abnormally high concentrations of uranium were found in the particulates settled from the same water sample ($1.19 \pm 0.07 \text{pCi g}^{-1}$, $3.53 \pm 0.21 \text{ppm}$), in the water sample itself ($2.76 \pm 0.12 \text{ug l}^{-1}$) or in another water sample of salinity 3.15%. ($0.45 \pm 0.02 \text{ug l}^{-1}$). It is unlikely, then, that the α -track clusters in the CLN are due solely to natural uranium given the low CLN : filter application time of 44 days. Table 3.15 contains the γ -spectrometry results for the settled particulates and shows a range of nuclides which are commonly found in the liquid effluent from the Magnox storage and decanning plant at BNFL, Sellafield (Hamilton and Clarke, 1984). The presence of these nuclides confirms BNFL as the source. Prior to discharge, the effluents are neutralised with ammonia and the iron-rich effluent should/

TABLE 3.15

Radionuclide activities in particulate material from the
Esk estuary, Cumbria. ($\pm 1.96 \sigma$ error, 0.582g sample).

<u>Radionuclide</u>	<u>Activity concentration (pCi g⁻¹)</u>
¹⁴⁴ Ce	42.2 \pm 10.4
⁶⁰ Co	8.8 \pm 1.90
¹³⁴ Cs	5.22 \pm 0.88
¹³⁷ Cs	161 \pm 8.8
⁹⁵ Nb	555 \pm 23.5
¹⁰⁶ Ru	559 \pm 38.0
⁹⁵ Zr	129 \pm 7.9

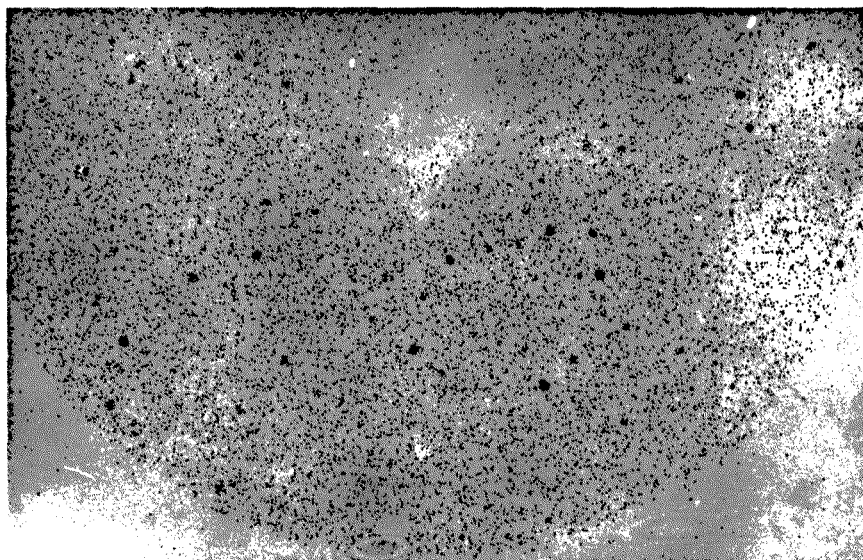


Figure 3.29. Alpha track clusters in cellulose nitrate from filtered particulates of the Esk estuary.

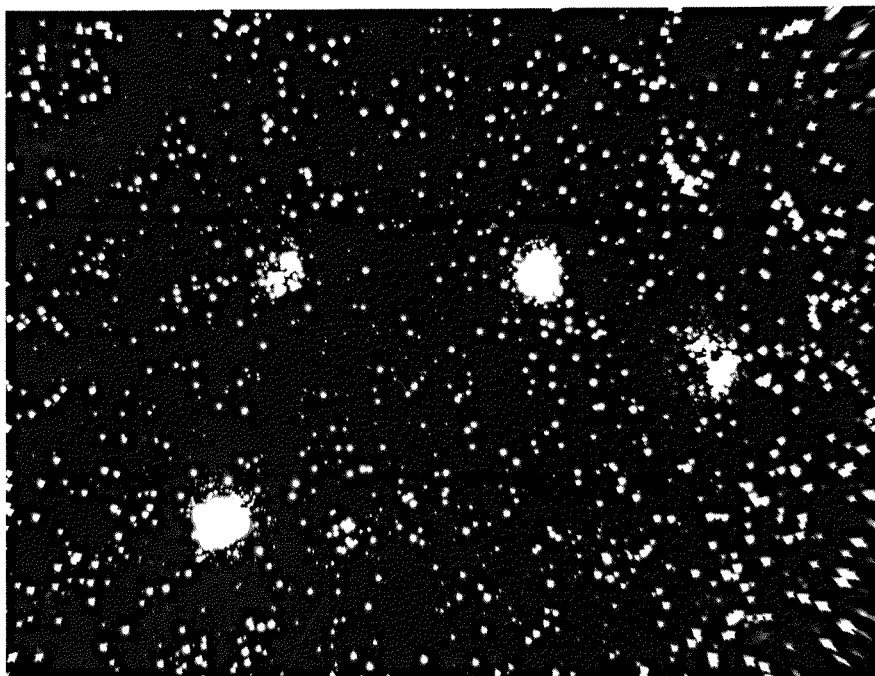


Figure 3.30. Enlarged alpha hot-spot from filtered particulates of the Esk estuary

should contain flocculant material and particulate debris, which is transported by the tides to the estuary with a transit time of about 10-12 months (Hamilton and Clarke, 1984). In the Esk, a large proportion of the radionuclides are retained in the sediments, especially in the silty muds, and these are stirred up by the ebb and flow of the tide, accounting for the occurrence of the 'hot particles' found in the water column.

A range of samples collected from an inlet East of Dounreay Nuclear Power Development Establishment (D.N.P.D.E.) were described in Table 2.2. Table 3.16 shows the uranium and plutonium results for these samples. As far as plutonium is concerned, the main observations are (1) that the scrapings from the rocks in the inlet have spatially and temporally-variable enrichments of plutonium compared to the soils and offshore sediment, and (2) the soil Pu inventories decrease inland by a factor of about 2 over 100 metres, a trend not unlike those described by Peirson et al., (1982) for coastal transects around Sellafield. This pattern reflects an on-land flux of material from the sea, such as wind-blown marine particulates/aerosols or foam, both of which are shown to be enriched in plutonium and some fission products (Cook et al., 1984). Fission track analysis was performed on samples 2, 3 and 5. The fission track distribution for the dried sea foam (sample 3) was completely homogeneous and comparison with a fission track glass standard yielded a uranium concentration of $0.68 \pm 0.03 \text{ pCig}^{-1}$ (2.0 ppm). However, the track distributions from 0.1g pellets of the 1981 rock scrapings (sample 2) and from a soil 50 metres inland (sample 5) were inhomogeneous, containing 21 and 2 fission stars respectively. The fission track analysis value of $2.18 \pm 0.07 \text{ pCig}^{-1}\text{U}$ (6.56 ppm) for sample 5 must therefore be taken as approximate. A realistic uranium value for sample 2, however, could only be obtained by total dissolution and α -spectrometry, since the fission stars in this sample were more abundant and more dense (see Figure 3.31a). Alpha-spectrometry gave values of $1.28 \pm 0.11 \text{ pCig}^{-1}\text{U}$ (3.8 ppm) and $2.20 \pm 0.08 \text{ pCig}^{-1}\text{U}$ (6.67 ppm) for samples 1 and 2 respectively. It appears, therefore, that there is no enrichment of uranium in these samples as there was for/

TABLE 3.16

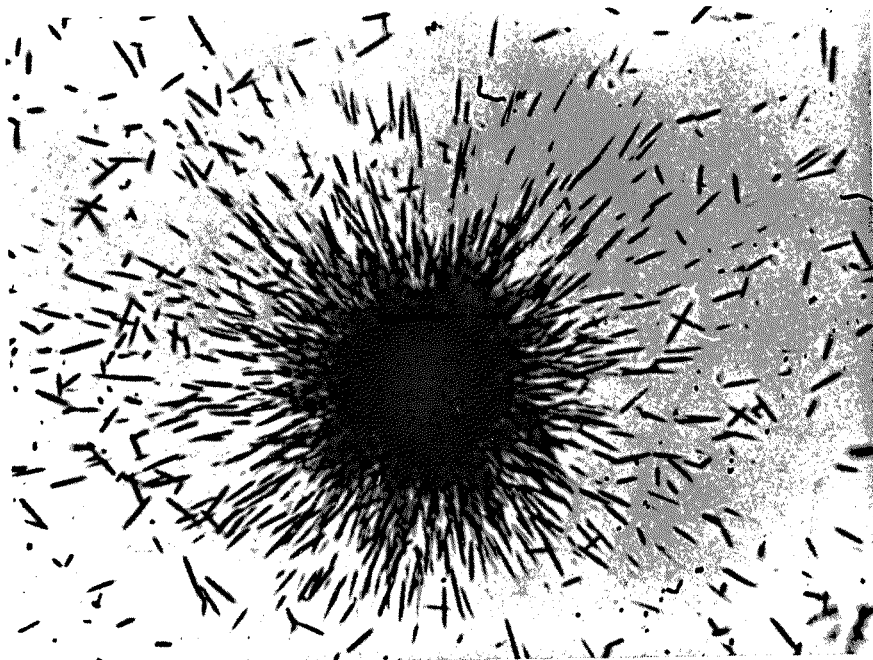
Plutonium and uranium concentrations of samples collected
in the vicinity of D.N.D.P.E., Caithness ($\pm 1\sigma$ error)

<u>Sample number</u> ^a	<u>^{238}U (pCig⁻¹)</u>	<u>$^{234}\text{U}/^{238}\text{U}$</u>	<u>$^{239,240}\text{Pu}$(pCig⁻¹)</u>
1	1.28 \pm 0.11	0.97 \pm 0.11	38.67 \pm 0.51
2	2.20 \pm 0.08	1.05 \pm 0.03	4.20 \pm 0.01
3	0.68 \pm 0.03 ^b	-	23.31 \pm 0.29
4	-	-	0.105 (1.47 ^c)
5	2.18 \pm 0.07 ^b	-	0.115 (1.04 ^c)
6	-	-	0.181 (1.70 ^c)
7	0.25 \pm 0.03	1.12 \pm 0.13	0.95 \pm 0.004

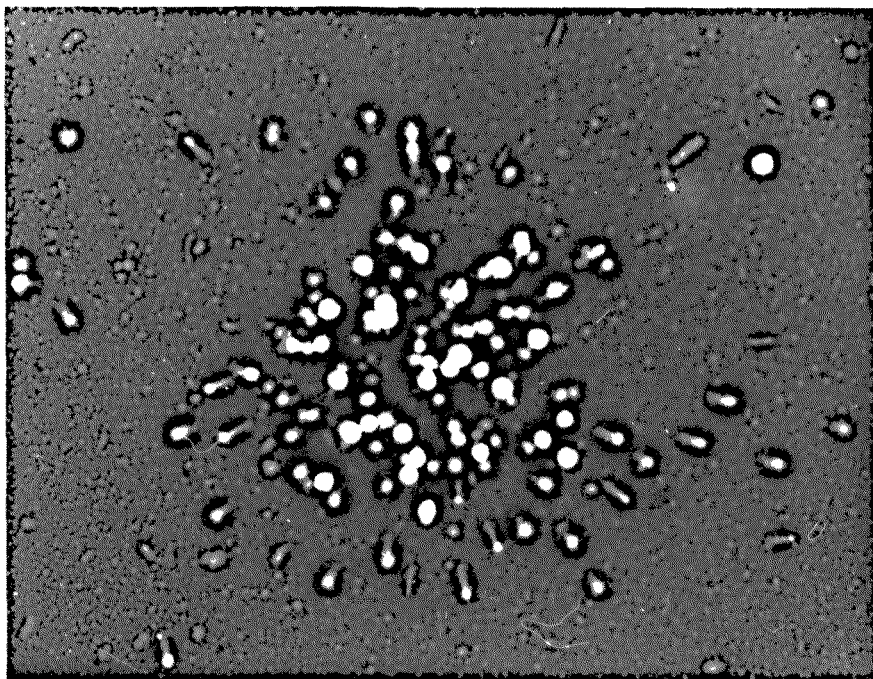
a - For sample descriptions see Table 2.2

b - Fission track analysis results

c.- Pu inventories to 30cm depth in pCicm⁻².



(a)



(b)

3.31 (a) Fission track and (b) alpha track hot-spots from material scraped from rocks near Dounreay, Caithness

for plutonium, its concentration being similar to that of the nearby soil (sample 5). The clay components of the material scraped from the rock may therefore derive from local soil weathering and erosion. The offshore sediment also required total dissolution / α -spectrometry because the sandy material was difficult to bind into a pellet. A relatively low concentration of $0.25 \pm 0.03 \text{ pCi g}^{-1} \text{U}$ (0.75 ppm) was found since the sediment comprised mainly coarse (97% >200um) quartz and carbonate.

It is interesting to note the $^{234}\text{U}/^{238}\text{U}$ activity ratio for sample 2 i.e. 1.05 ± 0.03 . This value is slightly higher than that expected for continental rocks or nearshore sediments (~ 1.00 Sackett and Cook, 1969) and may indicate a uranium contribution from sea-spray which has an activity ratio of about 1.15.

Fission stars such as that shown in Figure 3.31a (from sample 2) were initially thought to be due to ^{239}Pu , present at a concentration of 4.02 pCi g^{-1} and possibly in 'hot particles' such as those found by Hamilton (1981) near Sellafield. However, abundant fission stars have recently been observed in 90um thick sections of white sandstone and organic-rich black shales from Sandside Bay, close to D.N.D.P.E. (Das, pers. comm.), and these can only be due to natural uranium inherent in the rock. In fact, by calculation alone, the fission stars observed here, which constitute about 13% of the total tracks from the sample must be due to ^{235}U and not ^{239}Pu fission since a plutonium/uranium alpha-activity ratio of 1.17×10^4 would be required for an equal probability of fission. So the nature of the plutonium-particle association cannot be unequivocally determined due to this overwhelming ^{235}U fission track contribution. From Figure 3.31a, the diameter of the hot particle is estimated at approximately 10um, and, if pure $^{239}\text{PuO}_2$, would have an α -activity of approximately 324 pCi. The α -track density in the CLN detector (Figure 3.31b) after 6 months exposure to the particulates gives an approximate hot-spot α -activity of 0.02 pCi, some four orders/

orders of magnitude less.

Alpha-autoradiography was also performed on a hydrothermal manganese deposit, collected from an elevated submarine volcanic ridge. The deposit was similar to one described by Cronan et al., (1982) which had an accumulation rate of at least 500mm Myr^{-1} , far higher than the rate for most hydrogenous nodules, and is consistent with it being of hydrothermal origin. The deposit was shown by X-ray diffraction to be a pure birnessite (Moorby, pers.comm.) and had a purplish-black crust and many internal laminations. It was thought that this internal structure may have resulted from a periodicity of its growth rate, and it was considered worthwhile to apply the CLN detector to a section of the nodule to determine whether bands of α -activity occurred along the laminae. Such an observation would be expected if periods of low nodule accumulation rate coincided with high levels of uranium and/or thorium uptake at its surface. Figure 3.32 is an α -autoradiograph of the upper edge of the deposit after a CLN application time of 196 days. An enhanced level of α -activity is found at the edges relative to the internal bulk of the deposit. This distribution is quite similar to the radial profiles of α -activity described by Andersen and Macdougall (1977) which were found for most of the slices of manganese nodules they studied. These authors found a simple exponential decrease in total α -activity with depth and interpreted this in terms of the decay of $^{230}\text{Th}_{\text{excess}}$ during diagenetic nodule growth, growth rates being between 2 and 10 mm Myr^{-1} in agreement with values found radiochemically by Ku and Broecker (1969). Such low nodule growth rates mean that all the $^{230}\text{Th}_{\text{excess}}$ ($t_{1/2} = 7.7 \times 10^4\text{ y}$) is located in the outermost 1mm of the nodule, requiring the high resolution sampling ($\sim 30\mu\text{m}$, Andersen and Macdougall, 1977) provided by the track technique. In the hydrothermal manganese deposit similar to the one here, however, the ^{230}Th activity was very low and variable with depth, the $^{230}\text{Th}/^{234}\text{U}$ ratio was low and the $^{234}\text{U}/^{238}\text{U}$ ratio lay between 1.06 and 1.24 (Cronan et al., 1982) and thus most/



Figure 3.32. Alpha-autoradiograph of the upper edge of a hydrothermal manganese deposit.

most of the α -tracks at the edges are due to the uranium isotopes. Figure 3.32 would therefore seem to indicate the surface adsorption of uranium nuclides from sea water.

Figure 3.33 illustrates another interesting phenomenon. Visible in the photograph are peculiar 'clouds' of α -tracks which lie outside the area of contact between the CLN and the manganese deposit. One of these clouds issued from a small crack which travelled along the deposit, the other from the bottom edge of the deposit. It is believed that these α -tracks are due to the diffusion of ^{222}Rn , its decay and that of its two short-lived daughters ^{218}Po and ^{214}Po . Such diffusion would also be expected from the top surface of the deposit but is not observed. This is a consequence of the top surface having been coated with a resin prior to sectioning in order to prevent splitting or crumbling and to facilitate the preparation of the flat surface required for CLN application. It is evident that ^{222}Rn cannot diffuse through this resin (at least during the timescale of autoradiography) and so the amount of this nuclide available for diffusion elsewhere is increased. Such diffusion of ^{222}Rn has previously been observed by Krishnaswami and Cochran (1978) in their study of authigenic nodules. Depth profiles of ^{210}Pb in these nodules exhibited large excesses over ^{226}Ra ($^{210}\text{Pb}/^{226}\text{Ra}$ activity ratios from 2.2 to 17.6) in the outermost layer of their upper face, $^{210}\text{Pb}/^{226}\text{Ra}$ ratios of < 1.0 in the intermediate layers, and ratios slowly increasing to the secular equilibrium value in the deeper layers. This deficiency of ^{210}Pb in the near-surface, intermediate layers (ratios < 1.0) was caused by the diffusive escape of ^{222}Rn , the precursor of ^{210}Pb . This loss was not reflected in the high $^{210}\text{Pb}/^{226}\text{Ra}$ ratios on the upper surface of the nodules because of the deposition there of ^{210}Pb from sea water.

Stainless steel planchets containing purified electrodeposited radionuclides/

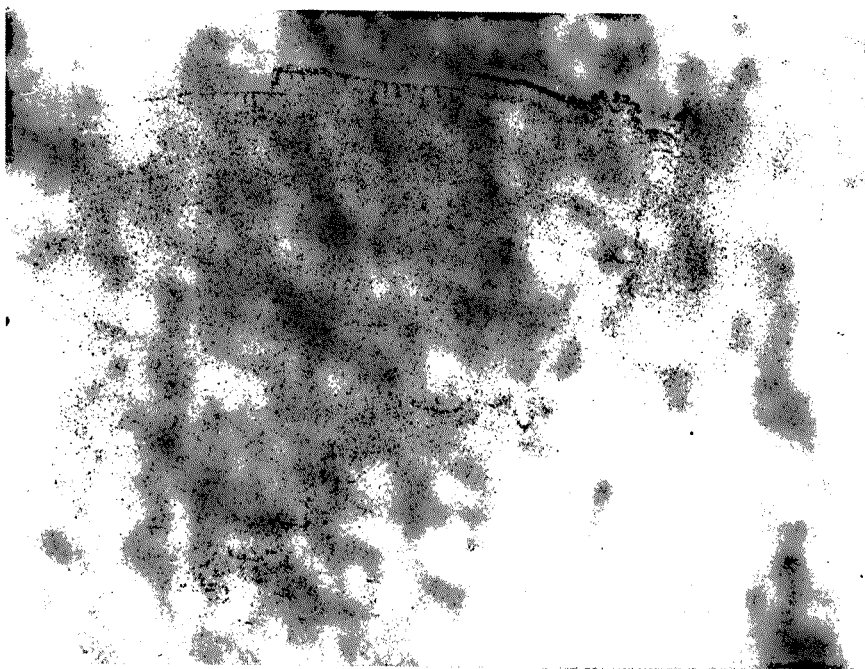


Figure 3.33. Complete alpha-autoradiograph of a hydrothermal manganese deposit.

radionuclides were also subjected to α -autoradiography. A thin aluminium absorber was used to slow down the α -particles for registration (Hashimoto, 1971) and the films were etched in 2.5 molar NaOH at 60°C for 2 hours (see section 2.7). The

α -track record produced in CLN from three of the planchets are shown in Figures 3.34, 3.35 and 3.36. Figure 3.34 shows the

α -tracks produced from a source of ^{232}U ($\sim 4\text{dpm}$) which had been applied to CLN for 25 days. The electroplating cell and plating parameters were as described in section 2.5.1. The ^{232}U α -tracks show an excellent homogeneous distribution over the planchet during plating. Figure 3.35, on the other hand, shows an inhomogeneous distribution of tracks obtained after a 40-day exposure of CLN to electroplated Pu isotopes on a planchet submitted by another laboratory. The observed pattern of tracks might be due to the Pt anode being positioned too close to the planchet during the plating procedure. It should be stressed, however, that such a distribution will have no effect on the quantitative α -spectrometric analysis of the Pu isotopes present, and there may actually be a slight gain in counting efficiency, depending on the relative dimensions of the deposit and surface barrier detector and on the source to detector clearance.

A slight inhomogeneous deposit of Pu isotopes (47.7 dpm total) was also found in a sample planchet from a different laboratory (Figure 3.36). A slight ridge of high α -activity can be seen which is present all the way round the deposit. Lexan polycarbonate was then applied to the same planchet and the package was irradiated for 6 hours in the research reactor at the γ -curtain (Figure 2.15). Subsequent etching yielded a fission track distribution (Figure 3.37) similar to the α -track distribution. Although more than half of the fission tracks will be due to the β -emitter ^{241}Pu ($\sigma_f = 1011\text{b}$), their distribution, when compared to the α -tracks, indicates that many are due to fission of ^{239}Pu ($\sigma_f = 742\text{b}$) and ^{238}Pu ($\sigma_f = 16.5\text{b}$). This demonstrates the viability of the fission track technique in the mapping of plutonium.

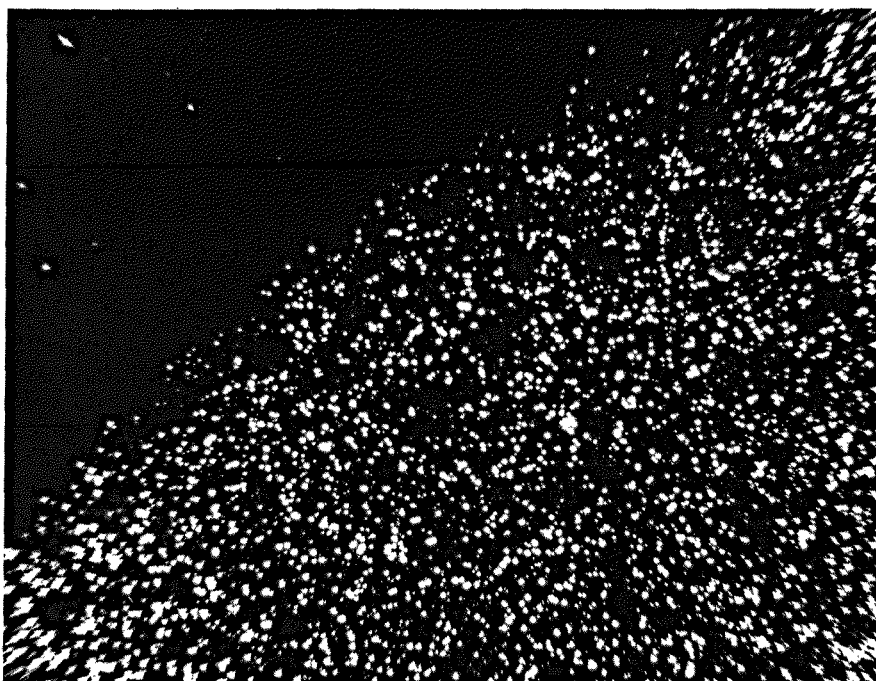


Figure 3.34. Alpha-autoradiograph of a planchet containing about 4dpm ^{232}U .

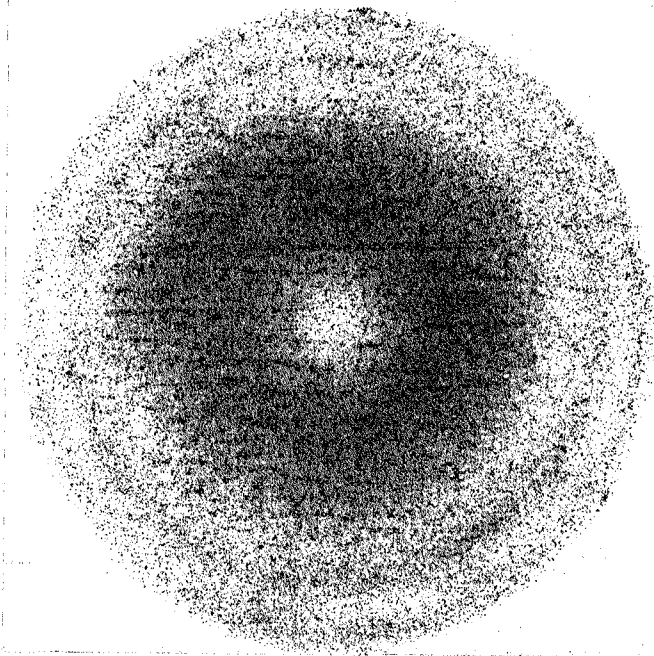


Figure 3.35. Alpha-autoradiograph of a planchet containing Pu isotopes.



Figure 3.36. Alpha-autoradiograph of a planchet containing 47.7 dpm of alpha-emitting Pu isotopes.

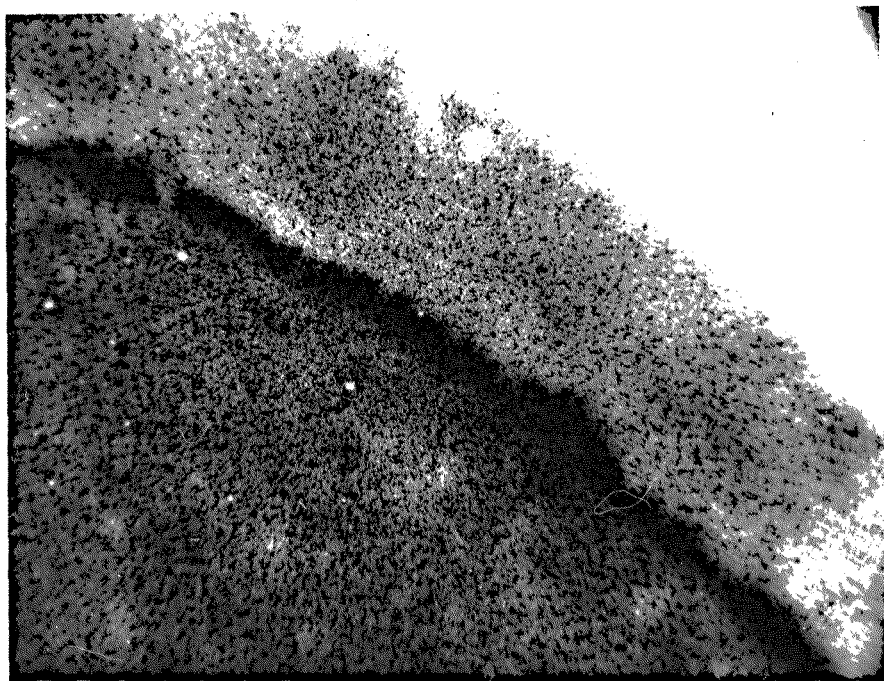


Figure 3.37. Fission track distribution produced by irradiation of a planchet containing Pu isotopes.

A sample of gypsum (calcium sulphate) was analysed for uranium by both α -spectrometry and fission track analysis. The gypsum was a waste product from a fertilizer factory at Leith on the Firth of Forth and is generated during the chemical processing of high-uranium-bearing calcium phosphate ore. It was therefore considered to be a possible source of uranium to the Forth estuary into which the waste was discharged. The results from both methods agreed within 2σ and were 3.65 ± 0.09 (fission track analysis, 1σ) and 4.12 ± 0.22 ppm (α -spectrometry, 1σ). The $^{234}\text{U}/^{238}\text{U}$ activity ratio was 0.92 ± 0.05 . The low uranium content of the gypsum relative to the calcium phosphate ore itself indicates that during the H_2SO_4 treatment of the ore, the uranium complexes with phosphate rather than the sulphate in solution, and ends up predominantly in the fertilizer (Spalding and Sackett, 1972).

APPENDIX A

SAMPLE CALCULATIONS, ERRORS AND STATISTICS

A physical magnitude can never be exactly determined; there is always an error associated with its measurement. These errors can be classified as either random or systematic, where the random error represents the unbiased fluctuations of the measuring system obtained after repeated measurement (precision). The systematic error, on the other hand, is caused by measurement bias and determines how closely mean experimental values correspond to the 'true' value (accuracy). Inaccuracies can be introduced by faulty equipment, incorrect calibration or poor technique.

In this study, random errors were evaluated by repeated measurements of replicates as illustrated in Tables 2.3, 2.5 and 2.6 for the fission track and α -track methods, while systematic errors were evaluated by interlaboratory or intersystem comparison - Table 2.4 (pore waters) and Tables 3.1 and 3.2 (sediments). The replicate analyses give an overall 1σ error value, where the standard deviation is given by

$$\sigma_{\text{REP}} = \left(\frac{\sum (x - \bar{x})^2}{n-1} \right)^{\frac{1}{2}}$$

where x is the value obtained for an individual measurement and \bar{x} is the mean value of n observations. The error associated with replicate measurements, σ_{REP} , can be regarded as a combined or total error, σ_{TOT} , divisible into two distinct components: (i) a statistical error, σ_{C} , derived from the observed number of counts, N , which, in radiocactivity measurement is equal to $N^{\frac{1}{2}}$, (ii) a non-counting error, σ_{NC} , arising from inaccuracies in, for example, weighing of sample or dispensing tracer by pipette - it is therefore non-quantifiable. The total error thus represents the maximum values of the experimental uncertainties, and

$$\sigma_{\text{TOT}} = \sigma_{\text{REP}} = \left(\sigma_{\text{C}}^2 + \sigma_{\text{NC}}^2 \right)^{\frac{1}{2}}$$

In the case of sea water replicates (Table 2.4), σ_{REP} was found to be 6.1%, and from the number of track counts (mean 1233),

$\sigma_{\text{C}} = 2.8\%$ and so $\sigma_{\text{NC}} = 5.4\%$. With the achievement of homogeneous track densities, it was assumed that since the number of fission tracks/

tracks was proportional to irradiation time, then the error on the track density (tracks/area) is equal to $(\text{tracks})^{1/2}/\text{area}$. From equation 2.2 therefore, the error on U_x by propagation of errors is

$$e(U_x) = U_s \left[\left(\frac{e(D_x)}{D_s} \right)^2 + \left(\frac{D_x}{D_s^2} \right)^2 e(D_s)^2 \right]^{1/2}$$

The following is a typical calculation for the uranium content of a pore water sample based on equation 2.2 and the above equation -

Mean background tracks	= 13.6
Total area counted	= $8.309 \times 10^{-2} \text{ cm}^2$
Mean background track density	= $163.7 \pm 44.4 \text{ cm}^{-2}$
Uranium standard track count	= 1589
Total area counted	= $6.985 \times 10^{-3} \text{ cm}^2$
Standard track density	= $227487 \pm 5707 \text{ cm}^{-2}$
Sample track count	= 1268
Total area counted	= $8.309 \times 10^{-2} \text{ cm}^2$
Sample track density	= $15260 \pm 429 \text{ cm}^{-2}$
Uranium content of standard	= 44.76 ug l^{-1}

Thus, from equation 2.2,

$$\begin{aligned} U_x &= \frac{(15260 \pm 429) - (164 \pm 44)}{(227487 \pm 5707) - (164 \pm 44)} \cdot 44.76 \\ &= \frac{(15096 \pm 431)}{(227323 \pm 5707)} \cdot 44.76 \\ &= 3.00 \pm 0.11 \text{ ug l}^{-1} \end{aligned}$$

The 1σ errors quoted for the analyses of uranium by the fission track method are those derived from counting statistics only, and as such do not represent the total uncertainty, which can be derived from σ_{REP} .

In the determination of the excess α -track density (R_{xs}) down a deep sea core, each of the terms R_i , R_∞ , U_i and U_∞ (equation 2.4) has its own associated error and the overall error function for R_{xs} can be expressed in the form of a Maclaurin expansion. Since variances are/

are linearly additive,

$$\text{var}(R_x) = \text{var}(R_T) + \text{var}\left(\frac{R_\infty}{U_\infty} \cdot U_i\right)$$

and

$$\text{var}\left(\frac{R_\infty}{U_\infty} \cdot U_i\right) = \text{var}(R_\infty) \cdot \left(\frac{U_i}{U_\infty}\right)^2 + \text{var}(U_\infty) \left(\frac{R_\infty U_i}{U_\infty^2}\right)^2 + \text{var}(U_i) \left(\frac{R_\infty}{U_\infty}\right)^2$$

The error on R_{xs} is then given by

$$(R_{xs}) = [\text{var}(R_{xs})]^{1/2}$$

From Table 3.1, this error ranges from about 7% to 36% for core 9936K.

APPENDIX BFORTRAN IV COMPUTER PROGRAMME FOR NEUTRON FLUX CALCULATION

```

C   This program evaluates neutron fluxes from activities obtained
C   from Geli
      DIMENSION A(100), FLUX (100), T1(100), C1174(100), C1333(100),
      *C1292(100), D1(100), D2(100), D3(100), ATFE(100), AOFE(100), X(100),
      *DELAY (100), WT(100), TIRRN(100)
      READ (5,1)N
C 1  FORMAT (I2)
C   N is the number of fluxes to be calculated
      DO 8, I=1,N
      READ (5,3) T1 (I), C1174(I), C1333(I), C1292(I),DELAY (I), WT(I),
      *TIRRN(I)
3  FORMAT (F8.5, 3F10.4, F4.2, 2F9.4)
8  CONTINUE
C
C   C1174, C1333 and C1292 ae taken to be in counts per second
C
      DO 2, I = 1,N
      A(I) = 3.7E4*11.67*EXP(-0.693*T1(I) /5.26)
      D1(I)= C1174(I) *100.0/A(I)
      D2(I)= C1333(I) * 100.0/A(I)
      D3(I)= D1(I) - (0.188/0.159)*(D1(I)-D2(I) )
      ATFE(I)=C1292(I) * 100.0/D3(I)
2  CONTINUE
C
      DO 4, I = 1,N
      AOFE(I) = ATFE(I)*EXP(0.693*DELAY(I)/45.1)*(100.0/42.75)
      X(I) = WT(I)*3.559E16
      FLUX (I) = AOFE(I) / (X(I)*1.23E-24*(1.0-EXP(-6.402E!4*TIRRN(I))))
4  CONTINUE
C
      WRITE (6,6)
6  FORMAT (1H, 10X, 'NUMBER', 15X, 'FLUX')
C
      DO 7, I=1,N
      WRITE (6,9) I, FLUX (I)
9  FORMAT (1H1, 12X, I2, 14X,E13.6)
7  CONTINUE
      STOP
      END

```

APPENDIX CFORTRAN IV COMPUTER PROGRAMME FOR EVALUATION OF THE URANIUM
ACTIVITY OF NATURAL WATERS.

```

1      Program Hydro 2
2      C      This program evaluates uranium-238 activity of natural waters
3      C      and the U234/U238 activity ratio
4      DIMENSION A(20), B(20), C(20), LT(20), SPIKE(20), Y(20), Z(20),
5      *      EA(20),EB(20),EC(20),EY(20),EZ(20),CU232(20), ECU232(20)
6      *      CU238(20), ECU238(20)
7      REAL LT
8      C
9      READ (5,1)N
10     1      FORMAT (2X,I2)
11     DO 3, I=1,N
12     READ (5,2)A(I),B(I),C(I),LT(I),SPIKE(I)
13     2      FORMAT (3F6.1,2F4.2)
14     3      CONTINUE
15     C
16     DO 5, I=1,N
17     EA(I) = SQRT(A(I))
18     EB(I) = SQRT(B(I))
19     EC(I) + SQRT(C(I))
20     Y(I) = B(I)/A(I)
21     EY(I)=Y(I) * SQRT(EA(I)**2+(EB(I)/B(I))**2)
22     Z(I) = C(I)/B(I)
23     EZ(I)=Z(I)*SQRT(EC(I)/C(I))**2+(EB(I)/B(I)**2)
24     CU232(I)=SPIKE(I)/LT(I)
25     ECU232(I) = CU232(I)*1.01E-2
26     CU238(I)=CU232(I)*Y(I)
27     ECU232(I)=CU238(I)*SQRT( (ECU232(I)/CU232(I))**2+(EY(I)/Y(I))**2)
28
29     5      CONTINUE
30     C      Concentration of U-238 is in DPM per litre
31/

```

```
31     WRITE (6,4)
32 4   FORMAT (6X,'NUMBER', 4X, '[U238]' , 5X, 'ERROR', 5X '234/238', 5X,
33 *   'ERROR' )
34 C
35     DO 6 I = 1,N
36     WRITE (6,7) I, CU238(I), ECU238 (I), Z(I), EZ(I)
37 7   FORMAT (9X,I2,7X,F4.3,5X,F4.3,5X,F4.3,7X,F4.3
38 6   CONTINUE
39     STOP
40     END
```

REFERENCES

- ALEXANDER W.R. (1984). Diagenesis in anoxic sediment interstitial waters, Tamar estuary, S.W. England. Ph.D. Thesis, Dept. of Earth Sciences, University of Leeds.
- ALLARD B., OLOFSSON U. and TORSTENFELT B. (1984). Environmental actinide chemistry. *Inorg.Chim.Acta*, 94, 205-221.
- ALLER R.C. and COCHRAN J.K. (1976). $^{234}\text{Th}/^{238}\text{U}$ disequilibrium in near-shore sediment : particle reworking and diagenetic timescales. *Earth Planet. Sci. Lett.*, 29, 37 -50.
- ANDERSEN M.E. and MACDOUGALL J.D. (1977). Accumulation rates of manganese nodules and sediments : an alpha track method. *Geophys.Res.Lett.*, 4, 351-353.
- ANDERSON R.F. (1984). A method for determining the oxidation state of uranium in natural waters. *Nucl.Instr.Meth.Phys. Res.*, 223, 213-217.
- ASIKAINEN M. (1981). State of disequilibrium between ^{238}U , ^{234}U , ^{226}Ra and ^{222}Rn in groundwater from bedrock. *Geochim. Cosmochim.Acta*, 45, 201-206.
- ASTON S.R. and STANNERS D.A. (1981). Plutonium transport to and deposition and mobility in intertidal sediments from the Irish sea. *Nature*, 289, 581-582.
- AUMENTO F. (1971). Uranium content in mid-oceanic basalts. *Earth Planet. Sci.Lett.*, 11, 90-94.
- BACON M.P. and ANDERSON R.F. (1983). Thorium isotope distributions in the eastern equatorial Pacific. *NATO Conf. Ser.*, 4, 367-378.
- BALLESTRA S., HOLM E. and FUKAI R. (1978). Low-level determination of radionuclides in environmental and biological materials. In : *Symp. on determ. radion. in environ. biol. mat.*, CEGB, London, paper 15.
- BALISTRIERI L. and MURRAY J.W. (1979). Surface of goethite ($\alpha\text{-FeOOH}$) in seawater. In : *Am.Chem.Soc.Symp.Ser.No.93*, 275-298.
- BALZER W. (1982). On the distribution of iron and manganese at the sediment/water interface : thermodynamic versus kinetic control. *Geochim.Cosmochim.Acta*, 46, 1153-1161.

- BARCELONA M.J. (1980). Dissolved organic carbon and volatile fatty acids in marine sediment pore waters. *Geochim. Cosmochim. Acta*, 44, 1977-1984.
- BATURIN G.N. (1971). Uranium in oceanic ooze solutions of the southeastern Atlantic. *Proc.Nat.Acad.Sci. USSR*, 198, 224-226.
- BATURIN G.N. (1973). Uranium in the modern marine sedimentary cycle. *Geochem. Internat.*, 10, 1031-1041.
- BATURIN G.N. and KOCHENOV A.V. (1973). Uranium in the interstitial waters of marine and oceanic sediments. *Geokhimiya*, 10, 1529-1536.
- BAXTER M.S., MCKINLEY I.G., MACKENZIE A.B. and JACK W. (1979). Windscale radiocaesium in the Clyde sea area. *Mar.Poll.Bull.*, 10, 116-120.
- BAXTER M.S., CRAWFORD R.W., SWAN D.S. and FARMER J.G. (1981). ²¹⁰Pb dating of a Loch Lomond sediment core by conventional and particle track methods and some geochemical observations. *Earth Planet. Sci.Lett.*, 53, 434-444.
- BENDER M., BROECKER W., GORNITZ V., MIDDEL U., KAY R., SUN S.S. and BISCAYE P. (1971). Geochemistry of three cores from the East Pacific Rise. *Earth Planet. Sci. Lett.*, 12, 425-433.
- BENDER M.L., FANNING K.A., FROELICH P.N., HEATH G.R. and MAYNARD V. (1977). Interstitial nitrate profiles and oxidation of sedimentary organic matter in the eastern equatorial Atlantic. *Science*, 198, 605-609.
- BERGER W.H. (1976). Biogenous deep sea sediments : production, preservation and interpretation. In: *Chemical Oceanography* (Riley J.P. and Chester R., eds.) Academic Press, London, 5, 266-388.
- BERNER R.A. (1971). *Principles of Chemical Sedimentology*, McGraw-Hill, New York, N.Y. 1971.
- BERNER R.A. (1981). A new geochemical classification of sedimentary environments. *J.Sed. Petrol.*, 51, 359-365.
- BERNER R.A., SCOTT M.R. and THOMLINSON C. (1970). Carbonate alkalinity in the porewaters of anoxic marine sediments. *Limnol. Oceanogr.*, 15, 544-549
- BERTINE K.K., CHAN L.H. and TUREKIAN K.K. (1970). Uranium determinations in deep sea sediments and natural waters using fission tracks. *Geochim.Cosmochim. Acta*, 34, 641-648

- BHAT S.G. and KRISHNASWAMI S. (1969). Isotopes of uranium and radium in Indian rivers. Proc.Ind.Acad.Sci., 70 (A), 1-17.
- BHAT S.G., KRISHNASWAMI S., LAL D., RAMA and MOORE W.S. (1969). $^{234}\text{Th}/^{238}\text{U}$ ratios in the ocean. Earth Planet. Sci. Lett., 5, 483-491.
- BISCAYE R.E., KOLLA V. and TUREKIAN K.K. (1976). Distribution of calcium carbonate in surface sediments of the Atlantic ocean. J. Geophys. Res., 81, 2595-2603.
- BISCHOFF J.L., GREER R.E. and LUISTRO A.O. (1970). Composition of interstitial waters of marine sediments : temperature of squeezing effects. Science, 167, 1245-1246.
- BISCHOFF J.L. and KU T.-L. (1971). Pore fluids of recent marine sediments : II. Anoxic sediments of 35° to 45° N, Gibraltar to mid-Atlantic Ridge. J. Sed.Petrol., 41, 1008-1017.
- BISCHOFF J.L. and SAYLES F.L. (1972). Pore fluid and mineralogical studies of recent marine sediments : Bauer depression region of East Pacific Rise, J. Sed. Petrol., 42, 711-724.
- BLANCHARD R.L. (1965). $^{234}\text{U}/^{238}\text{U}$ ratios in coastal marine waters and calcium carbonates. J. Geophys.Res., 70, 4055-4061.
- BLANCHARD R.L. and OAKES D. (1965). Relationships between uranium and radium in coastal marine shells and their environment. J. Geophys.Res., 70, 2911-2921.
- BLOCH S. (1980). Some factors controlling the concentration of uranium in the world ocean. Geochim. Cosmochim. Acta, 44, 373-377.
- BLOOMFIELD C. and KELSO W.I. (1973). The mobilisation and fixation of Mo, V and U by decomposing plant matter. J. Soil Sci., 24, 368-379.
- BONATTI E., FISHER D.E., JOENSUU O. and RYDELL H.S. (1971). Post-depositional mobility of some transition elements, phosphorus and thorium in deep sea sediments, Geochim. Cosmochim. Acta, 35, 189-201.
- BOROLE D.V., KRISHNASWAMI S. and SOMAYAJULU B.L.K. (1977). Investigations on dissolved uranium, silicon and particulate trace elements in estuaries. Estuar. Coast. Mar.Sci., 5, 743-754.
- BOROLE D.V., KRISHNASWAMI S. and SOMAYAJULU B.L.K. (1982). Uranium isotopes in rivers, estuaries and adjacent coastal sediments of western India : Their weathering, transport and oceanic budget. Geochim.Cosmochim.Acta, 46, 125-137.

- BOULAD A.P. and MICHARD G. (1976). Etude de l'uranium, du thorium et de leurs isotopes dans quelques carottes du bassin Angolais (Atlantique Sud-Est). *Earth Planet. Sci. Lett.*, 32, 77-83.
- BOYLE E., COLLIER R., DENGLER A.T., EDMOND J.M., NG A.C. and STALLARD R.F. (1974). On the chemical mass-balance in estuaries. *Geochim. Cosmochim. Acta*, 38, 1719-1728.
- BOYLE E.A., SCLATER F.R. and EDMOND J.M. (1977). The distribution of dissolved copper in the Pacific. *Earth Planet Sci. Lett.*, 37, 38-54.
- BRAY J.T., BRICKER O.P. and TROUP B.N. (1973). Phosphate in interstitial waters of anoxic sediments : oxidation effects during sampling procedure. *Science*, 180, 1362-1363.
- BROECKER W.S. (1965). An application of natural radon to problems in ocean circulation. In : *Symp. on Diffusion in Oceans and Fresh Waters* (Ichiye T. ed.), Lamont-Doherty Geological Observatory, Palisades, New York, 116-145.
- BROECKER W.S., CROMWELL J. and Li Y.H. (1968). Rates of vertical eddy diffusion near the ocean floor based on measurements of the distribution of excess ^{222}Rn . *Earth Planet. Sci. Lett.*, 5, 101-105.
- BROECKER W.S. and PENG T-H. (1982). *Tracers in the sea*. Lamont-Doherty Geological Observatory, Eldigio Press 1982.
- BURTON J.D. (1975). Radioactive nuclides in the marine environment. In : *Chemical Oceanography* (Riley J.P. and Skirrow G., eds.) Academic Press, London, 3, 91-191.
- BUTLER E.I. and TIBBITTS S. (1972). Chemical survey of the Tamar Estuary. I. Properties of the waters. *J. Mar. Biol. Ass. U.K.*, 52, 681-699.
- CALVERT S.E. (1976). The mineralogy and geochemistry of nearshore sediment. In : *Chemical Oceanography* (Riley J.P. and Chester R. eds.) Academic Press, London, 6, 187-280.
- CALVERT S.E. and PRICE N.B. (1972). Diffusion and reaction profiles of dissolved manganese in the pore water of marine sediments. *Earth Planet. Sci. Lett.*, 16, 245-249.
- CALVERT S.E. et al. (1979). RRS Discovery Cruise 99 : 16-27 January 1979. Geochemical sampling in the Cape basin. Institute of Oceanographic Sciences, Cruise Report, No. 78.
- CARPENTER B.S. and CHEEK C.H. (1970). Trace determination of uranium in biological material by fission track counting. *Anal. Chem.*, 42, 121-123.

- CARPENTER B.S. and REIMER G.M. (1974). Standard Reference Materials : Calibrated glass standards for fission track use. Nat.Bur. Stand.(U.S.), Spec. Publ. 260-49, 27pp.
- CHERDYNTSEV V.V., CHALOV P.I., KHITRIK M.E., MAMBETOV D.M., and KHAIDAROV G.Z. (1955). In : Trans.3rd Session Commis. Determ.Abs.Age Geol.Formns. Akad.Nauk SSSR, 3, 175-233.
- CHESTER R. and ASTON S.R. (1976). The geochemistry of deep-sea sediments. In : Chemical Oceanography (Riley J.P. and Chester R. eds.) Academic Press, London, 6, 281-390.
- CHUNG Y.C. (1974). Radium-226 and Ra-Ba relationships in Antarctic and Pacific waters. Earth Planet. Sci, Lett., 23, 125-135.
- CHUNG Y.C., CRAIG H., KU T-L., GODDARD J. and BROECKER W.S. (1974). Radium-226 measurements from three GEOSECS intercalibration stations. Earth Planet. Sci.Lett., 23, 116-124.
- CHUNG Y.C. and CRAIG H. (1980). ²²⁶Ra in the Pacific Ocean. Earth Planet. Sci.Lett., 49, 267-292.
- CLIFTON R.J. and HAMILTON E.I. (1979). Lead-210 chronology in relation to levels of elements in dated sediment core profiles. Estuar. Coast. Mar.Sci., 8, 259-269.
- CLYDE RIVER PURIFICATION BOARD (1971-78). Annual Reports.
- COCHRAN J.K. (1980). The flux of ²²⁶Ra from deep-sea sediments. Earth Planet, Sci. Lett., 49, 381-392.
- COCHRAN J.K. (1982). The oceanic chemistry of the U- and Th-series nuclides. In : Uranium Series Disequilibrium : Applications to Environmental Problems (Ivanovich M. and Harmon R.S.ed.), Clarendon Press, Oxford, 384-430.
- COCHRAN J.K. (1983). Personal communication.
- COCHRAN J.K. and KRISHNASWAMI S. (1980). Radium, thorium, uranium and Pb-210 in deep sea sediments and sediment porewaters from the North equatorial Pacific. Amer.J.Sci., 280, 849-889.
- COLLEY S., THOMSON J., WILSON T.R.S and HIGGS N.C. (1984). Post-depositional migration of elements during diagenesis in brown clay and turbidite sequences in the North East Atlantic. Geochim.Cosmochim.Acta, 48, 1223-1235.
- CONLAN B., HENDERSON P. and WALTON A. (1969). A simplified procedure for the assay of picocurie concentrations of radium-226 and its application to a study of the natural radioactivity in surface water in Scotland. Analyst, 94, 15-19.

- COOK G.T., BAXTER M.S., DUNCAN H.J., TOOLE J. and MALCOLMSON R. (1984). Geochemical association of plutonium in the Caithness environment. Nucl.Instr.Meth.Phys.Res., 223, 517-522.
- COWART J.B. (1980). The relationship of uranium isotopes to oxidation/reduction in the Edwards Carbonate Aquifer of Texas. Earth Planet. Sci.Lett., 48, 277-283.
- CRAIB J.S. (1965). A sampler for taking short, undisturbed marine cores. J.Cons.Perm.Int.Explor.Mer., 30, 34-39.
- CRAWFORD R.W. (1982). Development of particle track techniques for radionuclide studies in sediments. Ph.D.Thesis, University of Glasgow.
- CRAWFORD R.W. and BAXTER M.S. (1981). Particle track analysis of natural decay series nuclides in sediments and porewaters. In : Proc.IAEA Conf.Meth.Low-level Counting Spectrometry, IAEA, Vienna, 263-276.
- CRAWFORD R.W., TOOLE J., BAXTER M.S. and THOMSON J. (1984). A comparison of the particle track and alpha-spectrometric techniques in excess Thorium-230 dating of E.Atlantic pelagic sediments. J. Environ.Rad., in press.
- CRONAN D.S., GLASBY G.P., MOORBY S.A., THOMSON J., KNEDLER K.E. and McDOUGALL J.C. (1982). A submarine hydrothermal manganese deposit from the south-west Pacific island arc. Nature, 298, 456-458.
- CULKIN F. et al. (1980). RRS Discovery Cruise 108 : 18 February - 3 March 1980. Geochemical sampling on the Nares abyssal plain. Institute of Oceanographic Sciences, Cruise Report, No. 99.
- DAS N. (1983). Personal communication.
- DAVIES T.A. and GORSLINE D. (1976). Oceanic sediments and sedimentary processes. In : Chemical Oceanography (Riley J.P. and Chester R. eds.) Academic Press, London, 5, 1-80.
- DELANEY M.L. and BOYLE E.A. (1983). U and Th isotope concentrations in foraminiferal calcite. Earth Planet. Sci.Lett., 62, 258-262.
- DONGARRA G. and LANGMUIR D. (1980). The stability of UO_2OH^+ and $UO_2[HPO_4]_2^-$ complexes at 25°C. Geochim.Cosmochim. Acta, 44, 1747-1751.
- DYER K.R. (1972). Sedimentation in estuaries. In : The Estuarine Environment (Barnes R.S.K. and Green J. eds.), Applied Science Publ., London, 10-31.

- DYMOND J. and VEEH H.H. (1975). Metal accumulation rates in the southeast Pacific and the origin of metaliferous sediments. *Earth Planet. Sci. Lett.*, 28, 13-22.
- DYSART J.E. and OSMOND J.K. (1975a). Uranium in pore waters of two southern ocean cores. *Antartic J. United States*, 10, 255.
- DYSART J.E. and OSMOND J.K. (1975b). Uranium and thorium in pore water of pelagic cores. *Am.Geophys.Union Trans.*, 56, 1006.
- EATON A. (1979). The impact of anoxia on Mn fluxes in the Chesapeake Bay. *Geochim.Cosmochim.Acta*, 43, 429-432.
- EDMOND J.M., MEASURES C., MANGUM B., GRANT B., SELATER F.R., COLLIER R., HUDSON A., GORDON L.I. and CORLISS J.B. (1979). On the fractionation of metal rich deposits at ridge crests. *Earth Planet. Sci. Lett.*, 46, 19-30.
- ELDERFIELD H. (1978). Chemical variability in estuaries. In : *Biogeochemistry of Estuarine Sediments* (Goldberg E.D. ed.), UNESCO publication, 171-178.
- ELDERFIELD H. (1981). Metal-organic associations in interstitial waters of Narragansett Bay sediments. *Amer. J.Sci.*, 281, 1184-1196.
- ELDERFIELD H. and Hepworth A. (1975). Diagenesis, metals and pollution in estuaries. *Mar.Poll.Bull.*, 6, 85-87.
- EMERSON S., JAHNKE R., BENDER M., FROELICH P.N., KLINKHAMMER G.P., BOWSER C. and SETLOCK G. (1980). Early diagenesis in sediments from the eastern equatorial Pacific. I. Pore water nutrient and carbonate results. *Earth Planet. Sci.Lett.*, 49, 57-80.
- EMERSON S., GRUNDMANIS V. and GRAHAM D. (1982). Carbonate chemistry in marine pore waters : MANOP sites C and S. *Earth Planet. Sci.Lett.*, 61, 220-232.
- EMERY K.O. and RITTENBERG S.C. (1952). Early diagenesis in California basin sediments in relation to origin of oil. *Bull. Am.Ass.Petrol.Geol.*, 36, 735-806.
- FAIRES R.A. and BOSWELL G.G.J. (1981). *Radioisotope Laboratory Techniques*, 4th edn., Butterworths, London.
- FANNING K.A. and PILSON M.E.Q. (1971). Interstitial silica and pH in marine sediments : some effects of sampling procedures. *Science*, 173, 1228-1231.

- FANNING K.A. and PILSON M.E.Q. (1974). The diffusion of dissolved silica out of deep-sea sediments. *J. Geophys. Res.*, 79, 1293-1297.
- FEWS A.P. and HENSHAW D.L. (1982). High resolution alpha-particle spectroscopy using CR-39 plastic track detector. In : *Solid state Nuclear Track Detectors, Proc. 11th Int.Conf.*, Bristol (Fowler P.H. and Clapham V.M. eds.), 641-645.
- FISHER D.E. (1977a). Fission/alpha particle track analysis of the U, Th families. *Nature*, 265, 227-229
- FISHER D.E. (1977b). Fission/alpha particle track analysis : a new geologic technique for the measurement of U, Th and isotopic disequilibria. *J. Radioanal. Chem.*, 38, 477-490.
- FISHER D.E. (1978). Sedimentation rates of deep-sea cores determined by f/alpha track counting. *Geophys. Res.Lett.*, 5, 233-236.
- FISHER D.E. and BOSTROM K. (1969). Uranium-rich sediments on the East Pacific Rise. *Nature*, 224, 64-65.
- FLEISCHER R.L. (1980). Isotopic disequilibrium of uranium: alpha recoil damage and preferential solution effects. *Science*, 207, 979-981.
- FLEISCHER R.L., PRICE P.B., WALKER R.M. and HUBBARD E.L. (1964). Track registration in various solid state nuclear track detectors. *Phys. Rev.*, 133A, 1443-1449.
- FLEISCHER R.L., PRICE P.B. and WALKER R.M. (1965). Ion explosion spike mechanism for formation of charged-particle tracks in solids. *J.Appl. Phys.*, 36, 3645-3652.
- FLEISCHER R.L. and LOVETT D.B. (1968). Uranium and boron content of water by particle track etching. *Geochim.Cosmochim. Acta*, 32, 1126-1128.
- FLEISCHER R.L., ALTER H.W., FURMAN S.C., PRICE P.B. and WALKER R.M. (1972). Particle track etching. *Science*, 178, 255-263.
- FLEISCHER R.L., PRICE P.B. and WALKER R.M. (1975). *Nuclear Tracks in Solids. Principles and Applications*, Univ.California Press. Berkeley, London.
- FLEISCHER R.L. and DELANY A.C. (1976). Determination of suspended and dissolved uranium in water. *Anal.Chem.*, 48, 642-645.

- FLEISCHER R.L. and RAABE O.G. (1978). Recoiling alpha-emitting nuclei. Mechanisms for uranium-series disequilibrium. *Geochim.Cosmochim.Acta*, 42, 973-978.
- FORTH RIVER PURIFICATION BOARD. (1982). Annual Report.
- FROELICH P.N., KLINKHAMMER G.P., BENDER M.L., LUEDTKE N.A., HEATH G.R., CULLEN D., DAUPHIN P., HAMMOND D., HARTMAN B. and MAYNARD V. (1979). Early oxidation of organic matter in pelagic sediments of the eastern equatorial Atlantic : suboxic diagenesis. *Geochim.Cosmochim.Acta*, 43, 1075-1090.
- FROELICH P.N., KIM K.H., JAHNKE R., BURNETT W.C., SOUTAR A. and DEAKIN M. (1983). Pore water fluoride in Peru continental margin sediments : uptake from seawater. *Geochim.Cosmochim.Acta*, 47, 1605-1612.
- GARDNER W.S. and MENZEL D.W. (1974). Phenolic aldehydes as indicators of terrestrially-derived organic matter in the sea. *Geochim.Cosmochim.Acta*, 38, 813-822.
- GARRELS RM. and CHRIST C.L. (1965). Solutions, Minerals and Equilibria. Harper and Row.
- GASCOYNE M. (1982). Geochemistry of the actinides and their daughters. In : Uranium Series Disequilibrium : Applications to Environmental Problems (Ivanovich M. and Harmon R.S. eds.), Clarendon Press, Oxford, 33-55.
- GERALDO L.P., CESAR M.F., MAFRA O.Y. and TANAKA E.M. (1979). Determination of uranium concentration in water samples by the fission track registration technique. *J. Radioanal. Chem.*, 49, 115-126.
- GIBLIN A.M., BATTIS B.D. and SWAINE D.J. (1981). Laboratory simulation studies of uranium mobility in natural waters. *Geochim.Cosmochim.Acta*, 45, 699-709.
- GOLDBERG E.D. and KOIDE M. (1958). Ionium-thorium chronology in deep-sea sediments of the Pacific. *Science*, 128, 1003.
- GOULDING F.S. and STONE Y. (1970). Semiconductor radiation detectors. *Science*, 170, 280-289.
- GRUNDMANIS V. and MURRAY J.W. (1982). Aerobic respiration in pelagic marine sediments. *Geochim. Cosmochim. Acta*, 46, 1101-1120.
- GUO S-L., ZHOU S-H., MENG W., SUN S-F. and SHI R-F. (1982). Detection efficiencies of solid state nuclear track detectors for fission fragments. In : Solid State Nuclear Track Detectors. Proc. 11th Int. Conf., Bristol (Fowler P.H. and Clapham V.M.eds.), 265-269.

- HALBACH P., VON BORSTEL D. and GUNDERMAN K-D. (1980). The uptake of uranium by organic substances in a peat bog environment on a granitic bedrock. *Chem.Geol.*, 29, 117-138.
- HAMER A.N. and ROBBINS E.J. (1960). A search for variations in the natural abundance of uranium - 235. *Geochim. Cosmochim. Acta*, 19, 143-145.
- HAMILTON E.I. (1966). Distribution of uranium in some natural minerals. *Science*, 151, 570-572.
- HAMILTON E.I. (1970). Uranium content of normal blood. *Nature*, 227, 501-502.
- HAMILTON E.I. (1980). Concentration and distribution of uranium in *Mytilus Edulis* and associated materials. *Mar.Ecol.Prog. Ser.*, 2, 61-73.
- HAMILTON E.I. (1981). Alpha-particle radioactivity of hot particles from the Esk estuary. *Nature*, 290, 690-693.
- HAMILTON E.I. and CLIFTON R.J. (1980). Concentration and distribution of the transuranium radionuclides ^{239,240}Pu and ²⁴¹Am in *Mytilus Edulis*, *Fucus Vesiculosus* and surface sediment of the Esk estuary. *Mar.Ecol.Prog.Ser.*, 3, 267-277.
- HAMILTON E.I. and CLARKE K.R. (1984). Sedimentation history of the Esk estuary, Cumbria, U.K. The application of radiochronological methods. *Sci. Total Environ.*, 35, 325-386.
- HARTLEY P.H.T. and SPOONER G.M. (1938). The ecology of the Tamar estuary. I. Introduction. *J. Mar.Biol.Ass.U.K.*, 22, 501-508.
- HARTMANN M. (1965). An apparatus for the recovery of interstitial water from recent sediments. *Deep-Sea Res.*, 12, 225-226.
- HASHIMOTO T. (1971a). Determination of the uranium content in sea water by a fission track method with condensed aqueous solution. *Anal.Chim.Acta*, 56, 347-354.
- HASHIMOTO T. (1971b). Electrodeposition of Am and observation of the surface by means of alpha-particle tracks on CLN film. *J. Radioanal.Chem.*, 9, 251-258.
- HENRICHS S.M. and FARRINGTON J.W. (1979). Amino acids in interstitial waters of marine sediments. *Nature*, 279, 319-322.
- HETHERINGTON J.A., JEFFERIES D.F. and LOVETT M.B. (1975). Some investigations into the behaviour of plutonium in the marine environment. In : *Proc. Conf. Impacts of Nuclear Releases into the Aquatic Environment*, IAEA, Vienna, 193-212.

- HOLMES C.W., OSMOND J.K. and GOODELL H.G. (1968). The geochronology of foraminiferal ooze deposits in the southern Ocean. *Earth Planet. Sci.Lett.*, 4, 368-374.
- HOSTETLER P.B. and GARRELS R.M. (1962). Transportation and precipitation of uranium and vanadium at low temperatures, with special reference to sandstone-type uranium deposits. *Econ.Geol.*, 57, 137-167.
- ISAAC N. and PICCIOTTO E. (1953). Ionium determination in deep-sea sediments. *Nature*, 171, 742-743.
- JAHNKE R., EMERSON S. and MURRAY J.W. (1982). A model of oxygen reduction, denitrification and organic matter mineralisation in marine sediments. *Limnol. Oceanogr.*, 27, 610-623.
- JESSE A. (1971). Quantitative image analysis in the field of nuclear materials. *Microscope*, 19, 65-76.
- JOSHI L.U. and GANGULY A.K. (1976). Anomalous behaviour of uranium isotopes in coastal marine environment of the west coast of India. *Geochim.Cosmochim.Acta*, 40, 1491-1496.
- KADKO D. (1980). Thorium-230, radium-226 and radon-222 in abyssal sediments. *Earth Planet. Sci. Lett.*, 49, 360-380.
- KALIL E.K. and GOLDHABER M. (1973). A sediment squeezer for removal of pore waters without air contact. *J.Sed.Petrol*, 43, 553-557.
- KENYON N. et al. (1980). RRS Discovery Cruise 104 : 27 July - 19 August 1979. Geological studies in the Mediterranean. Institute of Oceanographic Sciences, Cruise Report, No. 105.
- KESTER D.R. and PYTKOWICZ R.M. (1967). Determination of the apparent dissociation constants of phosphoric acid in sea water. *Limnol. Oceanogr.*, 12, 243-252.
- KEY R.M., GUINASSO N.L.Jr. and SCHINK D.R. (1979). Emanation of radon-222 from marine sediments. *Mar.Chem.*, 7, 221-250.
- KHAN H.A. and DURRANI S.A. (1972). Efficiency calibration of solid state nuclear track recorders. *Nucl.Instr.Meth.*, 98, 229-236.
- KIGOSHI K. (1971). Alpha-recoil thorium-234 : dissolution into water and the uranium-234/uranium-238 disequilibrium in nature. *Science*, 173, 47-48.
- KLEEMAN J.D. AND LOVERING J.F. (1967). Uranium distribution in rocks by fission-track registration in Lexan plastic. *Science*, 156, 512-513.

- KLINKHAMMER G.P. (1980). Early diagenesis in sediments from the eastern equatorial Pacific, II. Pore water metal results. *Earth Planet. Sci. Lett.*, 49, 81-101.
- KLINKHAMMER G.P., HEGGIE D.T. and GRAHAM D.W. (1982). Metal diagenesis in oxic marine sediments. *Earth Planet. Sci. Lett.*, 61, 211-219.
- KOCZY F.F. (1958). Natural radium as tracer in the ocean. In : *Proc. 2nd U.N. Int. Conf. Peaceful Uses of Atomic Energy*, 18, 351-357.
- KOCZY F.F. (1963). Age determination in sediments by natural radioactivity. In : *The Sea* (Hill M.N. ed.), Wiley-Interscience, New York, 3, 816-831.
- KOLODNY Y. and KAPLAN I.R. (1973). Deposition of uranium in the sediment and interstitial water of an anoxic fjord. In : *Proc. Symp. Hydrogeochem. Biogeochem.* (Ingerson E. ed.), Clarke Co., Washington D.C., 1, 418-442.
- KORKISCH J. (1969). *Modern Methods for the Separation of Rarer Metal Ions*, Pergamon Press, Oxford.
- KRAUS K.A. and MOORE G.E. (1950). Adsorption of protactinium from hydrochloric acid solutions by anion exchange resins. *J. Amer. Chem. Soc.*, 72, 4293-4294.
- KRAUS K.A., MOORE G.E. and NELSON F. (1956). Anion-exchange studies. XXI. Th(IV) and U(IV) in hydrochloric acid. Separation of thorium, protactinium and uranium. *J. Amer. Chem. Soc.*, 78, 2692-2695.
- KRESSIN I.K. (1977). Electrodeposition of plutonium and americium for high resolution alpha-spectrometry. *Anal. Chem.*, 49, 842-846.
- KRISHNASWAMI S. (1976). Authigenic transition elements in Pacific pelagic clays. *Geochem. Cosmochim. Acta*, 40, 425-434.
- KRISHNASWAMI S. and COCHRAN J.K. (1978). Uranium and thorium series nuclides in oriented ferromanganese nodules : growth rates, turnover times and nuclide behaviour. *Earth Planet. Sci. Lett.*, 40, 45-62.
- KROLL V. St. (1953). Vertical distribution of radium in deep-sea sediments. *Nature*, 171, 742.
- KROLL V. St. (1954). On the age-determination in deep sea sediments by radium measurements. *Deep-Sea Res.*, 1, 211-215.
- KROM M.D. and SHOLKOVITZ E.R. (1977). Nature and reactions of dissolved organic matter in the interstitial waters of marine sediments. *Geochim. Cosmochim. Acta*, 41, 1565-1573.

- KROM M.D. and SHOLKOVITZ E.R. (1978). On the association of Fe and Mn with organic matter in anoxic marine porewaters. *Geochim.Cosmochim.Acta*, 42, 607-611.
- KU T-L (1965). An evaluation of the $^{234}\text{U}/^{238}\text{U}$ method as a tool for dating pelagic sediments. *J.Geophys.Res.*, 70, 3457-3474.
- KU T-L. (1976). The uranium-series methods of age determination. *Ann. Rev. Earth Planet. Sci.*, 4, 347-379.
- KU T-L. and BROECKER W.S. (1969). Radiochemical studies on manganese nodules of deep-sea origin. *Deep Sea Res.*, 16, 625-637.
- KU T-L., KNAUSS K.G. and MATHIEU G.G. (1977). Uranium in open ocean : concentration and isotopic composition. *Deep Sea Res.*, 24, 1005-1017.
- LALLY A.E. (1982). Chemical procedures. In : *Uranium Series Disequilibrium : Applications to Environmental Problems* (Ivanovich M. and Harmon R.S. eds.), Clarendon Press, Oxford, 79-106.
- LALLY A.E. and EAKINS J.D. (1978). Some recent advances in environmental analysis at A.E.R.E. Harwell. In : *Symp.Determ. Radionuclides Environ. Bio. Mat.*, C.E.G.B., London, paper 12.
- LALOU C. and BRICHET E. (1980). Anomalously high uranium contents in the sediment under Galapagos hydrothermal mounds. *Nature*, 284, 251-253.
- LANGMUIR D. (1978). Uranium solution-mineral equilibria at low temperatures with applications to sedimentary ore deposits. *Geochim.Cosmochim. Acta*, 42, 547-569.
- LEATHERLAND T.M. (1983). Personal communication.
- LEDERER C.M. and SHIRLEY V.S. (1978). *Table of Isotopes*, 7th edn., Wiley-Interscience, New York.
- LERMAN A. (1979). *Geochemical Processes : Water and Sediment Environments*, Wiley-Interscience, New York.
- LEVINSON A.A., BLAND C.J. and LIVELY R.S. (1982). Exploration for U ore deposits. In : *Uranium Series Disequilibrium : Applications to Environmental Problems* (Ivanovich M. and Harmon R.S. eds.), Clarendon Press, Oxford, 351-383.
- Li Y.H. and CHAN L.H. (1979). Desorption of Ba and Ra-226 from river-borne sediments in the Hudson estuary. *Earth Planet. Sci.Lett.*, 43, 343-350

- LI Y.H. and GREGORY S. (1974). Diffusion of ions in sea water and in deep-sea sediments. *Geochim.Cosmochim.Acta*, 38, 703-714.
- LISS P.S. (1976). Conservative and non-conservative behaviour of dissolved constituents during estuarine mixing. In : *Estuarine Chemistry* (Burton J.D. and Liss P.S. eds), Academic Press, London, 93-130.
- LISS P.S., HERRING J.R. and GOLDBERG E.D. (1973). Iodide/iodate system in sea water as a possible measure of redox potential. *Nature Phys. Sci.*, 242, 108-109.
- LIVINGSTONE D.A. (1963). Chemical composition of rivers and lakes. In : *The Data of Geochemistry*, 6th edn, (Fleischer M. ed.), U.S. Geological Survey Professional Paper 440, 1-64.
- LODER T.C., LYONS W.B., MURRAY S. and MCGUINNESS H.D. (1978). Silicate in anoxic pore waters and oxidation effects during sampling. *Nature*, 273, 373-374.
- LYCOS T. and BESANT C.B. (1976). Measurement of fast reactor reaction rates using solid-state track recorders. *Microscope*, 24, 199-212
- LYLE M. (1983). The brown-green color transition in marine sediments : a marker of the Fe (III) - Fe(II) redox boundary. *Limnol. Oceanogr.*, 28, 1026-1033.
- LYMAN J. and FLEMING R.H. (1940). Composition of sea water. *J. Mar.Res.*, 3, 134-146.
- LYNN D.C. and BONATTI. (1965). Mobility of manganese in diagenesis of deep-sea sediments. *Mar.Geol.*, 3, 457-474.
- LYONS W.B., GAUDETTE H.E. and HEWITT A.D. (1979a). Dissolved organic matter in pore water of carbonate sediments from Bermuda. *Geochim.Cosmochim.Acta*, 43, 433-437.
- LYONS W.B., GAUDETTE H.E. and SMITH G.M. (1979b). Pore water sampling in anoxic carbonate sediments : oxidation artefacts. *Nature*, 277, 48-49.
- MACDOUGALL J.D. (1977). Uranium in marine basalts : concentration, distribution and implications. *Earth Planet. Sci. Lett.*, 35, 67-70.
- MACKAY D.W. and LEATHERLAND T.M. (1976). Chemical processes in an estuary receiving major inputs of industrial and domestic wastes. In : *Estuarine Chemistry* (Burton J.D. and Liss P.S.eds), Academic Press, London, 185-218.

- MACKENZIE A.B. (1977). A radionuclide study of the Clyde Sea Area. Ph.D. Thesis, University of Glasgow.
- MACKENZIE A.B. and SCOTT R.D. (1982) Radiocaesium and plutonium in intertidal sediments from southern Scotland. *Nature*, 299, 613-616.
- MCCORKELL R.H. and HUANG Y.F. (1977). Discharge counter for the determination of uranium in water by the fission track method. *Rev.Sci.Instr.*, 48, 1005-1009.
- MCCRONE A.W. (1967). The Hudson river estuary : sedimentary and geochemical properties between Kingston and Haverstraw, New York. *J.Sed. Petrol.* 37, 475-486.
- McKAY W.A. (1983). Marine chemistry and tracer applications of radiocaesium. Ph.D. Thesis, University of Glasgow.
- MAEDA M. and WINDOM H.L. (1982). Behaviour of uranium in two estuaries of the south-eastern United States, *Mar.Chem.*, 11, 427-436.
- MAHAJAN G.R., CHAUDHURI N.K. SAMPATHKUMAR R. and IYER R.H. (1978). Application of track registration technique in the estimation of fissile materials : analysis of uranium in rock samples. *Nucl. Instr. Meth.*, 153, 253-257
- MAGELSDORF P.C., WILSON T.R.S. and DANIELL E.(1969). Potassium enrichments in interstitial waters of recent marine sediments. *Science*, 165, 171-173.
- MANGINI A. and DOMINIK J. (1979). Late quaternary sapropel on the Mediterranean ridge : U-budget and evidence for low sedimentation rates. *Sed.Geol.*, 23, 113-125.
- MANGINI A., SONNTAG C., BERTSCH G. and MULLER E. (1979). Evidence for a higher natural uranium content in world rivers. *Nature*, 278, 337-339.
- MANHEIM F.T. and SAYLES F.L. (1974). Composition and origin of interstitial waters of marine sediments, based on deep sea drill cores. In : *The Sea* (Goldberg E.D. ed.), Wiley-Interscience, New York, 5, 527-568.
- MARTIN J-M., NIJAMPURKAR V. and SALVADORI F. (1978a). Uranium and thorium isotope behaviour in estuarine systems. In: *Biogeochemistry of Estuarine Sediments* (Goldberg E.D. ed.), UNESCO publication, 111-127.

- MARTIN J-M., MEYBECK M. and PUSSET M. (1978b). Uranium behaviour in the Zaire estuary. *Neth. J. Sea Res.*, 12, 338-344.
- MARTIN J-M. and MEYBECK M. (1979). Elemental mass-balance of material carried by major world rivers. *Mar. Chem.*, 7, 173-206.
- MILNE A. (1938). The ecology of the Tamar estuary III. The salinity and temperature conditions in the lower estuary. *J. Mar. Biol. Ass. U.K.*, 22, 529-542.
- MO T., O'BRIEN B.C. and SUTTLE A.D. (1971). Uranium : further investigation of uranium content of Caribbean cores P6304-8 and P6304-9. *Earth Planet. Sci. Lett.*, 10, 175-178.
- MO T., SUTTLE A.D. and SACKETT W.H. (1973). Uranium concentrations in marine sediments. *Geochim.Cosmochim.Acta*, 37, 35-51.
- MOOK W.C. and KOENE B.K.S. (1975). Chemistry of dissolved inorganic carbon in estuarine and coastal brackish waters. *Estuar. Coast.Mar.Sci.*, 3, 325-336.
- MOORBY S.A. (1983). Personal communication.
- MOORE W.S. (1969). Measurement of radium-228 and thorium-228 in sea water. *J.Geophys. Res.*, 74, 694-704.
- MOORE W.S. (1969). Oceanic concentrations of ²²⁸Radium. *Earth Planet. Sci.Lett.*, 6, 437-446.
- MOORE W.S. (1981). The thorium isotope content of ocean water. *Earth Planet. Sci. Lett.*, 53, 419-426.
- MOORE W.S. and SACKETT W.M. (1964). Uranium and thorium series inequilibrium in sea water. *J. Geophys.Res.*, 69, 5401-5405.
- MORONEY M.J. (1979). *Facts from Figures*. Penguin Books Ltd.
- MORSE J.W., SHANBHAG P.M., SAITO A. and CHOPPIN G.R. (1984). Interaction of uranyl ions in carbonate media. *Chem.Geol.*, 42, 85-99.
- MORY J., DEQUILLEBON D. and DELSARTE G. (1970). Mesure du parcours moyen des fragments de fission avec le mica comme detecteur - influence de la texture cristalline. *Rad. Effects*, 5, 37-40.
- MULLER P.J. and MANGINI A. (1980). Organic carbon decomposition rates in the sediments of the Pacific manganese nodule belt dated by ²³⁴Th and ²³¹Pa. *Earth Planet Sci. Lett.*, 51, 94-114.

MURRAY C.N., KAUTSKY H., HOPPENHEIT M. and DOMIAN M. (1978). Actinide activities in water entering the northern North Sea. *Nature*, 276, 225-230.

MURRAY J.W., GRUNDMANIS V. and SMETHIE W.M. (1978). Interstitial water chemistry in the sediments of Saanich Inlet. *Geochim.Cosmochim.Acta*, 42, 1011-1026.

MURRAY J.W., EMERSON S. and JAHNKE R. (1980). Carbonate saturation and the effect of pressure on the alkalinity of interstitial waters from the Guatemala Basin. *Geochim. Cosmochim.Acta*, 44, 963-972.

NATURAL ENVIRONMENT RESEARCH COUNCIL (1974). The Clyde Estuary and Firth. An assessment of present knowledge compiled by members of the Clyde Study Group. N.E.R.C. Publications Series C, No. 11.

NIKILAYEV D.S., OKUNEV N.S., DROZHZHIN V.M., YEFIMOVA Ye. I. and BELYAYAV B.N. (1979). ²³⁴U/²³⁸U ratios for seas and rivers. *Geochem.Int.*, 16, 134-144. Transl. from *Geokhimiya*, 4, 586-597 (1979).

NISHIWAKI Y., TSURUTA T. and YAMAZAKI K. (1971). Detection of fast neutrons by etch-pit method of nuclear track registration in plastics. *J. Nucl.Sci. Technol.*, 8, 162-166.

NISSENBAUM A., BAEDECKER M.J. and KAPLAN I.R. (1971). Studies on dissolved organic matter from interstitial water of a reducing marine fjord. In: *Advances in Organic Geochemistry*, Pergamon Press, Oxford, 427-440.

NISSENBAUM A. and KAPLAN I.R. (1972). Chemical and isotopic evidence for the in-situ origin of marine humic substances. *Limnol. Oceanogr.*, 17, 570-582.

NISSENBAUM A., PRESLEY B.J. and KAPLAN I.R. (1972). Early diagenesis in a reducing fjord, Saanich Inlet, British Columbia - I. Chemical and isotopic changes in the major components of the interstitial water. *Geochim. Cosmochim. Acta*, 36, 1007-1027.

NISSENBAUM A. and SWAINE D.J. (1976). Organic matter-metal interactions in recent sediment: the role of humic substances. *Geochim. Cosmochim. Acta*, 40, 809-816.

NOZAKI Y., COCHRAN J.K., TUREKIAN K.K. and KELLER G. (1977). Radiocarbon and ²¹⁰Pb distribution in submersible-taken deep-sea cores from Project FAMOUS. *Earth Planet. Sci.Lett.*, 34, 167-173.

OSMOND J.K. (1979). Accumulation models of ²³⁰Th and ²³¹Pa in deep sea sediments. *Earth Sci. Rev.*, 15, 95-150.

OSMOND J.K. and COWART J. B. (1976). Theory and uses of natural uranium isotopic variations in hydrology. *At. Energy Rev.*, 14, 621-679.

OSMOND J.K. and COWART J.B. (1982). Ground water. In : *Uranium Series Disequilibrium : Applications to Environmental Problems* (Ivanovich M. and Harmon R.S. eds.), Clarendon Press, Oxford, 202-245.

PEIRSON D.H., CAMBRAY R.S., CAWSE P.A., EAKINS J.D. and PATTENDEN N.J. (1982). Environmental radioactivity in Cumbria. *Nature*, 300, 27-31.

PETERS R.D., TIMMINS N.T., CALVERT S.E. and MORRIS R.J. (1980). The I.O.S. box corer : Its design, development, operation and sampling. Institute of Oceanographic Sciences, Report No. 106.

PIESCH E. and WENG P.S. (1972). Application of fission track etching process for determination of low-level uranium concentration in liquids and aerosols. KFK 1552, Karlsruhe.

PILLAI K.C., MATHEW E., MATKAR V.M., DEY N.N., ABANI M.C., CHHAPGAR B.F. and MULLAY C.D. (1982). Behaviour of transuranic nuclides in coastal environment. In : *Transuranic Cycling Behaviour in the Marine Environment*, IAEA-TECDOC-265, 61-82.

POWERS M.C. (1967). Adjustment of land derived clays to the marine environment. *J.Sed. Petrol.*, 27, 355-372.

PRESLEY B.J., KOLODNY Y., NISSENBAUM A. and KAPLAN I.R. (1972). Early diagenesis in a reducing fjord, Saanich Inlet, British Columbia - II. Trace element distribution in interstitial water and sediment. *Geochim.Cosmochim.Acta*, 36, 1073-1090.

PRESLEY B.J. and TREFRY J.H. (1980). Sediment-water interactions and the geochemistry of interstitial waters. In : *Chemistry and Biogeochemistry of Estuaries* (Olausson E. and Cato I. eds.), Wiley-Interscience, 187-232.

PUPHAL K.W. and OLSEN D.R. (1972). Electrodeposition of alpha-emitting nuclides from a mixed oxalate-chloride electrolyte. *Anal. Chem.*, 44, 284-289.

QAQUISH A.Y. and BESANT C.B. (1976). Detection efficiency and range determination of alpha particles in cellulose nitrate. *Nucl.Instr.Meth.*, 138, 493-505.

REDFIELD A.C. (1958). The biological control of chemical factors in the environment. *Am.Sci.*, 46, 206-226.

- REEBURGH W.S. (1967). An improved interstitial water sampler. *Limnol. Oceanogr.*, 12, 163-165.
- RIDOUT P.S. (1981). A shipboard system for extracting interstitial water from deep ocean sediments. Institute of Oceanographic Sciences, Report No. 121.
- RILEY J.E. (1981). Analysis of ceramic semiconductor packages for trace uranium by fission track counting. *Anal.Chem.*, 53, 407-411.
- ROBBINS J.A. and CALLENDER E. (1975). Diagenesis of manganese in Lake Michigan sediments. *Amer.J.Sci.*, 275, 512-533.
- ROBERTSON D.E. (1968). The adsorption of trace elements in sea water on various container surfaces. *Anal.Chim.Acta*, 42, 533-536.
- ROGERS J.J.W. and ADAMS J.A.S. (1969). Handbook of Geochemistry (Wedepohl K.H. ed.), 2.5, Springer-Verlag, Berlin
- RONA E. and EMILIANI C. (1969). Absolute dating of Caribbean cores P6304-8 and P6304-9. *Science*, 163, 66-68.
- ROSHOLT J.N., DOE B.R. and TATSUMOTO M. (1966). Evolution of the isotope composition of uranium and thorium in soil profiles. *Geol. Soc. Am. Bull.*, 77, 987-1003.
- ROSSIGNOL-STRICK M., NESTEROFF W. and VERGNAUD-GRAZZINI P.O. and C. (1982). After the deluge : Mediterranean stagnation and sapropel formation. *Nature*, 295, 105-110.
- RYDELL H. and FISHER D.E. (1971). Uranium content of Caribbean core P6304-9. *Bull. Mar. Sci.*, 21, 787-789.
- SACKETT W.M. and THOMPSON R.R. (1963). Isotopic organic carbon composition of recent continental derived clastic sediments of east Gulf coast, Gulf of Mexico. *Bull.Am.Ass.Petrol.Geol.*, 47, 525-528.
- SACKETT W.M. and COOK G. (1969). Uranium geochemistry of the Gulf of Mexico. *Trans. Gulf Coast Assoc. Geol. Soc.*, 19, 233-238.
- SARMIENTO J.L., FEELY H.W., MOORE W.S., FAINBRIDGE A.E. and BROECKER W.S. (1976). The relationship between vertical eddy diffusion and buoyancy gradient of the deep sea. *Earth Planet. Sci.Lett.*, 32, 357-370.

SAWLAN J.J. and MURRAY J.W. (1983). Trace metal remobilisation in the interstitial waters of red clay and hemipelagic marine sediments. *Earth Planet Sci.Lett.*, 64, 213-230.

SAYLES F.L. (1970). Preliminary geochemistry. In : Initial Reports of the Deep sea Drilling Project, U.S. Government Printing Office, Washington D.C., 4, 645-655.

SAYLES F.L. (1979). The composition and diagenesis of interstitial solutions - I. Fluxes across the sea water - sediment interface in the Atlantic Ocean. *Geochim. Cosmochim. Acta*, 43, 527-545.

SAYLES F.L. (1981). The composition and diagenesis of interstitial solutions - II. Fluxes and diagenesis at the water-sediment interface in the high latitude North and South Atlantic. *Geochim.Cosmochim.Acta*, 45, 1061-1086.

SAYLES F.L., MANGELSDORF P.C. Jr., WILSON T.R.S. and HUME D.N. (1976). A sampler for the in-situ collection of marine sedimentary pore waters. *Deep-Sea Res.*, 23, 259-264.

SCOTT M.R. (1968). Thorium and uranium concentrations and isotope ratio in river sediments. *Earth Planet Sci. Lett.*, 4, 245-252.

SCOTT M.R. (1982). The chemistry of U-and Th-series nuclides in rivers. In : Uranium Series Disequilibrium : Applications to Environmental Problems (Ivanovich M. and Harmon R.S. eds.), Clarendon Press, Oxford, 181-201.

SEARLE R.C. et al. (1980). RRS Discovery Cruise 110 : 22 April - 18 June 1980. Geophysics and geochemistry in the east Pacific ocean. Institute of Oceanographic Sciences, Cruise Report, No. 102.

SHANBHAG P.M. and CHOPPIN G.R. (1981). Binding of uranyl by humic acid. *J. Inorg.Nucl.Chem.*, 43, 3369-3372.

SHEN G.T., SHOLKOVITZ E.R. and MANN D.R. (1983). The coagulation of dissolved ^{239,240}Pu in estuaries as determined from a mixing experiment. *Earth Planet. Sci. Lett.*, 64, 437-444.

SHOLKOVITZ E.R. (1976). Flocculation of dissolved organic matter and inorganic matter during the mixing of river water and seawater. *Geochim.Cosmochim.Acta*, 40, 831-845.

SHOLKOVITZ E.R., COCHRAN J.K. and CAREY A.E. (1983). Laboratory studies of the diagenesis and mobility of ^{239,240}Pu and ¹³⁷Cs in nearshore sediments. *Geochim.Cosmochim.Acta*, 47, 1369-1379.

- SILL C.W. (1974). Purification of radioactive tracers for use in high sensitivity alpha spectrometry. *Anal.Chem.*, 46, 1426-1431.
- SILL C.W. and OLSEN D.G. (1970). Sources and prevention of recoil contamination of solid-state alpha detectors. *Anal Chem.*, 42, 1596-1607.
- SMITH-BRIGGS J.L. (1983). A combined trace metal/radionuclide study of the Clyde Sea Area. Ph.D. Thesis, University of Glasgow.
- SOMAYAJULU B.L.K. and CHURCH T.M. (1973). Radium, thorium and uranium isotopes in the interstitial water from the Pacific ocean sediment. *J. Geophys.Res.*, 78, 4529-4531.
- SORENSEN J. and WILSON T.R.S. (1984). A headspace technique for oxygen measurements in deep-sea sediment cores. *Limnol. Oceanogr.*, 29, 650-652.
- SORENSEN J., HYDES D.J. and WILSON T.R.S. (1984). Denitrification in a deep-sea sediment core from the eastern equatorial Atlantic. *Limnol. Oceanogr.*, 29, 653-657.
- SPALDING R.F. and SACKETT W.M. (1972). Uranium in runoff from the Gulf of Mexico distributive province. *Science*, 175, 629-631.
- STANLEY D.J. (1978). Ionian Sea sapropel distribution and late Quaternary palaeoceanography in the eastern Mediterranean. *Nature*, 274, 149-152.
- STUMM W. and MORGAN J.J. (1981). *Aquatic Chemistry. An introduction emphasising chemical equilibria in natural waters.* John Wiley and Sons.
- SUESS E. (1970). Interaction of organic compounds with calcium carbonate. *Geochim. Cosmochim. Acta*, 34, 157-169.
- SUTHERLAND H.E., CALVERT S.E. and MORRIS R.J. (1984). Geochemical studies of the recent sapropel and associated sediment from the Hellenic outer ridge, eastern Mediterranean sea. 1. Mineralogy and chemical composition. *Mar.Geol.*, 56, 79-92.
- SWAN D.S. (1978). Some geochronological applications of lead-210 in the coastal marine and freshwater environment. Ph.D. Thesis, University of Glasgow.
- SZALAY A. (1964). Cation exchange properties of humic acids and their importance in the geochemical enrichment of UO_2^{2+} and other cations. *Geochim. Cosmochim. Acta*, 28, 1605-1614.
- TALVITIE N.A. (1971). Radiochemical determination of plutonium in environmental and biological samples by ion exchange. *Anal. Chem.*, 43, 1827-1830.
- TALVITIE N.A. (1972). Electrodeposition of actinides for alpha spectrometric determination. *Anal.Chem.*, 44, 280-283.

- THOMSON J. (1971). Natural radioactive series dating of Pleistocene oceanic materials. Ph.D. Thesis, University of Glasgow.
- THOMSON J. (1978). Oceanography related to deep sea waste disposal. Institute of Oceanographic Sciences, NERC, Report No.77.
- THOMSON J. (1982). A total dissolution method for determination of alpha-emitting isotopes of U and Th in deep-sea sediments. *Anal. Chim. Acta*, 142, 259-268.
- THOMSON J. (1982). Personal communication.
- THURBER D.L. (1962). Anomalous $^{234}\text{U}/^{238}\text{U}$ in nature. *J. Geophys. Res.*, 67, 4518-4520.
- TOOLE J., THOMSON J., WILSON T.R.S. and BAXTER M.S. (1984). A sampling artefact affecting the uranium content of deep-sea porewaters obtained from cores. *Nature*, 308, 263-266.
- TRIPATHI V.S. (1979). Comments on 'Uranium solution-mineral equilibria at low temperatures with applications to sedimentary ore deposits.' *Geochim. Cosmochim. Acta*, 43, 1989-1990.
- TROUP B.N., BRICKER O.P. and BRAY J.T. (1974). Oxidation effect on the analysis of iron in the interstitial water of recent anoxic sediments. *Nature*, 249, 237-239.
- TUREKIAN K.K. (1967). Estimates of the average Pacific deep-sea clay accumulation rate from material balance calculations. *Prog. Oceanogr.*, 4, 227-244.
- TUREKIAN K.K. and CHAN L.H. (1971). The marine geochemistry of the uranium isotopes, Th^{230} and Pa^{231} . In: *Activation Analysis in Geochemistry and Cosmochemistry* (Brunfeld A.O. and Steinnes E. eds.), Universitetsforlaget, Oslo, 311-320.
- TUREKIAN K.K. and COCHRAN J.K. (1978). Determination of marine chronologies using natural radionuclides. In: *Chemical Oceanography* (Riley J.P. and Chester R. eds.), Academic Press, London, 7, 313-360.
- UPSTILL-GODDARD R.C. (1984). Diagenesis of the halogens in anoxic estuarine sediments. Ph.D. Thesis, Dept. of Earth Sciences, University of Leeds.
- UPSTILL-GODDARD R.C. and ALEXANDER W.R. (1982). Sampling and handling procedures for the extraction of interstitial waters from anoxic, estuarine sediments. *Oceanography Internal Report No. 1*, Dept. of Earth Sciences, University of Leeds.

- URRY W.D. (1941). The radioactive determination of small amounts of uranium. *Amer. J. Sci.*, 239, 191-203.
- URRY W.D. (1942). The radio-elements in non-equilibrium systems. *Amer. J. Sci.*, 240, 426-436.
- URRY W.D. (1948). Radioactivity of ocean sediments. VII. Rate of deposition of deep-sea sediments. *J. Mar. Res.*, 7, 618-634.
- URRY W.D. (1949). Radioactivity of ocean sediments. VI. Concentrations of the radioelements in marine sediments of the southern hemisphere. *Amer. J. Sci.*, 247, 257-275,
- VEEH H.H. (1967). Deposition of uranium from the ocean. *Earth Planet. Sci. Lett.*, 3, 145-150.
- VEEH H.H. and BOSTROM K. (1971). Anomalous $^{234}\text{U}/^{238}\text{U}$ on the east Pacific rise. *Earth Planet. Sci. Lett.*, 10, 372-374.
- VEEH H.H., CALVERT S.E. and PRICE N.B. (1974). Accumulation of uranium in sediments and phosphorites on the South West African shelf. *Mar. Chem.*, 2, 189-202.
- WEAVER P.P.E. and KUIJPERS A. (1983). Climatic control of turbidite deposition on the Madeira abyssal plain. *Nature*, 306, 360-363.
- WEST R. (1976). Natural nuclear reactors. *J. Chem. Ed.*, 53, 336-340.
- WHITFIELD M. (1974). Thermodynamic limitations on the use of platinum electrode in Eh measurement. *Limnol. Oceanogr.*, 19, 857-865.
- WILSON T.R.S. et al. (1982). RRS Discovery Cruise 129 : 22 May - 22 June 1982. Geochemical sampling in the tropical and subtropical eastern Atlantic. Institute of Oceanographic Sciences, Cruise Report, No. 138.
- WISH L. (1959). Anion exchange behaviour in mixed acid solutions and development of a sequential separation scheme. *Anal. Chem.*, 31, 326-330.
- YAFFE L. (1962). Preparation of thin films, sources and targets. *Ann. Rev. Nucl. Sci.*, 12, 153-188.
- YAMADA M. and TSUNOGAI S. (1984). Postdepositional enrichment of uranium in sediment from the Bering Sea. *Mar. Geol.*, 54, 263-276.
- ZHOVOROV V.A., BOGUSLAVSKIY S.G., BABINETS A. Ye., SOLOV'YEVA L.V., KIRCHANOVA A.I. and KIR'YAKOV P.A. (1982). Geochemistry of uranium in the Black Sea. *Geokhimiya*, 8, 1195-1203.